MINISTRY OF EDUCATION AND SCIENCE OF THE REPUBLIC OF ARMENIA

YEREVAN STATE UNIVERSITY

Saharyan Nvard Aram

Some quantum phenomena in gravitational fields

Thesis

Speciality: 01.04.02 - "Theoretical Physics"

Presented for the degree of Doctor of Philosophy

in physical and mathematical sciences

Scientific supervisor: Doctor of physical and

mathematical sciences, professor R. M. Avagyan

YEREVAN - 2019

Contents

INTRODUCTION

In quantum field theory the vacuum is defined as a state with zero number of quanta. The field operator and the operator of the number of quanta do not commute and from the uncertainty relations it follows that in the vacuum state the field fluctuates. These fluctuations are called vacuum or zero-point fluctuations. The properties of vacuum fluctuations of quantum fields depend on external fields and on the geometry of the background spacetime. Among the most interesting effects of this kind is the dependence of the properties of the vacuum on boundary conditions imposed on a quantum field. The boundary conditions modify the spectrum of vacuum fluctuations and, as a result of that, the vacuum expectation values (VEVs) of physical observables are changed. For the electromagnetic field and in the geometry of two parallel neutral conducting plates this effect was predicted by Casimir in 1948 [1]. Casimir has shown that for an indealized case of infinite plates they attract by the force per unit surface $\pi^2\hbar c/(240a^4)$, where a is the separation between the plates. The forces acting on constraining boundaries as a consequence of the change in the spectrum of vacuum fluctuations for quantum fields are known as Casimir forces. In general, the change in the vacuum properties induced by boundary conditions is called the Casimir effect. Currently it has been investigated in large number of the bulk and boundary geometries (for reviews see [2]-[12]).

Among the most popular boundary geometries was the case of a spherical shell. Historically, the investigation of the corresponding Casimir effect for electromagnetic field was motivated by the Casimir semiclassical model for a charged particle [13]. In this model, the Casimir force appears in the role of the stress stabilizing the charged particle against the repulsive electrostatic forces. Assuming that the Casimir force is attractive (in analogy of the case for planar boundaries), from the equilibrium condition between the Casimir end electrostatic forces the fine structure constant is expressed in terms of the coefficient of the Casimir energy for a conducting sphere. Though the Casimir model was suggested in 1953, the Casimir energy for a conducting sphere has been evaluated only in 1968 by Boyer [14]. This was conditioned by the fact that in the case of a spherical boundary the vacuum energy is expressed in terms of series over the zeros of the Bessel functions. These zeros are given implicitly and the corresponding

calculations were more involved compared to the planar geometry. Boyer has shown that for a perfectly conducting sphere the Casimir energy is positive and, hence, the corresponding forces are repulsive. Consequently, the Casimir model with a perfectly reflecting sphere does not work. The Casimir effect for a perfectly conducting sphere has been later reconsidered by other authors [15]-[17]. New methods have been developed that include direct summation over the complete set of modes, the generalized zeta function technique [18]-[26], semiclassical methods [27]-[29], the optical approach [30]-[32], worldline numerics [33]-[35], the path integral approach [36]-[42], methods based on scattering theory [43]-[53], numerical methods based on evaluation of the stress tensor via the fluctuation-dissipation theorem [54, 55]. It is also of interest to consider the dependence of the Casimir energy on the number of spatial dimensions. For a spherical shell this problem has been analyzed in [56, 57] in the case of a massless scalar field satisfying Dirichlet and a special type of Robin boundary conditions using the Green's function method and in [58, 59] for the electromagnetic, massless scalar and spinor fields with various boundary conditions on the basis of the zeta function approach. The Casimir effect for a massive vector field and for a sphere in an arbitrary number of spatial dimensions is considered in [60].

In the references mentioned above qlobal quantities were considered, such as the vacuum energy and the force acting on the boundary. It is also of interest to consider local characteristics of the vacuum, for example, the energy density or, more generally, the VEV of the energy-momentum tensor. The energy density inside a perfectly reflecting spherical shell was studied in [61],[62]. The distribution of the remaining components for the energy-momentum tensor of the electromagnetic field inside and outside a shell and in the region between two concentric spherical shells is considered in [63]-[66]. The corresponding results have been summarized in [67],[68]. For a massive scalar field with Robin boundary conditions on spherical boundaries in $(D+1)$-dimensional Minkowski spacetime the VEV of the energy-momentum tensor is investigated in [69].

The Casimir effect can be considered as a consequence of the vacuum polarization by boundaries. Another kind of vacuum polarization arises in an external gravitational field. Currently a reliable theory of quantum gravity is absent and the influence of the gravitational field on

quantum matter is investigated within the framework of semiclassical theory. In this theory the gravitational field is considered as the classical background and the back reaction of quantum effects is described by quasiclassical Einstein equations with the expectation value of the energy-momentum tensor for quantum fields in the right-hand side (for reviews see [3],[70]-[76]). Though the quantum field theory in curved spacetime is not a fundamental theory, it should have a very broad range of physical applicability, from the smallest distance accessible in experiments to cosmological scales. This hybrid but very useful scheme is an important intermediate step to the development of quantum gravity. Among the most interesting effects in this field are the particle production and the vacuum polarization by strong gravitational fields.

The investigation of quantum effects in curved backgrounds is motivated by several reasons. During the cosmological expansion of the Universe, the back reaction of the particles created by a time dependent gravitational field at early stages leads to a rapid isotropization of the expansion. According to the inflationary scenario, the quantum vacuum fluctuations of a scalar field, amplified by the gravitational field during the quasi-de Sitter like expansion, serve as seeds for the large scale structure formation in the Universe [77, 78]. The information on the properties of these fluctuations are encoded in the thermal anisotropies of the cosmic microwave background which are measured with high accuracy by a number of recent cosmological projects. An important feature of quantum field theory in curved backgrounds is a possible breakdown of the energy conditions in the formulations of Hawking-Penrose singularity theorems, by the expectation value of the energy-momentum tensor of quantum fields. This opens a possibility to solve the singularity problem within the framework of classical general relativity. An additional motivation for the study of quantum field theoretical effects in curved backgrounds appeared recently in condensed matter physics related to various analog models. In particular, the long wavelength properties of the electronic subsystem in a graphene sheet are well described by the Dirac-like model with the speed of light replaced by the Fermi velocity. In curved graphene structures (for example, in fullerenes) the corresponding field theory is formulated on curved geometry and the curvature effects should be taken into account in the calculations of physical properties of these structures [79, 80].

An interesting topic in the theory of the Casimir effect is the investigation of the dependence

of the local characteristics, like the energy density and stresses, on the background gravitational field. In the corresponding calculations the knowledge of a complete set of the field modes is required and exact results can be obtained for bulk and boundary geometries having high degree of symmetry. The vacuum densities induced by spherical boundaries in a curved background of global monopole and in Rindler-like spacetimes have been discussed in [81]-[87] and [88]-[90], respectively. The Casimir stresses on spherical boundaries in de Sitter (dS) spacetime were considered in [91, 92] for a conformally coupled massless scalar field. The corresponding problem is conformally related to the problem for a sphere in Minkowski spacetime and the VEVs are generated from those for the Minkowski counterpart with an additional the conformal factor. The situation is qualitatively different for a spherical shell in dS spacetime in the case of non-conformal coupling [93]. In this case the curvature of the background spacetime essentially changes the behavior of sphere-induced VEVs at distances larger than the curvature scale of dS spacetime. In [94] the Wightman function, the VEVs of the field squared, and the energy-momentum tensor were investigated for a massive scalar field with general curvature coupling in a spherically symmetric static background geometry described by two distinct metric tensors inside and outside a spherical boundary.

The boundary conditions imposed on quantum fields in the Casimir effect may have different physical natures and can be divided into two main classes. In the first one, the constraints are induced by the presence of boundaries, like macroscopic bodies in QED, interfaces separating different phases of a physical system, extended topological defects, horizons in gravitational physics, branes in high-energy theories with extra dimensions and in string theories. In the corresponding models the field operator obeys the boundary condition on some spacelike surfaces (static or dynamical). In the second class, the boundary conditions on the field operator are induced by the nontrivial topology of the space. The changes in the properties of the vacuum state generated by this type of conditions are referred to as the topological Casimir effect. The importance of this effect is motivated by that the presence of compact dimensions is an inherent feature in many high-energy theories of fundamental physics, in cosmology and in condensed matter physics. In particular, supergravity and superstring theories are formulated in spacetimes having extra compact dimensions. The compactified higher-dimensional models

provide a possibility for the unification of known interactions. Models of a compact universe with nontrivial topology may also play an important role by providing proper initial conditions for inflation in the early stages of the Universe expansion [95]. In condensed matter physics, a number of planar systems in the low-energy sector are described by an effective field theory. The compactification of these systems leads to the change in the ground state energy which is the analog of the topological Casimir effect. A well-known example of this type of systems is a graphene sheet. In the long wavelength limit, the dynamics of the quasiparticles for the electronic subsystem is described in terms of the Dirac-like theory in two-dimensional space (see [96, 97]). The corresponding effective 3-dimensional relativistic field theory, in addition to Dirac fermions, involves scalar and gauge fields. The single-walled carbon nanotubes are generated by rolling up a graphene sheet to form a cylinder and for the corresponding Dirac model one has the spatial topology $R^1 \times S^1$. For another class of graphene-made structures, called toroidal carbon nanotubes, the background topology is a 2-dimensional torus, T^2.

Many authors have investigated the Casimir energies and stresses associated with the presence of compact dimensions (for reviews see [5, 98]-[103]). In higher-dimensional models the Casimir energy of bulk fields induces an effective potential for the compactification radius. This has been used as a stabilization mechanism for the corresponding moduli fields and as a source for dynamical compactification of the extra dimensions during the cosmological evolution. The Casimir effect has also been considered as a possible origin for the dark energy in both Kaluza-Klein-type and braneworld models [104]-[112]. Extra-dimensional theories with low-energy compactification scale predict Yukawa-type corrections to Newton's gravitational law and the measurements of the Casimir forces between macroscopic bodies provide a sensitive test for constraining the parameters of the corresponding long-range interactions [113]-[116]. The influence of extra compactified dimensions on the Casimir effect in the classical configuration of two parallel plates has been recently discussed for scalar [117]-[122], electromagnetic [123]-[127] and fermionic [128]-[130] fields.

The main part of the works on the influence of the copmactification on the properties of the quantum vacuum in the Casimir effect has considered global quantities such as the force or the total energy. More detailed information on the vacuum fluctuations is contained in the local

characteristics. Among the most important local quantities, because of their close connection with the structure of spacetime, are the VEVs of the vacuum energy density and stresses. For charged fields, another important characteristic is the VEV of the current density. Due to the global nature of the vacuum, this VEV carries information on both global and local properties of the vacuum state. Besides, the VEV of the current density appears as a source of the electromagnetic field in semiclassical Maxwell equations, and, hence, it is needed in modeling a self-consistent dynamics involving the electromagnetic field.

In models with nontrivial topology, the nonzero current densities in the vacuum state may appear as a consequence of quasiperiodicity conditions along compact dimensions or by the presence of gauge field fluxes enclosed by these dimensions. Note that the gauge field fluxes in higher-dimensional models will also generate a potential for moduli fields and this provides another mechanism for moduli stabilization (for a review see [131]). The VEV of the fermionic current density in spaces with toroidally compactified dimensions has been considered in [132]. In the special case of a 2-dimensional space, application are given to the electrons in cylindrical and toroidal carbon nanotubes, described within the framework of the effective field theory in terms of Dirac fermions. The vacuum currents for charged fields in dS and anti-de Sitter (AdS) spacetimes with toroidally compact spatial dimensions are investigated in [133, 134]. Finite temperature effects on the charge density and on the current densities along compact dimensions have been discussed in [135] and [136] for scalar and fermionic fields, respectively. The changes in the fermionic vacuum currents induced by the presence of parallel plane boundaries, with the bag boundary conditions on them, are investigated in [137]. The effects of branes on the vacuum current density in locally AdS spacetime with toroidally compact dimensions were studied in [138]-[141].

In addition to spherical boundaries, the investigation of the vacuum effects in geometries involving cylindrical boundaries was among the most popular directions in the study of the Casimir effect. The applications include the traditional problems of QED in the presence of material boundaries (for example conductors), the flux tube models of confinement in QCD [142, 143], the structure of the vacuum state in interacting field theories [144]. From the experimental perspective, by taking into account that in cylindrical geometries of boundaries

the effective area of interaction is larger than that for spherical boundaries, they are among the most optimal candidates for measurements of the Casimir force [145]-[147].

For a perfectly conducting cylindrical shell the Casimir energy has been evaluated in [148] by using the Green function technique and an ultraviolet regulator for the coincidence limit divergences. The result was rederived by a number of other methods such as the zeta function technique [26, 149] and the direct summation over the modes [150]. A more general problem with a dielectric-diamagnetic cylinder has been considered as well (see, for example, [151] and references cited there). The VEV of the energy-momentum tensor for the electromagnetic field in the geometries of a single and two coaxial conducting cylindrical shells was discussed in [152]-[155] (see also [67, 68]). The scalar Casimir effect for a single and two coaxial cylindrical shells with Robin boundary conditions is investigated in [156, 157]. By employing the mode summation technique, the vacuum energy in the geometry of an arbitrary number of perfectly conducting coaxial cylindrical shells is evaluated in [158]. The problem with two eccentric cylinders is considered in [159]-[166]. The Casimir energy for an elliptic cylinder is studied in [167]-[169]. The Casimir forces in the hybrid geometry of two parallel plates inside a conducting cylindrical shell are investigated in [170]. Another combined geometry consisting a wedge and coaxial cylindrical boundary is discussed in [171]-[179]. In most studies of the Casimir effect with cylindrical boundaries the geometry of the background spacetime is Minkowskian. Combined effects of a cylindrical boundary and nontrivial topology induced by a cosmic string are discussed in [180]-[184].

In the present thesis we investigate combined effects of a cylindrical boundary and background geometry on the local characteristics of the electromagnetic vacuum. As a background geometry the dS spacetime is considered. This choice is motivated by several reasons. The dS spacetime has maximal number of symmetries and because of this a large number of physical problems can be solved exactly on its background. A better understanding of the influence of classical gravitational field on quantum matter in dS spacetime serves as a way to deal with less symmetric geometries. The quantum effects in dS bulk play an important role in inflationary scenarios (see [185]-[189]). Quantum fluctuations of the inflaton field in the inflationary universe with dS geometry produce density perturbations in the post-inflationary stage. They have

nearly scale-invariant spectrum and form the base of the currently most popular mechanism for the generation of large scale structures. The corresponding predictions are in good agreement with the recent observational data on the temperature anisotropies of the cosmic microwave background radiation. The importance of dS spacetime as a gravitational background further increased after the discovery of the accelerating expansion of the Universe at recent epoch [190]-[197]. Within the framework of general relativity, among the most popular cosmological models is the one with a positive cosmological constant as a driving source behind the accelerating expansion. In this model the dS spacetime is the future attractor for the geometry of our universe.

The scalar Casimir effect for a massive field with general curvature coupling and with Robin boundary conditions on planar boundaries in the background of $(D+1)$-dimensional dS spacetime has been investigated in [198]-[201]. The geometry with a cylindrical boundary with Robin boundary condition was discussed in [202]. Depending on the mass of the field, at distances from the boundaries larger than the dS curvature radius, two different regimes are realized with monotonic or oscillatory decay of the vacuum expectation values. The electromagnetic Casimir effect for planar boundaries with generalized perfect conductor boundary conditions in dS bulk, having an arbitrary number of spatial dimensions, has been studied in [203, 204]. The propagators of vector fields on dS background in the absence of boundaries were evaluated in [205]-[209]. The background geometry of Friedmann-Robertson-Walker cosmologies with power-law scale factors was discussed in [210].

Another highly symmetric geometry that plays an important role in gravitational physics is AdS spacetime. It appears in two recent exciting developments of theoretical physics: AdS/conformal field theory (CFT) duality [211]-[213] and braneworld models with large extra dimensions [214]. In particular, motivated by the problems of the radion stabilization and the cosmological constant generation in braneworld models, the Casimir effect for planar boundaries in AdS space has been widely discussed [215]-[233]. Higher-dimensional generalizations of the AdS background having compact internal spaces have been considered as well [234]-[241]. The Casimir effect for a brane perpendicular to AdS boundary has been studied in [242].

As it has been emphasized above, the properties of the quantum vacuum are sensitive

to both the local and global geometrical characteristics of the background spacetime. In the thesis we investigate the electromagnetic vacuum polarization sourced by the gravitational field and by the nontrivial topology due to the presence of a straight cosmic string (for the effects of inflation on the cosmic strings see, for instance, [243]-[246]). In order to have an exactly solvable problem, for the cosmic string a simplified model is taken in which the local geometry outside the core is not changed by the presence of the string: the only effect is the planar angle deficit depending on the mass density of the string. Though the cosmic strings produced in phase transitions before or during early stages of inflation are diluted by the expansion to at most one per Hubble radius, the formation of defects near or at the end of inflation can be triggered by several mechanisms (see [247] for possible distinctive signals from such models). They include a coupling of the symmetry breaking field to the inflaton field or to the curvature of the background spacetime. Moreover, one can have various inflationary stages, with linear defects being formed in between them [248]. Depending on the underlying microscopic model, there exist several kinds of cosmic strings. They can be either nontrivial field configurations or more fundamental objects in superstring theories.

The cosmic strings are among the most popular topological defects formed by the symmetry breaking phase transitions in the early universe within the framework of the Kibble mechanism [249]. They are sources of a number of interesting physical effects that include the generation of gravitational waves, high-energy cosmic rays, and gamma ray bursts. Among the other signatures are the gravitational lensing and the creation of small non-Gaussianities in the cosmic microwave background. The cosmic superstrings, which are fundamental quantum strings stretched to cosmological scales, were first considered in [250]. More recently, a mechanism for the generation of this type of objects with low values of the string tensions is proposed within the framework of brane inflationary models [247, 251, 252]. In these models the accelerated expansion of the universe is a consequence of the motion of branes in warped and compact extra dimensions.

Although the specific properties of cosmic strings are model-dependent, they produce similar gravitational effects. In the simplified model with the string induced planar angle deficit, the nontrivial spatial topology results in the distortion of the vacuum fluctuations spectrum of

quantized fields and induces shifts in vacuum expectation values (VEVs) of physical characteristics of the vacuum state such as the field squared and the energy-momentum tensor. Explicit calculations of this effect have been done for scalar, fermion and vector fields. For charged fields, another important characteristic of the vacuum state is the VEV of the current density. The analysis of the vacuum polarization effects induced by a cosmic string in dS spacetime for massive scalar and fermionic fields has been presented in [253, 254, 255]. Here we will be concerned with the combined effects of the background gravitational field and of a cosmic string on the correlators for the electric and magnetic fields and on the VEVs of the energy density and squared electric and magnetic fields. The problem will be considered on the bulk of dS spacetime with an arbitrary number of spatial dimensions D. This is motivated by several reasons. In discussions of cosmic superstrings, depending on the compactification scheme of extra dimensions, one can have $3 \leqslant D \leqslant 9$. In particular, this is the case for superstrings formed at the end of brane inflation. The consideration of electrodynamics in spatial dimensions $D > 3$ is a natural way to break the conformal invariance of the $D = 3$ theory. The breaking of conformal invariance is required in inflationary models for the generation of large scale magnetic fields. Usually this is done by adding additional couplings of the electromagnetic field (for example, to the inflaton field) [256]-[259]. A mechanism for the generation of cosmological magnetic fields, based on the dynamics of electromagnetic fluctuations in models with $D > 3$, has been discussed in [260]. The consideration of quantum field theories in spatial dimensions other than 3 is also required in dimensional regularization procedure for the ultraviolet divergences.

The aim of the thesis is the investigation of combined effects of constraining boundaries, background geometry and nontrivial topology on the local properties of the vacuum state for scalar and electromagnetic fields. We have studied:

- Wightman function, the VEVs of the field squared and of the energy-momentum tensor for a quantum scalar field on the background of a negatively curved constant curvature space in the presence of a spherical boundary with Robin boundary condition on it,

- Effect of two parallel plane boundaries on the VEV of the current density for a charged scalar field in flat spacetime with toroidally compactified spatial dimensions,

- Electromagnetic field modes, the VEVs of the electric and magnetic fields squared and of the energy-momentum tensor inside and outside a cylindrical shell in dS spacetime,
- Influence of a cosmic string on the vacuum fluctuations of the electromagnetic field in background of dS spacetime.

Scientific novelty. The Wightman function, the mean field squared and the VEV of the energy-momentum tensor are evaluated for a scalar field with Robin boundary condition on a spherical shell in the background of a constant negative curvature space. For the coefficient in the boundary condition there is a critical value above which the scalar vacuum becomes unstable. At distances from the sphere larger than the curvature scale of the background space the suppression of the vacuum fluctuations in the gravitational field corresponding to the negative curvature space is stronger compared with the case of the Minkowskian bulk. The Hadamard function and the VEV of the current density are investigated for a charged scalar field in the geometry of flat boundaries with an arbitrary number of toroidally compactified spatial dimensions and in the presence of a constant gauge field. The latter induces Aharonov-Bohm-type effect on the VEVs. The vacuum stability condition depends on the lengths of compact dimensions and is less restrictive than that for background with trivial topology. Complete set of cylindrical modes is constructed for the electromagnetic field inside and outside a cylindrical shell in the background of dS spacetime and the VEVs of the electric field squared and of the energy-momentum tensor are evaluated. The vacuum energy-momentum tensor has a nonzero off-diagonal component that corresponds to the energy flux. For a cosmic string in dS spacetime, the electromagnetic field correlators are presented in the form with explicitly separated topological parts. Near the string the VEVs are dominated by the topological contributions and the effects induced by the gravitational field are small. At distances from the string larger than the curvature radius of the background geometry, the pure dS parts in the VEVs dominate.

Practical importance. The methods used in the thesis can be used for the investigation of the VEVs of local physical observables for other geometries of background spacetime. In particular, they include spaces with spherical bubbles and for cosmological models with negative curvature spaces. The expressions for the two-point functions can be used for the study of the response of Unruh-de Witt type particle detectors in a given state of motion. The generalized

Abel-Plana-type summation formula for series over the zeros of the linear combination of the associated Legendre function and its derivative can be used in other problems of mathematical physics on background of negatively curved space.

Basic results to be defended:

1. For a scalar field with Robin boundary condition on a spherical shell in the background of a constant negative curvature the boundary-induced parts are explicitly extracted from the VEVs of the field squared and of the energy-momentum tensor. At large distances from the sphere the decay of those parts is stronger compared with the case of a sphere in Minkowski bulk. Depending on the coefficient in the boundary condition, the vacuum energy density can be either positive or negative.

2. In spacetimes with toroidally compactified spatial dimensions, the nontrivial phases in quasiperiodicity conditions for a charged scalar field and a constant gauge field induce vacuum currents along compact dimensions. The current density is a periodic function of the magnetic flux, enclosed by compact dimensions, with the period equal to the flux quantum. Depending on the boundary conditions, the presence of planar boundaries may decrease or increase the VEV of the current density.

3. In both the problems with spherical and planar boundaries, there is a region in the space of the parameters in Robin boundary conditions where the vacuum state is unstable. The stability condition depends on the background geometry and topology.

4. For a cylindrical shell in dS spacetime, the boundary-induced contribution in the VEV of the electric field squared is positive for both the interior and exterior regions and the corresponding Casimir-Polder forces are directed toward the shell. The vacuum energy density, as a function of the distance from the shell, may change the sign. The presence of the cylindrical shell induces an energy flux directed from the shell.

5. For the electromagnetic field around a cosmic string in dS spacetime, the topological contributions in the local characteristics of the vacuum are explicitly separated. At distances from the string smaller than the dS curvature radius the influence of the gravitational

field is weak and those contributions dominate in the VEVs. At larger distances from the string the effect of the gravity is essential and the behavior of the VEVs may crucially differ from that for a string in Minkowski bulk. Depending on the planar angle deficit induced by the string, the vacuum energy density can be either positive or negative.

The structure of the remaining part of the thesis is the following.

In Chapter 1 we investigate the influence of background gravitational field and of a spherical shell with Robin boundary condition on local properties of the vacuum for a scalar field with general curvature coupling parameter. In Section 1.1, the bulk and boundary geometries are described and a complete sets of mode functions are presented in both the interior and exterior regions. For the interior geometry with a negative constant curvature space, the eigenmodes of a quantum scalar field with Robin boundary condition are expressed in terms of the zeros of the associated Legendre function with respect to its order. The positive-frequency Wightman function is evaluated for the boundary-free space and in the regions inside and outside the sphere. Having decomposed the Wightman function into the boundary-free and sphere-induced contributions, the renormalization of the VEVs in the coincidence limit is reduced to the one in the boundary-free geometry. In Section 1.2, the sphere-induced contribution in the VEV of the field squared is evaluated and its properties are investigated in asymptotic regions of the parameters. The expectation value of the energy-momentum tensor is studied in Section 1.3 for the both interior and exterior regions. In Section 1.4, we consider the background spacetime with the geometry described by distinct metric tensors inside and outside a spherical boundary. Two cases are investigated. In the first one the interior geometry is described by a general spherically symmetric static metric and the exterior metric corresponds to a constant negative curvature space. An example is considered with an interior Minkowskian geometry. In the second case, a constant curvature space is realized in the interior region whereas the exterior geometry is the Minkowski one. In Section 1.4.2, we discuss the properties of the zeros of the associated Legendre function with respect to its order. The expression of the Wightman function inside the spherical shell contains the summation over these zeros. In Section 1.4.2, by making use of the generalized Abel-Plana formula, a summation formula is derived for the series of this type.

In Chapter 2 the combined effects of nontrivial topology and boundaries on the vacuum current density for a charged scalar field are studied. As a background geometry we take a flat spacetime with toroidally compact spatial dimensions and the boundaries are presented by two planar parallel plates on which the field obeys Robin boundary conditions with, in general, different coefficients. In Section 2.1, the complete set of modes is specified and on the base of that the Hadamard function is evaluated. In the region between the plates, the latter is presented in the form of the sum of three terms. The first one corresponds to the Hadamard function in the geometry without boundaries, the second one is induced by a single boundary and the third one is generated by the presence of the second boundary. By using the expression for the Hadamard function, in Section 2.2, we evaluate the current density in the geometry of a single plate. The corresponding asymptotics are discussed in various limiting cases and numerical results are presented. In Section 2.3 the current density is investigated in the region between two plates. An alternative representation of the Hadamard function is given in Section 2.4.

Chapter 3 is devoted to the study of the effects of gravitational field and of a cylindrical shell on local characteristics of the electromagnetic vacuum. As a background geometry we take the dS spacetime and on the cylindrical shell a boundary condition is imposed which is a generalization of the perfect conductor boundary condition for an arbitrary number of spatial dimensions. The complete set of the electromagnetic field cylindrical modes are sepciefied and on the base of them, in Section 3.2, the VEV of the electric field squared inside the shell is evaluated. Various asymptotic regions of the parameters are discussed. The corresponding VEV of the energy-momentum tensor is studied in section 3.3. The VEVs of the electric field squared and of the energy-momentum tensor in the exterior region are investigated in section 3.4. In Section 3.4.2 the cylindrical modes in $(D+1)$-dimensional Minkowski spacetime are discussed. The integrals, appearing in the expressions for the VEVs for the special case $D=4$, are evaluated in Section 3.4.2. In the numerical evaluations of the VEVs we consider this special case.

In Chapter 4 the electromagnetic field vacuum fluctuations are investigated around a straight cosmic string in background of dS spacetime. By using the corresponding set of elec-

tromagnetic modes, realizing the Bunch-Davies vacuum state, the two-point functions for the vector potential and for the electric field strength are evaluated. The VEV of the electric field squared is discussed in Section 4.3. The part induced by the nontrivial topology of the cosmic string is explicitly separated and its asymptotic behavior in various limiting regions is investigated. The two-point functions corresponding to the Lagrangian density and the magnetic field are considered in Section 4.4. The topological contributions in the VEVs of the squared magnetic field and of the vacuum energy density are investigated. In Section 4.5 we present the main steps for the evaluation of the integrals appearing in the expressions for the two-point functions.

1 CHAPTER: VACUUM DENSITIES FOR A ROBIN SPHERE IN A CONSTANT CURVATURE SPACE

We evaluate the Wightman function, the mean field squared and the vacuum expectation value of the energy-momentum tensor for a scalar field with Robin boundary condition on a spherical shell in the background of a constant negative curvature space. For the coefficient in the boundary condition there is a critical value above which the scalar vacuum becomes unstable. In both interior and exterior regions, the vacuum expectation values are decomposed into the boundary-free and sphere-induced contributions. For the latter, rapidly convergent integral representations are provided. In the region inside the sphere, the eigenvalues are expressed in terms of the zeros of the combination of the associated Legendre function and its derivative and the decomposition is achieved by making use of the Abel-Plana type summation formula for the series over these zeros. The sphere-induced contribution to the vacuum expectation value of the field squared is negative for Dirichlet boundary condition and positive for Neumann one. At distances from the sphere larger than the curvature scale of the background space the suppression of the vacuum fluctuations in the gravitational field corresponding to the negative curvature space is stronger compared with the case of the Minkowskian bulk. In particular, the decay of the vacuum expectation values with the distance is exponential for both massive and massless fields. The corresponding results are generalized for spaces with spherical bubbles and for cosmological models with negative curvature spaces.

1.1 Wightman function

1.1.1 Geometry of the problem

We consider a quantum scalar field $\varphi(x)$ with the curvature coupling parameter ξ in a $(D+1)$-dimensional spacetime with the metric tensor g_{ik} and the Ricci scalar $\mathcal{R}$. The most important special cases of this parameter $\xi = 0$ and $\xi = \xi_c$, with

$$\xi_c = \frac{D-1}{4D},$$

correspond to minimally and conformally coupled scalars, respectively. The field dynamics is described by the Klein-Gordon equation in curved spacetime (in natural units $\hbar = 1$ and $c = 1$) [70]

$$(\nabla_l \nabla^l + m^2 + \xi \mathcal{R})\varphi(x) = 0, \tag{1.1}$$

where m is the mass of the field quanta, the covariant d'Alembertian is given by $\nabla_l \nabla^l = (1/\sqrt{|g|})\partial_l \left(\sqrt{|g|} g^{lk} \partial_k\right)$ and g is the determinant of the metric tensor.

In this Chapter the background geometry is described by the line element

$$ds^2 = dt^2 - a^2(dr^2 + \sinh^2 r d\Omega_{D-1}^2), \tag{1.2}$$

with a constant a and with $d\Omega_{D-1}^2$ being the line element on the $(D-1)$-dimensional sphere with unit radius, S^{D-1}. The corresponding angular coordinates we denote by (ϑ, ϕ) with $\vartheta = (\theta_1, \ldots, \theta_n)$, $n = D-2$, and $0 \leqslant \theta_k \leqslant \pi$, $k = 1, \ldots, n$, $0 \leqslant \phi \leqslant 2\pi$. The spatial part of the line element (1.2) describes a constant negative curvature space. The spaces with negative curvature play a significant role in cosmology and in holographic theories. For the Ricci scalar corresponding to (1.2) one has

$$\mathcal{R} = -\frac{D(D-1)}{a^2}. \tag{1.3}$$

Note that in Eq. (1.1) the curvature coupling term appears in the form of the effective mass squared $m^2 - D(D-1)\xi/a^2$. Depending on the value of the curvature coupling parameter, the latter can be either negative or positive.

Quantum effects on the background of constant curvature spaces have been widely discussed in the literature (see, for instance, [3, 5, 7, 70, 99, 100]). These effects play an important role in the physics of the early Universe, in inflationary models, and in a number of condensed matter systems described by effective curved geometries. Here we are interested in combined effects of the background gravitational field and boundaries on the properties of the quantum vacuum for a scalar field. As a boundary geometry we consider a spherical shell with the radius $r = r_0$ on which the field operator obeys Robin boundary condition

$$\left(A + Bn^l \nabla_l\right)\varphi(x) = 0, \tag{1.4}$$

where A and B are constants, and n^l is the unit inward normal to the sphere. In the geometry

under consideration one has

$$n^l = -\delta_{(j)}\frac{\delta_1^l}{a},\ j = i, e, \tag{1.5}$$

with $\delta_{(i)} = 1$ for the interior region ($r < r_0$) and $\delta_{(e)} = -1$ for the exterior region ($r > r_0$). With this, for $B \neq 0$, the boundary condition can also be written in the form $\left(\beta - \delta_{(j)}\partial_r\right)\varphi(x) = 0$, $r = r_0$, with the notation

$$\beta = aA/B. \tag{1.6}$$

Of course, all the physical results will depend on this ratio. We wrote the condition in the form (1.4) to keep the transition to special cases of Dirichlet ($B = 0$) and Neumann ($A = 0$) boundary conditions transparent. Robin type conditions appear in a variety of situations, including the considerations of vacuum effects for a confined charged scalar field in external fields [261] gauge field theories, quantum gravity and supergravity [72, 262], braneworld models [218, 223, 263] and in a class of models with boundaries separating the spatial regions with different gravitational backgrounds [94, 264]. In some geometries, these conditions may be useful for depicting the finite penetration of the field into the boundary with the "skin-depth" parameter related to the coefficient β. It is interesting to note that the quantum scalar field constrained by Robin condition on the boundary of cavity violates the Bekenstein's entropy-to-energy bound near certain points in the space of the parameter β [265].

For a free field theory all the properties of the quantum vacuum are contained in two-point functions. Here we shall consider the positive-frequency Wightman function defined as the vacuum expectation value

$$W(x, x') = \langle 0|\varphi(x)\varphi(x')|0\rangle, \tag{1.7}$$

where $|0\rangle$ stands for the vacuum state. The expectation values of physical characteristics bilinear in the field operator, such as the field squared and the energy-momentum tensor, are obtained from this function in the coincidence limit. In addition to this, the positive-frequency Wightman function determines the response function for the Unruh–De Witt particle detector in a given state of motion [70]. Let $\{\varphi_\alpha(x), \varphi_\alpha^*(x)\}$ be a complete set of normalized positive- and negative-energy mode functions obeying the field equation (1.1) and the boundary condition (1.4). Here, the collective index α is the set of quantum numbers specifying the solutions. Expanding the field operator in terms of the complete set $\{\varphi_\alpha(x), \varphi_\alpha^*(x)\}$ with the annihilation

and creation operators as coefficients and by using the condition that the vacuum state is nullified by the annihilation operator, the mode-sum formula

$$W(x,x') = \sum_{\alpha} \varphi_{\alpha}(x)\varphi_{\alpha}^{*}(x'), \tag{1.8}$$

is obtained. Here $\sum_{\alpha}$ is understood as summation for discrete components of the collective index α and as integration for continuous ones. In (1.8) the modes are normalized by the standard orthonormalization condition

$$\int d^{D}x \sqrt{|g|}\varphi_{\alpha}(x)\varphi_{\alpha'}^{*}(x) = \frac{\delta_{\alpha\alpha'}}{2E}, \tag{1.9}$$

where the symbol $\delta_{\alpha\alpha'}$ is understood as Kronecker delta for discrete indices and as the Dirac delta function for continuous ones.

For the problem under consideration, the positive-energy mode functions can be presented in the factorized form

$$\varphi_{\alpha}(x) = R_{l}(r)Y(m_{k};\vartheta,\phi)e^{-iEt}, \tag{1.10}$$

where $Y(m_{k};\vartheta,\phi)$ is the spherical harmonic of degree l. For the angular quantum numbers one has $l = 0, 1, 2\ldots$, $m_{k} = (m_{0} = l, m_{1}, \ldots, m_{n})$, where m_{1}, m_{2},..., m_{n} are integers obeying the relations

$$0 \leqslant m_{n-1} \leqslant m_{n-2} \leqslant \cdots \leqslant m_{1} \leqslant l, \tag{1.11}$$

and $-m_{n-1} \leqslant m_{n} \leqslant m_{n-1}$. By taking into account the equation for the spherical harmonics,

$$\Delta_{(\vartheta,\phi)}Y(m_{k};\vartheta,\phi) = -b_{l}Y(m_{k};\vartheta,\phi), \tag{1.12}$$

with

$$b_{l} = l(l+D-2), \tag{1.13}$$

from the field equation (1.1) for the radial function $R_{l}(r)$ one gets

$$\frac{1}{\sinh^{D-1}r}\frac{d}{dr}\left(\sinh^{D-1}r\frac{dR_{l}}{dr}\right) + \left[(E^{2}-m^{2})a^{2} + D(D-1)\xi - \frac{b_{l}}{\sinh^{2}r}\right]R_{l}(r) = 0. \tag{1.14}$$

Introducing a new function $f_{l}(r) = \sinh^{D/2-1}(r)R_{l}(r)$, we can see that the general solution for this function is a linear combination of the associated Legendre functions of the first and

second kinds, $P^{-\mu}_{iz-1/2}(\cosh r)$ and $Q^{-\mu}_{iz-1/2}(\cosh r)$ (here the definition of the associated Legendre functions follows that of [266]) with the order and degree determined by

$$\mu = l + D/2 - 1, \; z^2 = E^2 a^2 - z_m^2. \tag{1.15}$$

Here and in what follows we use the notation

$$z_m = \sqrt{m^2 a^2 - D(D-1)\,(\xi - \xi_c)}. \tag{1.16}$$

For a conformally coupled field one gets $z_m = ma$. The relative coefficient in the linear combination depends on the spatial region under consideration and will be determined below. Now, as a set of quantum numbers α, specifying the mode functions in Eq. (1.10), we can take $\alpha = (z, l, m_1, \ldots, m_n)$. The energy is expressed in terms of z by the formula

$$E(z) = a^{-1}\sqrt{z^2 + z_m^2}. \tag{1.17}$$

Below we shall assume that $z_m^2 \geqslant 0$. In particular, this condition is satisfied in the most important special cases of minimally and conformally coupled fields. If it is not obeyed there are modes with imaginary values of the energy which signal the vacuum instability. Note that the condition $z_m^2 \geqslant 0$ is different from the non-negativity condition for the effective mass squared $m^2 - D(D-1)\xi/a^2$.

In order to investigate the effects induced by the spherical boundary it is convenient to separate from the Wightman function the part corresponding to the boundary-free geometry when the spherical boundary is absent.

1.1.2 Wightman function in the boundary-free geometry

For the boundary-free geometry with $0 \leq r < \infty$, the solution of the radial equation (1.14), regular at the origin, is given in terms of the associated Legendre function of the first kind. The corresponding positive-energy mode functions have the form

$$\varphi_\alpha^{(0)}(x) = A_\alpha^{(0)} p^{-\mu}_{iz-1/2}(u) Y(m_k; \vartheta, \phi) e^{-iEt}, \tag{1.18}$$

with $0 \leqslant z < \infty$ and with the notations

$$p_\nu^{-\mu}(u) = \frac{P_\nu^{-\mu}(u)}{(u^2-1)^{(D-2)/4}}, \; u = \cosh r. \tag{1.19}$$

From the property $P_{iz-1/2}^{-\mu}(u)=P_{-iz-1/2}^{-\mu}(u)$ it follows that the radial function in (1.18) is real.

In the case $z=z'$ the normalization integral (1.9), with the integration over $r\in[0,\infty)$, diverges and, hence, the main contribution comes from large values r. By using the asymptotic formula for the associated Legendre function for large values of the argument, we can see that

$$\int_1^\infty du\, P_{iz-1/2}^{-\mu}(u)P_{iz'-1/2}^{-\mu}(u)=\frac{\pi}{z\sinh(\pi z)}\frac{\delta(z-z')}{|\Gamma(\mu+1/2+iz)|^2}, \tag{1.20}$$

where $\Gamma(x)$ is the Euler gamma function. With this result, for the normalization coefficient in (1.18) one finds

$$|A_\alpha^{(0)}|^2=\frac{z\sinh(\pi z)}{2\pi N(m_k)a^D E}|\Gamma(\mu+1/2+iz)|^2. \tag{1.21}$$

Here we have used the result $\int d\Omega\ |Y(m_k;\vartheta,\phi)|^2=N(m_k)$ (the specific form for $N(m_k)$ is given in Ref. [267] and will not be required in the following discussion). For $D=3$, the modes (1.18) with the coefficient (1.21) reduce to the ones discussed in Refs. [3, 268].

Substituting the functions (1.18) into the mode-sum (1.8), we use the addition theorem

$$\sum_{m_k}\frac{Y(m_k;\vartheta,\phi)}{N(m_k)}Y^*(m_k;\vartheta',\phi')=\frac{2l+n}{nS_D}C_l^{n/2}(\cos\theta), \tag{1.22}$$

where $S_D=2\pi^{D/2}/\Gamma(D/2)$ is the surface area of the unit sphere in D-dimensional space, $C_l^{n/2}(\cos\theta)$ is the Gegenbauer polynomial and θ is the angle between the directions determined by (ϑ,ϕ) and (ϑ',ϕ'). For the corresponding Wightman function we find the formula

$$\begin{aligned} W_0(x,x') &= \frac{a^{-D}}{2\pi nS_D}\sum_{l=0}^\infty(2l+n)C_l^{n/2}(\cos\theta)\int_0^\infty dz\, z\sinh(\pi z) \\ &\quad\times|\Gamma(iz+\mu+1/2)|^2 p_{iz-1/2}^{-\mu}(u)p_{iz-1/2}^{-\mu}(u')\frac{e^{-iE(z)\Delta t}}{E(z)}. \end{aligned} \tag{1.23}$$

with $u'=\cosh r'$ and with $E(z)$ given by Eq. (1.17).

1.1.3 Wightman function inside the sphere

In the presence of a spherical shell with the radius r_0, the mode functions for the interior region $r<r_0$, regular at the origin, are written in the form similar to Eq. (1.18):

$$\varphi_\alpha(x)=A_\alpha p_{iz-1/2}^{-\mu}(u)Y(m_k;\vartheta,\phi)e^{-iE(z)t}. \tag{1.24}$$

Now we should impose the boundary condition (1.4) on these modes. From that condition it follows that the eigenvalues for the quantum number z are solutions of the equation

$$\bar{P}^{-\mu}_{iz-1/2}(u_0)=0,\ u_0=\cosh r_0. \tag{1.25}$$

Here and in the following discussion of this chapter, for a given function $F(u)$ we use the notation

$$\bar{F}(u)=A(u)F(u)+B(u)F'(u), \tag{1.26}$$

with the coefficients

$$A(u)=A\sqrt{u^2-1}+(D/2-1)\delta_{(j)}\frac{B}{a}u,\ B(u)=-\delta_{(j)}\frac{B}{a}(u^2-1). \tag{1.27}$$

An equivalent expression for the function in the left-hand side of (1.25) is obtained by using the recurrence relation for the associated Legendre function:

$$\begin{aligned}\bar{P}^{-\mu}_{iz-1/2}(u) &= \left(A\sqrt{u^2-1}-\delta_{(j)}l\frac{B}{a}u\right)P^{-\mu}_{iz-1/2}(u)\\ &\quad+\delta_{(j)}\frac{B}{a}\left[(1/2+\mu)^2+z^2\right]\sqrt{u^2-1}P^{-\mu-1}_{iz-1/2}(u).\end{aligned} \tag{1.28}$$

For given r_0 and l, the equation (1.25) has an infinite set of positive roots with respect to z. We shall denote them, arranged in ascending order of magnitude, as $z=z_k$, $k=1,2,\ldots$. Note that these roots do not depend on the curvature coupling parameter and on the mass of the field. As is discussed in appendix 1.4.2, in addition to the real roots with respect to z, depending on the value of β, a purely imaginary root may appear. First we consider the case when all the roots are real. This case is realized for $\beta<\beta_0^{(1)}(u_0)$ (see appendix 1.4.2).

Substituting the mode functions (1.24) into the orthonormalization condition, with the integration over the region inside the spherical shell, for the normalization coefficient one finds

$$|A_\alpha|^{-2}=2Ea^DN(m_k)\int_1^{u_0}du\,|P^{-\mu}_{iz-1/2}(u)|^2. \tag{1.29}$$

The integral is evaluated by using the integration formula

$$\int_1^b du\,[P^{-\mu}_{iz-1/2}(u)]^2=\frac{b^2-1}{2z}\{[\partial_zP^{-\mu}_{iz-1/2}(b)]\partial_bP^{-\mu}_{iz-1/2}(b)-P^{-\mu}_{iz-1/2}(b)\partial_z\partial_bP^{-\mu}_{iz-1/2}(b)\}. \tag{1.30}$$

For the roots of Eq. (1.25), $z=z_k$, and for $b=u_0$, the expression in the figure braces is equal to $-P^{-\mu}_{iz-1/2}(u_0)\partial_z\bar{P}^{-\mu}_{iz-1/2}(u_0)/B(u_0)$. With this result, the normalization coefficient is written

in terms of $T_\mu(z,u)$, defined by (1.128) in appendix 1.4.2, by the expression

$$|A_\alpha|^2 = \frac{e^{i\mu\pi} z T_\mu(z,u_0)}{\pi a^D N(m_k) E(z)} \Gamma(\mu + iz + 1/2)\Gamma(\mu - iz + 1/2), \tag{1.31}$$

with $z = z_k$.

Having determined the normalized mode functions, we turn to the evaluation of the Wightman function in the region inside the sphere with the help of Eq. (1.8). Substituting the eigenfunctions, one finds

$$\begin{aligned} W(x,x') &= \frac{a^{-D}}{\pi n S_D} \sum_{l=0}^{\infty} (2l+n) C_l^{n/2}(\cos\theta) e^{i\mu\pi} \sum_{k=1}^{\infty} z_k T_\mu(z_k,u_0) \\ &\quad \times |\Gamma(iz_k + \mu + 1/2)|^2 p^{-\mu}_{iz_k - 1/2}(u) p^{-\mu}_{iz_k - 1/2}(u') \frac{e^{-iE(z_k)\Delta t}}{E(z_k)}, \end{aligned} \tag{1.32}$$

where $u' = \sinh r'$ and $\Delta t = t - t'$. The roots z_k are given implicitly and the representation (1.32) is not convenient for the evaluation of the vacuum expectation values of the field squared and the energy-momentum tensor. Additionally, the terms with large k are highly oscillatory. Both these difficulties are avoided by applying to the series over k the summation formula (1.125) with the function

$$h(z) = z\Gamma(\mu + iz + 1/2)\Gamma(\mu - iz + 1/2) P^{-\mu}_{iz-1/2}(u) P^{-\mu}_{iz-1/2}(u') \frac{e^{-iE(z)\Delta t}}{E(z)}. \tag{1.33}$$

The corresponding conditions are obeyed if $r + r' + \Delta t/a < 2r_0$. Note that the function (1.33) has branch points $z = \pm i z_m$.

The part in the Wightman function obtained from the first integral in the right-hand side of Eq. (1.125) coincides with the boundary-free function $W_0(x,x')$. In the second integral, the part over the interval $(0, z_m)$ vanishes and for the Wightman function we find

$$W(x,x') = W_0(x,x') + W_{\rm s}(x,x'), \tag{1.34}$$

where for the sphere-induced part one has

$$\begin{aligned} W_{\rm s}(x,x') &= -\frac{a^{1-D}}{\pi n S_D} \sum_{l=0}^{\infty} (2l+n) C_l^{n/2}(\cos\theta) e^{-i\mu\pi} \int_{z_m}^{\infty} dz\, z \\ &\quad \times \frac{\bar{Q}^{\mu}_{z-1/2}(u_0)}{\bar{P}^{-\mu}_{z-1/2}(u_0)} p^{-\mu}_{z-1/2}(u) p^{-\mu}_{z-1/2}(u') \frac{\cosh(\sqrt{z^2 - z_m^2}\,\Delta t/a)}{\sqrt{z^2 - z_m^2}}. \end{aligned} \tag{1.35}$$

In deriving this formula we have used the relation [266]

$$Q^{-\mu}_{z-1/2}(u) = e^{-2i\mu\pi}\frac{\Gamma(z-\mu+1/2)}{\Gamma(z+\mu+1/2)}Q^{\mu}_{x-1/2}(u), \tag{1.36}$$

for the associated Legendre function. Formula (1.35) provides our final expression for the sphere-induced part of the Wightman function in the interior region. In this form the knowledge of the roots z_k is not required and for $r + r' + \Delta t/a < 2r_0$ the integrand exponentially decays in the upper limit. In the special case $D = 3$ and for Dirichlet boundary condition, by taking into account Eq. (1.36), we see that Eq. (1.35) is reduced to the expression given in [175].

We have considered the case when all the zeros z_k of the function $\bar{P}^{-\mu}_{iz-1/2}(u_0)$ are real. As is noticed in appendix 1.4.2, for given r_0 and l, started from some critical value of β, for $\beta > \beta^{(1)}_l(\cosh r_0)$, a single purely imaginary zero $z = i\eta_l$, $\eta_l > 0$, appears. This zero first appears for the angular mode $l = 0$ and, hence, for a given r_0 the purely imaginary zeros are absent if $\beta < \beta^{(1)}_0(\cosh r_0)$. In order to have a stable vacuum state we assume that $E(i\eta_l) > 0$ or $\eta_l < z_m$. In the left panel of figure 1, for the spatial dimension $D = 3$, we have plotted the critical value $\beta^{(1)}_l(\cosh r_0)$ for the Robin coefficient, at which the purely imaginary zero appears, as a function of the sphere radius r_0 for $l = 0, 1, 5$ (the numbers near the curves).

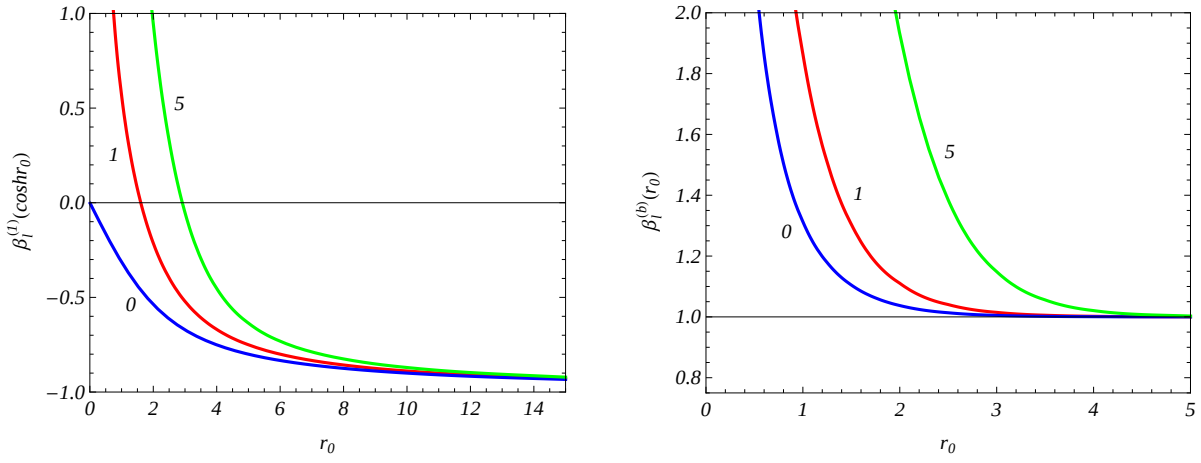

Figure 1: The critical values of the Robin coefficient for the appearance of the purely imaginary roots of the eigenvalue equation (1.25) in the interior region (left panel) and for the appearance of the bound states in the exterior region (right panel) versus the radius of the sphere. The graphs are plotted for the spatial dimension $D = 3$.

In the presence of the imaginary eigenmode, the corresponding contribution in the Wight-

man function should be added to the expression (1.32). This contribution is evaluated in a way similar to that we have used for the modes with real z and has the form

$$W^{(\mathrm{im})}(x,x')=\sum_{l=0}^{\infty}\frac{(2l+n)}{nS_Da^D}\frac{C_l^{n/2}(\cos\theta)}{u_0^2-1}\frac{\eta_l B(u_0)}{E(i\eta_l)}\frac{p_{\eta_l-1/2}^{-\mu}(u)p_{\eta_l-1/2}^{-\mu}(u')e^{-iE(i\eta_l)\Delta t}}{P_{\eta_l-1/2}^{-\mu}(u_0)\partial_\eta\bar{P}_{\eta-1/2}^{-\mu}(u_0)|_{\eta=\eta_l}}. \tag{1.37}$$

In the part of the Wightman function corresponding to the contribution of the modes with real z, given by Eq. (1.32), again we apply the summation formula (1.125). But now, as is explained in appendix 1.4.2, in the right-hand side of this formula we should add the term (1.131). By taking into account the expression (1.33) for the function $h(z)$, we can see that this term exactly cancels the contribution (1.37). Hence, the expression for the Wightman function given by Eq. (1.35) is also valid in the presence of the purely imaginary zeros for the function $\bar{P}_{iz-1/2}^{-\mu}(u_0)$ with $\eta_l<z_m$.

As an additional check of Eq. (1.35) let us consider the Minkowskian limit which corresponds to large values of a with fixed $ar=\rho$, where ρ is the Minkowskian radial coordinate. Firstly we introduce in Eq. (1.35) a new integration variable $y=z/a$ and then use the asymptotic formulae

$$P_\nu^{-\mu}[\cosh(x/\nu)]\approx\frac{I_\mu(x)}{\nu^\mu},\ Q_\nu^{\mu}[\cosh(x/\nu)]\approx e^{i\mu\pi}\nu^\mu K_\mu(x), \tag{1.38}$$

valid for $\nu\gg 1$. By taking also into account that for large a one has $z_m=am$, we can see that from Eq. (1.35) the expression for the Wightman function is obtained inside a Robin sphere in Minkowski spacetime with the radius $\rho_0=ar_0$ (see [69]).

1.1.4 Exterior region

In the region outside the sphere, $r>r_0$, the radial part of the mode functions is a linear combination of the two linear independent solutions of the Legendre equation. As such solutions it is convenient to take the functions $Q_{iz-1/2}^{-\mu}(\cosh r)$ and $Q_{-iz-1/2}^{-\mu}(\cosh r)$. The relative coefficient of the linear combination of these functions is determined from the boundary condition (1.4) and the mode functions are written in the form

$$\varphi_\alpha(x)=B_\alpha\frac{Z_{iz}^{-\mu}(u)Y(m_k;\vartheta,\phi)}{(u^2-1)^{(D-2)/4}}e^{-iE(z)t}, \tag{1.39}$$

where, as before, $u=\cosh r$, and

$$Z_{iz}^{-\mu}(u)=\bar{Q}_{iz-1/2}^{-\mu}(u_0)Q_{-iz-1/2}^{-\mu}(u)-\bar{Q}_{-iz-1/2}^{-\mu}(u_0)Q_{iz-1/2}^{-\mu}(u). \tag{1.40}$$

The notation with the bar is defined by Eq. (1.26) with the coefficients given in Eq. (1.27). In addition to the modes with real z, depending on the values of the coefficients in Robin boundary condition, the modes can be present with purely imaginary z. These modes correspond to bound states. First we consider the case when the bound states are absent.

From the normalization condition (1.9), for the modes (1.39) we have

$$B_\alpha^2 \int_{u_0}^{\infty} du Z_{iz}^{-\mu}(u)[Z_{iz'}^{-\mu}(u)]^* = \frac{\delta(z-z')}{2a^D N(m_k)E(z)}. \tag{1.41}$$

The u-integral diverges in the upper limit for $z=z'$ and, hence, the main contribution comes from large values u. So, we can replace the associated Legendre functions with the arguments u by their asymptotic expressions for large values of the argument. To find this asymptotic we use the expression of the associated Legendre function in terms of the hypergeometric function,

$$\begin{aligned} Q_{iz-1/2}^{-\mu}(\cosh r) &= \sqrt{\pi}\frac{\Gamma(1/2+iz-\mu)}{e^{i\mu\pi}\Gamma(1+iz)}\frac{e^{-(iz+1/2)r}}{(1-e^{-2r})^\mu} \\ &\quad \times F(1/2-\mu,1/2+iz-\mu;1+iz;e^{-2r}). \end{aligned} \tag{1.42}$$

From here, for large values u to the leading order we find

$$Q_{iz-1/2}^{-\mu}(u) \approx \sqrt{\pi}\frac{\Gamma(1/2+iz-\mu)}{e^{i\mu\pi}\Gamma(1+iz)}\frac{e^{-iz\ln(2u)}}{\sqrt{2u}}\left(1+O(1/u^2)\right). \tag{1.43}$$

Substituting this asymptotic into the integral (1.41), for the normalization coefficient one finds

$$B_\alpha^2 = \frac{V^{-2}(z)}{2\pi^2 a^D N(m_k)E}, \tag{1.44}$$

where

$$V(z) = \left| e^{i\mu\pi}\bar{Q}_{iz-1/2}^{-\mu}(u_0)\frac{\Gamma(1/2-iz-\mu)}{\Gamma(1-iz)}\right|. \tag{1.45}$$

By using the mode functions (1.39) with the normalization coefficient (1.44), from the mode-sum formula (1.8) for the Wightman function in the exterior region we find

$$W(x,x') = \frac{a^{-D}}{2\pi^2 n S_D}\sum_{l=0}^{\infty}\frac{(2l+n)C_l^{n/2}(\cos\theta)}{(\sinh r\sinh r')^{D/2-1}}\int_0^\infty dz\frac{e^{-iE\Delta t}}{E(z)V^2(z)}Z_{iz}^{-\mu}(u)[Z_{iz}^{-\mu}(u')]^*. \tag{1.46}$$

Introducing instead of the function $Q_{-iz-1/2}^{-\mu}(u)$ the function $P_{iz-1/2}^{-\mu}(u)$ and using the properties of the gamma function, the Wightman function is also expressed in the form

$$\begin{aligned} W(x,x') &= \frac{a^{-D}}{2\pi n S_D}\sum_{l=0}^{\infty}\frac{(2l+n)C_l^{n/2}(\cos\theta)}{(\sinh r\sinh r')^{D/2-1}}\int_0^\infty dz\, z\sinh(\pi z) \\ &\quad \times|\Gamma(iz+\mu+1/2)|^2\frac{Y_{iz-1/2}^{-\mu}(u)[Y_{iz-1/2}^{-\mu}(u')]^*}{\bar{Q}_{iz-1/2}^{-\mu}(u_0)[\bar{Q}_{iz-1/2}^{-\mu}(u_0)]^*}\frac{e^{-iE(z)\Delta t}}{E(z)}, \end{aligned} \tag{1.47}$$

where

$$Y_\nu^{-\mu}(u)=P_\nu^{-\mu}(u)\bar{Q}_\nu^{-\mu}(u_0)-\bar{P}_\nu^{-\mu}(u_0)Q_\nu^{-\mu}(u). \tag{1.48}$$

Here we are interested in the part of the Wightman function induced by the spherical shell. To obtain this contribution we subtract from the function (1.47) the Wightman function for the geometry without boundaries which is given by Eq. (1.23). For the further evaluation of the difference we use the identity

$$\frac{Y_{iz-1/2}^{-\mu}(u)[Y_{iz-1/2}^{-\mu}(u')]^*}{\bar{Q}_{iz-1/2}^{-\mu}(u_0)[\bar{Q}_{iz-1/2}^{-\mu}(u_0)]^*}-P_{iz-1/2}^{-\mu}(u)P_{iz-1/2}^{-\mu}(u')=\frac{e^{i\mu\pi}}{\pi i\sinh(\pi z)}$$
$$\times\sum_{s=\pm1}s\cos[\pi(siz-\mu)]\frac{\bar{P}_{iz-1/2}^{-\mu}(u_0)}{\bar{Q}_{siz-1/2}^{-\mu}(u_0)}Q_{siz-1/2}^{-\mu}(u)Q_{siz-1/2}^{-\mu}(u'). \tag{1.49}$$

Substituting this in the expression for the part of the Wightman function induced by the sphere, we rotate the integration contour over z by the angle $\pi/2$ for the term with $s=-1$ and by the angle $-\pi/2$ for the term with $s=1$. This leads to the following result:

$$\begin{aligned}W_{\rm s}(x,x') &= -\frac{a^{1-D}}{\pi nS_D}\sum_{l=0}^{\infty}(2l+n)C_l^{n/2}(\cos\theta)e^{-i\mu\pi}\int_{z_m}^{\infty}dz\,z\\ &\times\frac{\bar{P}_{z-1/2}^{-\mu}(u_0)}{\bar{Q}_{z-1/2}^{\mu}(u_0)}q_{z-1/2}^{\mu}(u)q_{z-1/2}^{\mu}(u')\frac{\cosh(\Delta t\sqrt{z^2-z_m^2})}{\sqrt{z^2-z_m^2}},\end{aligned} \tag{1.50}$$

with the notation

$$q_\nu^\mu(u)=\frac{Q_\nu^\mu(u)}{(u^2-1)^{(D-2)/4}}. \tag{1.51}$$

Here, once again, we have used Eq. (1.36). Comparing the expression (1.50) with Eq. (1.35), we see that the sphere-induced parts in the Wightman function for interior and exterior regions are obtained from each other by the replacements $P_{z-1/2}^{-\mu}\rightleftarrows Q_{z-1/2}^{\mu}$.

Now, let us turn to the case when bound states are present. For these states $z=i\eta$, $\eta>0$, and the mode functions are given by the expression

$$\varphi_\alpha(x)=B_{{\rm b}\alpha}q_{\eta-1/2}^{-\mu}(u)Y(m_k;\vartheta,\phi)e^{-iE(i\eta)t}, \tag{1.52}$$

with the energy $E(i\eta)=a^{-1}\sqrt{z_m^2-\eta^2}$. In order to have a stable vacuum state we assume that $\eta<z_m$. From the boundary condition (1.4) we see that, for a given r_0, the possible bound states are solutions of the equation

$$\bar{Q}_{\eta-1/2}^{-\mu}(u_0)=0. \tag{1.53}$$

Note that this equation does not involve the field mass and the curvature coupling parameter. The numerical analysis shows that there are no bound states for $\beta \leqslant (D-1)/2$. With fixed r_0 and l, a single bound state appears started from some critical value $\beta_l^{(b)}(r_0) > (D-1)/2$. We shall denote the corresponding root by $\eta = \eta_{(b)l}$. This critical value increases with increasing l. In the right panel of figure 1, for the $D = 3$ case, we have plotted $\beta_l^{(b)}(r_0)$ as a function of the sphere radius r_0 for several values of l (numbers near the curves). From the asymptotic expression for the function $Q^{-\mu}_{\eta-1/2}(u_0)$ it can be seen that $\beta_l^{(b)}(r_0) \to (D-1)/2$ for $r_0 \to \infty$.

In order to find the normalization coefficient in Eq. (1.52) we use the integration formula

$$\int_u^\infty dx\, [Q^{-\mu}_{\eta-1/2}(x)]^2 = \frac{u^2-1}{2\eta}\{[\partial_\eta Q^{-\mu}_{\eta-1/2}(u)]\partial_u Q^{-\mu}_{\eta-1/2}(u) - Q^{-\mu}_{\eta-1/2}(u)\partial_\eta\partial_u Q^{-\mu}_{\eta-1/2}(u)\}. \quad (1.54)$$

This formula is obtained by making use of the differential equation for the associated Legendre function. For the roots of Eq. (1.53) from Eq. (1.54) we get

$$\int_{u_0}^\infty dx\, [Q^{-\mu}_{\eta-1/2}(x)]^2 = \frac{1-u_0^2}{2\eta B(u_0)} Q^{-\mu}_{\eta-1/2}(u_0)\partial_\eta \bar{Q}^{-\mu}_{\eta-1/2}(u_0)|_{\eta=\eta_{(b)l}}. \quad (1.55)$$

By using this result, the normalization coefficient for the bound states is presented in the form

$$|B_{\mathrm{b}\alpha}|^2 = \frac{a^{-D}\eta B(u_0)}{N(m_k)E(\eta)} \frac{(1-u_0^2)^{-1}}{Q^{-\mu}_{\eta-1/2}(u_0)\partial_\eta \bar{Q}^{-\mu}_{\eta-1/2}(u_0)}|_{\eta=\eta_{(b)l}}. \quad (1.56)$$

With this coefficient, for the contribution of the bound states to the Wightman function one gets

$$W^{(\mathrm{bs})}(x,x') = \sum_{l=0}^\infty \frac{(2l+n)}{nS_D a^D} \frac{B(u_0)C_l^{n/2}(\cos\theta)}{E(\eta)\,(1-u_0^2)} \frac{\eta q^{-\mu}_{\eta-1/2}(u) q^{-\mu}_{\eta-1/2}(u')}{Q^{-\mu}_{\eta-1/2}(u_0)\partial_\eta \bar{Q}^{-\mu}_{\eta-1/2}(u_0)} e^{-iE(i\eta)\Delta t}|_{\eta=\eta_{(b)l}}. \quad (1.57)$$

In the presence of the bound states, the contribution to the Wightman function from the modes with real z is still given by Eq. (1.47). Again, for this expression we use the identity (1.49). The difference from the previous case arises at the step when one rotates the integration contour over z. Now, the integrands have simple poles on the imaginary axis corresponding to the zeros of the functions $\bar{Q}^{-\mu}_{siz-1/2}(u_0)$ in the denominator of Eq. (1.49). Rotating the integration contours for the terms with $s = -1$ and $s = 1$, we escape these poles by semicircles of small radius in the right-half plane. The integrals over these semicircles combine in the residue at the point $z = e^{\pi i/2}\eta_{(b)l}$. As a result, for the part in the Wightman function coming from the modes with real z we get the expression (1.50) plus the contribution coming from

the residue at the pole $z = e^{\pi i/2}\eta_{(b)l}$. Now, it can be seen that the latter is exactly canceled by the contribution from the bound state, given by Eq. (1.57). Hence, we conclude that the expression (1.50) for the shell-induced Wightman function in the exterior region is valid in the presence of bound states as well.

Similarly to the case of the interior region, we can see that in the limit $a \to \infty$ from (1.50) the corresponding expression is obtained for the sphere in Minkowski spacetime.

1.2 Vacuum expectation value of the field squared

Among the most important local characteristics of the vacuum state are the vacuum expectation values of the field squared and the energy-momentum tensor. We start with the mean field squared. It is obtained from the Wightman function in the coincidence limit of the arguments. This limit is divergent and a renormalization procedure is required. In curved backgrounds the structure of divergences is determined by the local geometry. In the problem under consideration, for points away from the sphere, the local geometry is the same as in the boundary-free case and, hence, the divergences in the local physical characteristics are the same as well. From here it follows that the renormalization procedure for these characteristics is the same as that in the boundary-free geometry. In the expressions given above for the both interior and exterior regions we have explicitly decomposed the Wightman function into the boundary-free and sphere-induced parts. For points outside the sphere, the renormalization is needed for the boundary-free vacuum expectation values only and the sphere-induced parts are directly obtained from the corresponding Wigthman function in the coincidence limit.

For the renormalized mean field squared we get

$$\langle\varphi^2\rangle = \langle\varphi^2\rangle_0 + \langle\varphi^2\rangle_{\rm s}, \tag{1.58}$$

where $\langle\varphi^2\rangle_0$ is the renormalized vacuum expectation value in the boundary-free space and the part $\langle\varphi^2\rangle_{\rm s}$ is induced by the sphere. For the latter, by taking into account that

$$C_l^{n/2}(1) = \frac{\Gamma(l+n)}{\Gamma(n)l!}, \tag{1.59}$$

in the interior region from Eq. (1.35) one finds

$$\langle\varphi^2\rangle_{\rm s} = -\frac{a^{1-D}}{\pi S_D}\sum_{l=0}^{\infty} D_l e^{-i\mu\pi}\int_{z_m}^{\infty} dz\, z\frac{\bar{Q}^{\mu}_{z-1/2}(u_0)}{\bar{P}^{-\mu}_{z-1/2}(u_0)}\frac{[p^{-\mu}_{z-1/2}(u)]^2}{\sqrt{z^2-z_m^2}}. \tag{1.60}$$

Here

$$D_l = 2\mu \frac{\Gamma(l+D-2)}{\Gamma(D-1)l!}, \tag{1.61}$$

is the degeneracy of the angular mode with given l. For the functions in the integrand, we have numerically checked that $e^{-i\mu\pi}\bar{Q}^{\mu}_{z-1/2}(u_0) > 0$ in both special cases of Dirichlet and Neumann boundary conditions, whereas $\bar{P}^{-\mu}_{z-1/2}(u_0) > 0$ for Dirichlet boundary condition and $\bar{P}^{-\mu}_{z-1/2}(u_0) < 0$ for Neumann one. Consequently, the sphere-induced vacuum expectation value of the field squared is negative for Dirichlet boundary condition and positive for Neumann boundary condition.

By using the asymptotic formulas

$$\begin{aligned} P^{-\mu}_{z-1/2}(u) &\approx \frac{z^{-\mu-1/2}e^{rz}}{\sqrt{2\pi\sinh r}}(1+O(1/z)), \\ Q^{\mu}_{z-1/2}(u) &\approx e^{i\mu\pi}\frac{\pi z^{\mu-1/2}e^{-rz}}{\sqrt{2\pi\sinh r}}(1+O(1/z)), \end{aligned} \tag{1.62}$$

valid for $z \gg 1$, we see that the integrand behaves as $e^{2z(r-r_0)}/z$. Hence, the sphere-induced vacuum expectation value (1.60) diverges on the boundary. In order to find the leading term in the asymptotic expansion over the distance from the sphere, we note that for points close to the boundary the dominant contribution in Eq. (1.60) comes from large values of z and l. In this case, instead of Eq. (1.62), we need to use the uniform asymptotic expansions for the associated Legendre functions for large values of both z and μ. The latter can be obtained from Eq. (1.38) by making use of the uniform asymptotic expansions for the modified Bessel functions (see, for instance, [266]). In this way, to the leading order, we get

$$\langle\varphi^2\rangle_{\rm s} \approx -\frac{a^{1-D}\Gamma((D-1)/2)\delta_B}{(4\pi)^{(D+1)/2}(r_0-r)^{D-1}}(1+O(r_0-r)), \tag{1.63}$$

with $\delta_B = 2\delta_{0B}-1$. As is seen, near the sphere the boundary-induced vacuum expectation value has opposite signs for Dirichlet and non-Dirichlet boundary conditions. By taking into account that $a(r_0-r)$ is the proper distance from the sphere, we see that the leading term coincides with that for the sphere in Minkowski bulk. Of course, this is natural, because near the sphere the contribution of the modes with the wavelengths smaller than the curvature radius dominate and they are relatively insensitive to the background geometry.

At the sphere center, by taking into account the asymptotic $p^{-\mu}_{z-1/2}(u) \approx 2^{-\mu}r^l/\Gamma(\mu+1)$ for

$r \to 0$, we see that the $l = 0$ mode contributes only:

$$\langle\varphi^2\rangle_{\rm s}|_{r=0} = \frac{(2a)^{1-D}e^{-i\pi D/2}}{\pi^{D/2+1}\Gamma(D/2)}\int_{z_m}^{\infty} dz\,\frac{z}{\sqrt{z^2-z_m^2}}\frac{\bar{Q}^{D/2-1}_{z-1/2}(u_0)}{\bar{P}^{1-D/2}_{z-1/2}(u_0)}. \tag{1.64}$$

Near the center the contribution of the modes with higher l decays as r^{2l}. Note that Eq. (1.64) is further simplified for $D = 3$. By taking into account the formulas

$$P^{-1/2}_{z-1/2}(u) = \frac{2\sinh(zr)}{z\sqrt{2\pi\sinh r}},\ Q^{1/2}_{z-1/2}(u) = \frac{i\pi e^{-zr}}{\sqrt{2\pi\sinh r}}, \tag{1.65}$$

we obtain

$$\frac{\bar{Q}^{1/2}_{z-1/2}(u_0)}{\bar{P}^{-1/2}_{z-1/2}(u_0)} = \frac{i\pi z}{\frac{\beta+u_0-z}{\beta+u_0+z}e^{2zr_0}-1}. \tag{1.66}$$

Hence, for $D = 3$, Eq. (1.64) is reduced to

$$\langle\varphi^2\rangle_{\rm s}|_{r=0} = -\frac{a^{-2}}{2\pi^2}\int_{z_m}^{\infty} dz\,\frac{z^2}{\sqrt{z^2-z_m^2}}\frac{1}{\frac{\beta+u_0-z}{\beta+u_0+z}e^{2zr_0}-1}, \tag{1.67}$$

with $z_m^2 = m^2a^2 + 1 - 6\xi$.

In the discussion below we shall also need the covariant Dalambertian of the boundary-induced part:

$$\nabla_p\nabla^p\langle\varphi^2\rangle_{\rm s} = \frac{2a^{-1-D}}{\pi S_D}\sum_{l=0}^{\infty} D_l e^{-i\mu\pi}\int_{z_m}^{\infty} dz\,z\frac{\bar{Q}^{\mu}_{z-1/2}(u_0)}{\bar{P}^{-\mu}_{z-1/2}(u_0)}\frac{F[p^{-\mu}_{z-1/2}(u)]}{\sqrt{z^2-z_m^2}}. \tag{1.68}$$

In this formula we have introduced the function

$$\begin{aligned} F[f(u)] &= \frac{1}{2}\left[(u^2-1)\partial_u^2 + Du\partial_u\right]f^2(u) \\ &= (u^2-1)f'^2(u) + \left[\frac{b_l}{u^2-1} - \frac{(D-1)^2}{4} + z^2\right]f^2(u). \end{aligned} \tag{1.69}$$

In the second expression, in order to exclude the second order derivative, we have used the differential equation obeyed by the function $p^{-\mu}_{z-1/2}(u)$.

In the exterior region, the shell-induced contribution in the vacuum expectation value of the field squared is obtained from Eq. (1.50) in the coincidence limit:

$$\langle\varphi^2\rangle_{\rm s} = -\frac{a^{1-D}}{\pi S_D}\sum_{l=0}^{\infty} D_l e^{-i\mu\pi}\int_{z_m}^{\infty} dz\,z\frac{\bar{P}^{-\mu}_{z-1/2}(u_0)}{\bar{Q}^{\mu}_{z-1/2}(u_0)}\frac{[q^{\mu}_{z-1/2}(u)]^2}{\sqrt{z^2-z_m^2}}. \tag{1.70}$$

This quantity is negative for Dirichlet boundary condition and positive for Neumann boundary condition. For points near the sphere, the leading term in the asymptotic expansion of this

expectation value is given by Eq. (1.63) with $r_0 - r$ replaced by $r - r_0$. In this limit, the effects of the background gravitational field are small. The curvature effects are crucial at distances from the sphere larger than the curvature radius of the background space. This corresponds to the limit of large r with a fixed value of the sphere radius r_0. For $r \gg 1$ we use the approximate formula

$$q^{\mu}_{z-1/2}(u) \approx 2^{D/2-1}\frac{e^{i\mu\pi}\sqrt{\pi}\Gamma(z+1/2+\mu)}{\Gamma(z+1)e^{(z+(D-1)/2)r}}(1+O(1/u^2)). \tag{1.71}$$

With this asymptotic, the dominant contribution in the integral of Eq. (1.70) comes from the region near the lower limit of the integration. For $z_m > 0$, assuming that $z_m r \gg 1$, to the leading order we get

$$\begin{aligned}\langle\varphi^2\rangle_{\rm s} &\approx -\frac{2^{D-3}\sqrt{\pi z_m/r}}{S_D a^{D-1}e^{(2z_m+D-1)r}}\sum_{l=0}^{\infty}D_l\frac{\bar{P}^{-\mu}_{z_m-1/2}(u_0)}{\bar{Q}^{\mu}_{z_m-1/2}(u_0)} \\ &\quad\times e^{i\mu\pi}\frac{\Gamma^2(z_m+l+D/2)}{\Gamma^2(z_m+1)}(1+O(1/r)).\end{aligned} \tag{1.72}$$

The boundary-induced vacuum expectation value is exponentially small and the suppression factor depends on the curvature coupling parameter. For $z_m = 0$ the leading term in the asymptotic expansion at large distance takes the form

$$\langle\varphi^2\rangle_{\rm s} \approx -\frac{2^{D-3}a^{1-D}}{S_D r e^{(D-1)r}}\sum_{l=0}^{\infty}D_l e^{i\mu\pi}\frac{\bar{P}^{-\mu}_{-1/2}(u_0)}{\bar{Q}^{\mu}_{-1/2}(u_0)}\Gamma^2(l+D/2)(1+O(1/r)). \tag{1.73}$$

In this case the decay is weaker, though, again exponential. In particular, for both minimally and conformally coupled massless scalars the suppression of the boundary induced vacuum expectation values at large distances is exponential.

For a spherical boundary in Minkowski bulk and for a massive field the vacuum expectation value at large distances is suppressed by the factor $e^{-2m\rho}$ with ρ being the Minkowskian radial coordinate. In this case the suppression factor does not depend on the curvature coupling. For a massless field in Minkowski spacetime, the dominant contribution at large distances comes from the angular mode $l = 0$ and the decay of the expectation value is of power-law, like $1/\rho^{2D-3}$ for $D \geqslant 3$. This shows that the suppression of the vacuum fluctuations in the gravitational field corresponding to the negative curvature space is stronger compared with the case of the Minkowskian bulk. A similar feature is observed in the geometry of planar boundaries on anti-de Sitter bulk (see Ref. [217]), then yielding another example of a negative curvature space.

For de Sitter geometry, having a positive curvature, the situation is essentially different: the boundary-induced contributions in the local vacuum expectation values decay at large distances as a power-law for both massive and massless fields.

1.3 Energy-momentum tensor

For the evaluation of the vacuum expectation value of the energy-momentum tensor we use the formula

$$\langle T_{ik} \rangle = \lim_{x' \to x} \partial_{i'} \partial_k W(x, x') + [(\xi - 1/4)\, g_{ik} \nabla_p \nabla^p - \xi \nabla_i \nabla_k - \xi \mathcal{R}_{ik}]\, \langle \varphi^2 \rangle, \tag{1.74}$$

where $\mathcal{R}_{ik}$ is the Ricci tensor. For the geometry under consideration one has (no summation over p) $\mathcal{R}_p^p = -(D-1)/a^2$ for $p = 1, \ldots, D$, and the remaining components vanish. In the right-hand side of Eq. (1.74) we have used the expression for the energy-momentum tensor for a scalar field which differs from the standard one by the term which vanishes on the solutions of the field equation and does not contribute to the boundary-induced vacuum expectation value (see [270]).

By taking into account the expressions for the Wightman function and for the expectation value of the field squared from the previous section, the vacuum energy-momentum tensor is presented in the decomposed form

$$\langle T_{ik} \rangle = \langle T_{ik} \rangle_0 + \langle T_{ik} \rangle_{\rm s}, \tag{1.75}$$

where the first and second terms in the right-hand side correspond to the boundary-free and sphere-induced contributions. Again, for points away the sphere, the renormalization is needed for the first term only.

In the interior region, after straightforward calculations, we find that the vacuum expectation value of the energy-momentum tensor is diagonal with the components (no summation over k)

$$\langle T_k^k \rangle_{\rm s} = \frac{a^{-1-D}}{\pi S_D} \sum_{l=0}^{\infty} D_l e^{-i\mu\pi} \int_{z_m}^{\infty} dz\, z \frac{\bar{Q}^{\mu}_{z-1/2}(u_0)}{\bar{P}^{-\mu}_{z-1/2}(u_0)} \frac{F^{(k)}[p^{-\mu}_{z-1/2}(u)]}{\sqrt{z^2 - z_m^2}}, \tag{1.76}$$

where we have introduced the notations

$$
\begin{aligned}
F^{(0)}[f(u)] &= 2\,(\xi-1/4)\,F[f(u)]+(z^2-z_m^2)f^2(u),\\
F^{(1)}[f(u)] &= \frac{1}{2}F[f(u)]+2(D-1)\xi u f(u)f'(u)\\
&\quad-\left[(D-1)\xi+\frac{b_l}{u^2-1}-\frac{(D-1)^2}{4}+z^2\right]f^2(u),\\
F^{(k)}[f(u)] &= 2(\xi-1/4)F[f(u)]-2\xi u f(u)f'(u)\\
&\quad+\frac{1}{D-1}\left[\frac{b_l}{u^2-1}-(D-1)^2\xi\right]f^2(u),
\end{aligned}
\tag{1.77}
$$

with $F[f(u)]$ defined in Eq. (1.69) and $k=2,3,\ldots,D$ in the last expression.

We can check that the part in the vacuum expectation value of the energy-momentum tensor induced by the spherical shell satisfies the covariant conservation equation $\nabla_k\langle T_i^k\rangle_{\rm s}=0$, which for the geometry under consideration takes the form

$$
(u^2-1)\frac{\partial}{\partial u}\langle T_1^1\rangle_{\rm s}+(D-1)u\left(\langle T_1^1\rangle_{\rm s}-\langle T_2^2\rangle_{\rm s}\right)=0. \tag{1.78}
$$

In addition, it can be seen that the boundary-induced parts in the vacuum expectation values satisfy the trace relation

$$
\langle T_k^k\rangle_{\rm s}=D(\xi-\xi_D)\nabla_p\nabla^p\langle\varphi^2\rangle_{\rm s}+m^2\langle\varphi^2\rangle_{\rm s}. \tag{1.79}
$$

In particular, for a conformally coupled massless scalar field the boundary-induced part in the expectation value of the energy-momentum tensor is traceless. The trace anomalies are contained in the boundary-free part.

The sphere-induced contribution in the vacuum expectation value of the energy-momentum tensor diverges on the boundary. The leading terms in the expansion over the distance from the sphere for the energy density and parallel stresses are found in a way similar to that we have used for the field squared. They are given by (no summation over k)

$$
\langle T_k^k\rangle_{\rm s}\approx\frac{D\Gamma((D+1)/2)(\xi-\xi_D)}{2^D\pi^{(D+1)/2}[a(r_0-r)]^{D+1}}\delta_B(1+O(r_0-r)), \tag{1.80}
$$

for the components $k=0,2,\ldots$. Again, these leading terms coincide with those for a sphere in the Minkowski bulk. The leading term for the radial stress vanishes and the next to the leading

terms in the relations (1.38) should be kept. Easier way is to use the continuity equation (1.78) with the result

$$\langle T_1^1 \rangle_{\rm s} \approx \left(1-\frac{1}{D}\right)\frac{u_0(r_0-r)}{\sqrt{u_0^2-1}}\langle T_0^0\rangle_{\rm s}, \tag{1.81}$$

with $\langle T_0^0\rangle_{\rm s}$ from Eq. (1.80).

At the sphere center only the terms with $l=0,1$ contribute, and one has (no summation over k)

$$\langle T_k^k \rangle_{\rm s} = \frac{a^{-1-D}}{\pi S_D}\int_{z_m}^{\infty} dz\,\frac{z}{\sqrt{z^2-z_m^2}}\sum_{l=0}^{1}\frac{D_l e^{-i\mu\pi}F_l^{(k)}}{2^{2\mu}\Gamma^2(\mu+1)}\frac{\bar{Q}^{\mu}_{z-1/2}(u_0)}{\bar{P}^{-\mu}_{z-1/2}(u_0)}, \tag{1.82}$$

where

$$\begin{aligned} F_0^{(0)} &= 2\left(\xi-\frac{1}{4}\right)\left[z^2-\frac{(D-1)^2}{4}\right]+z^2-z_m^2, \\ F_0^{(k)} &= \left[2\left(1-\frac{1}{D}\right)\xi-\frac{1}{2}\right]\left[z^2-\frac{(D-1)^2}{4}\right]-(D-1)\xi, \end{aligned} \tag{1.83}$$

and

$$\begin{aligned} F_1^{(0)} &= 2D\,(\xi-1/4)\,, \\ F_1^{(k)} &= 2(D-1)\xi-D/2+1. \end{aligned} \tag{1.84}$$

In Eqs. (1.83) and (1.84), $k=1,2,\ldots,D$ and the stresses are isotropic at the center. For $D=3$, Eq. (1.82) is further simplified by using Eq. (1.66). The functions $P^{-3/2}_{z-1/2}(u)$ and $Q^{3/2}_{z-1/2}(u)$ in the $l=1$ term of Eq. (1.82) are expressed in terms of the hyperbolic functions by using Eq. (1.65) and the recurrence relations for the associated Legendre functions.

For the shell-induced contribution in the vacuum expectation value of the energy-momentum tensor in the exterior region, $r>r_0$, we get

$$\langle T_k^k \rangle_{\rm s} = \frac{a^{-1-D}}{\pi S_D}\sum_{l=0}^{\infty} D_l e^{-i\mu\pi}\int_{z_m}^{\infty} dz\,z\frac{\bar{P}^{-\mu}_{z-1/2}(u_0)}{\bar{Q}^{\mu}_{z-1/2}(u_0)}\frac{F^{(k)}[q^{\mu}_{z-1/2}(u)]}{\sqrt{z^2-z_m^2}}. \tag{1.85}$$

For points near the sphere the corresponding asymptotic for the energy density and parallel stresses are given by Eq. (1.80) with the replacement $(r_0-r)\to(r-r_0)$. Hence, for a non-conformally coupled field, near the boundary these components have the same sign in the exterior and interior regions. For the radial stress we have the same relation (1.81) and for a non-conformally coupled field it has opposite signs inside and outside the sphere.

Now we turn to the asymptotic behavior of the vacuum energy-momentum tensor at large distances from the sphere. In this limit we use Eq. (1.71). The dominant contribution to the integral in Eq. (1.85) comes form the region near the lower limit. For $z_m > 0$, to the leading order we get (no summation over k)

$$\begin{aligned}\langle T_k^k \rangle_{\rm s} &\approx \frac{2^{D-3}\sqrt{\pi z_m/r}F^{(k)}(z_m)}{S_D a^{D+1} e^{(2z_m+D-1)r}} \sum_{l=0}^{\infty} D_l e^{i\mu\pi} \\ &\times \frac{\bar{P}^{-\mu}_{z_m-1/2}(u_0)}{\bar{Q}^{\mu}_{z_m-1/2}(u_0)} \frac{\Gamma^2(z_m+1/2+\mu)}{\Gamma^2(z_m+1)}(1+O(1/r)), \end{aligned} \tag{1.86}$$

where we have defined the functions

$$\begin{aligned} F^{(0)}(z) &= (4\xi-1)\, z[z+(D-1)/2], \\ F^{(1)}(z) &= -\frac{1}{2}(D-1)\left[(4\xi-1)\, z + 2D\,(\xi-\xi_D)\right], \end{aligned} \tag{1.87}$$

and $F^{(k)}(z) = 2zF^{(1)}(z)/(1-D)$ for $k = 2, \ldots, D$. For minimally and conformally coupled fields $F^{(0)}(z) < 0$ and from Eq. (1.86) it follows that the sphere-induced contribution to the vacuum energy of these fields is negative for Dirichlet boundary condition and positive for Neumann boundary condition.

For $z_m = 0$, the leading term in the asymptotic expansion at large distances has the form (no summation over k)

$$\langle T_k^k \rangle_{\rm s} \approx \frac{2^{D-3} D F^{(k)}_{\rm (e)} e^{-(D-1)r}}{S_D a^{D+1} r^{2-\delta_1^k}} \sum_{l=0}^{\infty} D_l e^{i\mu\pi} \frac{\bar{Q}^{\mu}_{-1/2}(u_0)}{\bar{P}^{-\mu}_{-1/2}(u_0)} \Gamma^2(1/2+\mu)(1+O(1/r)), \tag{1.88}$$

with the coefficients

$$\begin{aligned} F^{(0)}_{\rm (e)} &= \xi_D\,(4\xi-1)\,, \\ F^{(1)}_{\rm (e)} &= (1-D)\,(\xi-\xi_D)\,,\ F^{(k)}_{\rm (e)} = \xi-\xi_D, \end{aligned} \tag{1.89}$$

and with $k = 2, \ldots, D$ in the last expression. In this case, for non-conformally coupled fields one has $|\langle T_1^1 \rangle_{\rm s}| \gg |\langle T_0^0 \rangle_{\rm s}|$. Again, at large distances we have an exponential suppression for both massive and massless fields. For minimally and conformally coupled fields the energy density corresponding to Eq. (1.88) is negative for Dirichlet boundary condition and positive for Neumann one. Note that for a sphere in Minkowski bulk the Casimir densities for massive fields are suppressed by the factor $e^{-2m\rho}$. For non-conformally coupled massless fields, at large

distances the contribution of the $l = 0$ mode dominates and all the diagonal components of the vacuum energy-momentum tensor in Minkowski bulk are of the same order. In this case the vacuum expectation values decay as $1/\rho^{2D-1}$ for $D \geqslant 3$ and as $1/(\rho^3 \ln \rho)$ for $D = 2$ (see [69]).

In figure 2, for a minimally coupled massless field, we have plotted the sphere-induced contribution in the vacuum energy density inside (left panel) and outside (right panel) the $D = 3$ spherical shell versus the radial coordinate r for the values of the radius $r_0 = 1, 1.5, 2$ (numbers near the curves). The full/dashed curves correspond to Dirichlet/Neumann boundary conditions.

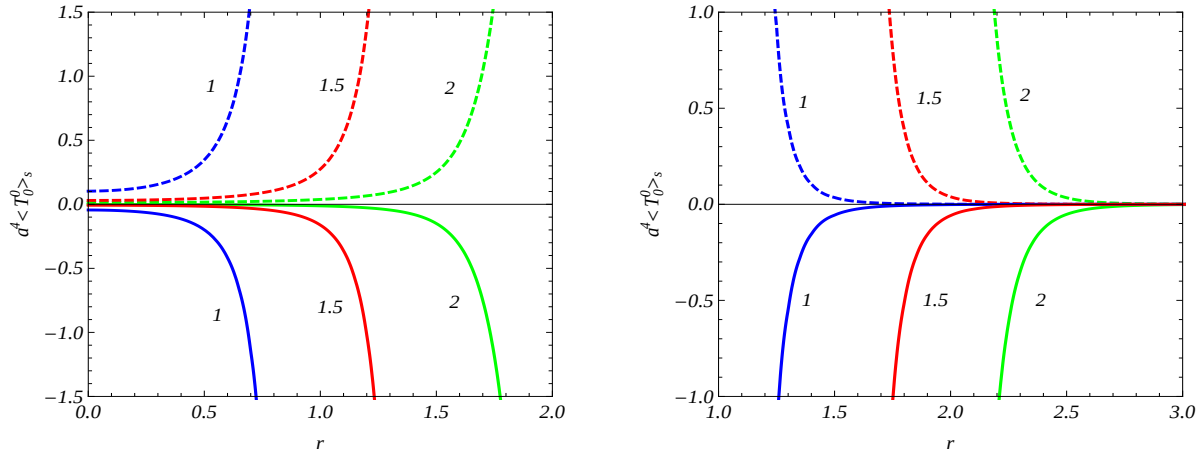

Figure 2: The sphere-induced vacuum energy density for a minimally coupled $D = 3$ massless scalar field as a function of the radial coordinate. The graphs are plotted for several values of the sphere radius ($r_0 = 1, 1.5, 2$, numbers near the curves). The left/right panel corresponds to the interior/exterior regions and the full and dashed curves are for Dirichlet and Neumann boundary conditions, respectively.

In figure 3, the sphere-induced contribution in the vacuum energy is displayed as a function of the parameter β in Robin boundary condition for fixed value of r (numbers near the curves) and for $D = 3$ sphere with the radius $r_0 = 2$. Again, the graphs are plotted for a minimally coupled massless field.

Here we have considered the vacuum expectation value of the bulk energy-momentum tensor. On manifolds with boundaries and for a scalar field with Robin boundary condition there is also a surface energy-momentum tensor located on the boundary. In the general case of bulk and boundary geometries the expression for the latter is given in [270] (see also the discussion in Ref.

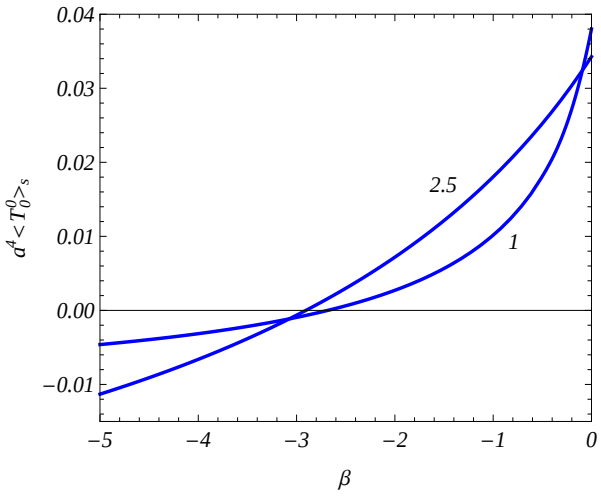

Figure 3: The sphere-induced vacuum energy density versus the coefficient in the Robin boundary condition in the case of a minimally coupled $D = 3$ massless field. For the sphere radius one has $r_0 = 2$ and the numbers near the curves correspond to the values of the radial coordinate r.

[271]-[274]). The expectation value of the surface energy-momentum tensor can be evaluated by making use of the corresponding mode-sum with the eigenfunctions given above. However, in this case the renormalization procedure is not reduced to the one in the boundary-free space and additional subtractions are necessary. This procedure can be realized, for example, by using the generalized zeta function technique and will be discussed elsewhere with the total Casimir energy.

For a conformally coupled massless scalar field, the generalization of the the results given above for the Friedmann-Robertson-Walker backgrounds, described by Eq. (1.2) with a time-dependent scale factor $a = a(t)$, is straightforward. For that, in the expressions for the Wightman function and for the vacuum expectation values of the field squared and the energy-momentum tensor one should make the replacement $a \to a(t)$. For non-conformally coupled fields the problem is more complicated. In particular, similar to the case of de Sitter background, we expect that in addition to the diagonal components, the vacuum energy-momentum tensor will have an off-diagonal component describing the energy flux along the radial direction.

1.4 Casimir densities induced by spherical bubbles

In this section we consider the background spacetime with the geometry described by distinct metric tensors inside and outside a spherical boundary. The interior and exterior gravitational backgrounds may correspond to different vacuum states of a physical system. In this case the sphere serves as a thin-wall approximation of a domain wall interpolating between two coexisting vacua [275]. In what follows we shall refer the interior region as a bubble.

1.4.1 Bubble in a constant curvature space

First we consider the geometry described by the line element (1.2) in the region $r > r_0$ and by

$$ds^2 = e^{2u(r)}dt^2 - a^2[e^{2v(r)}dr^2 + e^{2w(r)}d\Omega_{D-1}^2], \tag{1.90}$$

in the region $r < r_0$, assuming that the corresponding metric tensor is regular. For generality, the presence of the surface energy-momentum tensor with nonzero components τ_0^0 and $\tau_2^2 = \cdots = \tau_D^D$, located at $r = r_0$, will be assumed. The continuity of the metric tensor at the separating boundary gives

$$u(r_0) = 0,\ v(r_0) = 0,\ w(r_0) = \ln(\sinh r_0). \tag{1.91}$$

From the Israel matching conditions on the sphere $r = r_0$ we get (no summation over $k = 2, 3, \ldots, D$)

$$\begin{aligned} 8\pi G a\tau_0^0 &= (D-1)\left[w'(r_0) - \coth r_0\right], \\ 8\pi G a\tau_k^k &= u'(r_0) + (D-2)\left[w'(r_0) - \coth r_0\right]. \end{aligned} \tag{1.92}$$

where G is the gravitational constant. For the trace of the surface energy-momentum tensor one has

$$\frac{8\pi G}{D-1}a\tau = u'(r_0) + (D-1)[w'(r_0) - \coth r_0]. \tag{1.93}$$

A general problem for the Casimir densities in spherically symmetric spaces with bubbles is considered in [94]. In that paper the exterior metric was assumed to be asymptotically flat. The latter is not the case for the problem under consideration. However, the main steps for the evaluation are similar and we omit the details.

The mode functions for a scalar field in the interior and exterior regions are presented in the form (1.10). We denote the regular solution of the equation for the radial function in the interior region by $R_{(i)\,l}(r,E)$ taking it being real. By taking into account that the energy appears in the equation for the radial function in the form E^2, we shall also assume that $R_{(i)\,l}(r,-E)=\text{const}\cdot R_{(i)\,l}(r,E)$. For the radial function in the exterior region one has

$$R_l(r)=A_1 q^{-\mu}_{iz-1/2}(u)+A_2 q^{-\mu}_{-i\lambda-1/2}(u). \tag{1.94}$$

The radial functions are continous at $r=r_0$ and for their derivatives one has the jump condition [94]

$$R_l'(r_0+0)-R_l'(r_0-0)=\frac{16\pi G\xi}{D-1}a\tau R(r_0). \tag{1.95}$$

This jump comes from the delta function term in the field equation (1.1) contained in the Ricci scalar. From these matching conditions, for the radial functions in the geometry at hand one gets

$$R_l(r)=C_\alpha V^{-\mu}_{iz}(u),\ r>r_0, \tag{1.96}$$

where

$$V^{-\mu}_{iz}(u)=\hat{q}^{-\mu}_{-iz-1/2}(u_0)q^{-\mu}_{iz-1/2}(u)-\hat{q}^{-\mu}_{iz-1/2}(u_0)q^{-\mu}_{-iz-1/2}(u), \tag{1.97}$$

and

$$C_\alpha=\frac{R_{(i)\,l}(r_0,E)}{W^{(12)}_l(r_0)}. \tag{1.98}$$

In Eq. (1.97), the notation with hat is defined as

$$\hat{F}(u)=\sqrt{u^2-1}F'(u)-\left[\frac{R'_{(i)\,l}(r_0,E)}{R_{(i)\,l}(r_0,E)}+\frac{16\pi G\xi}{D-1}a\tau\right]F(u), \tag{1.99}$$

where $R'_{(i)\,l}(r_0,E)=\partial_r R_{(i)\,l}(r,E)|_{r=r_0}$, and

$$W^{(12)}_l(r)=\sqrt{u^2-1}W\{q^{-\mu}_{iz-1/2}(u),q^{-\mu}_{-iz-1/2}(u)\}, \tag{1.100}$$

with $W\{f(u),g(u)\}$ being the Wronskian for the enclosed functions. In the normalization condition, similar to Eq. (1.9), the integration goes over both the interior and exterior regions. However, the dominant contribution comes from large values of r. By using the asymptotic for the associated Legendre function, similar to the case of the region outside a spherical boundary

with Robin boundary condition, one gets

$$C_\alpha^2=\frac{|\hat{q}_{iz-1/2}^{-\mu}(u_0)|^{-2}|\Gamma(1-iz)|^2}{2\pi^2a^DN(m_k)E(z)|\Gamma(1/2-iz-\mu)|^2}. \tag{1.101}$$

Now substituting the exterior mode functions with the normalization coefficient (1.101) into the mode-sum for the Wightman function, in the exterior region we get the formula

$$\begin{aligned}W(x,x') &= \sum_{l=0}^{\infty}\frac{(2l+n)C_l^{n/2}(\cos\theta)}{2\pi nS_Da^D}\int_0^\infty dz\, z\sinh(\pi z)\\ &\quad\times|\Gamma(iz+\mu+1/2)|^2\frac{y_{iz-1/2}^{-\mu}(u)[y_{iz-1/2}^{-\mu}(u')]^*}{\hat{q}_{iz-1/2}^{-\mu}(u_0)[\hat{q}_{iz-1/2}^{-\mu}(u_0)]^*}\frac{e^{-iE(z)\Delta t}}{E(z)},\end{aligned} \tag{1.102}$$

with the function

$$y_{iz-1/2}^{-\mu}(u)=\hat{q}_{iz-1/2}^{-\mu}(u_0)p_{iz-1/2}^{-\mu}(u)-\hat{p}_{iz-1/2}^{-\mu}(u))q_{iz-1/2}^{-\mu}(u). \tag{1.103}$$

In deriving Eq. (1.102) we have used the relation

$$V_{iz}^{-\mu}(u)=-i\pi\frac{e^{-i\mu\pi}\sinh(\pi z)}{\cos[\pi(iz+\mu)]}y_{iz-1/2}^{-\mu}(u). \tag{1.104}$$

Now by comparing Eq. (1.102) with the expression (1.47) for the corresponding function outside the Robin sphere, we see that Eq. (1.102) differs from Eq. (1.47) by the replacement

$$\beta\to-\frac{R'_{(i)\,l}(r_0,E)}{R_{(i)\,l}(r_0,E)}-\frac{16\pi G\xi}{D-1}a\tau. \tag{1.105}$$

The further evaluation of the Wightman function is similar to that we have given in section 1.1 for the exterior region. The only difference is that, after using the identity (1.49) in the integral representation (1.47), in the rotation of the contours of the integrations we should take into account that now the effective Robin coefficient depends on z through $E=E(z)$ (see Eq. (1.105)). Because of our choice of the interior radial function, the logarithmic derivative in Eq. (1.105) is an even function of the energy and the dependence on z gives no additional difficulties in the evaluation process. As a result, the bubble-induced part in the Wightman function is given by Eq. (1.50) where now, in the notation (1.26), we should make the replacement

$$\beta\to-\frac{R'_{(i)\,l}(r_0,e^{\pi i/2}\sqrt{z^2-z_m^2})}{R_{(i)\,l}(r_0,e^{\pi i/2}\sqrt{z^2-z_m^2})}-\frac{16\pi G\xi}{D-1}a\tau, \tag{1.106}$$

where the second term in the right-hand side is given by Eq. (1.93). With the same replacement in Eqs. (1.70) and (1.85), we obtain the vacuum expectation values of the field squared and the energy-momentum tensor.

Similar to the case of the Robin sphere, in the geometry of the bubble under consideration, the expectation values of the field squared and the energy-momentum tensor diverge on the separating boundary. It can be seen that (see also [94]), because of the dependence of the effective Robin coefficient in Eq. (1.106) on the integration variable z, the leading terms in the asymptotic expansion of the vacuum expectation values over the distance from the boundary vanish and the divergences are weaker compared to the case of the Robin sphere. In particular, the expectation value of the field squared diverges as $(r-r_0)^{2-D}$ and the energy density behaves as $(r-r_0)^{-D}$.

As a simple application of the general results, consider a bubble with the Minkowskian interior with the functions $v(r) = 0$ and $w(r) = \ln r$ in Eq. (1.90). For the surface energy density one finds

$$\tau_0^0 = \frac{D-1}{8\pi G a}\left(1/r_0 - \coth r_0\right), \tag{1.107}$$

and for the stresses we get (no summation over $k = 2, \ldots, D$) $\tau_k^k = (D-2)\tau_0^0/(D-1)$. Note that $-1 < 1/r_0 - \coth r_0 \leqslant 0$ for $\infty > r_0 \geqslant 0$ and the corresponding energy density is always negative. In this special case for the regular radial function in the interior region one has

$$R_{(i)\,l}(r, E) = \frac{\text{const}}{r^{n/2}} J_{l+n/2}(ar\sqrt{E^2 - m^2}), \tag{1.108}$$

with $J_\nu(x)$ being the Bessel function. Hence, the Casimir densities in the region $r > r_0$, induced by the interior Minkowskian geometry are given by Eqs. (1.70) and (1.85), making the replacement

$$\beta \to -\frac{1}{r_0}\left[y\frac{I'_{l+n/2}(y)}{I_{l+n/2}(y)} - \frac{n}{2} + 2\xi(D-1)\left(1 - r_0\coth r_0\right)\right], \tag{1.109}$$

with the notation

$$y = r_0\sqrt{z^2 - z_m^2 + m^2a^2}, \tag{1.110}$$

and with the modified Bessel function $I_\nu(x)$. For the example of a minimally coupled massless scalar field we have checked that there are no bound states in the geometry under consideration.

1.4.2 Bubble of a constant curvature in Minkowski spacetime

Now we consider a background geometry with the line element (1.2) in the region $r < r_0$ and with the Minkowskian spacetime in the region $r > r_0$. The components of the surface

energy-momentum tensor are given by Eq. (1.107) with the opposite signs. In particular, the corresponding energy density is always positive. The Casimir densities in the exterior region are obtained from the general results of [94] for the special interior geometry under consideration.

For the Wightman function one has the decomposition

$$W(x,x') = W_M(x,x') + W_{\rm b}(x,x'), \tag{1.111}$$

where $W_M(x,x')$ is the Wightman function in the Minkowski spacetime and the part

$$\begin{aligned} W_{\rm b}(x,x') &= -\sum_{l=0}^{\infty} \frac{(2l+n)\, C_l^{n/2}(\cos\theta)}{\pi n S_D a^{D-1}\,(rr')^{n/2}} \int_{ma}^{\infty} dz\, z \frac{\tilde{I}_{l+n/2}(zr_0,z)}{\tilde{K}_{l+n/2}(zr_0,z)} \\ &\quad \times \frac{\cosh((\Delta t/a)\sqrt{z^2-m^2a^2})}{\sqrt{z^2-m^2a^2}} K_{l+n/2}(zr) K_{l+n/2}(zr'), \end{aligned} \tag{1.112}$$

is induced by the constant curvature bubble. In Eq. (1.112), we have defined the notation

$$\tilde{F}(y,z) = y\partial_y F(y) - \left[r_0 \sinh r_0 \frac{p^{-\mu'}_{w(z)-1/2}(u_0)}{p^{-\mu}_{w(z)-1/2}(u_0)} + 2\xi(D-1)\,(r_0 \coth r_0 - 1) + \frac{n}{2} \right] F(y), \tag{1.113}$$

with

$$w(z) = \sqrt{z^2 - m^2a^2 + z_m^2}. \tag{1.114}$$

Note that under the condition $z_m^2 \geqslant 0$ the function $w(z)$ is real and the Minkowskian vacuum in the exterior region is stable. The corresponding Casimir densities in the exterior region are obtained from the expressions in [94] by the replacements $\tilde{F}(y) \to \tilde{F}(y,z)$ with Eq. (1.113) and $F = I_{l+n/2}, K_{l+n/2}$.

Appendix A1: On the eigenvalues inside a sphere

As has been shown in section 1.1, the eigenvalues of the quantum number z in the region inside a spherical shell with the boundary condition (1.4) are zeros of the function $\bar{P}^{-\mu}_{iz-1/2}(u)$ for a given value of $u > 1$. The corresponding positive roots we have denoted by z_k, $k = 1, 2, \ldots$. From the relation $\bar{P}^{-\mu}_{iz-1/2}(u) = \bar{P}^{-\mu}_{-iz-1/2}(u)$ it follows that $z = -z_k$ are zeros of the function $\bar{P}^{-\mu}_{iz-1/2}(u)$ as well. Note that the latter can also be written in the form

$$\bar{P}^{-\mu}_{iz-1/2}(u) = (u^2-1)^{D/4} \tilde{p}^{-\mu}_{iz-1/2}(u), \tag{1.115}$$

where, for a given function $F(u)$ we have defined the notation

$$\tilde{F}(u) = AF(u) - \delta_{(j)} \frac{B}{a} \sqrt{u^2-1}\, \partial_u F(u), \tag{1.116}$$

and for the interior region $\delta_{(j)} = 1$. From (1.115) we see that for $u > 1$ the points $z = z_k$ are the zeros of the function $\tilde{p}^{-\mu}_{iz-1/2}(u)$. First of all let us show that these zeros are simple.

By taking into account that the function $R_l(r) = p^{-\mu}_{iz-1/2}(\cosh r)$ is a solution of Eq. (1.14), the following integration formula can be obtained

$$\int_1^u dx\,(x^2-1)^{D/2-1}[p^{-\mu}_{iz-1/2}(x)]^2 = \frac{(u^2-1)^{D/2}}{2z} \times\{[\partial_z p^{-\mu}_{iz-1/2}(u)]\partial_u p^{-\mu}_{iz-1/2}(u) - p^{-\mu}_{iz-1/2}(u)\partial_z\partial_u p^{-\mu}_{iz-1/2}(u)\}. \tag{1.117}$$

From here, for $z = z_k$ one gets

$$\int_1^u dx\,(x^2-1)^{D/2-1}[p^{-\mu}_{iz-1/2}(x)]^2 = \frac{(u^2-1)^{(D-1)/2}}{2zB_1/a} p^{-\mu}_{iz-1/2}(u)\partial_z\tilde{p}^{-\mu}_{iz-1/2}(u)|_{z=z_k}. \tag{1.118}$$

The left-hand side of this relation is positive (recall that $p^{-\mu}_{iz-1/2}(x)$ is a real function) and, hence, $\partial_z\tilde{p}^{-\mu}_{iz-1/2}(u)|_{z=z_k} \neq 0$. This shows that the zeros z_k are simple.

The asymptotic expression for large positive zeros is found by using the asymptotic formula

$$P^{-\mu}_{iz-1/2}(u) \sim \sqrt{\frac{2}{\pi}}\frac{z^{-\mu-1/2}}{\sqrt{u^2-1}}\sin(z\,\mathrm{arccosh}\,u - \pi\mu/2 + \pi/4)(1+O(1/z^2)), \tag{1.119}$$

for $z \gg 1$. From here we see that

$$z_k \approx \pi\frac{2k+\mu+1/2-\delta_{0B}}{2\,\mathrm{arccosh}\,u} + O(1/k). \tag{1.120}$$

Now let us discuss possible purely imaginary zeros. With fixed u and l, the function $\bar{P}^{-\mu}_{iz-1/2}(u)$ has no purely imaginary zeros for sufficiently small values of the ratio $\beta = Aa/B$. With increasing β, started from some critical value $\beta^{(1)}_l(u)$, a pair of purely imaginary zeros $z = \pm i\eta$, $\eta > 0$, appears. The critical value $\beta^{(1)}_l(u)$ increases with increasing l and, hence, the purely imaginary zero first appears for the mode $l = 0$ (see the left panel of figure 1, where in the case $D = 3$ the critical value is plotted versus $r_0 = \mathrm{arccosh}\,u$ for different values of l). By taking into account that for $r \gg 1$ one has

$$P^{-\mu}_{z-1/2}(\cosh r) \approx \frac{\Gamma(z)e^{(z-1/2)r}}{\sqrt{\pi}\Gamma(1/2+z+\mu)}, \tag{1.121}$$

it is seen that for large values of u we have $\eta \approx \beta + (D-1)/2$ and $\beta^{(1)}_l(u) \to -(D-1)/2$ for $u \to \infty$. There are no purely imaginary zeros for $\beta < -(D-1)/2$. With the further increase of $\beta > \beta^{(1)}_l(u)$ the value of η increases and for the second critical value $\beta = \beta^{(2)}_l(u)$ the energy of the corresponding mode becomes zero. This corresponds to $\eta = z_m$. For $\beta > \beta^{(2)}_l(u)$ the energy of the mode becomes imaginary which signals the instability of the vacuum.

Appendix B1: Summation formula

In this appendix, by making use of the generalized Abel-Plana formula [276] (see also, [67, 68]), we derive a summation formula for the series over the zeros of the function

$$\bar{P}^{-\mu}_{iz-1/2}(u) = A(u)P^{-\mu}_{iz-1/2}(u) + B(u)\partial_u P^{-\mu}_{iz-1/2}(u), \tag{1.122}$$

with respect to z, for given $u > 1$ and $\mu \geqslant 0$. In general, the functions $A(u)$ and $B(u)$ can be different from those in Eq. (1.27). We shall denote the positive zeros, arranged in ascending order, by z_k, $k = 1, 2, \ldots$, assuming that they are simple. The summation formula can be obtained in a way similar to that used in Ref. [269] for the special case $A(u) = 1$ and $B(u) = 0$ and we shall outline the main steps only (for the summation formula over the zeros of the combination of the associated Legendre functions of the first and second kinds see [277]).

We substitute in the generalized Abel-Plana formula

$$\begin{aligned} f(z) &= \sinh(\pi z)h(z), \\ g(z) &= \frac{e^{i\mu\pi}h(z)}{\pi i\bar{P}^{-\mu}_{iz-1/2}(u)} \sum_{j=\pm} \cos[\pi(\mu - jiz)]\bar{Q}^{-\mu}_{jiz-1/2}(u), \end{aligned} \tag{1.123}$$

where the function $h(z)$ is analytic in the right-half plane of the complex variable $z = x + iy$. The function $g(z)$ has simple poles at $z = z_k$. For functions obeying the condition

$$|h(z)| < \varepsilon(x)\exp(cy\,\mathrm{arccosh}\,u),\ |z| \to \infty, \tag{1.124}$$

with $c < 2$, $\varepsilon(x)e^{\pi x} \to 0$ for $x \to +\infty$, the following formula is obtained

$$\begin{aligned} \sum_{k=1}^{\infty} T_\mu(z_k, u)h(z_k) = \frac{e^{-i\mu\pi}}{2}\int_0^\infty dx\ \sinh(\pi x)h(x) \\ -\frac{1}{2\pi}\int_0^\infty dx\,\frac{\bar{Q}^{-\mu}_{x-1/2}(u)}{\bar{P}^{-\mu}_{x-1/2}(u)}\cos[\pi(\mu + x)]\sum_{j=\pm} h(xe^{j\pi i/2}). \end{aligned} \tag{1.125}$$

Here we have introduced the notation

$$T_\mu(z, u) = \frac{\bar{Q}^{-\mu}_{iz-1/2}(u)}{\partial_z\bar{P}^{-\mu}_{iz-1/2}(u)}\cos[\pi(\mu - iz)]. \tag{1.126}$$

Formula (1.125) is also valid for some functions having branch-points on the imaginary axis, for example, in the case of functions of the form $h(z) = F(z)/(z^2 + z_0^2)^{1/2}$, with $F(z)$ being

an analytic function. Note that, in the physical problem we have considered the branch points correspond to $z = \pm iz_m$. Adding the corresponding residue terms in the right-hand side, the formula (1.125) can be generalized for functions $h(z)$ having poles in the right-half plane.

An equivalent expression for $T_\mu(z,u)$ is obtained by using the relation

$$\bar{Q}^{-\mu}_{iz-1/2}(u) = \frac{B(u)e^{-i\mu\pi}\Gamma(iz-\mu+1/2)}{\Gamma(iz+\mu+1/2)(1-u^2)P^{-\mu}_{iz-1/2}(u)}, \tag{1.127}$$

with $z = z_k$. This formula follows from the Wronskian relation for the associated Legendre functions. Now, from Eq. (1.126) for $z = z_k$ one gets

$$T_\mu(z,u) = \frac{\pi e^{-i\mu\pi}B(u)|\Gamma(\mu+iz+1/2)|^{-2}}{(1-u^2)P^{-\mu}_{iz-1/2}(u)\partial_z\bar{P}^{-\mu}_{iz-1/2}(u)}. \tag{1.128}$$

Formula (1.125) can be generalized for the case when the function $\bar{P}^{-\mu}_{iz-1/2}(u)$ has purely imaginary zeros at the points $z = \pm iy_k$, $y_k > 0$, $k = 1, 2, \ldots$, under the assumption that the function $h(z)$ obeys the condition

$$h(z) = -h(ze^{-\pi i}) + o(z - iy_k),\ z \to iy_k. \tag{1.129}$$

Assuming that the zeros are simple, in this case, on the right-hand side of Eq. (1.125) we have to add the term

$$-i\sum_k \frac{\bar{Q}^{-\mu}_{y-1/2}(u)}{\partial_y\bar{P}^{-\mu}_{y-1/2}(u)}\cos[\pi(\mu-y)]h(iy)|_{y=y_k}, \tag{1.130}$$

at these poles and take the principal value of the second integral on the right-hand side. The latter exists due to the condition (1.129). By using the relation (1.127) the term (1.130) can also be written in the form

$$i\sum_k \frac{\pi B(u)e^{-i\mu\pi}}{P^{-\mu}_{y-1/2}(u)\partial_y\bar{P}^{-\mu}_{y-1/2}(u)}\frac{(u^2-1)^{-1}h(iy)}{\Gamma(\mu+y+1/2)\Gamma(\mu-y+1/2)}|_{y=y_k}. \tag{1.131}$$

A physical example with purely imaginary modes using this result is discussed in section 1.1.

1.5 Summary

In this chapter we have investigated the properties of the scalar vacuum in a constant negative curvature space induced by a spherical boundary on which the field operator obeys Robin boundary condition. General values of the spatial dimension and of the curvature coupling

parameter are considered. For the coefficient in the Robin boundary condition there is a critical value above which the scalar vacuum becomes unstable. The properties of the quantum vacuum are encoded in two-point functions. We have considered the positive-frequency Wightman function and the other function can be evaluated in a similar way. In order to evaluate the Wightman function we employed the direct summation over the complete set of modes. In the region inside the sphere, the eigenmodes of the field are expressed in terms of the zeros of the combination of the associated Legendre function and its derivative with respect to the order (see Eq. (1.25)). In the mode-sum for the Wightman function, for the summation of the series over these zeros we have used the formula (1.125), derived from the generalized Abel-Plana formula. This allowed us to separate the part corresponding to the boundary-free geometry and to present the sphere-induced part in terms of a rapidly convergent integral. In this form the explicit knowledge of the eignemodes is not required. In addition, with the decomposition into the boundary-free and boundary-induced contributions, the renormalization of the vacuum expectation values in the coincidence limit is reduced to the one for the boundary-free geometry. We have provided a similar decomposition for the exterior region as well.

As an important local characteristic of the vacuum state, in section 1.2 we consider the vacuum expectation value of the field squared. The corresponding expressions for the sphere-induced parts in the interior and exterior regions are given by Eqs. (1.60) and (1.70). These parts are negative for Dirichlet boundary condition and positive for Neumann boundary condition. The expectation value of the field squared diverges on the boundary. The leading term in the asymptotic expansion over the distance from the sphere is given by Eq. (1.63) and coincides with that for a sphere in Minkowski bulk. In this limit the dominant contribution comes from the wavelengths smaller than the curvature radius of the background and the effects of the gravitational field are small. In the opposite limit of large distances, the effects of gravity are decisive. The asymptotic behavior in this region depends on whether the parameter z_m, defined by Eq. (1.16), is zero or not. For $z_m > 0$, the leading term is given by Eq. (1.72) and the boundary-induced vacuum expectation value is exponentially suppressed. For $z_m = 0$ the leading term is given by Eq. (1.73). The decay in this case is again exponential, though relatively weaker. Consequently, for both massive and massless fields the suppression of the

boundary-induced vacuum expectation values at large distances is exponential. This is in contrast to the case of Minkowskian bulk, where the decay for massless fields has a power-law behavior.

Another important characteristic of the vacuum is the vacuum expectation value of the energy-momentum tensor. This expectation value is diagonal and the expressions for the sphere-induced contributions are given by Eqs. (1.76) and (1.85) for the interior and exterior regions, respectively. Near the sphere, the leading term in the energy density and parallel stresses is given by Eq. (1.80). Once again, this term coincides with the corresponding asymptotic for a spherical shell in flat spacetime. For the leading term in the normal stress one has the expression (1.81) and the corresponding divergence is weaker. The asymptotics at large distances are given by Eqs. (1.86) and (1.88) for the cases $z_m > 0$ and $z_m = 0$, respectively. In both cases the vacuum expectation values are suppressed by the factor $e^{-(2z_m+D-1)r}$. At large distances and for non-conformally coupled fields one has $|\langle T_1^1\rangle_{\rm s}| \gg |\langle T_0^0\rangle_{\rm s}|$. Again, in contrast to the Minkowskian case, the expectation values are exponentially suppressed for both massive and massless fields. This feature is observed also in the Casimir problems on the background of anti-de Sitter spacetime, which presents another example of a negative curvature space. In de Sitter spacetime, having a positive curvature, the situation is opposite: at large distances from the boundary the local vacuum expectation values for both massive and massless fields exhibit a power-law behavior.

We have generalized the results for the vacuum expectation values to the backgrounds described by two distinct spherically symmetric metric tensors in the regions separated by a spherical boundary. The geometry of one region affects the properties of the vacuum in the other region leading to the gravitationally induced Casimir effect. We have considered the interior geometry described by the line element (1.90) and the exterior geometry, as before, corresponds to a constant curvature space. In addition, we have assumed the presence of the surface energy-momentum tensor located on the separating boundary. The corresponding jump conditions on the normal derivatives of the metric tensor are obtained from the Israel matching conditions, whereas the boundary conditions on the field operator are obtained from the field equation. In this way, we have shown that the bubble-induced contributions in the Wightman

function and in the vacuum expectation values of the field squared and the energy-momentum tensor are obtained from the expressions for the spherical shell with Robin boundary condition by the replacement (1.106) of the coefficient. As an example of the exterior geometry we have considered the case of the Minkowskian bubble. In this case the replacement needed is given by Eq. (1.109). Note that in the geometry with bubbles the divergences on the boundary are weaker compared with the case of the Robin sphere. We have also considered a bubble with a negative constant curvatures space in the Minkowski bulk. The corresponding expressions for the local characteristics are obtained from the general formulas in [94] with the notation with tilde defined by Eq. (1.113).

The generalization of the results given above for the Friedmann-Robertson-Walker cosmological models with a time-dependent scale factor is straightforward in the case of a conformally coupled massless field. This requires the replacement $a \to a(t)$ in the expressions for the Wightman function and for the vacuum expectation values. In the special case $D = 2$, the results obtained can be applied to negatively curved graphene structures (for this type of structures see [80]), described in the long-wavelength regime by an effective 3-dimensional relativistic field theory. The latter, in addition to the well-known Dirac fermions describing the low-energy excitations of the electronic subsystem, involves scalar and gauge fields originating from the elastic properties and describing disorder phenomena, like the distortions of the graphene lattice and structural defects. In this setup, the spherical boundary models the edge of a negatively curved graphene sheet. The boundary condition we have used ensures the zero flux of a scalar field through the boundary.

2 CHAPTER: VACUUM CURRENT DENSITIES IN TOPOLOGICALLY NONTRIVIAL SPACES

The Hadamard function and the VEV of the current density are investigated for a charged scalar field in the geometry of flat boundaries with an arbitrary number of toroidally compactified spatial dimensions. The field operator obeys the Robin conditions on the boundaries and quasiperiodicity conditions with general phases along compact dimensions. In addition, the presence of a constant gauge field is assumed. The latter induces Aharonov-Bohm-type effect on the VEVs. There is a region in the space of the parameters in Robin boundary conditions where the vacuum state becomes unstable. The stability condition depends on the lengths of compact dimensions and is less restrictive than that for background with trivial topology. The vacuum current density is a periodic function of the magnetic flux, enclosed by compact dimensions, with the period equal to the flux quantum. It is explicitly decomposed into the boundary-free and boundary-induced contributions. In sharp contrast to the VEVs of the field squared and the energy-momentum tensor, the current density does not contain surface divergences. Moreover, for Dirichlet condition it vanishes on the boundaries. The normal derivative of the current density on the boundaries vanish for both Dirichlet and Neumann conditions and is nonzero for general Robin conditions. When the separation between the plates is smaller than other length scales, the behavior of the current density is essentially different for non-Neumann and Neumann boundary conditions. In the former case, the total current density in the region between the plates tends to zero. For Neumann boundary condition on both plates, the current density is dominated by the interference part and is inversely proportional to the separation.

2.1 Formulation of the problem and the Hadamard function

Compact spatial dimensions appear in a number of models in high-energy physics (Kaluza-Klein type models, supergravity, string theories) and in condensed matter physics (carbon nanotubes and nanoloops, topological insulators). In this chapter we consider the simplest case of toroidal compactification that does not change the local geometrical characteristics. Namely,

we consider $(D+1)$-dimensional flat spacetime with coordinates $(x^0, x^1, \ldots, x^D)$ having a spatial topology $R^{p+1} \times T^q$, $p+q+1=D$, where T^q stands for a q-dimensional torus (for a review of quantum field-theoretical effects in toroidal topology see [103]). The set of coordinates in the uncompactified subspace R^{p+1} will be denoted by $\mathbf{x}_{p+1} = (x^1, ..., x^{p+1})$ and for the compactified coordinates we denote $\mathbf{x}_q = (x^{p+2}, ..., x^D)$. One has $-\infty < x^l < \infty$ for $l = 1, .., p$, and $0 \leqslant x^l \leqslant L_l$ for $l = p+2, ..., D$, where L_l is the length of the lth compact dimension.

We are interested in the VEV of the current density for a quantum scalar field $\varphi(x)$. The mass and the charge of the field quanta will be denoted by m and e, respectively. In the presence of an abelian gauge field A_μ the field equation reads

$$\left(g^{\mu\nu} D_\mu D_\nu + m^2\right) \varphi = 0, \tag{2.1}$$

where $g^{\mu\nu} = \mathrm{diag}(1, -1, \ldots, -1)$ and $D_\mu = \partial_\mu + ieA_\mu$ is the gauge extended derivative. The background geometry is flat and the related Ricci scalar becomes zero, $\mathcal{R} = 0$. Consequently, the nonminimal curvature coupling term is absent in (2.1). We assume the presence of two parallel flat boundaries placed at $x^{p+1} = a_1$ and $x^{p+1} = a_2$. On the boundaries the field obeys Robin boundary conditions (compare with (1.4))

$$(1 + \beta_j n_j^\mu D_\mu)\varphi(x) = 0, \quad x^{p+1} \equiv z = a_j, \tag{2.2}$$

with constant coefficients β_j, $j = 1, 2$, and with n_j^μ being the inward pointing normal to the boundary at $x^{p+1} = a_j$. Here, for the further convenience we have introduced a special notation $z = x^{p+1}$ for the $(p+1)$th spatial dimension. Note that Robin boundary conditions in the form (2.2) are gauge invariant (for the discussion of various types of gauge invariant boundary conditions see [72]). In what follows we will consider the region between the plates, $a_1 \leqslant z \leqslant a_2$. For this region one has $n_j^\mu = (-1)^{j-1}\delta_{p+1}^\mu$. The expressions for the VEVs in the regions $z \leqslant a_1$ and $z \geqslant a_2$ are obtained by the limiting transitions. The results for Dirichlet and Neumann boundary conditions are obtained from those for the condition (2.2) in the limits $\beta_j \to 0$ and $\beta_j \to \infty$, $A_\mu = 0$, respectively.

In addition to the boundary conditions on the plates, for the theory to be completely defined, we should also specify the periodicity conditions along the compact dimensions. Different conditions correspond to topologically inequivalent field configurations [278]. Here, we consider

generic quasiperiodicity conditions,

$$\varphi(t,x^1,\ldots,x^l+L_l,\ldots,x^D)=e^{i\alpha_l}\varphi(t,x^1,\ldots,x^l,\ldots,x^D), \tag{2.3}$$

with constant phases α_l, $l=p+2,\ldots,D$. The special cases of the condition (2.3) with $\alpha_l=0$ and $\alpha_l=\pi$ correspond to the most frequently discussed cases of untwisted and twisted scalar fields, respectively. As it will be seen below, one of the effects of nontrivial phases in (2.3) is the appearance of nonzero vacuum currents along compact dimensions (for a discussion of physical effects of phases in periodicity conditions along compact dimensions see [279]-[285] and references therein).

For a scalar field, the operator of the current density is given by the expression

$$j_\mu(x)=ie[\varphi^+(x)D_\mu\varphi(x)-(D_\mu\varphi(x))^+\varphi(x)], \tag{2.4}$$

where the cross stands for the hermitian conjugate. Its VEV is obtained from the Hadamard function

$$G(x,x')=\langle 0|\varphi(x)\varphi^+(x')+\varphi^+(x')\varphi(x)|0\rangle, \tag{2.5}$$

with $|0\rangle$ being the vacuum state, by using the formula

$$\langle 0|j_\mu(x)|0\rangle\equiv\langle j_\mu(x)\rangle=\frac{i}{2}e\lim_{x'\to x}(\partial_\mu-\partial'_\mu+2ieA_\mu)G(x,x'). \tag{2.6}$$

In the discussion below we will assume a constant gauge field A_μ. Though the corresponding field strength vanishes, the nontrivial topology of the background spacetime leads to the Aharonov-Bohm-like effects on physical observables. A constant gauge field A_μ can be excluded from the field equation and from the expression for the VEV of the current density by the gauge transformation $A_\mu=A'_\mu+\partial_\mu\chi$, $\varphi(x)=e^{-ie\chi}\varphi'(x)$, with the function $\chi=A_\mu x^\mu$. In the new gauge one has $A'_\mu=0$. However, unlike to the case of trivial topology, here the constant vector potential does not completely disappear from the problem. It appears in the periodicity conditions for the new field operator:

$$\varphi'(t,x^1,\ldots,x^l+L_l,\ldots,x^D)=e^{i\tilde{\alpha}_l}\varphi'(t,x^1,\ldots,x^l,\ldots,x^D), \tag{2.7}$$

where now the phases are given by the expression

$$\tilde{\alpha}_l=\alpha_l+eA_lL_l. \tag{2.8}$$

In the discussion below we shall consider the problem in the gauge $(\varphi'(x), A'_\mu = 0)$ omitting the prime. For this gauge, in (2.1), (2.2), (2.4) one has $D_\mu = \partial_\mu$ and in the expressions (2.6) the term with the vector potential is absent.

As it is seen from (2.8), the presence of a constant gauge field is equivalent to the shift in the phases of the periodicity conditions along compact dimensions. The shift in the phase is expressed in terms of the magnetic flux Φ_l enclosed by the lth compact dimension as

$$eA_l L_l = -e\mathbf{A}_l L_l = -2\pi\Phi_l/\Phi_0, \tag{2.9}$$

where $\Phi_0 = 2\pi/e$ is the flux quantum and $\mathbf{A}_l$ is the lth component of the spatial vector $\mathbf{A} = (-A_1, \ldots, -A_D)$. In the discussion below the physical effects of a constant gauge field will appear through the phases $\tilde{\alpha}_l$. In particular, the VEVs of physical observables are periodic functions of these phases with the period 2π. In terms of the magnetic flux, this corresponds to the periodicity of the VEVs, as functions of the magnetic flux, with the period equal to the flux quantum.

Expanding the field operator in terms of the annihilation and creation operators, in a way similar to that for (1.8), the expression of the Hadamard function is preented in the form

$$G(x, x') = \sum_{\mathbf{k}} \sum_{s=\pm} \varphi_{\mathbf{k}}^{(s)}(x) \varphi_{\mathbf{k}}^{(s)*}(x'), \tag{2.10}$$

where $\varphi_{\mathbf{k}}^{(\pm)}(x)$ form a complete set of normalised positive- and negative-energy solutions to the classical field equation obeying the boundary conditions of the model. In the region between the plates, introducing the wave vectors $\mathbf{k}_p = (k_1, \ldots, k_p)$ and $\mathbf{k}_q = (k_{p+2}, \ldots, k_D)$, these mode functions can be written in the form

$$\varphi_{\mathbf{k}}^{(\pm)}(x) = C_{\mathbf{k}} \cos\left[k_{p+1}\left(z - a_j\right) + \gamma_j(k_{p+1})\right] e^{i\mathbf{k}_\parallel \cdot \mathbf{x}_\parallel \mp i\omega_{\mathbf{k}} t}, \tag{2.11}$$

where $\mathbf{k}_\parallel = (\mathbf{k}_p, \mathbf{k}_q)$, $\mathbf{k} = (\mathbf{k}_p, k_{p+1}, \mathbf{k}_q)$, $\omega_{\mathbf{k}} = \sqrt{\mathbf{k}^2 + m^2}$, and $\mathbf{x}_\parallel$ stands for the coordinates parallel to the plates. For the momentum components along the dimensions x^i, $i = 1, \ldots, p$, one has $-\infty < k_i < +\infty$, whereas the components along the compact dimensions are quantized by the periodicity conditions (2.7):

$$k_l = \frac{2\pi n_l + \tilde{\alpha}_l}{L_l}, \quad n_l = 0, \pm 1, \pm 2, \ldots, \tag{2.12}$$

with $l = p+2, ..., D$. We will denote by ω_0 the smallest value for the energy in the compact subspace, $\sqrt{\mathbf{k}_q^2 + m^2} \geqslant \omega_0$. Assuming that $|\tilde{\alpha}_l| \leqslant \pi$, we have

$$\omega_0 = \sqrt{\sum_{l=p+2}^{D} \tilde{\alpha}_l^2/L_l^2 + m^2}. \tag{2.13}$$

This quantity can be considered as the effective mass for the field quanta.

Now we should impose on the modes (2.11) the boundary conditions (2.2) with $D_\mu = \partial_\mu$. From the boundary condition on the plate at $z = a_j$, for the function $\gamma_j(k_{p+1})$ in (2.11) one gets

$$e^{2i\gamma_j(k_{p+1})} = \frac{ik_{p+1}\beta_j(-1)^j + 1}{ik_{p+1}\beta_j(-1)^j - 1}. \tag{2.14}$$

The boundary condition on the second plate determines the eigenvalues for k_{p+1}. They are solutions of the transcendental equation

$$e^{2iy} = \frac{1 + ib_2 y}{1 - ib_2 y}\frac{1 + ib_1 y}{1 - ib_1 y}, \tag{2.15}$$

where we have defined

$$y = k_{p+1}a, \ b_j = \beta_j/a, \tag{2.16}$$

and $a = a_2 - a_1$ is the separation between the plates. In terms of dimensionless quantity y, equation (2.15) is rewritten in the form

$$\left(1 - b_1 b_2 y^2\right)\sin y - (b_2 + b_1) y \cos y = 0. \tag{2.17}$$

Unlike to the cases of Dirichlet and Neumann conditions, for Robin boundary condition the eigenvalues of k_{p+1} are given implicitly, as solutions of the equation (2.17). The latter has an infinite number of positive roots which will be denoted by $y = \lambda_n$, $n = 1, 2, \ldots$, and for the corresponding eigenvalues of k_{p+1} one has $k_{p+1} = \lambda_n/a$. For $b_j \leqslant 0$ or $\{b_1 + b_2 \geqslant 1, b_1 b_2 \leqslant 0\}$ there are no other roots in the right-half plane of a complex variable y, $\mathrm{Re}\, y \geqslant 0$ (see [273]). In the remaining region of the plane (b_1, b_2), the equation (2.17) has purely imaginary roots $\pm iy_l$, $y_l > 0$. Depending on the values of b_j, the number of y_l can be one or two. In the presence of purely imaginary roots, under the condition $\omega_0 < y_l$, there are modes of the field for which the energy $\omega_{\mathbf{k}}$ becomes imaginary. This would lead to the instability of the vacuum state. In the discussion below we will assume that $\omega_0 > y_l$. Note that in the corresponding problem

on background of spacetime with trivial topology the stability condition is written as $m > y_l$. Now, by taking into account that $\omega_0 > m$, we conclude that the compactification, in general, enlarges the stability range in the space of parameters of Robin boundary conditions.

Having specified the parameters in the mode functions, it remains to determine the coefficient $C_{\mathbf{k}}$ in (2.11). It is found from the orthonormalization condition

$$\int d^D x \varphi_{\mathbf{k}}^{(\lambda)}(x) \varphi_{\mathbf{k}'}^{(\lambda')*}(x) = \frac{\delta_{\lambda\lambda'}}{2\omega_{\mathbf{k}}} \delta(\mathbf{k}_p - \mathbf{k}'_p) \delta_{nn'} \delta_{n_{p+2},n'_{p+2}} .... \delta_{n_D,n'_D}, \tag{2.18}$$

with the integration over x^{p+1} in the region between the plates. Substituting the functions (2.11), after the standard integrations, one gets

$$|C_{\mathbf{k}}|^2 = \frac{\{1 + \cos[y + 2\tilde{\gamma}_j(y)] \sin(y)/y\}^{-1}}{(2\pi)^p a V_q \omega_{\mathbf{k}}}, \tag{2.19}$$

where y is a root of the equation (2.17) and $V_q = L_{p+1}....L_D$ is the volume of the compact subspace. The function $\tilde{\gamma}_j(y)$ is defined by the relation

$$e^{2i\tilde{\gamma}_j(y)} = \frac{iyb_j - 1}{iyb_j + 1}. \tag{2.20}$$

First we shall consider the case when all the roots of (2.17) are real and $y = \lambda_n$.

Substituting the modes $\varphi_{\mathbf{k}}^{(\pm)}(x)$ in the mode-sum (2.10), the expression for the Hadamard function takes in the form

$$\begin{aligned} G(x,x') &= \frac{1}{aV_q} \int \frac{d\mathbf{k}_p}{(2\pi)^p} \sum_{\mathbf{n}_q} \sum_{n=1}^{\infty} \frac{1}{\omega_{\mathbf{k}}} g_j(z, z', \lambda_n/a) \\ &\times \frac{\lambda_n \cos(\omega_{\mathbf{k}} \Delta t) e^{i\mathbf{k}_p \cdot \Delta \mathbf{x}_p + i\mathbf{k}_q \cdot \Delta \mathbf{x}_q}}{\lambda_n + \cos\left[\lambda_n + 2\tilde{\gamma}_j(\lambda_n)\right] \sin \lambda_n}, \end{aligned} \tag{2.21}$$

where $\Delta \mathbf{x}_p = \mathbf{x}_p - \mathbf{x}'_p$, $\Delta \mathbf{x}_q = \mathbf{x}_q - \mathbf{x}'_q$, $\Delta t = t - t'$, and $\mathbf{n}_q = (n_{p+2}, \ldots, n_D)$, $-\infty < n_l < +\infty$. In (2.21), the energy for the mode with a given $\mathbf{k}$ is written as

$$\omega_{\mathbf{k}} = \sqrt{\mathbf{k}_p^2 + \lambda_n^2/a^2 + \omega_{\mathbf{n}_q}^2}, \tag{2.22}$$

and

$$\omega_{\mathbf{n}_q} = \sqrt{\mathbf{k}_q^2 + m^2}, \ \mathbf{k}_q^2 = \sum_{l=p+2}^{D} \left(\frac{2\pi n_l + \tilde{\alpha}_l}{L_l} \right)^2. \tag{2.23}$$

The summation over $\mathbf{n}_q$ is understood as $\sum_{\mathbf{n}_q} = \sum_{n_{p+2}=-\infty}^{+\infty} \cdots \sum_{n_D=-\infty}^{+\infty}$. In (2.21) and in what follows we use the notation

$$g_j(z, z', u) = \cos(u\Delta z) + \frac{1}{2} \sum_{s=\pm 1} e^{siy|z+z'-2a_j|} \frac{iu\beta_j - s}{iu\beta_j + s}. \tag{2.24}$$

Note that $g_j(z,z',-y)=g_j(z,z',y)$ and $g_j(z,z',0)=0$.

The eigenvalues λ_n are given implicitly and the expression (2.21) is not convenient for the evaluation of the VEVs. In order to obtain an expression in which the explicit knowledge of λ_n is not required, we apply to the series over n the Abel-Plana-type summation formula [273, 68]

$$\sum_{n=1}^{\infty}\frac{\pi\lambda_n f(\lambda_n)}{\lambda_n+\cos[\lambda_n+2\tilde{\gamma}_j(\lambda_n)]\sin\lambda_n} = -\frac{\pi f(0)/2}{1-b_2-b_1}+\int_0^{\infty}duf(u) +i\int_0^{\infty}du\frac{f(iu)-f(-iu)}{c_1(u)c_2(u)e^{2u}-1}, \tag{2.25}$$

where, for the further convenience, the notation

$$c_j(u)=\frac{b_ju-1}{b_ju+1} \tag{2.26}$$

is introduced. In (2.25) we have assumed that $b_j\leqslant 0$. The changes in the evaluation procedure in the case $b_j>0$ will be discussed below. In order to evaluate the series in (2.21), we take in the summation formula

$$f(\lambda_n)=\frac{\cos(\omega_{\mathbf{k}}\Delta t)}{\omega_{\mathbf{k}}}g_j(z,z',\lambda_n/a). \tag{2.27}$$

For this function one has $f(0)=0$ and the first term in the right-hand side of (2.25) becomes zero.

Applying the summation formula (2.25) with (2.27), the Hadamard function is decomposed into the following separate contributions:

$$G(x,x') = G_j(x,x')+\frac{2}{\pi V_q}\int\frac{d\mathbf{k}_p}{(2\pi)^p}\sum_{\mathbf{n}_q}\int_{a\omega_{\mathbf{k}_\parallel}}^{\infty}du\,g_j(z,z',iu/a) \times\frac{e^{i\mathbf{k}_p\cdot\Delta\mathbf{x}_p+i\mathbf{k}_q\cdot\Delta\mathbf{x}_q}}{c_1(u)c_2(u)e^{2u}-1}\frac{\cosh(\Delta t\sqrt{u^2/a^2-\omega_{\mathbf{k}_\parallel}^2})}{\sqrt{u^2-a^2\omega_{\mathbf{k}_\parallel}^2}}, \tag{2.28}$$

where $\omega_{\mathbf{k}_\parallel}=\sqrt{\mathbf{k}_p^2+\omega_{\mathbf{n}_q}^2}$. The first term in the right-hand side, given by

$$G_j(x,x') = \frac{1}{\pi V_q}\int\frac{d\mathbf{k}_p}{(2\pi)^p}\sum_{\mathbf{n}_q}e^{i\mathbf{k}_p\cdot\Delta\mathbf{x}_p+i\mathbf{k}_q\cdot\Delta\mathbf{x}_q} \times\int_0^{\infty}dk_{p+1}\frac{\cos(\omega_{\mathbf{k}}\Delta t)}{\omega_{\mathbf{k}}}g_j(z,z',k_{p+1}), \tag{2.29}$$

comes from the first integral in the right-hand side of (2.25) and corresponds to the Hadamard function in the geometry of a single plate at $x^{p+1}=a_j$ when the second plate is absent. This

follows from the fact that the last term in 2.28 tends to zero for a fixed location $z = a_j$ of the plate when the location of the second plate tends to infinity.

The Hadamard function (2.29) is further decomposed by taking into account that the part in (2.24) coming from the first term in the right-hand side of (2.24),

$$G_0(x,x') = \frac{1}{V_q}\int \frac{d\mathbf{k}_{p+1}}{(2\pi)^{p+1}} \sum_{\mathbf{n}_q} e^{i\mathbf{k}_{p+1}\cdot\Delta\mathbf{x}_{p+1}+i\mathbf{k}_q\cdot\Delta\mathbf{x}_q}\frac{\cos(\omega_{\mathbf{k}}\Delta t)}{\omega_{\mathbf{k}}}, \tag{2.30}$$

is the corresponding function for the boundary-free geometry. After the integration over the components of the momentum along uncompactified dimensions, this function can be presented in the form

$$G_0(x,x') = \frac{2V_q^{-1}}{(2\pi)^{p/2+1}} \sum_{\mathbf{n}_q} e^{i\mathbf{k}_q\cdot\Delta\mathbf{x}_q}\omega_{\mathbf{n}_q}^p f_{p/2}(\omega_{\mathbf{n}_q}\sqrt{|\Delta\mathbf{x}_{p+1}|^2-(\Delta t)^2}), \tag{2.31}$$

with the notations

$$f_\nu(x) = K_\nu(x)/x^\nu, \tag{2.32}$$

where $K_\nu(x)$ is the Macdonald function.

Consequently, the Hadamard function in the geometry of a single plate is written as

$$\begin{aligned} G_j(x,x') &= G_0(x,x') + \frac{1}{2\pi V_q}\int \frac{d\mathbf{k}_p}{(2\pi)^p}\sum_{\mathbf{n}_q} e^{i\mathbf{k}_p\cdot\Delta\mathbf{x}_p+i\mathbf{k}_q\cdot\Delta\mathbf{x}_q} \\ &\times \sum_{s=\pm 1}\int_0^\infty dk_{p+1}\frac{\cos(\omega_{\mathbf{k}}\Delta t)}{\omega_{\mathbf{k}}} e^{sik_{p+1}|z+z'-2a_j|}\frac{ik_{p+1}\beta_j - s}{ik_{p+1}\beta_j + s}, \end{aligned} \tag{2.33}$$

where the second term in the right-hand side is induced by the presence of the plate at $x^{p+1} = a_j$. For the further transformation of the boundary-induced part in (2.33) we rotate the integration contour over k_{p+1} by the angle $s\pi/2$. In the summation over s the integrals over the intervals $(0, \pm i\omega_{\mathbf{k}_\parallel})$ cancel each other and we get

$$\begin{aligned} G_j(x,x') &= G_0(x,x') + \frac{1}{\pi V_q}\int \frac{d\mathbf{k}_p}{(2\pi)^p}\sum_{\mathbf{n}_q} e^{i\mathbf{k}_p\cdot\Delta\mathbf{x}_p+i\mathbf{k}_q\cdot\Delta\mathbf{x}_q} \\ &\times \int_{\omega_{\mathbf{k}_\parallel}}^\infty du \frac{\cosh(\Delta t\sqrt{u^2-\omega_{\mathbf{k}_\parallel}^2})}{\sqrt{u^2-\omega_{\mathbf{k}_\parallel}^2}}\frac{u\beta_j+1}{u\beta_j-1}e^{-u|z+z'-2a_j|}. \end{aligned} \tag{2.34}$$

This expression is well suited for the investigation of the current density. With the representation (2.34), the Hadamard function in the region between the plates, given by (2.28), is

decomposed into the boundary-free, single plate-induced and second plate-induced contributions. An alternative expression for the Hadamard function is obtained in Appendix A2.

In deriving (2.28) and (2.34) we have assumed that $\beta_j \leqslant 0$. In the case $\beta_j > 0$, the quantum scalar field in the geometry of a single plate at $z = a_j$ has modes with $k_{p+1} = i/\beta_j$ for which the dependence on the coordinate x^{p+1} has the form e^{-z_j/β_j}. In the case $1/\beta_j > \omega_0$, for a part of these modes the energy is imaginary and the vacuum is unstable. In order to have a stable vacuum, in what follows, for non-Dirichlet boundary conditions, we shall assume that $1/\beta_j < \omega_0$ and the mode with $k_{p+1} = i/\beta_j$ corresponds to a bound state. For $\beta_j > 0$ and in the absence of purely imaginary roots of (2.17), in the right-hand side of the summation formula (2.25) the residue terms at $u = \pm i/b_j$ should be added (see [273]). Now the integrand in (2.33) has a simple pole at $k_{p+1} = is/\beta_j$ and after the rotation the contribution of the residue at that pole should be added. This contribution cancels the additional residue term in the right-hand side of (2.25). In the case when the equation (2.17) has purely imaginary roots the corresponding contributions have to be added to the mode-sum (2.21) for the Hadamard function. But the corresponding contributions should also be added in the left-hand side of (2.25) and the further evaluation procedure remains the same. Hence, the expressions (2.28) and (2.34) are valid for all values of the coefficients in the Robin boundary conditions. The only restrictions come from the stability of the vacuum state: $1/\beta_j < \omega_0$ and $y_l < \omega_0$. In the presence of compact dimensions with $\tilde{\alpha}_l \neq 0$ one has $\omega_0 > m$ and these conditions are less restrictive than those in the case of trivial topology.

The current density in the boundary-free geometry is obtained by using the Hadamard function (2.31) and has been investigated in [135]. The corresponding charge density and the current densities along uncompact dimensions vanish. As it can be seen from (2.28) and (2.34), the same holds in the case of the boundary-induced contributions in the VEVs. Hence, the only nonzero components correspond to the current density along compact dimensions.

2.2 Vacuum currents in the geometry of a single plate

In this section we investigate the VEV of the vacuum current density in the geometry of a single plate at $x^{p+1} = a_j$. This VEV is obtained with the help of the formula (2.6) by using the

Hadamard function from (2.34). The component of the VEV of the current density along the lth compact dimension is presented in the decomposed form

$$\langle j^l \rangle_j = \langle j^l \rangle_0 + \langle j^l \rangle_j^{(1)}, \tag{2.35}$$

where $\langle j^l \rangle_0$ is the current density in the boundary-free geometry and $\langle j^l \rangle_j^{(1)}$ is the contribution induced by the presence of the plate.

The current density in the boundary-free geometry has been investigated in [135] and for the completeness we will recall the main results. The current density is given by the formula

$$\langle j^l \rangle_0 = \frac{4eL_l m^{D+1}}{(2\pi)^{(D+1)/2}} \sum_{n_l=1}^{\infty} n_l \sin(n_l \tilde{\alpha}_l) \sum_{\mathbf{n}_{q-1}} \cos(\mathbf{n}_{q-1} \cdot \tilde{\boldsymbol{\alpha}}_{q-1}) f_{\frac{D+1}{2}}(m g_{\mathbf{n}_q}(\mathbf{L}_q)), \tag{2.36}$$

where $\tilde{\boldsymbol{\alpha}}_{q-1} = (\tilde{\alpha}_{p+2}, \ldots, \tilde{\alpha}_{l-1}, \tilde{\alpha}_{l+1}, \ldots, \tilde{\alpha}_D)$, $\mathbf{n}_{q-1} = (n_{p+2}, \ldots, n_{l-1}, n_{l+1}, \ldots, n_D)$, and $g_{\mathbf{n}_q}(\mathbf{L}_q) = (\sum_{i=p+2}^{D} n_i^2 L_i^2)^{1/2}$. The current density $\langle j^l \rangle_0$ is an odd periodic function of $\tilde{\alpha}_l$ with the period 2π and an even periodic function of $\tilde{\alpha}_r$, $r \neq l$, with the same period. This corresponds to the periodicity in the magnetic flux with the period of flux quantum. An alternative expression for the current density in the boundary-free geometry is given by the formula [135]

$$\langle j^l \rangle_0 = \frac{4eL_l/V_q}{(2\pi)^{(p+3)/2}} \sum_{n=1}^{\infty} \frac{\sin(n\tilde{\alpha}_l)}{(nL_l)^{p+2}} \sum_{\mathbf{n}_{q-1}} g_{\frac{p+3}{2}}(nL_l \omega_{\mathbf{n}_{q-1}}), \tag{2.37}$$

where we have defined the function

$$g_\nu(x) = x^\nu K_\nu(x), \tag{2.38}$$

and

$$\omega_{\mathbf{n}_{q-1}}^2 = \omega_{\mathbf{n}_q}^2 - k_l^2. \tag{2.39}$$

In the model with a single compact dimension ($q = 1$) the representations (2.36) and (2.37) are identical.

When the length of the lth compact dimension, L_l, is much larger than the other length scales, the behavior of the current density crucially depends whether the parameter

$$\omega_{0l} = \left(\sum_{i=p+2, \neq l}^{D} \tilde{\alpha}_i^2 / L_i^2 + m^2 \right)^{1/2}, \tag{2.40}$$

is zero or not. For $\omega_{0l} = 0$, which is realised for a massless field with $\tilde{\alpha}_i = 0$, $i \neq l$, to the leading order we have

$$\langle j^l \rangle_0 \approx \frac{2e\Gamma((p+3)/2)}{\pi^{(p+3)/2} L_l^{p+1} V_q} \sum_{n=1}^{\infty} \frac{\sin(n\tilde{\alpha}_l)}{n^{p+2}}. \tag{2.41}$$

In this case, the leading term in the expansion of $V_q\langle j^l\rangle_0/L_l$ coincides with the current density in $(p+2)$-dimensional space with a single compact dimension of the length L_l. For $\omega_{0l}\neq 0$ and for large values of L_l one has

$$\langle j^l\rangle_0 \approx \frac{2eV_q^{-1}\sin(\tilde{\alpha}_l)\omega_{0l}^{p/2+1}}{(2\pi)^{p/2+1}L_l^{p/2}}e^{-L_l\omega_{0l}}, \tag{2.42}$$

and the current density is exponentially suppressed. In the opposite limit of small values for L_l, to the leading order we get

$$\langle j^l\rangle_0 \approx \frac{2e\Gamma((D+1)/2)}{\pi^{(D+1)/2}L_l^D}\sum_{n=1}^{\infty}\frac{\sin(n\tilde{\alpha}_l)}{n^D}. \tag{2.43}$$

The leading term does not depend on the mass and on the lengths of the other compact dimensions and coincides with the current density for a massless scalar field in the space with topology $R^{D-1}\times S^1$.

Now we turn to the investigation of the plate-induced contribution in the current density. By using the expression for the corresponding part in the Hadamard function from (2.34), we get the following expression

$$\langle j^l\rangle_j^{(1)} = \frac{eC_p}{2^pV_q}\sum_{\mathbf{n}_q}k_l\int_{\omega_{\mathbf{n}_q}}^{\infty}dy\,(y^2-\omega_{\mathbf{n}_q}^2)^{(p-1)/2}e^{-2yz_j}\frac{y\beta_j+1}{y\beta_j-1}, \tag{2.44}$$

with the notations $z_j=|z-a_j|$ for the distance from the plate and

$$C_p = \frac{\pi^{-(p+1)/2}}{\Gamma((p+1)/2)}. \tag{2.45}$$

Recall that, in order to have a stable vacuum state with $\langle\varphi\rangle=0$, we have assumed that $1/\beta_j<\omega_0$. Under this condition, the integrand in (2.44) is regular everywhere in the integration range. The integral in (2.44) is evaluated in the special cases of Dirichlet and Neumann boundary conditions with the result

$$\langle j^l\rangle_j^{(1)} = \mp\frac{2e/V_q}{(2\pi)^{p/2+1}}\sum_{\mathbf{n}_q}k_l\omega_{\mathbf{n}_q}^p f_{p/2}(2\omega_{\mathbf{n}_q}z_j), \tag{2.46}$$

where the upper and lower signs correspond to Dirichlet and Neumann boundary conditions, respectively. Note that, in the problem with a fermionic field, obeying the bag boundary condition on the plate, the boundary-induced contribution vanishes for a massless field [137].

Let us consider the behavior of the plate-induced contribution in asymptotic regions of the parameters. At large distances from the plate, $z_j \gg L_i$, one has $z_j\omega_{\mathbf{n}_q} \gg 1$. Assuming that $|\tilde{\alpha}_i| < \pi$, the dominant contribution in (2.44) comes from the region near the lower limit of the integration and from the term with $n_i = 0$, $i = p+2, \ldots, D$. To the leading order we find

$$\langle j^l \rangle_j^{(1)} \approx \frac{e\tilde{\alpha}_l \omega_0^{(p-1)/2} e^{-2\omega_0 z_j}}{(4\pi)^{(p+1)/2} V_q L_l z_j^{(p+1)/2}} \frac{\omega_0\beta_j + 1}{\omega_0\beta_j - 1}, \tag{2.47}$$

and the current density is exponentially small. Note that the suppression is exponential for both massive and massless field.

For points close to the plate, $z_j \ll L_i$, in (2.44) the contribution of the terms with large values of $|n_i|$ dominates and this formula is not convenient for the asymptotic analysis and for numerical evaluations. In the case $\beta_j \leqslant 0$, an alternative expression is obtained by using the representation (2.93) for the Hadamard function. The first term in the right-hand side of this representation corresponds to the geometry with uncompactified lth dimension and does not contribute to the current density along that direction. In the geometry of a single plate at $x^{p+1} = a_j$ the part in the Hadamard function induced by the compactification is given by the first term in the figure braces of (2.93). From this part, by making use of (2.6), for the VEV of the lth component of the current density we get

$$\langle j^l \rangle_j = \frac{2^{1-p/2} e L_l}{\pi^{p/2+2} V_q} \sum_{n=1}^{\infty} \frac{\sin(n\tilde{\alpha}_l)}{(nL_l)^{p+1}} \sum_{\mathbf{n}_{q-1}} \int_0^{\infty} dy\, g(z_j, y) g_{p/2+1}(nL_l\sqrt{y^2 + \omega_{\mathbf{n}_{q-1}}^2}), \tag{2.48}$$

where we have defined the function

$$\begin{aligned} g(z_j, y) &= g_j(z, z, y) = 1 + \frac{1}{2}\sum_{s=\pm 1} e^{2siyz_j} \frac{iy\beta_j - s}{iy\beta_j + s} \\ &= 1 - \frac{(1 - y^2\beta_j^2)\cos(2yz_j) + 2y\beta_j \sin(2yz_j)}{1 + y^2\beta_j^2}. \end{aligned} \tag{2.49}$$

The part with the first term in the right-side of (2.49) corresponds to the current density in the boundary-free geometry. In this part the integration over y is done with the help of the formula

$$\int_0^{\infty} dy\, g_{\frac{p}{2}+1}(nL_l\sqrt{y^2 + b^2}) = \sqrt{\pi/2}(nL_l)^{-1} g_{\frac{p+3}{2}}(nL_l b), \tag{2.50}$$

and one gets the expression (2.37).

Extracing the boundary-free part, for the plate-induced contribution from (2.48) we find

$$\langle j^l \rangle_j^{(1)} = \frac{2^{-p/2} e L_l}{\pi^{p/2+2} V_q} \sum_{n=1}^{\infty} \frac{\sin(n\tilde{\alpha}_l)}{(nL_l)^{p+1}} \sum_{\mathbf{n}_{q-1}} \int_0^{\infty} dy\, g_{\frac{p}{2}+1}(nL_l \sqrt{y^2+\omega_{\mathbf{n}_{q-1}}^2}) \sum_{s=\pm 1} e^{2siyz_j} \frac{iy\beta_j - s}{iy\beta_j + s}. \quad (2.51)$$

In the case of single compact dimension one has $q=1$, $p=D-2$, and the corresponding formula for the plate-induced contribution in the current density is obtained from (2.51) omitting the summation over $\mathbf{n}_{q-1}$ and putting $\omega_{\mathbf{n}_{q-1}} = m$.

An important issue in quantum field theory with boundaries is the appearance of surface divergences in the VEVs of local physical observables. Examples of the latter are the VEVs of the field squared and of the energy density. These divergences are a consequence of the oversimplification of a model where the physical interactions are replaced by the imposition of boundary conditions for all modes of a fluctuating quantum field. Of course, this is an idealization, as real physical systems cannot constrain all the modes (for a discussion of surface divergences and their physical interpretation see [5],[286]-[294] and references therein). The appearance of divergences in the VEVs of physical quantities indicates that a more realistic physical model should be employed for their evaluation on the boundaries. An important feature, which directly follows from the representation (2.51), is that the VEV of the current density is finite on the plate. This is in sharp contrast with the behavior of the VEVs for the field squared and energy-momentum tensor. The finiteness of the current density on the boundary may be understood from general arguments. The divergences in local physical observables are determined by the local bulk and boundary geometries. If we consider the model with the topology $R^{p+2} \times T^{q-1}$ with the lth dimension having the topology R^1, then in this model the lth component of the current density vanishes by the symmetry. The compactification of the lth dimension to S^1 does not change both the bulk end boundary local geometries and, hence, does not add new divergences to the VEVs compared with the model on $R^{p+2} \times T^{q-1}$.

In deriving (2.51) we have assumed that $\beta_j \leqslant 0$. In the case $\beta_j > 0$ the contribution of the bound state should be added to (2.51). For $1/\beta_j < \omega_{0l}$, this contribution is obtained from the corresponding part in the Hadamard function, given by (2.94), and has the form

$$\langle j_l \rangle_{bj}^{(1)} = -\frac{2^{2-p/2} e L_l e^{-2z_j/\beta_j}}{\pi^{p/2+1} V_q \beta_j} \sum_{n=1}^{\infty} \frac{\sin(n\tilde{\alpha}_l)}{(nL_l)^{p+1}} \sum_{\mathbf{n}_{q-1}} g_{\frac{p}{2}+1}(nL_l \sqrt{\omega_{\mathbf{n}_{q-1}}^2 - 1/\beta_j^2}). \quad (2.52)$$

In what follows for simplicity we shall consider the case $\beta_j \leqslant 0$. Recall that, the representation (2.44) is valid for all values of β_j from the range of the vacuum stability.

For Dirichlet and Neumann boundary conditions, after the evaluation of the integral in (2.51) by using the formula

$$\int_0^\infty dy\, \cos(2yz_j) g_{\frac{p}{2}+1}(nL_l\sqrt{y^2+b^2}) = \sqrt{\frac{\pi}{2}}(nL_l)^{p+2}\frac{g_{\frac{p+3}{2}}(b\sqrt{4z_j^2+n^2L_l^2})}{(4z_j^2+n^2L_l^2)^{(p+3)/2}}, \tag{2.53}$$

one gets

$$\langle j^l\rangle_j^{(1)} = \mp\frac{4eL_l^2/V_q}{(2\pi)^{(p+3)/2}}\sum_{n=1}^\infty \frac{n\sin(n\tilde{\alpha}_l)}{(4z_j^2+n^2L_l^2)^{(p+3)/2}}\sum_{\mathbf{n}_{q-1}} g_{\frac{p+3}{2}}(\omega_{\mathbf{n}_{q-1}}\sqrt{4z_j^2+n^2L_l^2}), \tag{2.54}$$

where the upper and lower signs correspond to Dirichlet and Neumann conditions, respectively. For a single compact dimension with the length L and with the phase $\tilde{\alpha}$ in the periodicity condition for a massless field this gives

$$\langle j^l\rangle_j^{(1)} = \mp\frac{2\Gamma((D+1)/2)e}{\pi^{(D+1)/2}L^D}\sum_{n=1}^\infty \frac{n\sin(n\tilde{\alpha})}{(n^2+4z_j^2/L^2)^{(D+1)/2}}. \tag{2.55}$$

Now, combining the expressions (2.37) and (2.54), we see that in the case of Dirichlet boundary condition the boundary-free and plate-induced parts of the current density cancel each other for $z_j = 0$ and, hence, the total current vanishes on the plate. For Neumann condition the current density on the plate is given by

$$\langle j^l\rangle_{j,z=a_j} = 2\langle j^l\rangle_0 = \frac{8eL_l/V_q}{(2\pi)^{(p+3)/2}}\sum_{n=1}^\infty \frac{\sin(n\tilde{\alpha}_l)}{(nL_l)^{p+2}}\sum_{\mathbf{n}_{q-1}} g_{\frac{p+3}{2}}(nL_l\omega_{\mathbf{n}_{q-1}}). \tag{2.56}$$

Note that the normal derivative of the current density on the plate vanishes for both Dirichlet and Neumann boundary conditions: $(\partial_z\langle j^l\rangle_j)_{z=a_j} = 0$. This is not the case for general Robin condition.

Let us consider the behavior of the plate-induced contribution in the current density in the limit $L_i \ll L_l$. In this investigation it is more convenient to use the representation (2.51). For $\sum_{i=p+2,\neq l}^D \tilde{\alpha}_i^2 \neq 0$, the dominant contribution in the integral of (2.51) comes from the region near the lower limit of the integration and from the term $n = 1$, $n_i = 0$, $i = p+2,\ldots,D$, in the summation. The argument of the function $g_{p/2+1}(x)$ in the integrand is large and we can use the asymptotic expression $g_\nu(x) \approx \sqrt{\pi/2}x^{\nu-1/2}e^{-x}$. After some intermediate calculations,

for the leading term we get

$$\langle j^l \rangle_j^{(1)} \approx \frac{2e(1-2\delta_{0\beta_j})}{(2\pi)^{p/2+1} V_q L_l^{p/2}} \frac{\omega_{0l}^{p/2+1} \sin\tilde{\alpha}_l}{e^{L_l\omega_{0l}(1+2z_j^2/L_l{}^2)}}. \tag{2.57}$$

Here, we have additionally assumed that $L_i \ll |\beta_j|$ for $\beta_j \neq 0$. For $\tilde{\alpha}_i = 0$, $i = p+2, \ldots, D$, $i \neq l$, the dominant contribution in (2.51) comes from the term $n_i = 0$, $i = p+2, \ldots, D$, with the leading term

$$\begin{aligned} \frac{V_q}{L_l}\langle j^l \rangle_j^{(1)} &\approx \langle j^l \rangle_{j,R^{p+1}\times S^1}^{(1)} = \frac{4e}{(2\pi)^{p/2+2}} \sum_{n=1}^{\infty} \frac{\sin(n\tilde{\alpha}_l)}{(nL_l)^{p+1}} \int_0^{\infty} dy \\ &\times g_{\frac{p}{2}+1}(nL_l\sqrt{y^2+m^2}) \sum_{s=\pm 1} e^{2siyz_j} \frac{iy\beta_j - s}{iy\beta_j + s}. \end{aligned} \tag{2.58}$$

Here, $\langle j^l \rangle_{j,R^{p+1}\times S^1}^{(1)}$ is the plate-induced contribution in the current density for $(p+2)$-dimensional space with topology $R^{p+1} \times S^1$ (see (2.51) for the case $q = 1$ and, hence, $\omega_{\mathbf{n}_{q-1}} = m$).

If the length of the ith compact dimension is large, $i \neq l$, the dominant contribution to the sum over n_i comes from large values of $|n_i|$ and in (2.51) we can replace the summation over n_i by the integration in accordance with

$$\sum_{n_i=-\infty}^{\infty} f(|k_i|) \to \frac{L_i}{\pi} \int_0^{\infty} dx\ f(x). \tag{2.59}$$

The integral over x is evaluated by using the formula (2.50). As a result, from (2.51), to the leading order, we obtain the current density along the lth compact dimension for the spatial topology $R^{p+2} \times T^{q-1}$ with the lengths of the compact dimensions $(L_{p+2}, \ldots, L_{i-1}, L_{i+1}, \ldots, L_D)$.

Now let us consider the limiting case when L_l is large compared with the other length scales in the problem, $L_l \gg L_i, z_j$, $i \neq l$. The dominant contribution in (2.51) comes from the term $n_i = 0$, $i \neq l$. For $\omega_{0l} \neq 0$ we find

$$\langle j^l \rangle_j^{(1)} \approx \frac{2e\left(2\delta_{\beta_j,\infty} - 1\right)}{(2\pi)^{p/2+1} V_q} \frac{\sin\tilde{\alpha}_l}{L_l{}^{p/2}} \omega_{0l}^{p/2+1} e^{-L_l\omega_{0l}}, \tag{2.60}$$

where, for non-Neumann boundary conditions ($\beta_j \neq \infty$), we have assumed that $\beta_j\omega_{0l} \ll (L_l\omega_{0l})^{1/2}$. For $\omega_{0l} = 0$ the leading term is given by the expression

$$\langle j^l \rangle_j^{(1)} \approx \frac{2e\left(2\delta_{\beta_j,\infty} - 1\right)}{\pi^{(p+3)/2} V_q L_l^{p+1}} \Gamma((p+3)/2) \sum_{n=1}^{\infty} \frac{\sin(n\tilde{\alpha}_l)}{n^{p+2}}. \tag{2.61}$$

Comparing with the corresponding asymptotics (2.41) and (2.42), we see that for non-Neumann boundary conditions, in the both cases $\omega_{0l} \neq 0$ and $\omega_{0l} = 0$, the leading terms in the boundary-induced and boundary-free parts of the current density cancel each other.

An equivalent representation for the plate-induced current density is obtained from (2.51) rotating the integration contour in the complex plane y by the angle $\pi/2$ for the term with $s=1$ and by the angle $-\pi/2$ for the term with $s=-1$. The integrals over the intervals $(0,\pm i\omega_{\mathbf{n}_{q-1}})$ are cancelled and we find

$$\begin{aligned}\langle j^l\rangle_j^{(1)} &= \frac{2^{-p/2}eL_l}{\pi^{p/2+1}V_q}\sum_{n=1}^{\infty}\frac{\sin(n\tilde{\alpha}_l)}{(nL_l)^{p+1}}\sum_{\mathbf{n}_{q-1}}\int_{\omega_{\mathbf{n}_{q-1}}}^{\infty}dy \\ &\quad\times e^{-2yz_j}\frac{y\beta_j+1}{y\beta_j-1}w_{p/2+1}(nL_l\sqrt{y^2-\omega_{\mathbf{n}_{q-1}}^2}),\end{aligned} \tag{2.62}$$

where

$$w_\nu(x)=x^\nu J_\nu(x), \tag{2.63}$$

and $J_\nu(x)$ is the Bessel function. The equivalence of the representations (2.44) and (2.62) can also be directly seen by applying to the series over n_l in (2.44) the relation

$$\sum_{n_l=-\infty}^{+\infty}k_l g(|k_l|)=\frac{2L_l}{\pi}\sum_{n=1}^{\infty}\sin(n\tilde{\alpha}_l)\int_0^{\infty}dx\,x\sin(nL_lx)g(x). \tag{2.64}$$

The latter is a direct consequence of the Poisson's resummation formula. After using (2.64) in (2.44), we introduce a new integration variable $u=\sqrt{y^2-x^2-\omega_{\mathbf{n}_{q-1}}^2}$ and then pass to polar coordinates in the (u,x)-plane. The integration over the polar angle is expressed in terms of the Bessel function and the representation (2.62) is obtained.

Another expression is obtained by applying to the series over n_l in (2.44) the summation formula (2.88). For the series in (2.44) one has $g(u)=u$ and the first integral vanishes. As a result, the plate-induced part in the VEV of the current density is presented as

$$\begin{aligned}\langle j^l\rangle_j^{(1)} &= -\frac{eC_pL_l\sin\tilde{\alpha}_l}{2^p\pi V_q}\sum_{\mathbf{n}_{q-1}}\int_0^{\infty}dx\,\frac{x}{\cosh(L_l\sqrt{x^2+\omega_{\mathbf{n}_{q-1}}^2})-\cos\tilde{\alpha}_l} \\ &\quad\times\int_0^x dy\frac{(1-y^2\beta_j^2)\cos(2yz_j)+2y\beta_j\sin(2yz_j)}{(1+y^2\beta_j^2)(x^2-y^2)^{(1-p)/2}}.\end{aligned} \tag{2.65}$$

For Dirichlet and Neumann boundary conditions we obtain

$$\langle j^l\rangle_j^{(1)}=\mp\frac{2eL_l\sin\tilde{\alpha}_l}{(4\pi)^{p/2+1}V_qz_j^{p/2}}\sum_{\mathbf{n}_{q-1}}\int_0^{\infty}dx\,\frac{x^{p/2+1}\,J_{p/2}(2xz_j)}{\cosh(L_l\sqrt{x^2+\omega_{\mathbf{n}_{q-1}}^2})-\cos\tilde{\alpha}_l}. \tag{2.66}$$

In figure 4, for the simplest Kaluza-Klein model with a single compact dimension of the length L and with the phase $\tilde{\alpha}$ ($D=4$), we have plotted the total current density, $L^D\langle j^l\rangle_j/e$,

for a massless scalar field in the geometry of a single plate as a function of the distance from the plate and of the phase $\tilde{\alpha}$. The left/right panel correspond to Dirichlet/Neumann boundary conditions. As has been already noticed before, in the Dirichlet case the total current density vanishes on the plate.

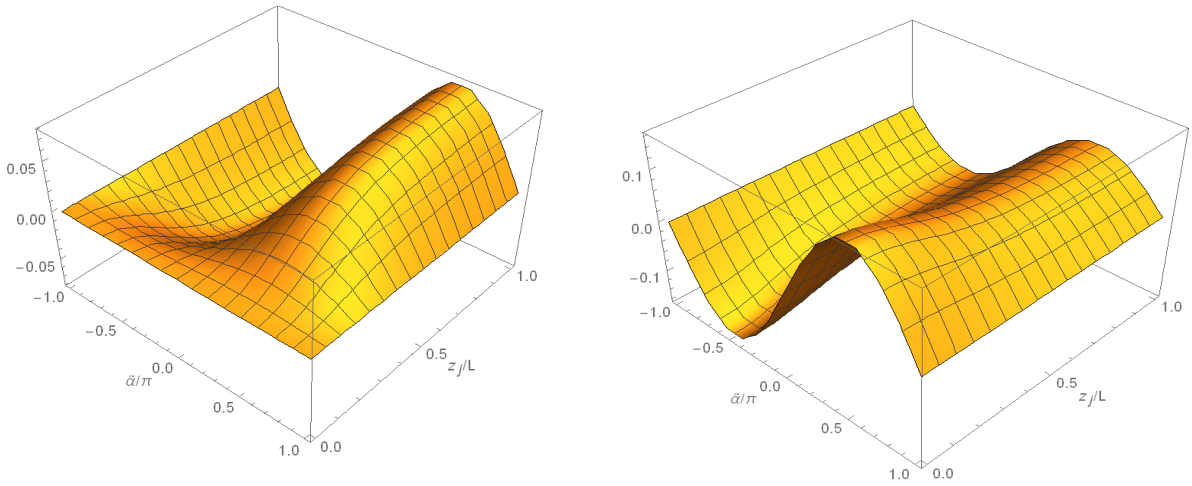

Figure 4: The total current density, $L^D\langle j^l\rangle_j/e$, in the topology $R^3\times S^1$ for a $D=4$ massless scalar field with Dirichlet (left panel) and Neumann (right panel) boundary conditions in the geometry of a single plate, as a function of the phase in the quasiperiodicity boundary condition and of the distance from the plate.

For the same model, figure 5 presents the plate-induced contribution to the current density as a function of the distance from the plate for various values of the coefficients in the Robin boundary condition (left panel) and as a function of the ratio β_j/L (right panel). The numbers near the curves on the right panel correspond to the value of β_j/L. The left panel is plotted for the fixed value of the relative distance from the plate $z_j/L=0.3$. On both panels, the dashed curves are plotted for Dirichlet and Neumann boundary conditions. For the phase in the quasiperiodicity condition we have taken $\tilde{\alpha}=\pi/2$. On the right panel, for the values of β_j/L between the ordinate axis and the vertical dotted line ($\beta_j/L=1/\tilde{\alpha}$) the vacuum is unstable.

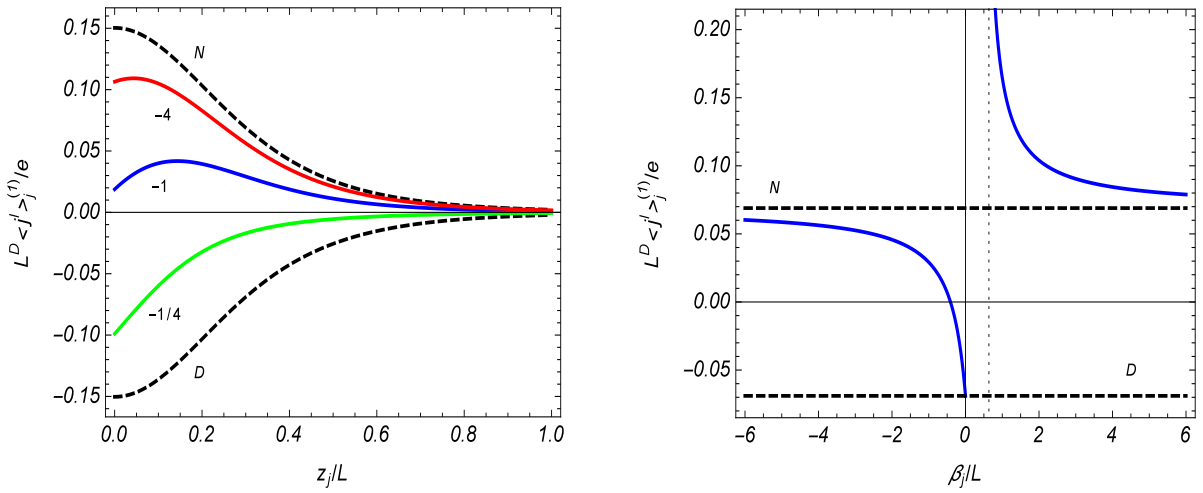

Figure 5: The plate-induced contribution to the current density for the model corresponding to figure 1 as a function of the distance from the plate (left panel) for different values of the ratio β_j/L (numbers near the curves) and as a function of β_j/L (right panel) for $z_j/L = 0.3$. The dashed curves correspond to Dirichlet and Neumann boundary conditions and the graphs are plotted for $\tilde{\alpha} = \pi/2$.

2.3 Current density between two plates

Now we turn to the geometry of two plates. In the region $a_1 \leqslant x^{p+1} \leqslant a_2$, by using the formula (2.28) for the Hadamard function, the VEV of the current density is decomposed as

$$\langle j^l \rangle = \langle j^l \rangle_j + \frac{eC_p}{2^{p-1}V_q} \sum_{\mathbf{n}_q} k_l \int_{\omega_{\mathbf{n}_q}}^{\infty} dy \frac{(y^2 - \omega_{\mathbf{n}_q}^2)^{(p-1)/2} g(z_j, iy)}{c_1(ay)c_2(ay)e^{2ay} - 1}. \tag{2.67}$$

Here, the second term in the right-hand side is induced by the plate at $x^{p+1} = a_{j'}$, $j' \neq j$.

Extracting from the second term in the right-hand side of (2.67) the part induced by the second plate when the first one is absent, the current density is written in a more symmetric form:

$$\langle j^l \rangle = \langle j^l \rangle_0 + \sum_{j=1,2} \langle j^l \rangle_j^{(1)} + \Delta\langle j^l \rangle, \tag{2.68}$$

where the interference part is given by the expression

$$\Delta\langle j^l \rangle = \frac{eC_p}{2^p V_q} \sum_{\mathbf{n}_q} k_l \int_{\omega_{\mathbf{n}_q}}^{\infty} dy \, (y^2 - \omega_{\mathbf{n}_q}^2)^{\frac{p-1}{2}} \frac{2 + \sum_{j=1,2} e^{-2yz_j}/c_j(ay)}{c_1(ay)c_2(ay)e^{2ay} - 1}. \tag{2.69}$$

By taking into account the expression for the current density in the geometry of a single plate,

for the total current density we can also write

$$\langle j^l\rangle = \langle j^l\rangle_0 + \frac{eC_p}{2^pV_q}\sum_{\mathbf{n}_q} k_l \int_{\omega_{\mathbf{n}_q}}^{\infty} dy\,(y^2-\omega_{\mathbf{n}_q}^2)^{\frac{p-1}{2}} \times \frac{2+\sum_{j=1,2} c_j(ay)e^{2yz_j}}{c_1(ay)c_2(ay)e^{2ay}-1}. \tag{2.70}$$

For special cases of Dirichlet and Neumann boundary conditions on both plates the general formula is simplified to

$$\langle j^l\rangle = \langle j^l\rangle_0 + \frac{eC_p}{2^pV_q}\sum_{\mathbf{n}_q} k_l \int_{\omega_{\mathbf{n}_q}}^{\infty} dy\,(y^2-\omega_{\mathbf{n}_q}^2)^{\frac{p-1}{2}} \frac{2\mp\sum_{j=1,2} e^{2yz_j}}{e^{2ay}-1}, \tag{2.71}$$

where, as before, the upper and lower signs correspond to Dirichlet and Neumann boundary conditions, respectively. In particular, for Dirichlet boundary condition the part induced by the second plate vanishes on the first plate. Note that in the system of two fields with Dirichlet and Neumann conditions the distribution of the total current density in the region between the plates is uniform and the current density vanishes in the regions $z<a_1$ and $z>a_2$. Another form for (2.71) is obtained by making use of the expansion

$$\frac{1}{e^{2ay}-1} = \sum_{n=1}^{\infty} e^{-2nay}, \tag{2.72}$$

After the integration over y we get

$$\langle j^l\rangle = \langle j^l\rangle_0 + \frac{2e/V_q}{(2\pi)^{p/2+1}}\sum_{n=1}^{\infty}\sum_{\mathbf{n}_q} k_l\omega_{\mathbf{n}_q}^p[2f_{\frac{p}{2}}(2na\omega_{\mathbf{n}_q}) \mp \sum_{j=1,2} f_{\frac{p}{2}}(2(na-z_j)\omega_{\mathbf{n}_q})]. \tag{2.73}$$

A similar representation for the interference part $\Delta\langle j^l\rangle$ is obtained from (2.73) by the replacement $z_j\to -z_j$. For Dirichlet boundary condition, on the plates, $z=a_j$, one has

$$\Delta\langle j^l\rangle_{z=a_j} = \frac{2e/V_q}{(2\pi)^{p/2+1}}\sum_{\mathbf{n}_q} k_l\omega_{\mathbf{n}_q}^p f_{\frac{p}{2}}(2a\omega_{\mathbf{n}_q}). \tag{2.74}$$

Combining this result with the formulas for single plates, we see that in the case of Dirichlet boundary condition the total current vanishes on the plates: $\langle j^l\rangle_{z=a_j}=0$.

An equivalent representation for the current density in the region between the plates and for Robin conditions is obtained by using the representation (2.93) for the corresponding Hadamard function:

$$\langle j^l\rangle = \langle j^l\rangle_j + \frac{2^{1-p/2}eL_l}{\pi^{p/2+1}V_q}\sum_{n=1}^{\infty}\frac{\sin(n\tilde{\alpha}_l)}{(nL_l)^{p+1}}\sum_{\mathbf{n}_{q-1}}\int_{\omega_{\mathbf{n}_{q-1}}}^{\infty} dy \times \frac{w_{p/2+1}(nL_l\sqrt{y^2-\omega_{\mathbf{n}_{q-1}}^2})}{c_1(ay)c_2(ay)e^{2ay}-1} g(z_j,iy). \tag{2.75}$$

Combining the expressions (2.62) and (2.75), for the total current density we find

$$\begin{aligned}\langle j^l\rangle &= \langle j^l\rangle_0+\frac{2^{-p/2}eL_l}{\pi^{p/2+1}V_q}\sum_{n=1}^{\infty}\frac{\sin(n\tilde{\alpha}_l)}{(nL_l)^{p+1}}\sum_{\mathbf{n}_{q-1}}\int_{\omega_{\mathbf{n}_{q-1}}}^{\infty}dy\\ &\times\frac{2+\sum_{j=1,2}e^{2yz_j}c_j(ay)}{c_1(ay)c_2(ay)e^{2ay}-1}w_{p/2+1}(nL_l\sqrt{y^2-\omega_{\mathbf{n}_{q-1}}^2}).\end{aligned}\tag{2.76}$$

Now, by taking into account the expression (2.62) for the single plate induced part, from (2.75) for the interference part we get

$$\begin{aligned}\Delta\langle j^l\rangle &= \frac{2^{-p/2}eL_l}{\pi^{p/2+1}V_q}\sum_{n=1}^{\infty}\frac{\sin(n\tilde{\alpha}_l)}{(nL_l)^{p+1}}\sum_{\mathbf{n}_{q-1}}\int_{\omega_{\mathbf{n}_{q-1}}}^{\infty}dy\\ &\times\frac{2+\sum_{j=1,2}e^{-2yz_j}/c_j(ay)}{c_1(ay)c_2(ay)e^{2ay}-1}w_{p/2+1}(nL_l\sqrt{y^2-\omega_{\mathbf{n}_{q-1}}^2}).\end{aligned}\tag{2.77}$$

The equivalence of the representations (2.70) and (2.75) can be seen directly by using the formula (2.64) in a way similar to that for the geometry of a single plate.

For Dirichlet and Neumann conditions, after using the expansion (2.72), the integral over y in (2.76) is expressed in terms of the MacDonald function and one gets the representation

$$\begin{aligned}\langle j^l\rangle &= \frac{2^{(1-p)/2}eL_l^2}{\pi^{(p+3)/2}V_q}\sum_{n=1}^{\infty}n\sin(n\tilde{\alpha}_l)\sum_{\mathbf{n}_{q-1}}\omega_{\mathbf{n}_{q-1}}^{p+3}\\ &\times\sum_{r=-\infty}^{\infty}\left\{f_{\frac{p+3}{2}}(\omega_{\mathbf{n}_{q-1}}\sqrt{4(ra)^2+n^2L_l^2})\right.\\ &\left.\mp f_{\frac{p+3}{2}}(\omega_{\mathbf{n}_{q-1}}\sqrt{4(ra-z+a_1)^2+n^2L_l^2})\right\},\end{aligned}\tag{2.78}$$

where we have taken into account the expression (2.37) for the current density in the boundary-free geometry. In the model with a single compact dimension with the length L and for a massless field, from (2.78) we find

$$\begin{aligned}\langle j^l\rangle &= \frac{2\Gamma((D+1)/2)e}{\pi^{(D+1)/2}L^D}\sum_{n=1}^{\infty}\sum_{r=-\infty}^{\infty}n\sin(n\tilde{\alpha})\\ &\times\left\{\left[4(ra/L)^2+n^2\right]^{-\frac{D+1}{2}}\mp\left[4(ra-z+a_1)^2/L^2+n^2\right]^{-\frac{D+1}{2}}\right\}.\end{aligned}\tag{2.79}$$

In the case of Dirichlet boundary condition on the left plate, $x^{p+1}=a_1$, and Neumann boundary condition on the right one, $x^{p+1}=a_2$, the corresponding formulas are obtained from (2.78) and (2.79) with the upper sign, adding the factor $(-1)^r$ in the summation over r. The corresponding current density vanishes on the left plate. From (2.78) we can also see that the

normal derivative of the current density vanishes on the plates for both Dirichlet and Neumann boundary conditions.

In the limit $a \ll L_i$, $i \neq l$, the dominant contribution to the series over $\mathbf{n}_{q-1}$ in (2.77) comes from large values of $|n_i|$, $i \neq l$, and we can replace the summation by the integration in accordance with

$$\sum_{\mathbf{n}_{q-1}} f(\omega_{\mathbf{n}_{q-1}}) \to \frac{2\,(4\pi)^{(1-q)/2}\,V_q}{\Gamma((q-1)/2)L_l} \int_0^\infty du\, u^{q-2}\, f(\sqrt{u^2+m^2}). \tag{2.80}$$

Changing the integration variable y to $x = \sqrt{y^2-u^2}$, we introduce polar coordinates in the (u,x)-plane. After the integration over the polar angle, we get

$$\Delta\langle j^l\rangle \approx \Delta\langle j^l\rangle_{R^D\times S^1}, \tag{2.81}$$

where $\Delta\langle j^l\rangle_{R^D\times S^1}$ is the corresponding quantity in the geometry of a single compact dimension with the length L_l. The expression for $\Delta\langle j^l\rangle_{R^D\times S^1}$ is obtained from (2.77) taking $p = D-2$, $V_q = L_l$, $\omega_{\mathbf{n}_{q-1}} = m$, and omitting the summation over $\mathbf{n}_{q-1}$. If, in addition, $am \ll 1$, one finds

$$\Delta\langle j^l\rangle \approx \frac{2e}{(2\pi)^{D/2}\,a} \sum_{n=1}^\infty \frac{\sin(n\tilde{\alpha}_l)}{(nL_l)^{D-1}} \int_0^\infty dy\, \frac{2+\sum_{j=1,2} e^{-2yz_j/a}/c_j(y)}{c_1(y)c_2(y)e^{2y}-1} w_{D/2}(nL_l y/a). \tag{2.82}$$

Now let us also assume that $a \ll L_i, m^{-1}$, for all $i = p+2,\ldots,D$. This means that the separation between the plates is smaller than all other length scales in the problem. In order to estimate the integral in (2.82), we note that for a fixed b and for $\lambda \to +\infty$, the dominant contribution to the integral $\int_0^\infty dy\, f(y)e^{-by}w_{D/2}(\lambda y)$ comes from the region with $y \lesssim a/L$. By taking into account that

$$\int_0^\infty dy\, e^{-by} w_{D/2}(\lambda y) = \frac{2^{D/2}\lambda^D\Gamma((D+1)/2)}{\sqrt{\pi}\,(b^2+\lambda^2)^{(D+1)/2}}, \tag{2.83}$$

to the leading order we get

$$\int_0^\infty dy\, f(y)e^{-by} w_{D/2}(\lambda y) \approx \frac{2^{D/2}}{\sqrt{\pi}\lambda}\Gamma((D+1)/2) f(0). \tag{2.84}$$

For the integral in (2.82) we take $b = 2$ and

$$f(y) = \frac{2+\sum_{j=1,2} e^{-2yz_j/a}/c_j(y)}{c_1(y)c_2(y)-e^{-2y}}. \tag{2.85}$$

In the case of non-Neumann boundary conditions one has $f(0) = 1$ and, hence,

$$\Delta\langle j^l\rangle \approx \frac{2e\Gamma((D+1)/2)}{\pi^{(D+1)/2}L^D}\sum_{n=1}^{\infty}\frac{\sin(n\tilde{\alpha}_l)}{n^D}. \tag{2.86}$$

Combining this result with the expressions from the previous section for the geometry of a single plate, we conclude that $\lim_{a\to 0}\langle j^l\rangle = 0$, i.e., for non-Neumann boundary conditions the total current density in the region between the plates tends to zero for small separations between the plates. For non-Neumann boundary condition on one plate and Neumann boundary condition on the other we have $f(0) = -1$ and the corresponding formula is obtained from (2.86) changing the sign of the right-hand side. In this case we have again $\lim_{a\to 0}\langle j^l\rangle = 0$.

For Neumann boundary condition on both plates, for the function in (2.85) we have $f(y) \sim 2/y$, $y \to 0$. In order to obtain the leading term in the asymptotic expansion for small values of a it is more convenient to use the expression (2.79) with the lower sign instead of the right-hand side of (2.82). For small a/L the dominant contribution in (2.79) comes from large values of r and, to the leading order, we replace the corresponding summation by the integration. For the leading term this gives

$$\langle j^l\rangle \approx \frac{2e\Gamma(D/2)}{\pi^{D/2}L^{D-1}a}\sum_{n=1}^{\infty}\frac{\sin(n\tilde{\alpha})}{n^{D-1}}, \tag{2.87}$$

and for Neumann boundary condition the current density diverges in the limit $a \to 0$ like $1/a$. The described features in the behavior of the vacuum current density, $L^D\langle j^l\rangle/e$, in the region between the plates located at $z = 0$ and $z = a$, as a function of the separation between the plates, is illustrated in figure 6 for a $D = 4$ massless scalar field in the model with a single compact dimension of the length L and of the phase $\tilde{\alpha}$. The graphs are plotted for $z = a/2$ and $\tilde{\alpha} = \pi/2$, in the cases of Dierichlet (D), Neumann (N) boundary conditions on both plates, for Dirichlet boundary condition at $z = 0$ and Neumann boundary condition at $z = a$ (DN), and for Robin boundary conditions with $\beta_j/L = -0.5$ and $\beta_j/L = -1$ (numbers near the curves). At large separations between the plates, the boundary-induced effects are small and the current density coincides with that in the boundary-free geometry.

In figure 7, in the model with a single compact dimension of the length L and for a $D = 4$ massless scalar field with Dirichlet (left panel) and Neumann (right panel) boundary conditions, we have plotted the total current density as a function of the ratio z/a in the region between the

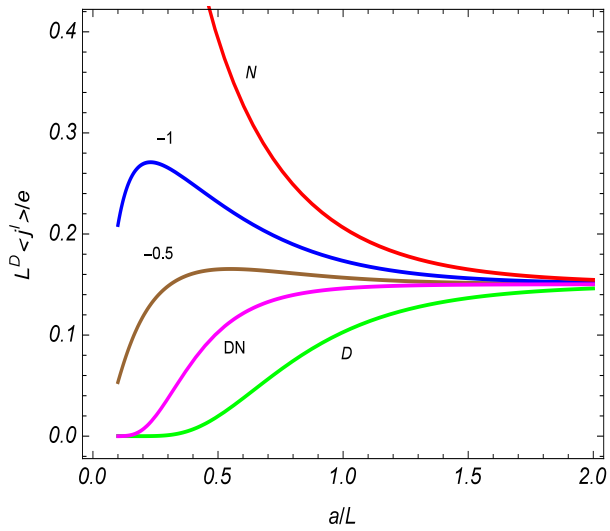

Figure 6: The VEV of the current density in the region between the plates evaluated at $z = a/2$, as a function of the separation between the plates. The graphs are plotted for Dirchlet and Neumann boundary conditions on both plates, for Dirichlet condition on the left plate and Neumann condition on the right one, and for Robin boundary conditions with the values of β_j/L given near the curves. For the phase we have taken the value $\tilde{\alpha} = \pi/2$.

plates. The numbers near the curves correspond to the values of a/L and the graphs are plotted for $\tilde{\alpha} = \pi/2$. The features, obtained before on the base of asymptotic analysis, are clearly seen from the graphs: the current density for Dirichlet/Neumann scalar decreases/increases with decreasing separation between the plates and for Dirichlet scalar it vanishes on the plates.

The same graphs for Dirichlet boundary condition on the left plate and Neumann condition on the right one are presented on the left panel of figure 8. The right panel in figure 8 is plotted for Robin boundary condition on both plates with $\beta_1/L = \beta_2/L = -1$. In the Robin case, the current density decreases with the further decrease of the separation between the plates and it tends to zero in the limit $a \to 0$, in accordance with the general analysis described above.

2.4 Appendix A2: Alternative representation of the Hadamard function

In this section we derive an alternative representation for the Hadamard function which is well suited for the investigation of the near-plate asymptotic of the current density. The starting

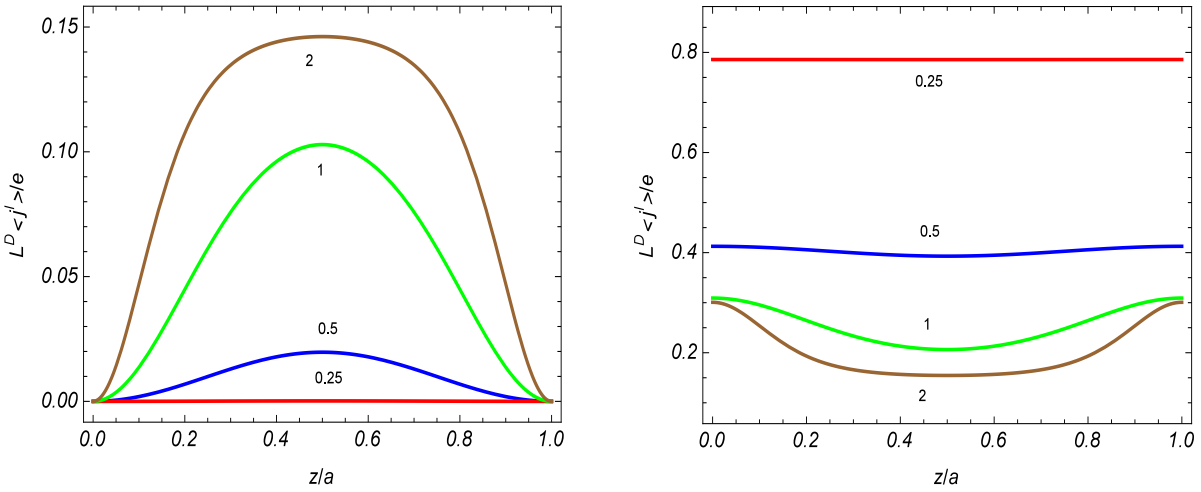

Figure 7: The current density between the plates as a function of the relative distance from the left plate in the model with a single compact dimension. The graphs are plotted for a massless field with the parameter $\tilde{\alpha} = \pi/2$ and with Dirichlet (left panel) and Neumann (right panel) boundary conditions. The numbers near the curves correspond to the values of a/L.

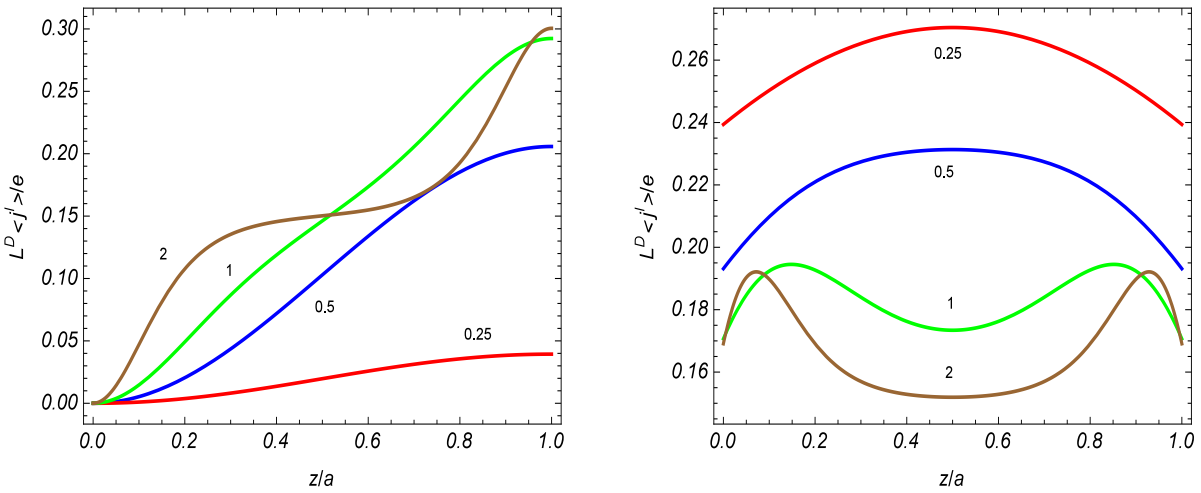

Figure 8: The same as in figure 7 for Dirichlet boundary condition on the left plate and Neumann condition on the right one (left panel). The right panel is plotted for Robin boundary condition on both plates with $\beta_1/L = \beta_2/L = -1$.

point is the representation (2.21). We apply to the corresponding series over n_l the summation formula [132, 295]

$$\frac{2\pi}{L_l}\sum_{n_l=-\infty}^{\infty} g(k_l)f(|k_l|) = \int_0^\infty du[g(u)+g(-u)]f(u) + i\int_0^\infty du\,[f(iu)-f(-iu)]\sum_{\lambda=\pm 1}\frac{g(i\lambda u)}{e^{uL_l+i\lambda\tilde{\alpha}_l}-1}, \tag{2.88}$$

where k_l is given by (2.12). The part in the Hadamard function coming from the first term in the right-hand side of (2.88) coincides with the Hadamard function for the geometry of two plates in D-dimensional space with topology $R^{p+2}\times T^{q-1}$ and with the lengths of the compact dimensions $(L_{p+2},\ldots,L_{l-1},L_{l+1},\ldots,L_D)$ (the lth dimension is uncompactified). We will denote this function by $G_{R^{p+2}\times T^{q-1}}(x,x')$. As a result, under the assumption $\beta_j \leqslant 0$, the Hadamard function is decomposed as

$$\begin{aligned} G(x,x') &= G_{R^{p+2}\times T^{q-1}}(x,x') + \frac{L_l}{\pi a V_q}\int\frac{d\mathbf{k}_p}{(2\pi)^p}\sum_{\mathbf{n}_{q-1}} \\ &\times\sum_{n=1}^{\infty}\frac{\lambda_n g(z,z',\lambda_n/a)e^{i\mathbf{k}_p\cdot\Delta\mathbf{x}_p+i\mathbf{k}^l_{q-1}\cdot\Delta\mathbf{x}^l_{q-1}}}{\lambda_n+\cos\left[\lambda_n+2\tilde{\gamma}_j(\lambda_n)\right]\sin\lambda_n} \\ &\times\int_{\omega^{(l)}_{\mathbf{k}}}^\infty du\,\frac{\cosh(\Delta t\sqrt{u^2-\omega^{(l)2}_{\mathbf{k}}})}{\sqrt{u^2-\omega^{(l)2}_{\mathbf{k}}}}\sum_{\lambda=\pm 1}\frac{e^{-\lambda u\Delta x^l}}{e^{uL_l+i\lambda\tilde{\alpha}_l}-1}, \end{aligned} \tag{2.89}$$

where $\mathbf{x}^l_{q-1} = (x^{p+2},...,x^{l-1},x^{l+1},\ldots x^D)$, $\mathbf{k}_{q-1} = (k_{p+2},\ldots,k_{l-1},k_{l+1},\ldots,k_D)$, and $\omega^{(l)}_{\mathbf{k}} = \sqrt{\omega^2_{\mathbf{k}}-k_l^2}$. Here, the second term in the right-hand side vanishes in the limit $L_l\to\infty$ and is induced by the compactification of the lth dimension from R^1 to S^1 with the length L_l.

By making use of the relation

$$\sum_{\lambda=\pm 1}\frac{e^{-\lambda u\Delta x^l}}{e^{uL_l+i\lambda\tilde{\alpha}_l}-1} = 2u\sum_{r=1}^{\infty}h_r(u,\Delta x^l), \tag{2.90}$$

with

$$h_r(\Delta x^l,u) = \frac{e^{-ruL_l}}{u}\cosh\left(u\Delta x^l+ir\tilde{\alpha}_l\right), \tag{2.91}$$

we rewrite the formula (2.89) in the form

$$
\begin{aligned}
G(x,x') &= G_{R^{p+2}\times T^{q-1}}(x,x') + \frac{2L_l}{\pi a V_q}\sum_{r=1}^{\infty}\int\frac{d\mathbf{k}_p}{(2\pi)^p} \\
&\times \sum_{\mathbf{n}_{q-1}}\int_0^{\infty} dy\,\cosh(y\Delta t)e^{i\mathbf{k}_p\cdot\Delta\mathbf{x}_p+i\mathbf{k}_{q-1}^l\cdot\Delta\mathbf{x}_{q-1}^l} \\
&\times \sum_{n=1}^{\infty}\frac{\lambda_n g(z,z',\lambda_n/a)h_r(\Delta x^l,\sqrt{\lambda_n^2/a^2+y^2+\omega_{p,\mathbf{n}_{q-1}}^2})}{\lambda_n+\cos\left[\lambda_n+2\tilde{\gamma}_j(\lambda_n)\right]\sin\lambda_n},
\end{aligned}
\tag{2.92}
$$

with $\omega_{p,\mathbf{n}_{q-1}}=\sqrt{\mathbf{k}_p^2+\omega_{\mathbf{n}_{q-1}}^2}$. Now, by using the summation formula (2.25) for the series over n we get the final representation

$$
\begin{aligned}
G(x,x') &= G_{R^{p+2}\times T^{q-1}}(x,x') + \frac{2L_l}{\pi^2 V_q}\sum_{r=1}^{\infty}\int\frac{d\mathbf{k}_p}{(2\pi)^p}\sum_{\mathbf{n}_{q-1}}e^{i\mathbf{k}_p\cdot\Delta\mathbf{x}_p+i\mathbf{k}_{q-1}^l\cdot\Delta\mathbf{x}_{q-1}^l} \\
&\times\int_0^{\infty}dy\,\cosh(\Delta t y)\Big\{\int_0^{\infty}du g_j(z,z',u)h_r(\Delta x^l,\sqrt{u^2+y^2+\omega_{p,\mathbf{n}_{q-1}}^2}) \\
&+\int_{\sqrt{y^2+\omega_{p,\mathbf{n}_{q-1}}^2}}^{\infty}du\frac{g_j(z,z',iu)}{c_1(au)c_2(au)e^{2au}-1}\sum_{s=\pm1}ih_{sr}(\Delta x^l,i\sqrt{u^2-y^2-\omega_{p,\mathbf{n}_{q-1}}^2})\Big\}.
\end{aligned}
\tag{2.93}
$$

In this expression, the part with the first term in the figure braces is the contribution to the Hadamard function induced by the compactification of the lth dimension for the geometry of a single plate at $x^{p+1}=a_j$ and the part with the second term in the figure braces is induced by the second plate. Note that the contribution of the first term in the right-hand side of (2.93) to current density along the lth dimension vanishes.

In deriving the representation (2.93) we have assumed that $\beta_j\leqslant 0$. For this case, in the region between the plates, all the eigenvalues for the momentum k_{p+1} are real and in the geometry of a single plate there are no bound states. For $\beta_j>0$, in the application of the summation formula (2.25) to the series over n in (2.92) the contribution from the poles $\pm i/b_j$ should be added to the right-hand side of (2.25). This contribution comes from the bound state in the geometry of a single plate at $x^{p+1}=a_j$. For this bound state the mode function has the form $\varphi_{\mathbf{k}}^{(\pm)}(x)\sim e^{-z_j/\beta_j}e^{i\mathbf{k}_{\parallel}\cdot\mathbf{x}_{\parallel}\mp i\omega_{\mathbf{k}}^{(b)}t}$ with $\omega_{\mathbf{k}}^{(b)}=\sqrt{\mathbf{k}_p^2+\omega_{\mathbf{n}_q}^2-1/\beta_j^2}$. Assuming that $\omega_{0l}>1/\beta_j$, the contribution from the bound state to the Hadamard function in the geometry of a single plate is given by the expression

$$
\begin{aligned}
G_{bj}^{(1)}(x,x') &= \frac{4\theta(\beta_j)L_l}{\pi V_q\beta_j}e^{-|z+z'-2a_j|/\beta_j}\sum_{r=1}^{\infty}\int\frac{d\mathbf{k}_p}{(2\pi)^p}\sum_{\mathbf{n}_{q-1}^l}\int_0^{\infty}dx\,e^{i\mathbf{k}_p\cdot\Delta\mathbf{x}_p+i\mathbf{k}_{q-1}^l\cdot\Delta\mathbf{x}_{q-1}^l} \\
&\times\cosh(x\Delta t)h_r(\Delta x^l,\sqrt{x^2+\mathbf{k}_p^2+\omega_{\mathbf{n}_{q-1}}^2-1/\beta_j^2}),
\end{aligned}
\tag{2.94}
$$

where $\theta(x)$ is the Heaviside unit step function. In the case $\omega_{0l} < 1/\beta_j < \omega_0$ the corresponding expression is more complicated.

2.5 Summary

We have investigated the influence of parallel flat boundaries on the VEV of the current density for a charged scalar field in a flat spacetime with toroidally compactified spatial dimensions, assuming the presence of a constant gauge field. The effect of the latter on the current is similar to the Aharonov-Bohm effect and is caused by the nontrivial topology of the background space. Along compact dimensions we have considered quasiperiodicity conditions with general phases. The special cases of twisted and untwisted fields are the configurations most frequently discussed in the literature. By a gauge transformation, the problem with a constant gauge field is mapped to the one with zero field, shifting the phases in the periodicity conditions by an amount proportional to the magnetic flux enclosed by a compact dimension in the initial representation of the model. On the plates we employed Robin boundary conditions, in general, with different coefficients on the left and right plates. The Robin boundary conditions for bulk fields naturally arise in braneworld scenario and the boundaries considered here may serve as a simple model for the branes.

We considered a free field theory and all the information on the properties of the vacuum state is encoded in two-point functions. Here we chose the Hadamard function. The VEV of the current density is obtained from this function in the coincidence limit by using (2.6). For the evaluation of the Hadamard function we have employed a direct summation over the complete set of modes. In the region between the plates the eigenvalues of the momentum component perpendicular to the plates are quantized by the boundary conditions on the plates and are given implicitly, in terms of solutions of the transcendental equation (2.17). Depending on the values of the Robin coefficients, this equation may have purely imaginary solutions $y = \pm iy_l$. In order to have a stable vacuum with $\langle\varphi\rangle = 0$, we assume that $\omega_0 > y_l$. Compared to the case of the bulk with trivial topology, this constraint in models with compact dimensions is less restrictive. The eigenvalues of the momentum components along compact dimensions are quantized by the periodicity conditions and are determined by (2.12). The application of the

generalized Abel-Plana formula for the summation over the roots of (2.17) allowed us to extract from the Hadamard function the part corresponding to the geometry with a single plate and to present the second-plate-induced contribution in the form which does not require the explicit knowledge of the eigenmodes for k_{p+1} (see (2.28)). In addition, the corresponding integrand decays exponentially in the upper limit. A similar representation, (2.34), is obtained for the Hadamard function in the geometry of a single plate. The second term in the right-hand side of this representation is the boundary-induced contribution. An alternative representation for the Hadamard function, (2.93), is obtained in Appendix, by making use of the summation formula (2.88). The second term in the right-hand side of this representation is the contribution induced by the compactification of the lth dimension.

The VEVs of the charge density and the components of the current density along uncompact dimensions vanish. The current density along compact dimensions is a periodic function of the magnetic flux with the period equal to the flux quantum. The component along the lth compact dimension is an odd function of the phase $\tilde{\alpha}_l$ and an even function of the remaining phases $\tilde{\alpha}_i$, $i \neq l$. First we have considered the geometry with a single plate. The VEV of the current density is decomposed into the boundary-free and plate-induced parts. The boundary-free contribution was investigated in [135] and we have been mainly concerned with the plate-induced part, given by (2.44). For special cases of Dirichlet and Neumann boundary conditions the corresponding expression is simplified to (2.46). The plate-induced part has opposite signs for Dirichlet and Neumann conditions. At distances from the plate larger than the lengths of compact dimensions the asymptotic is described by (2.47) and the plate-induced contribution is exponentially small. For the investigation of the near-plate asymptotic of the current density it is more convenient to use the representation (2.51) for the general Robin case and (2.54) for Dirichlet and Neumann conditions. From these representations it follows that the current density is finite on the plate. This property is in sharp contrast with the behavior of the VEVs of the field squared and of the energy-momentum tensor which diverge on the plate. For Dirichlet boundary condition the current density vanishes on the plate and for Neumann condition its value on the plate is two times larger than the current density in the boundary-free geometry. The normal derivative of the current density vanishes on the plate for both Dirichlet and Neumann conditions. This is

not the case for general Robin condition. The behavior of the plate-induced part of the current density along lth dimension, in the limit when the lengths of the other compact dimensions are much smaller than L_l, crucially depend wether the phases $\tilde{\alpha}_i$, $i \neq l$, are zero or not. For $\sum_{i\neq l} \tilde{\alpha}_i^2 \neq 0$ one has $\omega_{0l} \neq 0$ and the corresponding asymptotic expression is given by (2.57). In this case the plate-induced contribution is exponentially suppressed. For $\tilde{\alpha}_i = 0$, $i \neq l$, the leading term in the asymptotic expansion, multiplied by V_q/L_l, coincides with the corresponding current density for $(p+2)$-dimensional space with topology $R^{p+1} \times S^1$. In the limit when the length of the lth dimension is much larger than the other length scales of the model, the behavior of the plate-induced contribution to the current density is essentially different for the cases $\omega_{0l} \neq 0$ and $\omega_{0l} = 0$. In the former case the leading term is given by (2.60) and the current density is suppressed by the factor $e^{-L_l\omega_{0l}}$. In the second case, for the leading term one has the expression (2.61) and its behavior, as a function of L_l, is power law. In both cases and for non-Neumann boundary conditions, the leading terms in the boundary-induced and boundary-free parts of the current density cancel each other.

For the current density in the region between the plates we have provided various decompositions ((2.67), (2.68), (2.70) for general Robin boundary conditions and (2.71), (2.73), (2.78) for special cases of Dirichlet and Neumann conditions). In the case of Dirichlet boundary condition the total current vanishes on the plates. The normal derivative vanishes on the plates for both Dirichlet and Neumann cases. In the limit when the separation between the plates is smaller than all the length scales in the problem, the behavior of the current density is essentially different for non-Neumann and Neumann boundary conditions. In the former case, the total current density in the region between the plates tends to zero. For Neumann boundary condition on both plates, for small separations the total current density is dominated by the interference part and it diverges inversely proportional to the separation (see (2.87)). The results of the present paper may be applied to Kaluza-Klein-type models in the presence of branes (for $D > 3$) and to planar condensed matter systems (for $D = 2$), described within the framework of an effective field theory. In particular, in the former case, the vacuum currents along compact dimensions generate magnetic fields in the uncompactified subspace. The boundaries discussed above can serve as a simple model for the edges of planar systems.

3 CHAPTER: ELECTROMAGNETIC CASIMIR EFFECT FOR A CYLINDRICAL SHELL ON DE SITTER SPACE

Complete set of cylindrical modes is constructed for the electromagnetic field inside and outside a cylindrical shell in the background of $(D+1)$-dimensional dS spacetime. On the shell, the field obeys the generalized perfect conductor boundary condition. For the Bunch-Davies vacuum state, we evaluate the expectation values (VEVs) of the electric field squared and of the energy-momentum tensor. The shell-induced contributions are explicitly extracted. In this way, for points away from the shell, the renormalization is reduced to the one for the VEVs in the boundary-free dS bulk. As a special case, the VEVs are obtained for a cylindrical shell in the $(D+1)$-dimensional Minkowski bulk. We show that the shell-induced contribution in the electric field squared is positive for both the interior and exterior regions. The corresponding Casimir-Polder forces are directed toward the shell. The vacuum energy-momentum tensor, in addition to the diagonal components, has a nonzero off-diagonal component corresponding to the energy flux along the direction normal to the shell. This flux is directed from the shell in both the exterior and interior regions. For points near the shell, the leading terms in the asymptotic expansions for the electric field squared and diagonal components of the energy-momentum tensor are obtained from the corresponding expressions in the Minkowski bulk replacing the distance from the shell by the proper distance in the dS bulk. The influence of the gravitational field on the local characteristics of the vacuum is essential at distances from the shell larger than the dS curvature radius. The results are extended for confining boundary conditions of flux tube models in QCD.

3.1 Electromagnetic field modes in dS spacetime

We consider a quantum electromagnetic field in background of a $(D+1)$-dimensional dS spacetime, in the presence of a perfectly conducting cylindrical shell having the radius a. In accordance with the problem symmetry, we write the dS line element in cylindrical coordinates

$(r, \phi, \mathbf{z})$:

$$ds^2 = dt^2 - e^{2t/\alpha}\left[dr^2 + r^2 d\phi^2 + (d\mathbf{z})^2\right], \tag{3.1}$$

where $\mathbf{z} = \left(z^3, ..., z^D\right)$. The parameter α is expressed in terms of the cosmological constant Λ through the relation

$$\alpha^2 = \frac{D(D-1)}{2\Lambda}. \tag{3.2}$$

Below, in addition to the synchronous time coordinate t we will use the conformal time τ, defined as

$$\tau = -\alpha e^{-t/\alpha}, \ -\infty < \tau < 0. \tag{3.3}$$

In terms of this coordinate the metric tensor takes a conformally flat form $g_{\mu\nu} = (\alpha/\tau)^2 g_{(\mathrm{M})\mu\nu}$, where $g_{(\mathrm{M})\mu\nu} = \mathrm{diag}(1, -1, -r^2, -1, \ldots, -1)$ is the Minkowskian metric tensor.

We are interested in the changes of the VEVs for the electromagnetic field induced by a cylindrical boundary $r = a$ in the background of the geometry given by (3.1). In the canonical quantization procedure a complete orthonormal set of solutions to the classical field equations is required and, in this section, we present this set for the geometry at hand. For a free electromagnetic field the Maxwell equations have the form

$$\frac{1}{\sqrt{|g|}}\partial_\nu\left(\sqrt{|g|}F^{\mu\nu}\right) = 0, \tag{3.4}$$

where $F_{\mu\nu}$ is the electromagnetic field tensor, $F_{\mu\nu} = \partial_\mu A_\nu - \partial_\nu A_\mu$. We assume that on the surface $r = a$ the field obeys the boundary condition

$$n^{\nu_1} {}^*F_{\nu_1\cdots\nu_{D-1}} = 0, \tag{3.5}$$

where n^v is the normal to the boundary, ${}^*F_{\nu_1\cdots\nu_{D-1}}$ is the dual of the field tensor $F_{\mu\nu}$. For $D = 3$ the condition (3.5) reduces to the boundary condition on the surface of a perfect conductor. We want to find the complete set of solutions to the equation (3.4) in the coordinates $(\tau, r, \phi, \mathbf{z})$.

In the Coulomb gauge one has $A_0 = 0$, $\partial_l(\sqrt{|g|}A^l) = 0$, $l = 1, ..., D$. For the geometry under consideration the latter equation is reduced to

$$\sum_{l=1}^{D}\partial_l(rA^l) = 0, \tag{3.6}$$

which is the same as that in the Minkowski spacetime. If we present the solution in the factorized form, $A_\mu(\tau, x^l) = T(\tau)S_\mu(x^l)$, then it can be shown that the parts of the mode

functions corresponding to $S_\mu(x^l)$ are found in a way similar to that for the $(D+1)$-dimensional Minkowski bulk. The corresponding modes are presented in appendix 3.4.2. From the field equations (3.4) for the function $T(\tau)$ one gets $T(\tau) = \eta^{D/2-1} Z_{D/2-1}(\omega\eta)$, where $\eta = |\tau|$ and $Z_\nu(x)$ is a cylinder function of the order ν. It can be taken as a linear combination of the Hankel functions $H_\nu^{(1,2)}(x)$. The relative coefficient in the linear combination depends on the vacuum state under consideration. We assume that the field is prepared in the Bunch-Davies vacuum [296] for which $Z_\nu(x) = H_\nu^{(1)}(x)$. Among a one-parameter family of maximally symmetric vacuum states in dS spacetime the Bunch-Davies vacuum is the only one with the Hadamard singularity structure.

As a result, by taking into account the expressions for the Minkwoskian modes (3.93) and (3.103), for the modes in dS spacetime realizing the Bunch-Davies vacuum state one finds the expressions

$$A_{(\beta)\mu} = c_\beta \eta^{D/2-1} H^{(1)}_{D/2-1}(\omega\eta)(0, im/r, -r\partial_r, 0, \ldots, 0) C_m(\gamma r) e^{im\phi + i\mathbf{k}\cdot\mathbf{z}}, \tag{3.7}$$

for the polarization $\sigma = 1$, and

$$A_{(\beta)\mu} = \omega c_\beta \eta^{D/2-1} H^{(1)}_{D/2-1}(\omega\eta) \left(0, \epsilon_{\sigma l} + i\omega^{-2}\mathbf{k}\cdot\epsilon_\sigma \partial_l\right) C_m(\gamma r) e^{im\phi + i\mathbf{k}\cdot\mathbf{z}}, \tag{3.8}$$

for the remaining polarizations $\sigma = 2, \ldots, D-1$, with $l = 1, \ldots, D$. Here, $m = 0, \pm 1, \pm 2, \ldots$, $C_m(x)$ is a cylinder function, $\mathbf{k}\cdot\mathbf{z} = \sum_{l=3}^{D} k_l z^l$, $\mathbf{k}\cdot\epsilon_\sigma = \sum_{l=3}^{D} k_l \epsilon_{\sigma l}$, and

$$\omega = \sqrt{\gamma^2 + k^2}, \tag{3.9}$$

with $k^2 = \sum_{l=3}^{D} k_l^2$. For the polarization vectors $\epsilon_{\sigma l}$ one has $\epsilon_{\sigma 1} = \epsilon_{\sigma 2} = 0$ and the relations (3.99), (3.100). The set of quantum numbers specifying the modes is reduced to $\beta = (\gamma, m, \mathbf{k}, \sigma)$. It can be easily checked that the modes (3.7) and (3.8) obey the gauge condition (3.6).

The eigenvalues for the quantum number γ are determined by the boundary condition (3.5). First we consider the region inside the cylindrical shell, $r < a$. From the regularity condition at $r = 0$ it follows that

$$C_m(\gamma r) = J_m(\gamma r), \tag{3.10}$$

with $J_m(x)$ being the Bessel function. For the mode $\sigma = 1$ the allowed values for γ are roots of the equation

$$J'_m(\gamma a) = 0, \tag{3.11}$$

where the prime means the derivative with respect to the argument of the function. For the modes $\sigma = 2, \ldots, D-1$, the radial derivative enters in the expression for the component A_1 only. For these modes the boundary condition is reduced to

$$J_m(\gamma a) = 0. \tag{3.12}$$

In what follows we will denote the eigenmodes by $\gamma a = \gamma_{m,n}^{(\lambda)}$, $n = 1, 2, ...$, where $\lambda = 1$ for $\sigma = 1$ and $\lambda = 0$ for $\sigma = 2, 3, \ldots, D-1$. Hence, one has $J_m^{(\lambda)}(\gamma_{m,n}^{(\lambda)}) = 0$, with $f^{(0)}(x) = f(x)$ and $f^{(1)}(x) = f'(x)$.

The normalization coefficients c_β in (3.7) and (3.8) are determined from the orthonormalization condition for the vector potential:

$$\int d^D x \sqrt{|g|} [A^*_{(\beta')\nu}(x) \nabla^0 A^\nu_\beta(x) - \nabla^0 A^*_{(\beta')\nu}(x) A^\nu_{(\beta)}(x)] = 4i\pi\delta_{\beta\beta'}, \tag{3.13}$$

where the integration over the radial coordinate goes over the region inside the cylinder and $\delta_{\beta\beta'}$ is understood as the Kronecker symbol for the discrete components of the collective index β and the Dirac delta function for the continuous ones. By using the relation (3.99) it can be seen that the modes (3.8) are orthogonal. From (3.13) one finds

$$|c_\beta|^2 = \frac{T_m(\gamma_{m,n}^{(\lambda)})}{2(2\pi\alpha)^{D-3}\gamma_{m,n}^{(\lambda)}}, \tag{3.14}$$

for $\sigma = 1, \ldots, D-1$, where we have introduced the notation

$$T_m(x) = x \left[x^2 J_m'^2(x) + \left(x^2 - m^2\right) J_m^2(x)\right]^{-1}. \tag{3.15}$$

Having the complete set of mode functions (3.7) and (3.8) we can evaluate the VEV of any physical quantity $F\{A_\mu(x), A_\nu(x)\}$ bilinear in the field. By expanding the operator of the vector potential in terms of the modes (3.7) and (3.8) and using the commutation relations for the annihilation and creation operators, the following mode-sum formula is obtained

$$\langle 0|F\{A_\mu(x), A_\nu(x)\}|0\rangle = \sum_\beta F\{A_{(\beta)\mu}(x), A^*_{(\beta)\nu}(x)\}, \tag{3.16}$$

where $|0\rangle$ stands for the vacuum state, $\sum_\beta$ includes the summation over the discrete quantum numbers and the integration over the continuous ones. The expression in the right-hand side of (3.16) is divergent and requires a regularization with the subsequent renormalization. The

regularization can be done by introducing a cutoff function or by the point splitting. The consideration below does not depend on the specific regularization scheme and we will not specify it.

3.2 VEV of the electric field squared

As a local characteristic of the vacuum state we consider the VEV of the squared electric field. This VEV is obtained by making use of the mode-sum formula

$$\langle 0|E^2(x)|0\rangle \equiv \langle E^2(x)\rangle = -g^{00}g^{il}\sum_{\beta}\partial_0 A_{(\beta)i}(x)\partial_0 A^*_{(\beta)l}(x). \tag{3.17}$$

Note that the VEV of the electric field squared determines the Casimir-Polder potential between the shell and a polarizable particle with a frequency-independent polarizability. Substituting the eigenfunctions (3.7) and (3.8), after the summation over σ with the help of (3.100), for the VEV inside the shell we find

$$\begin{aligned}\langle E^2\rangle &= \frac{2^6 A_D \eta^{D+2}}{\alpha^{D+1}a^4}\sum_{m=0}^{\infty}{}'\int_0^{\infty}dk k^{D-3}\sum_{\lambda=0,1}\sum_{n=1}^{\infty}T_m(\gamma_{m,n}^{(\lambda)}) \\ &\quad\times\gamma_{m,n}^{(\lambda)3}F_m^{(\lambda)}[k,J_m(\gamma_{m,n}^{(\lambda)}r/a)]L_{D/2-2}(\omega_{m,n}^{(\lambda)}\eta),\end{aligned} \tag{3.18}$$

where $\omega_{m,n}^{(\lambda)}=\sqrt{\gamma_{m,n}^{(\lambda)}/a^2+k^2}$, the prime on the sign of the sum means that the term $m=0$ should be taken with the coefficient $1/2$,

$$A_D = \frac{1}{(4\pi)^{D/2}\Gamma(D/2-1)}, \tag{3.19}$$

and we have used the notation

$$L_\nu(x) = K_\nu(xe^{-i\pi/2})K_\nu(xe^{i\pi/2}). \tag{3.20}$$

Here, instead of the Hankel functions we have introduced the Macdonald function $K_\nu(x)$. The function $F_m^{(\lambda)}[k,f(x)]$ is defined by the relations

$$F_m^{(\lambda)}[k,f(x)] = \begin{cases} \frac{k^2r^2}{x^2}\left[f'^2(x)+\frac{m^2}{x^2}f^2(x)\right]+\left[(D-3)\left(1+\frac{k^2r^2}{x^2}\right)+1\right]f^2(x), & \lambda=0, \\ (1+\frac{k^2r^2}{x^2})\left[f'^2(x)+\frac{m^2}{x^2}f^2(x)\right], & \lambda=1. \end{cases} \tag{3.21}$$

The eigenvalues $\gamma_{m,n}^{(\lambda)}$ are given implicitly and the representation (3.18) is not convenient for the further investigation of the VEV. For the further evaluation of the mode-sum in (3.18), we

apply to the series over n the generalized Abel-Plana summation formula [68]

$$\sum_{n=1}^{\infty} T_m(\gamma_{m,n}^{(\lambda)}) f(\gamma_{m,n}^{(\lambda)}) = \frac{1}{2}\int_0^{\infty} dx f(x) + \frac{\pi}{4}\mathrm{Res}_{z=0} f(z)\,\frac{Y_m^{(\lambda)}(z)}{J_m^{(\lambda)}(z)}$$
$$-\frac{1}{2\pi}\int_0^{\infty} dz\,\frac{K_m^{(\lambda)}(z)}{I_m^{(\lambda)}(z)}\left[e^{-m\pi i} f(ze^{i\pi/2}) + e^{m\pi i} f(ze^{-i\pi/2})\right], \tag{3.22}$$

where $Y_m(z)$ is the Neumann function and $I_m(x)$ is the modified Bessel function of the first kind. In (3.22) it is assumed that the function $f(z)$ is analytic in the right half plane of the complex variable z. For the series in (3.18), the corresponding function $f(z)$ is given by

$$f(x) = x^3 L_{D/2-2}(\eta\sqrt{x^2/a^2+k^2}) F_m^{(\lambda)}[k, J_m(xr/a)]. \tag{3.23}$$

Note that this function has branch points $x = \pm ika$ on the imaginary axis. For the function (3.23) one has the relation

$$\sum_{j=-1,1} e^{jm\pi i} f(ze^{-ji\pi/2}) = ie^{-m\pi i} z^3 F_m^{(\lambda)}\left[k, J_m\left(ze^{i\pi/2}r/a\right)\right]$$
$$\times \sum_{j=-1,1} jL_{D/2-2}(\eta\sqrt{z^2e^{-ji\pi}/a^2+k^2}), \tag{3.24}$$

with

$$\sum_{j=-1,1} jL_\nu(\eta\sqrt{z^2e^{-ji\pi}/a^2+k^2}) = i\pi\begin{cases} 0, & z<ka \\ f_\nu(\eta\sqrt{z^2/a^2-k^2}), & z>ka \end{cases}. \tag{3.25}$$

Here and in what follows we use the notation

$$f_\nu(x) = K_\nu(x)\left[I_{-\nu}(x) + I_\nu(x)\right]. \tag{3.26}$$

After the application of the summation formula (3.22), the VEV of the electric field squared is decomposed as

$$\langle E^2\rangle = \langle E^2\rangle_{\mathrm{dS}} + \langle E^2\rangle_{\mathrm{b}}. \tag{3.27}$$

Here, the first term in the right-hand side comes from the first integral in (3.22). It does not depend on the shell radius a and corresponds to the VEV in dS spacetime in the absence of boundaries:

$$\langle E^2\rangle_{\mathrm{dS}} = \frac{2^5 A_D \eta^{D+2}}{\alpha^{D+1}}\,{\sum_{m=0}}'\int_0^{\infty} dk\,k^{D-3}\int_0^{\infty} dx\,x^3 F_m[k, J_m(xr)] L_{D/2-2}(\eta\sqrt{k^2+x^2}), \tag{3.28}$$

where

$$F_m\left[k,f(x)\right]=\left(1+2\frac{k^2r^2}{x^2}\right)\left[f'^2(x)+\frac{m^2}{x^2}f^2(x)\right]+\left[(D-3)\left(1+\frac{k^2r^2}{x^2}\right)+1\right]f^2(x). \quad (3.29)$$

The part of the VEV $\langle E^2\rangle_{\rm b}$ is the contribution of the last integral in (3.22). This part is induced by the presence of the cylindrical boundary and is given by the expression

$$\begin{aligned}\langle E^2\rangle_{\rm b} &= \frac{2^5A_D}{\alpha^{D+1}}\sum_{m=0}^{\infty}{}'\sum_{\lambda=0,1}\int_0^{\infty}dx\,x^{D+1}\frac{K_m^{(\lambda)}(xa/\eta)}{I_m^{(\lambda)}(xa/\eta)}\\ &\quad\times\int_0^1 ds\,s\left(1-s^2\right)^{D/2-2}G_m^{(\lambda)}\left[s,I_m(xr/\eta)\right]f_{D/2-2}(xs),\end{aligned} \quad (3.30)$$

with the notation

$$G_m^{(\lambda)}\left[s,f(x)\right]=\begin{cases}(1-s^2)\left[f'^2(x)+m^2f^2(x)/x^2\right]+\left[s^2(D-3)+1\right]f^2(x), & \lambda=0,\\ -s^2\left[f'^2(x)+m^2f^2(x)/x^2\right], & \lambda=1.\end{cases} \quad (3.31)$$

In deriving (3.30), after using (3.24) and (3.25), we have introduced a new integration variable u in accordance with $z=\sqrt{u^2+a^2k^2}$ and then passed to polar coordinates in the plane (u,ak). The representation (3.30) is valid for all even values of D and for $D<7$ in the case of odd D. The shell-induced contribution (3.30) depends on the variables η, a, r in the form of the ratios a/η and r/η. This feature is a consequence of the maximal symmetry of dS spacetime. Note that the combination $\alpha a/\eta$ is the proper radius of the cylindrical shell and, hence, a/η is the proper radius measured in units of the dS curvature scale α. Similarly, the ratio r/η is the proper distance from the cylinder axis measured in units of α.

As is seen from (3.28) and (3.30), in the new representation of the VEV the explicit knowledge of the eigenvalues $\gamma_{m,n}^{(\lambda)}$ is not required. Another advantage is that we have explicitly separated the part corresponding to the boundary-free dS spacetime. The presence of the boundary does not change the local geometry for points outside the shell. This means that at those points the divergences are the same in both the problems, in the absence and in the presence of the cylindrical shell. From here it follows that the divergences in (3.27) are contained in the part $\langle E^2\rangle_{\rm dS}$ only, whereas the boundary-induced contribution $\langle E^2\rangle_{\rm b}$ is finite for points away from the boundary and the regularization, implicitly assumed in the discussion above, can be safely removed in that part. Hence, the renormalization is required for the boundary-free part

only. Note that the expression for the latter can be further simplified after the summation over m by using the standard result for the series involving the square of the Bessel function.

Let us consider the properties of the boundary-induced contribution in the VEV of the field squared. First of all, by taking into account that for $D \geqslant 3$ one has $G_m^{(0)}[s, f(x)] > 0$, $G_m^{(1)}[s, f(x)] < 0$, and the function $f_{D/2-2}(x)$ is positive for the values of D for which the representation (3.30) is valid, from (3.30) it follows that $\langle E^2 \rangle_{\rm b}$ is always positive. The VEV of the electric field squared inside a cylindrical shell in Minkowski spacetime is obtained by the limiting transition $\alpha \to \infty$ for a fixed value of t. In this limit one has $\eta \approx \alpha - t$ and, hence, η is large. Passing to a new integration variable $y = x/\eta$, we see that η appears in the argument of the function $f_{D/2-2}(ys\eta)$. By taking into account that for large arguments one has $f_{D/2-2}(u) \approx 1/u$, after the integration over s, we get $\lim_{\alpha\to\infty} \langle E^2 \rangle_b = \langle E^2 \rangle_b^{(\rm M)}$, where

$$\langle E^2 \rangle_{\rm b}^{(\rm M)} = \frac{4(4\pi)^{(1-D)/2}}{\Gamma((D+1)/2)} \sum_{m=0}^{\infty}{}' \sum_{\lambda=0,1} \int_0^{\infty} dx\, x^D \frac{K_m^{(\lambda)}(ax)}{I_m^{(\lambda)}(ax)} G_{({\rm M})m}^{(\lambda)}[I_m(rx)], \tag{3.32}$$

with

$$G_{({\rm M})m}^{(\lambda)}[f(x)] = \begin{cases} (D-2)[f'^2(x) + (m^2/x^2+2)f^2(x)], & \lambda = 0, \\ -f'^2(x) - m^2 f^2(x)/x^2, & \lambda = 1, \end{cases} \tag{3.33}$$

is the VEV of the electric field squared inside a cylindrical shell in the Minkowski bulk.

In the special case of 4-dimensional dS spacetime one has $D = 3$ and $f_{-1/2}(u) = 1/u$. After the integration over s in (3.30), we find

$$\langle E^2 \rangle_{\rm b} = (\eta/\alpha)^4 \langle E^2 \rangle_{\rm b}^{(\rm M)}, \tag{3.34}$$

where $\langle E^2 \rangle_b^{(\rm M)}$ is given by (3.32) with $D = 3$. In this case, the VEV of the field squared is related to the corresponding result in Minkowski spacetime by standard conformal transformation with the conformal factor $(\eta/\alpha)^4$. This is a direct consequence of the conformal invariance of the electromagnetic field in $D = 3$ spatial dimensions and of the conformal flatness of the background geometry. The VEV of the electric field squared for a conducting cylindrical shell coaxial with a cosmic string in 4-dimensional spacetime ($D = 3$) is investigated in [297]. In the absence of planar angle deficit, the corresponding expression is reduced to (3.32) with $D = 3$. The corresponding Casimir-Polder forces were discussed in [298, 299].

On the axis of the shell, $r=0$, the only nonzero contribution to the boundary-induced VEV comes from the terms in (3.30) with $m=0,1$:

$$\begin{aligned}\left\langle E^2\right\rangle_{\mathrm{b},r=0} &= \frac{2^4 A_D}{\alpha^{D+1}}\left(\frac{\eta}{a}\right)^{D+2}\int_0^\infty dx\, x^{D+1}\int_0^1 ds\, s\left(1-s^2\right)^{D/2-2} f_{D/2-2}\left(xs\eta/a\right)\\ &\times\left[\left((D-3)\,s^2+1\right)\frac{K_0\left(x\right)}{I_0\left(x\right)}+\left(1-s^2\right)\frac{K_1\left(x\right)}{I_1\left(x\right)}-s^2\frac{K_1'\left(x\right)}{I_1'\left(x\right)}\right].\end{aligned}\tag{3.35}$$

The shell-induced VEV diverges on the cylindrical boundary. The surface divergences in the VEVs of local physical observables are well-known in the theory of the Casimir effect [5]. Near the shell the dominant contribution to the VEV comes from large values of m. For $m\neq 0$, introducing in (3.30) a new integration variable $y=x/m$, we use the uniform asymptotic expansions for the modified Bessel functions with the order m and the asymptotic for the function $f_{D/2-2}\left(u\right)$ for large arguments (see, for instance, [266]). To the leading order one finds

$$\left\langle E^2\right\rangle_{\mathrm{b}}\approx\frac{3\left(D-1\right)\Gamma\left(\left(D+1\right)/2\right)}{2^D\pi^{(D-1)/2}\left[\alpha\left(a-r\right)/\eta\right]^{D+1}}.\tag{3.36}$$

Note that the combination $\alpha\left(a-r\right)/\eta$ is the proper distance from the boundary. The leading term (3.36) is obtained from that for the cylindrical shell with the radius a in Minkowski spacetime by the replacement $\left(a-r\right)\to\alpha\left(a-r\right)/\eta$. For points near the boundary the contribution of the modes with small wavelengths dominate and at distances from the shell smaller than the curvature radius of the dS spacetime the influence of the gravitational field is small.

For the numerical evaluations we have taken the model with $D=4$. In this case for the function $f_\nu(y)$ in (3.30) one has

$$f_\nu(y)=2I_\nu(y)K_\nu(y),\tag{3.37}$$

and the integrals over s are of the form

$$\mathcal{I}_{n,\nu}(x)=\int_0^1 ds\, s^n f_\nu(xs),\tag{3.38}$$

with $n=1,3$. These integrals are evaluated in appendix 3.4.2. For the shell-induced part one gets

$$\begin{aligned}\left\langle E^2\right\rangle_{\mathrm{b}} &= \frac{2}{\pi^2\alpha^5}{\sum_{m=0}^{\infty}}'\sum_{\lambda=0,1}\int_0^\infty dx\, x^5\frac{K_m^{(\lambda)}\left(xa/\eta\right)}{I_m^{(\lambda)}\left(xa/\eta\right)}\\ &\times\left\{\left[I_m'^2(y)+\left(m^2/y^2+1\right)I_m^2(y)\right]\delta_{0\lambda}\mathcal{I}_{1,0}(x)\right.\\ &\left.-\left[I_m'^2(y)+\left(m^2/y^2-\delta_{0\lambda}\right)I_m^2(y)\right]\mathcal{I}_{3,0}(x)\right\}_{y=xr/\eta},\end{aligned}\tag{3.39}$$

with $\mathcal{I}_{1,0}(x)$ and $\mathcal{I}_{3,0}(x)$ given by (3.104), (3.110). In figure 9, this contribution is plotted versus the proper distance from the shell axis, measured in units of α. For the proper radius of the shell, in the same units, we have taken $a/\eta = 2$. The corresponding Casimir-Polder force is expressed in terms of the derivative $\partial_r \langle E^2 \rangle_{\rm b}$. This force is directed toward the cylindrical shell.

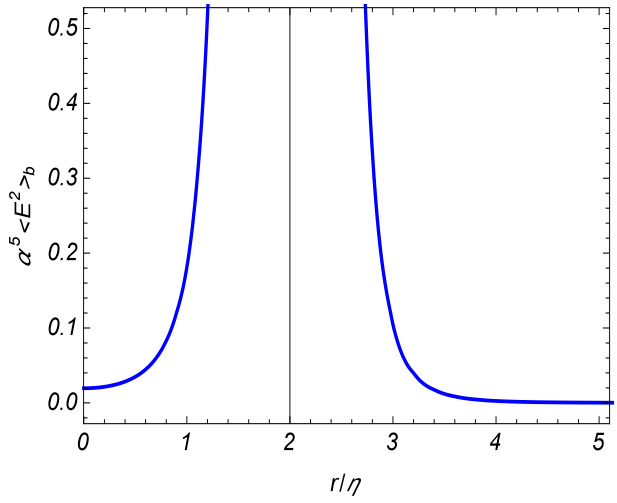

Figure 9: Shell-induced contribution in the VEV of the squared electric field versus the proper distance from the shell axis for the $D = 4$ model. For the corresponding value of the shell radius we have taken $a/\eta = 2$.

3.3 VEV of the energy-momentum tensor

Another important local characteristic of the vacuum state is the VEV of the energy-momentum tensor. This VEV is evaluated by using the mode-sum formula

$$\langle T_\mu^\nu \rangle = \frac{1}{16\pi}\delta_\mu^\nu g^{\rho l} g^{\sigma m} \sum_\beta F_{(\beta)\rho\sigma} F^*_{(\beta)lm} - \frac{1}{4\pi} g^{\nu\kappa} g^{\rho\sigma} \sum_\beta F_{(\beta)\mu\rho} F^*_{(\beta)\kappa\sigma}, \tag{3.40}$$

where $F_{(\beta)\mu\rho} = \partial_\mu A_{(\beta)\rho} - \partial_\rho A_{(\beta)\mu}$ is the field strength corresponding to the mode functions (3.7) and (3.8). By using the expressions for the mode functions, the mode-sums for the diagonal components of the VEV are presented in the form (no summation over i)

$$\begin{aligned} \langle T_i^i \rangle &= \frac{2B_D \eta^{D+2}}{\alpha^{D+1} a^2} {\sum_{m=0}^{\infty}}' \int_0^\infty dk k^{D-3} \sum_{\lambda=0,1} \sum_{n=1}^{\infty} \gamma_{m,n}^{(\lambda)} \\ &\times T_m(\gamma_{m,n}^{(\lambda)}) \sum_{l=0,1} t_{\lambda l}^{(i)}[k, \gamma_{m,n}^{(\lambda)}/a, J_m(\gamma r)] L_{D/2-1-l}(\omega_{m,n}^{(\lambda)} \eta), \end{aligned} \tag{3.41}$$

where

$$B_D = \frac{2^{2-D}}{\pi^{D/2+1}\Gamma(D/2-1)}. \tag{3.42}$$

Here we have used the notations

$$t_{\lambda l}^{(i)}[k,\gamma,f(y)] = (a_{\lambda l}^{(i)}k^2 + b_{\lambda l}^{(i)}\gamma^2)Z_m^{(i)}[f(y)] + ((D-3)\,c_{\lambda l}^{(i)}k^2 + d_{\lambda l}^{(i)}\gamma^2)f^2(y), \tag{3.43}$$

and

$$\begin{aligned} Z_m^{(i)}[f(y)] &= f'^2(y) + m^2 f^2(y)/y^2,\ i = 0,3,\ldots,D, \\ Z_m^{(i)}[f(y)] &= f'^2(y) - m^2 f^2(y)/y^2,\ i = 1,2. \end{aligned} \tag{3.44}$$

For the energy density the coefficients in (3.43) are given by the expressions

$$\begin{aligned} a_{\lambda l}^{(0)} &= \begin{pmatrix} 1 & 1 \\ 1 & 1 \end{pmatrix},\ b_{\lambda l}^{(0)} = \begin{pmatrix} D-2 & 0 \\ 0 & 1 \end{pmatrix}, \\ c_{\lambda l}^{(0)} &= \begin{pmatrix} 1 & 1 \\ 0 & 0 \end{pmatrix},\ d_{\lambda l}^{(0)} = \begin{pmatrix} 0 & D-2 \\ 1 & 0 \end{pmatrix}, \end{aligned} \tag{3.45}$$

where the rows and columns are numbered by $\lambda = 0,1$ and $l = 0,1$, respectively. For the coefficients in the radial and azimuthal components one has

$$a_{\lambda l}^{(1)} = \begin{pmatrix} -1 & 1 \\ 1 & -1 \end{pmatrix},\ c_{\lambda l}^{(1)} = \begin{pmatrix} 1 & -1 \\ 0 & 0 \end{pmatrix}, \tag{3.46}$$

and $a_{\lambda l}^{(2)} = -a_{\lambda l}^{(1)}$, $b_{\lambda l}^{(2)} = -b_{\lambda l}^{(1)} = b_{\lambda l}^{(0)}$, $c_{\lambda l}^{(2)} = c_{\lambda l}^{(1)}$, $d_{\lambda l}^{(1)} = d_{\lambda l}^{(2)} = -d_{\lambda l}^{(0)}$. For the axial components, $i = 3,\ldots,D$, we get

$$\begin{aligned} a_{\lambda l}^{(i)} &= \frac{1}{D-2}\begin{pmatrix} D-4 & 2-D \\ D-4 & 2-D \end{pmatrix},\ b_{\lambda l}^{(i)} = \begin{pmatrix} D-4 & 0 \\ 0 & -1 \end{pmatrix}, \\ c_{\lambda l}^{(i)} &= \frac{1}{D-2}\begin{pmatrix} D-6 & 4-D \\ 0 & 0 \end{pmatrix},\ d_{\lambda l}^{(i)} = \begin{pmatrix} 0 & 4-D \\ 1 & 0 \end{pmatrix}. \end{aligned} \tag{3.47}$$

In addition to the diagonal component, the VEV of the energy-momentum tensor has a nonzero off-diagonal component

$$\begin{aligned} \langle T_0^1 \rangle &= \frac{2^{3-D} i \eta^{D+2}}{\pi^D \alpha^{D+1} a^3} \sum_{m=0}^{\infty}{}' \int d\mathbf{k} \sum_{n=1}^{\infty} \sum_{\lambda=0,1} (-1)^\lambda N_\lambda T_m(\gamma_{m,n}^{(\lambda)}) \omega_{m,n}^{(\lambda)} \gamma_{m,n}^{(\lambda)2} \\ &\quad \times K_{D/2-2}(\omega_{m,n}^{(\lambda)}\eta e^{-\frac{i\pi}{2}}) K_{D/2-1}(\omega_{m,n}^{(\lambda)}\eta e^{\frac{i\pi}{2}}) J_m(\gamma_{m,n}^{(\lambda)} r/a) J'_m(\gamma_{m,n}^{(\lambda)} r/a). \end{aligned} \tag{3.48}$$

where $N_0 = D-2$, $N_1 = 1$. This component describes energy flux along the radial direction (along the direction normal to the boundary).

After the application of the summation formula (1.125), with the function

$$f(x) = xL_{D/2-1-l}(\eta\sqrt{x^2/a^2+k^2})t_{\lambda l}^{(i)}[k, x/a, J_m(xr/a)], \tag{3.49}$$

to the series over n in (3.41), the VEV of the energy-momentum tensor is presented in the form

$$\langle T_\mu^\nu \rangle = \langle T_\mu^\nu \rangle_{\rm dS} + \langle T_\mu^\nu \rangle_{\rm b}, \tag{3.50}$$

where $\langle T_\mu^\nu \rangle_{\rm dS}$ is the corresponding VEV in the boundary-free dS spacetime and the contribution $\langle T_\mu^\nu \rangle_b$ is induced by the presence of the cylindrical shell. The boundary-free contribution corresponds to the first integral in the right-hand side of the formula (3.22) and the boundary-induced contribution comes from the second integral. For points outside the cylindrical shell the boundary-induced contribution in (3.50) is finite and the renormalization is reduced to the one for the boundary-free part. From the maximal symmetry of the Bunch-Davies vacuum state it follows that the latter does not depend on the spacetime point and has the form $\langle T_\mu^\nu \rangle_{\rm dS} = {\rm const}\cdot\delta_\mu^\nu$.

With the help of the transformations similar to those we have used for the VEV of the field squared, for the boundary-induced parts in the diagonal components we get (no summation over i)

$$\begin{aligned}\langle T_i^i \rangle_{\rm b} &= \frac{B_D}{\alpha^{D+1}}\sum_{m=0}^{\infty}{}'\sum_{\lambda=0,1}\int_0^\infty dx\, x^{D+1}\frac{K_m^{(\lambda)}(ax/\eta)}{I_m^{(\lambda)}(ax/\eta)}\int_0^1 ds\, s \\ &\quad\times\left(1-s^2\right)^{D/2-2}\sum_{l=0,1}P_{\lambda l}^{(i)}[s, I_m(xr/\eta)]f_{D/2-1-l}(xs),\end{aligned} \tag{3.51}$$

where we have defined the functions

$$P_{\lambda l}^{(i)}[s, f(y)] = (A_{\lambda l}^{(i)} + B_{\lambda l}^{(i)}s^2)Z_m^{(i)}[f(y)] + (C_{\lambda l}^{(i)} + (D-3)\,D_{\lambda l}^{(i)}s^2)f^2(y), \tag{3.52}$$

with $Z_m^{(i)}[f(y)]$ given by (3.44). For the energy density the coefficients in (3.52) are given by the expressions

$$A_{\lambda l}^{(0)} = C_{\lambda l}^{(0)} = \begin{pmatrix} 3-D & 1 \\ 1 & 0 \end{pmatrix},\ B_{\lambda l}^{(0)} = -\begin{pmatrix} 1 & 1 \\ 1 & 1 \end{pmatrix},\ D_{\lambda l}^{(0)} = \begin{pmatrix} 1 & 1 \\ 0 & 0 \end{pmatrix}. \tag{3.53}$$

For the radial and azimuthal stresses one has

$$A_{\lambda l}^{(i)} = (-1)^i C_{\lambda l}^{(i)} = -(-1)^i \begin{pmatrix} D-3 & 1 \\ 1 & 0 \end{pmatrix},$$
$$B_{\lambda l}^{(i)} = (-1)^i \begin{pmatrix} -1 & 1 \\ 1 & -1 \end{pmatrix}, \; D_{\lambda l}^{(i)} = \begin{pmatrix} 1 & -1 \\ 0 & 0 \end{pmatrix}, \tag{3.54}$$

with $i = 1, 2$. And finally, for the axial stresses ($i = 3, \ldots, D$) we get:

$$A_{\lambda l}^{(i)} = \frac{1}{D-2} \begin{pmatrix} (D-4)(3-D) & 2-D \\ D-4 & 0 \end{pmatrix}, \; B_{\lambda l}^{(i)} = \frac{1}{D-2} \begin{pmatrix} 4-D & D-2 \\ 4-D & D-2 \end{pmatrix},$$
$$C_{\lambda l}^{(i)} = \frac{1}{D-2} \begin{pmatrix} (3-D)(D-6) & 4-D \\ D-2 & 0 \end{pmatrix}, \; D_{\lambda l}^{(i)} = \frac{1}{D-2} \begin{pmatrix} D-6 & 4-D \\ 0 & 0 \end{pmatrix}. \tag{3.55}$$

Note that, unlike to the case of the Minkowski bulk (see below), for the dS bulk the axial stresses do not coincide with the energy density.

For the off-diagonal component (3.48), the contribution of the first integral in (3.22) to the VEV vanishes. This directly follows from the relations $\sum_{m=0}^{\prime\infty} J_m(x) J_m'(x) = (1/2)\partial_x \sum_{m=0}^{\prime\infty} J_m^2(x)$ and $\sum_{m=0}^{\prime\infty} J_m^2(x) = 1/2$. The nonzero part is induced by the presence of the shell and is given by the expression

$$\langle T_0^1 \rangle_{\rm b} = -\frac{2B_D}{\alpha^{D+1}} \sum_{m=0}^{\infty\prime} \int_0^\infty dx\, x^{D+1} \left[(D-2) \frac{K_m(xa/\eta)}{I_m(xa/\eta)} - \frac{K_m'(xa/\eta)}{I_m'(xa/\eta)} \right] I_m(xr/\eta) I_m'(xr/\eta)$$
$$\times \int_0^1 ds\, s^2 \left(1-s^2\right)^{D/2-2} \left[K_{D/2-1}(y)\, I_{2-D/2}(y) - K_{D/2-2}(y)\, I_{D/2-1}(y) \right]_{y=xs} \tag{3.56}$$

In the special case $D = 3$ the off-diagonal component vanishes. For other values of D, for which the representation (3.56) is valid both the functions in the square brackets are positive and, hence, $\langle T_0^1 \rangle_{\rm b} < 0$ for $0 < r < a$. On the axis, the energy flux vanishes, $\langle T_0^1 \rangle_{{\rm b},r=0} = 0$. Similar to the case of the field squared, the boundary-induced VEVs (3.51) and (3.56) depend on η, a, r in the form of the ratios a/η and r/η.

With the expressions (3.51) and (3.56), we can see that the boundary-induced contributions obey the covariant continuity equation $\nabla_\nu \langle T_\mu^\nu \rangle_b = 0$. For the geometry at hand, this equation

is reduced to the following relations between the VEVs:

$$\begin{aligned}\left(\partial_\eta-\frac{D+1}{\eta}\right)\langle T_0^0\rangle_{\rm b} &= \left(\partial_r+\frac{1}{r}\right)\langle T_0^1\rangle_{\rm b}-\frac{1}{\eta}\langle T_k^k\rangle_{\rm b},\\ \left(\partial_\eta-\frac{D+1}{\eta}\right)\langle T_0^1\rangle_{\rm b} &= \frac{1}{r}\langle T_2^2\rangle_{\rm b}-\left(\partial_r+\frac{1}{r}\right)\langle T_1^1\rangle_{\rm b}.\end{aligned} \tag{3.57}$$

Let us denote by $\mathcal{E}_{{\rm b},r\leqslant r_0}$ the shell-induced contribution in the vacuum energy in the region $r\leqslant r_0<a$, per unit coordinate lengths along the directions $z^3,\ldots,z^D$:

$$\mathcal{E}_{{\rm b},r\leqslant r_0}=2\pi\,(\alpha/\eta)^D\int_0^{r_0}dr\,r\langle T_0^0\rangle_{\rm b}. \tag{3.58}$$

By taking into account the first equation in (3.57), the corresponding derivative with respect to the synchronous time coordinate t is expressed as

$$\partial_t\mathcal{E}_{{\rm b},r\leqslant r_0}=\frac{2\pi}{\alpha}\,(\alpha/\eta)^D\int_0^{r_0}dr\,r\sum_{l=1}^{D}\langle T_l^l\rangle_{\rm b}-2\pi r_0\,(\alpha/\eta)^{D-1}\,\langle T_0^1\rangle_{{\rm b},r=r_0}. \tag{3.59}$$

This relation shows that $\langle T_0^1\rangle_b$ is the energy flux per unit proper surface area. The quantity $-\langle T_l^l\rangle_b$ is the shell-induced contribution to the vacuum pressure along the l-th direction and the first term in the right-hand side of (3.59) is the work done by the surrounding on the selected volume. The last term in (3.59) is the energy flux through the surface $r=r_0$. Inside the shell one has $\langle T_0^1\rangle_{\rm b}<0$ and the flux is directed from the shell to the axis $r=0$.

Let us discuss special cases of the general expressions for the VEVs of the energy-momentum tensor components. First we consider the Minkowskian limit, corresponding to $\alpha\to\infty$. Introducing in (3.51) a new integration variable $y=x/\eta$, we see that the argument of the functions $f_\nu(u)$ is large and we can use the asymptotic expression $f_\nu(u)\approx 1/u$. After the integration over s, to the leading order we get $\langle T_i^i\rangle_b\approx\langle T_i^i\rangle_b^{({\rm M})}$, where for the VEVs on the Minkowski bulk one has (no summation over i)

$$\langle T_i^i\rangle_{\rm b}^{({\rm M})}=\frac{2(4\pi)^{-(D+1)/2}}{\Gamma((D+1)/2)}\sum_{m=0}^{\infty}{}'\sum_{\lambda=0,1}\int_0^\infty dx x^D\frac{K_m^{(\lambda)}(ax)}{I_m^{(\lambda)}(ax)}\left\{A_\lambda^{(i)}Z_m^{(i)}[I_m(rx)]+B_\lambda^{(i)}I_m^2(rx)\right\}, \tag{3.60}$$

with the coefficients

$$\begin{aligned}A_0^{(0)} &= (2-D)\,(D-3),\ A_1^{(0)}=D-3,\\ B_0^{(0)} &= (2-D)\,(D-5)\,,\ B_1^{(0)}=D-1,\\ A_\lambda^{(l)} &= (-1)^l\,B_\lambda^{(l)},\ B_0^{(l)}=(2-D)\,(D-1)\,,\ B_1^{(l)}=1-D,\end{aligned} \tag{3.61}$$

for $l=1,2$. For the stresses along the directions $i=3,\ldots,D$ we have $\langle T_i^i\rangle_b^{(\mathrm{M})}=\langle T_0^0\rangle_b^{(\mathrm{M})}$. In the special case $D=3$, from (3.60) we obtain the results previously derived in [152]. As is seen, for the Minkowski bulk the axial stresses are equal to the energy density. This result could be directly obtained on the base of the invariance of the problem with respect to the Lorentz boosts along the directions of the axis x^i, $i=3,\ldots,D$. The off-diagonal component vanishes in the Minkowskian limit. For the leading term in the corresponding asymptotic expansion from (3.56) we find

$$\langle T_0^1\rangle_{\mathrm{b}}\approx\frac{3-D}{\alpha}\frac{2^{1-D}\pi^{-(D+1)/2}}{\Gamma((D-1)/2)}{\sum_{m=0}}'\int_0^\infty dx\,x^{D-1}\left[(D-2)\frac{K_m(ax)}{I_m(ax)}-\frac{K_m'(ax)}{I_m'(ax)}\right]I_m(xr)I_m'(xr). \tag{3.62}$$

In the special case $D=3$ the off-diagonal component of the vacuum energy-momentum tensor vanishes, $\langle T_0^1\rangle_{\mathrm{b}}=0$, and the diagonal components are connected to the corresponding quantities for a cylindrical shell in the Minkowski bulk by the relation (no summation over i)

$$\langle T_i^i\rangle_{\mathrm{b}}=(\eta/\alpha)^4\langle T_i^i\rangle_{\mathrm{b}}^{(\mathrm{M})}. \tag{3.63}$$

In this special case $A_\lambda^{(i)}=0$ for $i=0,3$, and $B_0^{(i)}=B_1^{(i)}$ for all i. Note that the Casimir self-stress for an infinite perfectly conducting cylindrical shell in background of 4-dimensional Minkowski spacetime has been evaluated in [148] on the base of a Green's function technique. The corresponding Casimir energy was investigated by using the zeta function technique in [149] and the mode-by-mode summation method in [150]. The geometry of a cylindrical shell coaxial with a cosmic string was considered in [180, 182, 184].

Near the cylindrical shell, the asymptotic expressions for the components of the energy-momentum tensor are found in the way similar to that for the VEV of the electric field squared, by using the uniform asymptotic expansions for the modified Bessel functions. The leading terms are given by the expressions (no summation over i)

$$\langle T_i^i\rangle_{\mathrm{b}}\approx-\frac{(D-1)\,(D-3)\Gamma((D+1)/2)}{2(4\pi)^{(D+1)/2}[\alpha\,(a-r)\,/\eta]^{D+1}}, \tag{3.64}$$

for $i=0,2,\ldots,D$, and

$$\langle T_0^1\rangle_{\mathrm{b}}\approx\frac{a-r}{\eta}\langle T_0^0\rangle_b,\ \langle T_1^1\rangle_{\mathrm{b}}\approx\frac{a-r}{Da}\langle T_0^0\rangle_b. \tag{3.65}$$

The leading terms for the diagonal components coincide with those for a cylindrical shell in Minkowski bulk with the distance from the shell replaced by the proper distance $\alpha\,(a-r)\,/\eta$. In the special case $D=3$ the leading terms vanish. The latter feature is related to the conformal invariance of the electromagnetic field in $D=3$.

In the special case $D=4$, the integrals over s in (3.51) are evaluated in appendix 3.4.2. The expression for the diagonal components takes the form (no summation over i)

$$\begin{aligned}\langle T_i^i\rangle_{\rm b} &= \frac{\alpha^{-5}}{4\pi^3}\sum_{m=0}^{\infty}{}'\sum_{\lambda=0,1}\int_0^\infty dx x^5\frac{K_m^{(\lambda)}\,(ax/\eta)}{I_m^{(\lambda)}\,(ax/\eta)}\\ &\times\sum_{l=0,1}\Big\{(A_{\lambda l}^{(i)}\mathcal{I}_{1,1-l}(x)+B_{\lambda l}^{(i)}\mathcal{I}_{3,1-l}(x))Z_m^{(i)}[I_m(xr/\eta)]\\ &+(C_{\lambda l}^{(i)}\mathcal{I}_{1,1-l}(x)+D_{\lambda l}^{(i)}\mathcal{I}_{3,1-l}(x))I_m^2(xr/\eta)\Big\}\,,\end{aligned}\tag{3.66}$$

where the coefficients are given by (3.53), (3.54) and (3.55) with $D=4$. In the expression (3.56) for the energy flux, with $D=4$, the integral over s is evaluated by using the formulas (3.106) and (3.107). This leads to the following result:

$$\begin{aligned}\langle T_0^1\rangle_{\rm b} &= -\frac{\alpha^{-5}}{2\pi^3}\sum_{m=0}^{\infty}{}'\int_0^\infty dx\,x^4\left[2\frac{K_m(ax/\eta)}{I_m(ax/\eta)}-\frac{K_m'(ax/\eta)}{I_m'(ax/\eta)}\right]\\ &\times I_m(xr/\eta)I_m'(xr/\eta)I_1\,(x)\,K_1\,(x)\,.\end{aligned}\tag{3.67}$$

In figure 10 we have plotted the boundary-induced contribution in the energy density and the energy flux as functions of the proper distance from the shell axis, measured in units of the dS curvature scale α. For the corresponding value of the shell radius we have taken $a/\eta=2$. As is seen, in the interior region the energy density is negative near the shell and positive near the axis of the shell. The energy flux is negative inside the shell. This means that the energy flux is directed from the shell. The corresponding energy density in the Minkowski bulk is negative everywhere.

3.4 Exterior region

In the region outside the shell, $r>a$, the radial functions $C_m(x)$ in (3.7) and (3.8) are linear combinations of the Bessel and Neumann functions. The relative coefficients in the linear combinations are determined from the boundary condition (3.5) on the cylindrical surface

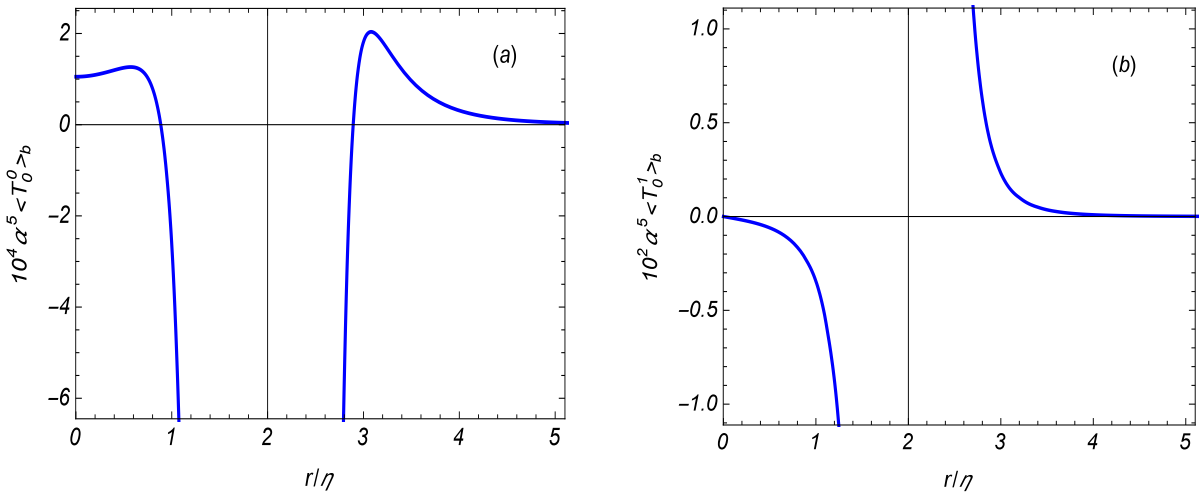

Figure 10: Shell-induced contribution in the VEV of the energy density (panel (a)) and the energy flux (panel (b)) as functions of the ratio r/η in the $D = 4$ model. The graphs are plotted for $a/\eta = 2$.

$r = a$. In this way we can see that

$$C_m(\gamma r) = g_m^{(\lambda)}(\gamma a, \gamma r) = J_m(\gamma r)Y_m^{(\lambda)}(\gamma a) - Y_m(\gamma r)J_m^{(\lambda)}(\gamma a), \tag{3.68}$$

for the modes $\lambda = 0, 1$. Now, in the normalization condition (3.13) the integration over the radial coordinate goes over the region $a \leqslant r < \infty$ and in the right-hand side the delta symbol for the quantum number γ is understood as the Dirac delta function $\delta(\gamma - \gamma')$. As the normalization integral diverges for $\gamma' = \gamma$, the main contribution to the integral comes from large values of r. By making use of the asymptotic formulas for the Bessel and Neumann functions with large arguments, for the normalization coefficients in (3.7) and (3.8) one gets

$$|c_\beta|^2 = \frac{[J_m^{(\lambda)2}(\gamma a) + Y_m^{(\lambda)2}(\gamma a)]^{-1}}{4\,(2\pi\alpha)^{D-3}\,\gamma}. \tag{3.69}$$

Similar to the case of the interior region, we consider the VEVs of the field squared and energy-momentum tensor separately.

3.4.1 VEV of the field squared

For the VEV of the electric field squared, by using the mode-sum formula (3.17), one finds

$$\begin{aligned}\langle E^2\rangle &= \frac{2^5 A_D \eta^{D+2}}{\alpha^{D+1}} \sum_{m=0}^{\infty}{}' \int_0^\infty dk k^{D-3} \int_0^\infty d\gamma \\ &\times \gamma^3 \sum_{\lambda=0,1} \frac{G_m^{(\lambda)}[k, g_m^{(\lambda)}(\gamma a, \gamma r)]}{J_m^{(\lambda)2}(\gamma a) + Y_m^{(\lambda)2}(\gamma a)} L_{D/2-2}(\omega\eta),\end{aligned} \tag{3.70}$$

with the same notations as in (4.15). With the help of the identity

$$\frac{G_m^{(\lambda)}[k, g_m^{(\lambda)}(\gamma a, \gamma r)]}{J_m^{(\lambda)2}(\gamma a) + Y_m^{(\lambda)2}(\gamma a)} = G_m^{(\lambda)}[J_m(\gamma r)] - \frac{1}{2} \sum_{j=0,1} \frac{J_m^{(\lambda)}(\gamma a)}{H_m^{(j)(\lambda)}(\gamma a)} G_m^{(\lambda)}[k, H_m^{(j)}(\gamma r)], \tag{3.71}$$

the VEV is presented in the decomposed form (3.27) where the shell-induced contribution is given by the expression

$$\begin{aligned}\langle E^2\rangle_{\rm b} &= -\frac{2^4 A_D \eta^{D+2}}{\alpha^{D+1}} \sum_{m=0}^{\infty}{}' \int_0^\infty dk k^{D-3} \sum_{j=0,1} \\ &\times \sum_{\lambda=0,1} \int_0^\infty d\gamma \gamma^3 \frac{J_m^{(\lambda)}(\gamma a)}{H_m^{(j)(\lambda)}(\gamma a)} L_{D/2-2}(\omega\eta).\end{aligned} \tag{3.72}$$

For the further transformation, in (3.72), we rotate the contour of integration in the complex plane γ by the angle $\pi/2$ for the term with $j = 1$ and by the angle $-\pi/2$ for $j = 2$. Introducing the modified Bessel functions, the expression (3.72) takes the form

$$\begin{aligned}\langle E^2\rangle_{\rm b} &= \frac{2^5 A_D}{\alpha^{D+1}} \sum_{m=0}^{\infty}{}' \sum_{\lambda=0,1} \int_0^\infty dx\, x^{D+1} \frac{I_m^{(\lambda)}(ax/\eta)}{K_m^{(\lambda)}(ax/\eta)} \\ &\times \int_0^1 ds s \left(1-s^2\right)^{D/2-2} G_m^{(\lambda)}\left[s, K_m(xr/\eta)\right] f_{D/2-2}(xs),\end{aligned} \tag{3.73}$$

where the functions $G_m^{(\lambda)}[s, f(x)]$ are defined by the formulae (3.31). Comparing this result with (3.30), we see that the expressions for the interior and exterior regions are related by the interchange $I_m \rightleftarrows K_m$. In particular, the result in the Minkowskian limit is obtained from (3.32) by the same replacements. In the special case $D = 3$ the electromagnetic field is conformally invariant and we have the relation (3.34). Similar to the case of the interior region, the shell-induced contribution (3.72) in the VEV of the electric field squared is positive. For points near the shell, the leading term in the asymptotic expansion over the distance from the boundary is obtained from (3.36) by the replacement $a - r \to r - a$.

At large proper distances from the shell compared with the dS curvature radius, we have $r/\eta \gg 1$. Introducing in (3.72) a new integration variable $y = xr/\eta$ and assuming that $r \gg a$, we use the expansions of the functions $I_m^{(\lambda)}(ya/r)/K_m^{(\lambda)}(ya/r)$ and $f_{D/2-2}(ys\eta/r)$ for small values of the arguments. The leading contribution comes from the term with $\lambda = 0$ and $m = 0$. For even $D > 4$ one gets

$$\langle E^2 \rangle_{\rm b} \approx \frac{4\,(4D^2-3D-4)\,\Gamma^3(D/2+1)}{\pi^{D/2}D(D-4)\Gamma(D+2)(\alpha r/\eta)^{D+2}}\frac{\alpha}{\ln(r/a)}. \tag{3.74}$$

In the case $D = 4$ the leading term is given by

$$\langle E^2 \rangle_{\rm b} \approx \frac{16\pi^{-2}\alpha(\alpha r/\eta)^{-6}}{5\ln(r/a)\ln(r/\eta)}. \tag{3.75}$$

For $D = 3$ and $D = 5$ we find

$$\begin{aligned} \langle E^2 \rangle_{\rm b} &\approx \frac{2(\alpha r/\eta)^{-4}}{3\pi\ln(r/a)},\ D=3, \\ \langle E^2 \rangle_{\rm b} &\approx \frac{7(\alpha r/\eta)^{-6}}{10\pi^2\ln(r/a)},\ D=5. \end{aligned} \tag{3.76}$$

At large distances, the total VEV is dominated by the boundary-free part $\langle E^2 \rangle_{\rm dS}$. For a cylindrical shell in the Minkowski bulk, at large distances, $r \gg a$, one has the following asymptotic behavior:

$$\left\langle E^2 \right\rangle_{\rm b}^{(\rm M)} \approx \frac{(D-2)\,(3D-1)}{\pi^{(D-1)/2}r^{D+1}\ln(r/a)}\frac{\Gamma^3((D+1)/2)}{(D-1)\,\Gamma(D+1)}, \tag{3.77}$$

for all values $D \geqslant 3$. Note that for $D = 3, 5$ the leading term (3.77) is obtained from (3.76) by the replacement of the proper distance from the axis, $\alpha r/\eta \to r$.

For the special case $D = 4$, the shell-induced contribution in the VEV of the squared electric field, for the exterior region, is presented in figure 1 as a function of the ratio r/η. Similar to the region inside the shell, the corresponding Casimir-Polder force is directed toward the shell.

3.4.2 Energy-momentum tensor

Now let us consider the VEV of the energy-momentum tensor outside the cylindrical shell. By using the mode-sum formula (3.40) with the exterior modes, for the VEV of the diagonal

components we get the following representation (no summation over i)

$$\langle T_i^i \rangle = \frac{B_D \eta^{D+2}}{\alpha^{D+1}} {\sum_{m=0}^{\infty}}' \int_0^\infty dk k^{D-3} \sum_{\lambda=0,1} \int_0^\infty d\gamma\gamma \times \sum_{l=1,2} \frac{t_{\lambda l}^{(i)}[k,\gamma,g_m^{(\lambda)}(\gamma a,\gamma r)]}{J_m^{(\lambda)2}(\gamma a)+Y_m^{(\lambda)2}(\gamma a)} L_{D/2-1-l}(\omega\eta), \tag{3.78}$$

with the notation (3.43). The expression for the off-diagonal component has the form

$$\langle T_0^1 \rangle = \frac{2iB_D \eta^{D+2}}{\alpha^{D+1}} {\sum_{m=0}^{\infty}}' \int_0^\infty dk k^{D-3} \int_0^\infty d\gamma\gamma \sum_{\lambda=0,1} (-1)^\lambda N_\lambda \omega\gamma^2 \times K_{D/2-2}(\omega\eta e^{-\frac{i\pi}{2}}) K_{D/2-1}(\omega\eta e^{\frac{i\pi}{2}}) \frac{g_m^{(\lambda)}(\gamma a,\gamma r) g_m^{(\lambda)\prime}(\gamma a,\gamma r)}{J_m^{(\lambda)2}(\gamma a)+Y_m^{(\lambda)2}(\gamma a)}, \tag{3.79}$$

where $g_m^{(\lambda)\prime}(x,y)=\partial_y g_m^{(\lambda)}(x,y)$.

Further transformation of the VEVs is similar to that we have used for the field squared. In the case of the diagonal components we employ the relation

$$\frac{t_{\lambda l}^{(i)}[k,\gamma,g_m^{(\lambda)}(\gamma a,\gamma r)]}{J_m^{(\lambda)2}(\gamma a)+Y_m^{(\lambda)2}(\gamma a)} = t_{\lambda l}^{(i)}[k,\gamma,J_m(\gamma r)] - \frac{1}{2}\sum_{j=1,2} \frac{J_m^{(\lambda)}(\gamma a)}{H_m^{(j)(\lambda)}(\gamma a)} t_{\lambda l}^{(i)}[k,\gamma,H_m^{(j)}(\gamma r)], \tag{3.80}$$

The part with the first term in the right-hand side coincides with the VEV in the boundary-free dS spacetime. In the part corresponding to the last term in (3.80) we rotate the integration contours by the angle $\pi/2$ for the term with $j=1$ and by the angle $-\pi/2$ for $j=2$. In this way for the boundary-induced contributions in the VEVs of the diagonal components we find (no summation over i)

$$\langle T_i^i \rangle_{\rm b} = \frac{B_D}{\alpha^{D+1}} {\sum_{m=0}^{\infty}}' \sum_{\lambda=0,1} \int_0^\infty dx x^{D+1} \frac{I_m^{(\lambda)}(ax/\eta)}{K_m^{(\lambda)}(ax/\eta)} \int_0^1 ds\, s \times \left(1-s^2\right)^{D/2-2} \sum_{l=0,1} P_{\lambda l}^{(i)}[s,K_m(xr/\eta)] f_{D/2-1-l}(xs). \tag{3.81}$$

In a similar way, the expression for the VEV of the off-diagonal component is presented as

$$\langle T_0^1 \rangle_{\rm b} = -\frac{2B_D}{\alpha^{D+1}} {\sum_{m=0}^{\infty}}' \int_0^\infty dx\, x^{D+1} \left[(D-2)\frac{I_m(xa/\eta)}{K_m(xa/\eta)} - \frac{I_m'(xa/\eta)}{K_m'(xa/\eta)}\right] K_m(xr/\eta) K_m'(xr/\eta) \times \int_0^1 ds\, s^2 \left(1-s^2\right)^{D/2-2} \left[K_{D/2-1}(y) I_{2-D/2}(y) - K_{D/2-2}(y) I_{D/2-1}(y)\right]_{y=xs}. \tag{3.82}$$

For $D \geqslant 4$, in the range of validity of this representation one has $\langle T_0^1 \rangle_{\rm b} > 0$. The corresponding energy flux is directed from the cylindrical shell to the infinity. Again, we can see that the shell-induced contributions obey the relations (3.57).

The VEVs in the Minkowskian limit, $\alpha \to \infty$, are obtained in the way similar to that for the interior region. In this limit the energy flux vanishes and the corresponding expressions for the diagonal components are obtained from (3.60) by the replacements $I_m \rightleftarrows K_m$. In the special case $D = 3$, the VEVs in the dS and Minkowski bulks are connected by the conformal relation (3.63).

For points near the shell, the leading terms in the asymptotic expansions over the distance from the boundary for the components $\langle T_i^i \rangle_{\rm b}$ with $i \neq 1$ are given by (3.64) with the replacement $a - r \to r - a$. For the normal stress and the energy flux we have the relations (3.65). Hence, near the shell and for $D > 3$, the boundary-induced contribution in the energy density has the same sign in the exterior and interior regions, whereas the normal stress and the energy flux have opposite signs.

Let us consider the asymptotics of the boundary-induced contributions at large distances from the shell. Introducing in (3.81) and (3.82) a new integration variable $y = xr$, we see that for $r \gg a, \eta$ the arguments of the functions $I_m^{(\lambda)}$, $K_m^{(\lambda)}$ and $f_{D/2-1-l}$ are small. By using the corresponding asymptotic expressions one can show that the dominant contribution comes from the term $m = 0$ and $\lambda = 0$. For even values of $D > 4$, to the leading order one gets the following expressions (no summation over i)

$$\begin{aligned} \langle T_i^i \rangle_{\rm b} &\approx \frac{2^{D-2}\Gamma^2(D/2+1)\Gamma^2(D/2)}{(D-2)\,(D-4)\,\Gamma(D+2)} \frac{\alpha B_D C_D^{(i)}}{(\alpha r/\eta)^{D+2}\ln(r/a)}, \\ \langle T_0^1 \rangle_{\rm b} &\approx \frac{2^{D-4} D \Gamma^4(D/2) B_D}{\Gamma(D)(\alpha r/\eta)^{D+1}\ln(r/a)}, \end{aligned} \tag{3.83}$$

with the coefficients

$$\begin{aligned} C_D^{(0)} &= D(D-1)\,(6-D) - 6, \\ C_D^{(1)} &= D\,(D-6) + 2, \\ C_D^{(2)} &= D^2\,(3-D) - 2, \\ C_D^{(l)} &= D^2\,(6-D) - 8D - 6, \end{aligned} \tag{3.84}$$

$l = 3, \ldots, D$. The corresponding energy density is positive. by taking into account that near the shell the energy density is negative for $D \geqslant 4$, we conclude that at some intermediate value of the radial coordinate the boundary-induced contribution in the energy density vanishes. The

asymptotic (3.83) for the energy flux is valid in the case $D = 4$ as well. For $D = 4$, the leading term in the expansion of the diagonal components is given by (no summation over i)

$$\langle T_i^i \rangle_{\rm b} \approx \frac{\alpha \ln(r/\eta) C_4^{(i)}}{20\pi^3 (\alpha r/\eta)^6 \ln(r/a)}, \tag{3.85}$$

where $C_4^{(0)} = -C_4^{(2)} = 3$, and $C_4^{(i)} = -1$ for $i = 1, 3, 4$. For the Minkowski bulk, the large distance asymptotic is given by (no summation over i)

$$\langle T_i^i \rangle_{\rm b}^{\rm (M)} \approx \frac{\pi^{-(D+1)/2} (2-D) \Gamma^3((D+1)/2)}{4 r^{D+1} \ln(r/a) (D-1) \Gamma(D+1)} C_{\rm (M)}^{(i)}, \tag{3.86}$$

where

$$\begin{aligned} C_{\rm (M)}^{(0)} &= D^2 - 4D + 1, \ i = 0, 3, \ldots, D, \\ C_{\rm (M)}^{(1)} &= 1 - D, \ C_{\rm (M)}^{(2)} = D(D-1). \end{aligned} \tag{3.87}$$

The corresponding energy density is positive for $D = 3$ and negative for $D \geqslant 4$.

The shell-induced contribution to the energy density and the energy flux in the exterior region are plotted in figure 2 for the $D = 4$ model. The large distance asymptotic is given by (3.85) and the energy density is positive. For points near the shell we have the asymptotic behavior (3.64), with the replacement $a - r \to r - a$, and the energy density is negative. Note that for the $D = 4$ Minkowski bulk the corresponding energy density is negative everywhere. For the $D = 3$ model, the energy density is positive in the exterior region and negative in the interior region.

In the discussion above we have considered the boundary condition (3.5) that generalizes the condition at the surface of a conductor for arbitrary number of spatial dimensions. Another type of boundary conditions for a gauge field is used in bag models of hadrons and in flux tube models of confinement in quantum chromodynamics (see, for instance, [142, 143, 300]). This boundary condition has the form

$$n^\mu F_{\mu\nu} = 0, \tag{3.88}$$

on the boundary of a volume inside of which the gluons are confined. In flux tube models the gauge field is confined inside a cylinder. The corresponding Casimir densities inside and outside a cylindrical shell are investigated in a way similar to that we have described above. The mode

functions still have the form (3.7) and (3.8). Imposing the boundary condition (3.88), we can see that, in the interior region, eigenvalues for γ are roots of the equation (3.12) for the mode $\sigma = 1$ and the roots of (3.11) for $\sigma = 2, \ldots, D-1$. The final expressions for the VEVs are obtained from those given above by the replacement

$$\frac{K_m^{(\lambda)}(xa/\eta)}{I_m^{(\lambda)}(xa/\eta)} \to \frac{K_m^{(1-\lambda)}(xa/\eta)}{I_m^{(1-\lambda)}(xa/\eta)}, \tag{3.89}$$

in both the interior and exterior regions. In particular, the VEV of the squared electric field is negative in these regions.

Appendix A3: Cylindrical modes in Minkowski spacetime

In this section we consider the cylindrical modes for the electromagnetic field in $(D+1)$-dimensional Minkowski spacetime. For the electromagnetic field one has $D-1$ polarization states specified by $\sigma = 1, 2, \ldots, D-1$. The vector potential for the polarization σ will be denoted by $A_{\sigma\mu}$, $\mu = 0, 1, \ldots, D$. We will impose the gauge condition $\nabla_{(\mathrm{M})\mu} A_\sigma^\mu = 0$, where $\nabla_{(\mathrm{M})\mu}$ is the covariant derivative operator associated with the Minkowskian metric tensor $g_{(\mathrm{M})\mu\nu} = \mathrm{diag}(1, -1, -r^2, -1, \ldots, -1)$. From the field equation $\nabla_{(\mathrm{M})\mu} F^{\mu\nu} = 0$ one gets

$$\left(\Delta - \partial_0^2\right) A_{\sigma\mu} = 0, \tag{3.90}$$

for $\mu = 0, 3, \ldots, D$, and

$$\begin{aligned} \left(\partial_0^2 - \Delta\right) A_{\sigma 1} + \frac{A_{\sigma 1}}{r^2} + \frac{2}{r^3}\partial_2 A_{\sigma 2} &= 0, \\ \partial_0^2 A_{\sigma 2} - \Delta A_{\sigma 2} + \frac{2}{r}\partial_1 A_{\sigma 2} - \frac{2}{r}\partial_2 A_{\sigma 1} &= 0, \end{aligned} \tag{3.91}$$

for the radial and azimuthal components. Here

$$\Delta = \frac{1}{r}\partial_1 (r\partial_1) + \frac{1}{r^2}\partial_2^2 + \sum_{l=3}^{D} \partial_l^2. \tag{3.92}$$

For the polarization $\sigma = 1$ we take

$$A_{\sigma\mu} = (0, -r^{-1}\partial_2, r\partial_1, 0, \ldots, 0)\psi_\sigma, \ \sigma = 1. \tag{3.93}$$

It can be easily checked that this function obeys the gauge condition. The field equations (3.91) are satisfied if the function ψ_σ obeys the equation

$$\left(\Delta - \partial_0^2\right)\psi_\sigma = 0. \tag{3.94}$$

For the polarizations $\sigma = 2, \ldots, D-1$ we present the vector potential in the form

$$A_{\sigma\mu} = \epsilon_{\sigma\mu}\psi_\sigma, \ \sigma = 2, \ldots, D-1, \tag{3.95}$$

with scalar functions ψ_σ and $\epsilon_{\sigma 1} = \epsilon_{\sigma 2} = 0$. From the field equations (3.90) it follows that the functions ψ_σ obey the wave equation (3.94). The gauge condition is reduced to

$$g^{\mu\nu}_{(\mathrm{M})}\epsilon_{\sigma\mu}\partial_\nu\psi_\sigma = 0. \tag{3.96}$$

The solutions for the scalar functions ψ_σ, $\sigma = 1, 2, \ldots, D-1$, have the form

$$\psi_\sigma = C_m(\gamma r)e^{i(m\phi + \mathbf{k}\cdot\mathbf{z} - \omega t)}, \tag{3.97}$$

where $C_m(x)$ is a cylinder function of the order $m = 0, \pm 1, \pm 2, \ldots$, $\mathbf{k}\cdot\mathbf{z} = \sum_{l=3}^{D} k_l z^l$, and ω is given by (3.9). We will normalize the polarization vectors in accordance with the relation

$$g^{\mu\nu}_{(\mathrm{M})}\epsilon_{\sigma\mu}\epsilon_{\sigma'\nu} = -\frac{\gamma^2}{\omega^2}\delta_{\sigma\sigma'}. \tag{3.98}$$

From the gauge condition one has $\epsilon_{\sigma 0} = -\mathbf{k}\cdot\epsilon_\sigma/\omega$, where $\mathbf{k}\cdot\epsilon_\sigma = \sum_{l=3}^{D} k_l\epsilon_{\sigma l}$. Combining with (3.98) the following relations are obtained:

$$\sum_{l,n=3}^{D}\left(\omega^2\delta_{nl} - k_l k_n\right)\epsilon_{\sigma l}\epsilon_{\sigma' n} = \gamma^2\delta_{\sigma\sigma'}, \tag{3.99}$$

and

$$\sum_{\sigma=2}^{D-1}\epsilon_{\sigma l}\epsilon_{\sigma n} = \omega^{-2}(k_l k_n + \gamma^2\delta_{ln}), \tag{3.100}$$

for $l, n = 3, \ldots, D$.

An alternative form for the cylindrical modes (3.95) with the polarizations $\sigma = 2, \ldots, D-1$ is obtained by making the gauge transformation

$$A'_{\sigma\mu} = A_{\sigma\mu} + \partial_\mu f_\sigma, \tag{3.101}$$

with the function

$$f_\sigma = i\omega^{-2}\mathbf{k}\cdot\epsilon_\sigma\psi_\sigma. \tag{3.102}$$

In the new gauge the scalar potential vanishes, $A'_{\sigma 0} = 0$, and one has

$$A'_{\sigma\mu} = \left(0, \left(\epsilon_{\sigma l} + i\omega^{-2}\mathbf{k}\cdot\epsilon_\sigma\partial_l\right)\psi_\sigma\right), \ l = 1, \ldots, D. \tag{3.103}$$

Hence, for $(D+1)$-dimensional Minkowski spacetime the cylindrical modes for the electromagnetic field in the gauge $A_{\sigma 0}=0$, $\partial_l(rA^l)=0$ are given by (3.93) and (3.103), where for the scalar function ψ_σ one has the expression (3.97). The radial function $C_m(\gamma r)$ is a linear combination of the Bessel and Neumann functions. The relative coefficient in this linear combination depends on the specific problem. For example, inside a cylindrical shell one has $C_m(\gamma r)\sim J_m(\gamma r)$. In the special case $D=3$, the modes (3.93) and (3.103) are reduced to the well known TE and TM modes in cylindrical waveguides (see, for instance, [301]). In the $(D+1)$-dimensional case we have a single mode of the TE type and $D-2$ modes of the TM type. The corresponding boundary conditions are discussed in section 4.1.

Appendix B3: Evaluation of the integrals in the model $D=4$

In this section we evaluate the integrals of the form (3.38) appearing in the expressions for the VEVs in the special case $D=4$. First of all, by using the integration formula from [302] we can see that

$$\begin{aligned}\mathcal{I}_{1,0}(x) &= \frac{1}{2}\left[f_0(x)+f_1(x)\right],\\ \mathcal{I}_{1,1}(x) &= \mathcal{I}_{1,0}(x)-\frac{2}{x}I_1(x)K_0(x).\end{aligned}\tag{3.104}$$

Our starting point in the evaluation of the remaining integrals is the formula (see, for instance, [302])

$$\int_0^1 ds\, sI_0(xs)\,K_0(ys)=-\frac{xI_1(x)\,K_0(y)+bI_0(x)\,K_1(y)-1}{y^2-x^2}.\tag{3.105}$$

Applying the operator $-\lim_{y\to x}\partial_y$ on the left and right hand sides of this formula we find

$$\int_0^1 ds\, s^2 I_0(xs)\,K_1(xs)=\frac{f_1(x)+1}{4x}.\tag{3.106}$$

Next, combining with the relation $I_0(x)\,K_1(x)=1/x-I_1(x)\,K_0(x)$ one gets

$$\int_0^1 ds s^2 I_1(xs)\,K_0(xs)=\frac{1-f_1(x)}{4x}.\tag{3.107}$$

For the evaluation of the integral $\mathcal{I}_{3,1}(x)$ we apply the operator $-2\lim_{y\to x}\partial_x\partial_y$ on the left- and right-hand sides of (3.105). This gives

$$\mathcal{I}_{3,1}(x)=\frac{2}{3x^2}\left[1-2xI_1(x)\,K_0(x)\right]+\frac{1}{6}\left[f_0(x)+\left(1-4/x^2\right)f_1(x)\right].\tag{3.108}$$

Integrating by parts the integral $\int_0^1 ds\, s^3 I_0'(xs)\, K_0'(xs)$ we can see that

$$\mathcal{I}_{3,0}(x) = \mathcal{I}_{3,1}(x) - \frac{2}{x} I_0(x)\, K_1(x) + \frac{4}{x}\int_0^1 ds s^2 I_0(sx)\, K_1(sx)\,. \tag{3.109}$$

By taking into account the relations (3.106) and (3.108) we obtain

$$\mathcal{I}_{3,0}(x) = \frac{1}{3x^2}\left[2xI_1(x)\, K_0(x) - 1\right] + \frac{1}{6}\left[f_0(x) + \left(1 + 2/x^2\right) f_1(x)\right]\,. \tag{3.110}$$

3.5 Summary

In the investigations of the Casimir effect the cylindrically symmetric boundaries are among the most popular geometries. In the present paper we have investigated the local Casimir densities for the electromagnetic field inside and outside a cylindrical shell in background of $(D+1)$-dimensional dS spacetime. On the shell, the field tensor obeys the boundary condition (3.5). In the special case $D = 3$ this corresponds to the perfect conductor boundary condition. The procedure, we employed for the evaluation of the VEVs bilinear in the field, is based on the mode-sum formula (3.16). In this procedure the complete set of cylindrical mode functions for the electromagnetic field, obeying the boundary condition, is required. In the problem under consideration one has a single mode of the TE type and $D-2$ modes of the TM type. For the Bunch-Davies vacuum state the corresponding vector potentials are given by the expressions (3.7) and (3.8) with the radial functions (3.10) and (3.68) for the exterior and interior regions, respectively.

We have investigated the combined effects of a cylindrical boundary and background gravitational field on the VEVs of the electric field squared and of the energy-momentum tensor. In the interior region the eigenvalues of the quantum number γ are expressed in terms of the zeros of the Bessel function $J_m(x)$ for the TM modes and in terms of the zeros of the derivative $J_m'(x)$ in the case of the TE mode. For the summation of the series over these zeros we have used the generalized Abel-Plana summation formula (1.125). This allowed us to extract from the VEVs the parts corresponding to the boundary-free dS spacetime and to present the shell-induced contributions in terms of strongly convergent integrals, for points away from the boundary. With this separation, the renormalization of the VEVs is reduced to the one for the boundary-free geometry. As a result, inside the shell, the VEVs are decomposed as (3.27) and

(3.50) with the shell-induced parts given by (3.30) for the electric field squared and by (3.51) for the diagonal components of the energy-momentum tensor. A similar decomposition is provided for the exterior region. The expressions for the shell-induced parts in this region differ from the ones inside the shell by the replacements $I_m \rightleftarrows K_m$ of the modified Bessel functions (see (3.73) and (3.81)). For both the interior and exterior regions the shell-induced contributions to the VEV of the electric field squared are positive. In addition to the diagonal components, the VEV of the energy-momentum tensor has nonzero off-diagonal component $\langle T_0^1 \rangle$. It corresponds to the energy flux along the radial direction and is given by the expressions (3.56) and (3.82) for the exterior and interior regions. The off-diagonal component is negative inside the shell and positive in the exterior region. This means that the energy flux is directed from the shell in both the regions. On the axis of the shell the flux vanishes.

We have considered various special cases of general formulas. In the limit $\alpha \to \infty$, the VEVs inside and outside a cylindrical shell in the background of $(D+1)$-dimensional Minkowski spacetime are obtained. The corresponding expressions generalize the results previously known for $D = 3$ to an arbitrary number of spatial dimensions. Note that for $D = 3$ the electromagnetic field is conformally invariant and the shell-induced VEVs in the dS bulk are obtained from those in Minkowski spacetime by the standard conformal transformation. For points near the cylindrical boundary the contribution of small wavelengths dominates in the shell-induced VEVs. The leading terms in the corresponding asymptotic expansions for the field squared and diagonal components of the energy-momentum tensor coincide with those for a cylindrical shell in the Minkowski bulk with the distance from the shell replaced by the proper distance in dS bulk. The leading term in the energy flux is given by the relation (3.65). The effects of the background gravitational field on the shell-induced VEVs are essential at distances from the boundary larger than the curvature radius of the dS spacetime. In particular, for the numerical example considered by us in the case $D = 4$, at large distances the shell-induced contribution to the vacuum energy density is negative for the Minkowski bulk and positive for dS background. Near the shell, the energy density is negative in both these cases. As a consequence, for the dS bulk it vanishes for some intermediate value of the radial coordinate.

Another boundary condition, used for the confinement of gauge fields in bag models of

hadrons and in flux tube models of QCD, is the one given by (3.88). The corresponding expressions for the VEVs of the field squared and energy-momentum tensor are obtained from those for generalized perfect conductor boundary condition by the replacement (3.89). In this case, the boundary-induced contribution on the VEV of the squared electric field is neagtive in both the interior and exterior regions.

4 CHAPTER: ELECTROMAGNETIC VACUUM FLUCTUATIONS AROUND A COSMIC STRING IN DE SITTER SPACETIME

The electromagnetic field correlators are evaluated around a cosmic string in background of $(D+1)$-dimensional dS spacetime assuming that the field is prepared in the Bunch-Davies vacuum state. The correlators are presented in the decomposed form where the string-induced topological parts are explicitly extracted. With this decomposition, the renormalization of the local VEVs in the coincidence limit is reduced to the one for dS spacetime in the absence of the cosmic string. The VEVs of the squared electric and magnetic fields, and of the vacuum energy density are investigated. Near the string they are dominated by the topological contributions and the effects induced by the background gravitational field are small. In this region, the leading terms in the topological contributions are obtained from the corresponding VEVs for a string on the Minkowski bulk multiplying by the conformal factor. At distances from the string larger than the curvature radius of the background geometry, the pure dS parts in the VEVs dominate. In this region, for spatial dimensions $D > 3$, the influence of the gravitational field on the topological contributions is crucial and the corresponding behavior is essentially different from that for a cosmic string on the Minkowski bulk. There are well-motivated inflationary models which produce cosmic strings. We argue that, as a consequence of the quantum-to-classical transition of super-Hubble electromagnetic fluctuations during inflation, in the postinflationary era these strings will be surrounded by large scale stochastic magnetic fields. These fields could be among the distinctive features of the cosmic strings produced during the inflation and also of the corresponding inflationary models.

4.1 Cylindrical electromagnetic modes

We consider $(D+1)$-dimensional locally dS background geometry described in cylindrical spatial coordinates $(r, \phi, \mathbf{z})$, $\mathbf{z} = \left(z^3, ..., z^D\right)$, by the interval

$$ds^2 = (\alpha/\tau)^2 \left[d\tau^2 - dr^2 - r^2 d\phi^2 - (d\mathbf{z})^2\right], \tag{4.1}$$

with the conformal time coordinate τ, $-\infty < \tau < 0$. The corresponding synchronous time t is expressed as $t = -\alpha \ln(|\tau|/\alpha)$, $-\infty < t < +\infty$. For the remaining coordinates we assume that $0 \leqslant r < \infty$, $0 \leqslant \phi \leqslant \phi_0$, $-\infty < z^l < +\infty$, $l = 3, \ldots, D$. For $\phi_0 = 2\pi$ the geometry is reduced to the standard dS one given in inflationary coordinates. In the case $\phi_0 < 2\pi$, though the local geometrical characteristics for $r \neq 0$ remain the same, the global properties are different. The special case $D = 3$ corresponds to a straight cosmic string with the core along the axis z^3 and with the planar angle deficit $2\pi - \phi_0$ determined by the linear mass density of the string. In [303, 304] it has been shown that the vortex solution of the Einstein-Abelian-Higgs equations in the presence of a cosmological constant induces a deficit angle into dS spacetime. The cosmological constant Λ is expressed in terms of the parameter α in the line element (4.1) by the relation $\Lambda = D(D-1)/(2\alpha^2)$.

The presence of the angle deficit gives rise to a number of interesting topological effect in quantum field theory. Here we are interested in the influence of the cosmic string on the vacuum fluctuations of the electromagnetic field. The properties of these fluctuations are encoded in the two-point functions which describe the correlations of the fluctuations at different spacetime points. These correlators are VEVs of bilinear combinations of the vector potential operator $A_\mu(x)$, where $x = (\tau, r, \phi, \mathbf{z})$ stands for the spacetime point. By expanding this operator in terms of a complete set $\{A_{(\beta)\mu}, A^*_{(\beta)\mu}\}$ of solutions to the classical Maxwell equations and by using the definition of the vacuum state $|0\rangle$, we can see that for a given bilinear combination $f(A_\mu(x), A_\nu(x'))$ the corresponding VEV is presented in the form of the mode sum

$$\langle 0|f(A_\mu(x), A_\nu(x'))|0\rangle = \sum_\beta f(A_{(\beta)\mu}(x), A^*_{(\beta)\nu}(x')). \tag{4.2}$$

Here, the set of quantum numbers β specifies the electromagnetic mode functions and in the right-hand side $\sum_\beta$ is understood as a summation over discrete quantum numbers and an integration over continuous ones. Hence, as the first stage, we need to find the complete set of cylindrical electromagnetic modes on dS bulk in the presence of the cosmic string.

It is convenient to fix the gauge degrees of the freedom by the Coulomb gauge with $A_0 = 0$ and $\partial_l(\sqrt{|g|}A^l) = 0$ for $l = 1, ..., D$. For the metric tensor

$$g_{\mu\nu} = (\alpha/\tau)^2 \operatorname{diag}(1, -1, -r^2, -1, \ldots, -1), \tag{4.3}$$

the latter equation is reduced to $\partial_l(rA^l) = 0$ and coincides with the corresponding equation in the Minkowski bulk. The procedure to find the complete set of solutions to the Maxwell equations is similar to that for the bulk in the absence of the cosmic string. The only difference is in the periodicity condition along the azimuthal direction ϕ. The corresponding part in the mode functions is given by $e^{iqm\phi}$ with $q = 2\pi/\phi_0$ and $m = 0, \pm 1, \pm 2, \ldots$. This leads to the dependence of the mode functions on the radial coordinate in terms of the Bessel function $J_{q|m|}(\gamma r)$ with $0 \leqslant \gamma < \infty$. The time-dependence appears in the form of the linear combination of the functions $\eta^{D/2-1}H^{(1)}_{D/2-1}(\omega\eta)$ and $\eta^{D/2-1}H^{(2)}_{D/2-1}(\omega\eta)$, where $\eta = |\tau| = \alpha e^{-t/\alpha}$ and $H^{(l)}_{\nu}(y)$, $l = 1, 2$, are the Hankel functions. The relative coefficient in the linear combination depends on the choice of the vacuum state under consideration. Here we assume that the field is prepared in the state that is the analog of the Bunch-Davies vacuum state for a scalar field. For this state the coefficient of the function $H^{(2)}_{D/2-1}(\omega\eta)$ is zero.

In $(D+1)$-dimensional spacetime, the electromagnetic field has $D-1$ polarization states. In what follows we specify them by the quantum number $\sigma = 1, \ldots, D-1$. For the polarization $\sigma = 1$ the cylindrical electromagnetic modes corresponding to the Bunch-Davies vacuum are presented as

$$A_{(\beta)\mu}(x) = c_\beta \eta^{D/2-1} H^{(1)}_{D/2-1}(\omega\eta) \left(0, \frac{iqm}{r}, -r\partial_r, 0, \ldots, 0\right) J_{q|m|}(\gamma r) e^{iqm\phi + i\mathbf{k}\cdot\mathbf{z}}, \tag{4.4}$$

and for the polarizations $\sigma = 2, \ldots, D-1$ we get

$$A_{(\beta)\mu}(x) = c_\beta \omega \eta^{D/2-1} H^{(1)}_{D/2-1}(\omega\eta) \left(0, \epsilon_{\sigma l} + i\frac{\mathbf{k}\cdot\epsilon_\sigma}{\omega^2}\partial_l\right) J_{q|m|}(\gamma r) e^{iqm\phi + i\mathbf{k}\cdot\mathbf{z}}, \tag{4.5}$$

with $l = 1, \ldots, D$. Here, $\mathbf{k} = (k_3, \ldots, k_D)$, $\omega = \sqrt{\gamma^2 + k^2}$ and $k^2 = \sum_{l=3}^{D} k_l^2$. For the scalar products one has $\mathbf{k}\cdot\mathbf{z} = \sum_{l=3}^{D} k_l z^l$ and $\mathbf{k}\cdot\epsilon_\sigma = \sum_{l=3}^{D} k_l \epsilon_{\sigma l}$. The spatial components in (4.4) and (4.5) are given in cylindrical coordinates $(r, \phi, \mathbf{z})$. For the components of the polarization vector we have $\epsilon_{\sigma 1} = \epsilon_{\sigma 2} = 0$, $\sigma = 2, \ldots, D-1$, and the relations

$$\begin{aligned} \sum_{l,n=3}^{D} \left(\omega^2\delta_{nl} - k_l k_n\right) \epsilon_{\sigma l}\epsilon_{\sigma' n} &= \gamma^2 \delta_{\sigma\sigma'}, \\ \omega^2 \sum_{\sigma=2}^{D-1} \epsilon_{\sigma n}\epsilon_{\sigma l} - k_n k_l &= \gamma^2 \delta_{nl}, \end{aligned} \tag{4.6}$$

for $l, n = 3, ..., D$. The mode functions are specified by the set of quantum numbers $\beta =$

$(\gamma, m, \mathbf{k}, \sigma)$ and in (4.2)

$$\sum_{\beta} = \sum_{\sigma=1}^{D-1} \sum_{m=-\infty}^{\infty} \int d\mathbf{k} \int_0^{\infty} d\gamma. \tag{4.7}$$

We have a single mode of the TE type ($\sigma = 1$) and $D-2$ modes of the TM type ($\sigma = 2, \ldots, D-1$).

The mode functions for vector fields are orthonormalized by the condition

$$\int d^D x \sqrt{|g|} g^{00} [A^*_{(\beta')\nu}(x) \nabla_0 A^{\nu}_{(\beta)}(x) - (\nabla_0 A^*_{(\beta')\nu}(x)) A^{\nu}_{(\beta)}(x)] = 4i\pi\delta_{\beta\beta'}, \tag{4.8}$$

where ∇_μ stands for the covariant derivative and $\delta_{\beta\beta'}$ is understood as the Kronecker symbol for discrete components of the collective index β (m and σ) and the Dirac delta function for the continuous ones (γ and $\mathbf{k}$). From (4.8) for the normalization coefficient c_β we get

$$|c_\beta|^2 = \frac{q}{4(2\pi\alpha)^{D-3}\gamma}, \tag{4.9}$$

for all the polarizations $\sigma = 1, \ldots, D-1$.

The Minkowskian limit of the problem under consideration corresponds to $\alpha \to \infty$ for a fixed value of the proper time t. In this limit one has $\eta = \alpha e^{-t/\alpha} \approx \alpha - t$ and, up to the phase (that can be absorbed into the normalization coefficient c_β), the function $\eta^{D/2-1} H^{(1)}_{D/2-1}(\omega\eta)$ is reduced to $\sqrt{2/(\pi\omega)}\alpha^{(D-3)/2} e^{-i\omega t}$. As a result, from (4.4) and (4.5) one gets the corresponding mode functions for a string in background of $(D+1)$-dimensional Minkowski spacetime. The case $D = 3$ has been considered previously in [297]. The electromagnetic field is conformally invariant in $D = 3$ and the modes (3.7) and (3.8) coincide with the Minkowskain modes having the time dependence $e^{-i\omega\eta}$.

4.2 Two-point functions

We consider a free field theory (the only interaction is with the background gravitational field) and all the information about the vacuum state is encoded in two-point functions. Given the complete set of normalized mode functions for the vector potential, we can evaluate the two-point function $\langle 0|A_l(x)A_m(x')|0\rangle \equiv \langle A_l(x)A_m(x')\rangle$ for the electromagnetic field by using the mode-sum formula (4.2):

$$\langle A_l(x)A_m(x')\rangle = \sum_{\beta} A_{(\beta)l}(x)\, A^*_{(\beta)m}(x'), \tag{4.10}$$

with $\sum_{\beta}$ from (4.7). Substituting the functions (4.4), (4.5) and using the relation (4.6), the two-point function is presented in the form

$$\begin{aligned}\langle A_l(x)A_p(x')\rangle &= \frac{q\left(\eta\eta'\right)^{D/2-1}}{\pi^2\left(2\pi\alpha\right)^{D-3}}\sum_{m=-\infty}^{\infty}e^{imq\Delta\phi}\int d\mathbf{k}\,e^{i\mathbf{k}\cdot\Delta\mathbf{z}} \\ &\times\int_0^{\infty}d\gamma\,\frac{\gamma}{\omega^2}K_{D/2-1}(e^{-i\pi/2}\eta\omega)K_{D/2-1}(e^{i\pi/2}\eta'\omega)f_{lp}\left(k,\gamma,r,r'\right), \quad (4.11)\end{aligned}$$

where $\Delta\phi=\phi-\phi'$, $\Delta\mathbf{z}=\mathbf{z}-\mathbf{z}'$ and instead of the Hankel function we have introduced the Macdonald function $K_{\nu}(x)$. In (4.11), the functions of the radial coordinates are defined by the expressions

$$\begin{aligned}f_{11}\left(k,\gamma,r,r'\right) &= k^2J'_{q|m|}(\gamma r)J'_{q|m|}(\gamma r')+\left(k^2+\gamma^2\right)\frac{q^2m^2}{\gamma^2rr'}J_{q|m|}(\gamma r)J_{q|m|}(\gamma r'), \\ f_{12}\left(k,\gamma,r,r'\right) &= -i\frac{qm}{\gamma r}\left[rk^2J'_{q|m|}(\gamma r)J_{q|m|}(\gamma r')+r'\omega^2J'_{q|m|}(\gamma r')J_{q|m|}(\gamma r)\right], \\ f_{22}\left(k,\gamma,r,r'\right) &= \frac{q^2m^2}{\gamma^2}k^2J_{q|m|}(\gamma r)J_{q|m|}(\gamma r')+rr'\omega^2J'_{q|m|}(\gamma r)J'_{q|m|}(\gamma r'), \quad (4.12)\end{aligned}$$

and

$$\begin{aligned}f_{1l}\left(k,\gamma,r,r'\right) &= ik_l\gamma J'_{q|m|}(\gamma r)J_{q|m|}(\gamma r'), \\ f_{2l}\left(k,\gamma,r,r'\right) &= -qmk_lJ_{q|m|}(\gamma r)J_{q|m|}(\gamma r'), \\ f_{lp}\left(k,\gamma,r,r'\right) &= \left(\omega^2\delta_{lp}-k_lk_p\right)J_{q|m|}(\gamma r)J_{q|m|}(\gamma r'), \quad (4.13)\end{aligned}$$

with $l,p=3,\ldots,D-1$. The remaining nonzero components are found by using the relation

$$f_{lp}\left(k,\gamma,r,r'\right)=f^{*}_{pl}\left(k,\gamma,r',r\right). \quad (4.14)$$

Having the two-point functions we can evaluate the VEVs of the squared electric and magnetic fields. For the VEV of the squared electric field one has

$$\langle E^2\rangle=\lim_{x'\to x}C_E(x,x'), \quad (4.15)$$

where the corresponding two-point function is expressed as

$$C_E(x,x')=-g^{00'}(x,x')g^{lp'}(x,x')\partial_0\partial'_0\langle A_l(x)A_p(x')\rangle, \quad (4.16)$$

with the parallel propagator $g^{\mu\nu'}(x,x')$. For the geometry under consideration the nonzero

components of the latter are given by

$$\begin{aligned} g^{00'}(x,x') &= -g^{ll'}(x,x') = \frac{\eta\eta'}{\alpha^2}, \\ g^{11'}(x,x') &= rr'g^{22'}(x,x') = -\frac{\eta\eta'}{\alpha^2}\cos\Delta\phi, \\ rg^{21'}(x,x') &= -r'g^{12'}(x,x') = \frac{\eta\eta'}{\alpha^2}\sin\Delta\phi, \end{aligned} \tag{4.17}$$

where $l = 3, \ldots, D$.

By taking into account the representation (4.11) we find the expression

$$\begin{aligned} C_E(x,x') &= \frac{8q\,(\eta\eta')^{D/2+1}}{(2\pi)^{D-1}\,\alpha^{D+1}}\sum_{m=0}^{\infty}{}' \Big\{\cos(mq\Delta\phi)\left[(D-2)\mathcal{J}^{(0,2)}_{D/2-2} + (D-3)\mathcal{J}^{(1,1)}_{D/2-2}\right] \\ &+ \left[\cos(mq\Delta\phi)\cos\Delta\phi\left(\partial_r\partial_{r'} + \frac{q^2m^2}{rr'}\right) + \frac{qm}{rr'}\sin(mq\Delta\phi)\sin\Delta\phi\right. \\ &\left.\times\,(r\partial_r + r'\partial_{r'})\right]\left(\mathcal{J}^{(0,1)}_{D/2-2} + 2\mathcal{J}^{(1,0)}_{D/2-2}\right)\Big\}, \end{aligned} \tag{4.18}$$

where

$$\mathcal{J}^{(n,p)}_{\nu} = \int d\mathbf{k}\, e^{i\mathbf{k}\cdot\Delta\mathbf{z}}\int_0^{\infty} d\gamma\, k^{2n}\gamma^{2p-1}K_{\nu}(e^{-i\pi/2}\omega\eta)K_{\nu}(e^{i\pi/2}\omega\eta')J_{qm}(\gamma r)J_{qm}(\gamma r'). \tag{4.19}$$

The prime on the summation sign in (4.18) means that the term $m = 0$ should be taken with an additional coefficient $1/2$. The integrals (4.19) for $n = 0, 1$ and $p = 0, 1, 2$ are evaluated in Appendix. By using the corresponding results (4.81), (4.83) and (4.84), the correlator is presented as

$$\begin{aligned} C_E(x,x') &= \frac{16q\,(\eta\eta')^{D/2+1}}{\pi^{D/2}\alpha^{D+1}}\int_0^{\infty} du\, u^{D/2}e^{u(\eta^2+\eta'^2-|\Delta\mathbf{z}|^2)}K_{D/2-2}(2\eta\eta'u) \\ &\times\left\{\left[\partial_w w + 2\left(D/2-1-|\Delta\mathbf{z}|^2u\right)\right]\left[\cos\Delta\phi\,(\partial_w + b) - \frac{1}{w}\sin\Delta\phi\partial_{\Delta\phi}\right]\right. \\ &\left.+(D-2)\partial_w w + (D-3)\left(D/2-1-|\Delta\mathbf{z}|^2u\right)\right\}\sum_{m=0}^{\infty}{}'\cos(mq\Delta\phi)e^{-bw}I_{qm}(w), \end{aligned} \tag{4.20}$$

with the notations

$$w = 2rr'u,\ b = \frac{r^2+r'^2}{2rr'}. \tag{4.21}$$

For the further transformation of the expression (4.20) we use the formula [134]

$$\sum_{m=0}^{\infty}{}'\cos(qm\Delta\phi)I_{qm}(w) = \frac{1}{2q}\sum_{l}e^{w\cos(2l\pi/q-\Delta\phi)} - \frac{1}{4\pi}\sum_{j=\pm1}\int_0^{\infty}dy\frac{\sin(q\pi+jq\Delta\phi)e^{-w\cosh y}}{\cosh(qy)-\cos(q\pi+jq\Delta\phi)}, \tag{4.22}$$

where the summation in the first term on the right-hand side goes under the condition

$$-q/2+q\Delta\phi/(2\pi)\leqslant l\leqslant q/2+q\Delta\phi/(2\pi). \tag{4.23}$$

If $-q/2+q\Delta\phi/(2\pi)$ or $q/2+q\Delta\phi/(2\pi)$ are integers, then the corresponding terms in the first sum on the right-hand side of (4.22) should be taken with the coefficient 1/2. The application of (4.22) leads to the expression

$$C_E(x,x')=C_E^{(1)}(x,x')+\sin\Delta\phi\partial_{\Delta\phi}C_E^{(2)}(x,x'). \tag{4.24}$$

Here and below we use the notation

$$\begin{aligned}C_J^{(i)}(x,x') &= \frac{8\,(\eta\eta')^{D/2+1}}{\pi^{D/2}\alpha^{D+1}}\left[\sum_l g_J^{(i)}(x,x',-\cos(2l\pi/q-\Delta\phi))\right.\\ &\left.-\frac{q}{2\pi}\sum_{j=\pm1}\int_0^\infty dy\frac{\sin(q\pi+jq\Delta\phi)g_J^{(i)}(x,x',\cosh y)}{\cosh(qy)-\cos(q\pi+jq\Delta\phi)}\right],\end{aligned} \tag{4.25}$$

for $i=1,2$ and $J=E,M$. The function with $J=M$ will appear in the expression for the VEV of the squared magnetic field. The functions $g_J^{(i)}(x,x',y)$ in (4.25) have the representation

$$g_J^{(i)}(x,x',y)=\int_0^\infty du\,u^{D/2}e^{u(\eta^2+\eta'^2-|\Delta\mathbf{z}|^2-r^2-r'^2-2rr'y)}K_{\nu_J}(2\eta\eta'u)h_J^{(i)}(y,u), \tag{4.26}$$

where

$$\nu_J=\begin{cases}D/2-2, & J=E\\ D/2-1, & J=M\end{cases}. \tag{4.27}$$

For the electric field, the functions in the integrand of (4.26) are given by the expressions

$$\begin{aligned}h_E^{(1)}(y,u) &= (D-2-y\cos\Delta\phi)\left[1-u\left(r^2+r'^2+2rr'y\right)\right]\\ &\quad+(D-3-2y\cos\Delta\phi)\left(D/2-1-|\Delta\mathbf{z}|^2u\right),\\ h_E^{(2)}(y,u) &= \frac{1}{2rr'u}\left[u\left(r^2+r'^2+2rr'y\right)-2\left(D/2-1-|\Delta\mathbf{z}|^2u\right)\right].\end{aligned} \tag{4.28}$$

The functions $h_M^{(i)}(y,u)$ for the magnetic field will be defined below.

The contribution of the $l=0$ term in (4.25) to the function (4.24) corresponds to the correlator in dS spacetime in the absence of the cosmic string (for the two-point functions of vector fields, including the massive ones, see [205]). It is simplified to

$$C_E^{(\mathrm{dS})}(x,x')=\frac{2(D-1)}{(2\pi)^{D/2}\alpha^{D+1}}\int_0^\infty du\,u^{D/2}e^{uZ(x,x')}\left(D-u\frac{|\Delta\mathbf{x}|^2}{\eta\eta'}\right)K_{D/2-2}(u), \tag{4.29}$$

where $|\Delta\mathbf{x}|^2 = r^2 + r'^2 - 2rr'\cos\Delta\phi + |\Delta\mathbf{z}|^2$ is the square of the spatial distance between the points x and x' and we have defined the dS invariant quantity

$$Z(x,x') = 1 + \frac{(\Delta\eta)^2 - |\Delta\mathbf{x}|^2}{2\eta\eta'}. \tag{4.30}$$

For the latter one has $Z(x,x') = \cos[\sigma(x,x')/\alpha]$, with $\sigma(x,x')$ being the proper distance along the shortest geodesic connecting the points x and x' if they are spacelike separated. The integral in (4.29) is expressed in terms of the hypergeometric function. Separating the $l = 0$ terms in the expressions for $C_E^{(1)}(x,x')$ and $C_E^{(2)}(x,x')$, the remaining part in (4.24) corresponds to the contribution induced by the presence of the cosmic string.

For points x and x' close to each other, the dominant contribution to the integral in (4.29) comes from large values of u and we can use the corresponding asymptotic for the function $K_{D/2-2}(u)$. To the leading order, for the pure dS part this gives

$$C_E^{(\mathrm{dS})}(x,x') \approx \frac{2(D-1)\Gamma((D+1)/2)}{\pi^{(D-1)/2}\sigma^{D+1}(x,x')}\left[D - \frac{(D+1)|\Delta\mathbf{x}|^2}{|\Delta\mathbf{x}|^2 - (\Delta\eta)^2}\right]. \tag{4.31}$$

In this limit the effects of the background curvature are small. Note that, for points outside the cosmic string core, $r \neq 0$, the divergences in the coincidence limit of $C_E(x,x')$ are contained in the pure dS part $C_E^{(\mathrm{dS})}(x,x')$ only. This is related to the fact that in our simplified model the presence of the cosmic string does not change the local geometry at those points.

4.3 VEV of the squared electric field

The VEV of the squared electric field is obtained from (4.24) in the coincidence limit. Separating the pure dS part $C_E^{(\mathrm{dS})}(x,x')$, the remaining topological contribution is finite in that limit for $r \neq 0$. Consequently, the renormalization is reduced to the one in dS spacetime. The contribution of the last term in (4.24) to the cosmic string induced part in the VEV of the field squared vanishes. As a result, the VEV of the squared electric field is presented in the decomposed form

$$\langle E^2\rangle = \langle E^2\rangle_{\mathrm{dS}} + \frac{8\alpha^{-D-1}}{(2\pi)^{D/2}}\left[\sum_{l=1}^{[q/2]} g_E(r/\eta, s_l) - \frac{q}{\pi}\sin(q\pi)\int_0^\infty dy \frac{g_E(r/\eta,\cosh y)}{\cosh(2qy) - \cos(q\pi)}\right], \tag{4.32}$$

where $[q/2]$ is the integer part of $q/2$. In (4.32), $\langle E^2\rangle_{\mathrm{dS}}$ is the renormalized VEV in the absence of the cosmic string and the remaining part is induced by the cosmic string (topological part).

Here and in what follows we use the notation $s_l = \sin(\pi l/q)$ and

$$g_E(x,y) = \int_0^\infty du\, u^{D/2} K_{D/2-2}(u) e^{u-2x^2y^2u} \left[2ux^2y^2\left(2y^2 - D + 1\right) + (D-1)\left(D/2 - 2y^2\right)\right]. \tag{4.33}$$

If the parameter q is equal to an even integer the term $l = q/2$ in (4.32) should be taken with an additional coefficient 1/2. The VEV (4.32) depends on r and η in the form of the combination r/η. The latter property is a consequence of the maximal symmetry of dS spacetime. Note that, for a given η, the ratio $\alpha r/\eta$ is the proper distance from the string. Hence, r/η is the proper distance measured in units of the dS curvature scale α. From the maximal symmetry of dS spacetime and of the Bunch-Davies vacuum state we expect that the pure dS part does not depend on the spacetime point and $\langle E^2\rangle_{\rm dS} = {\rm const}\cdot\alpha^{-D-1}$.

For odd values of D the integral in (4.33) is expressed in terms of elementary functions. In particular, for $D = 3$ and $D = 5$ one has

$$\begin{aligned} g_E(x,y) &= -\sqrt{\frac{\pi}{2}}\frac{1}{4x^4y^4},\ D=3, \\ g_E(x,y) &= -\sqrt{\frac{\pi}{2}}\frac{1+y^2}{2x^6y^6},\ D=5. \end{aligned} \tag{4.34}$$

In these cases, the topological part in the squared electric field is written in terms of the function

$$c_n(q) = \sum_{l=1}^{[q/2]} s_l^{-n} - \frac{q}{\pi}\sin(q\pi)\int_0^\infty dy \frac{\cosh^{-n} y}{\cosh(2qy) - \cos(q\pi)}. \tag{4.35}$$

For even n, this function can be found by using the recurrence scheme described in [181]. In particular, one has $c_2(q) = (q^2-1)/6$ and

$$\begin{aligned} c_4(q) &= \frac{q^2-1}{90}\left(q^2+11\right), \\ c_6(q) &= \frac{q^2-1}{1890}(2q^4+23q^2+191). \end{aligned} \tag{4.36}$$

As a result, the corresponding VEVs are presented as

$$\langle E^2\rangle = \langle E^2\rangle_{\rm dS} - \frac{(q^2-1)\,(q^2+11)}{180\pi(\alpha r/\eta)^4}, \tag{4.37}$$

for $D = 3$ and

$$\langle E^2\rangle = \langle E^2\rangle_{\rm dS} - \frac{(q^2-1)\,(q^4+22q^2+211)}{1890\pi^2\,(\alpha r/\eta)^6}, \tag{4.38}$$

for $D=5$. In the case $D=3$ the electromagnetic field is conformally invariant and the topological part in (4.37) is obtained from the corresponding result for a cosmic string in Minkowski bulk by the standard conformal transformation. The latter is reduced to the multiplication of the Minkowskian result by the factor $(\eta/\alpha)^4$.

As it has been mentioned before, the Minkowskian limit corresponds to $\alpha\to\infty$ for a fixed value of the time coordinate t. In this case one has $\eta\approx\alpha-t$ and η is large. Hence, we need the asymptotic of the function (4.33) for small values of x. In this limit the dominant contribution to the integral comes from large values of u and using the asymptotic expression for the Macdonald function for large argument, to the leading order we find

$$g_E(x,y)\approx-\sqrt{\pi}\frac{\Gamma\left((D+1)/2\right)}{2^{D/2+2}x^{D+1}y^{D+1}}\left[2\left(D-3\right)y^2+D-1\right]. \tag{4.39}$$

As a consequence, for a string in the Minkowski bulk one gets

$$\langle E^2\rangle^{(M)}=-\frac{2\Gamma\left((D+1)/2\right)}{(4\pi)^{(D-1)/2}r^{D+1}}\left[\left(D-3\right)c_{D-1}(q)+\frac{D-1}{2}c_{D+1}(q)\right]. \tag{4.40}$$

For $D=3$, this result is conformally related to the topological part in (4.37). It is of interest to note that, though the electromagnetic field is not conformally invariant for $D=5$, the latter property is valid in this case as well: $\langle E^2\rangle^{(M)}=\left(\langle E^2\rangle-\langle E^2\rangle_{\rm dS}\right)(\alpha/\eta)^{D+1}$, for $D=3,5$.

Now let us consider the asymptotic behavior of the VEV (4.32) at large and small distances from the string. At large distances, $r/\eta\gg1$, we need the asymptotic expressions for the function $g_E(x,y)$ in the limit $x\gg1$. In this limit the dominant contribution to the integral in (4.33) comes from the region near the lower limit of the integration. By using the asymptotic expression for the Macdonald function for small argument, to the leading order we get

$$g_E(x,y)\approx\frac{2^{D/2-5}}{y^6x^6}\Gamma\left(\frac{D}{2}-2\right)\left[\left(D-1\right)\left(\frac{D}{2}-3\right)+2\left(4-D\right)y^2\right], \tag{4.41}$$

for $D>4$ and $g_E(x,y)\approx-3\ln(yx)/(2y^6x^6)$ for $D=4$. In the case $D>4$ this gives

$$\langle E^2\rangle\approx\langle E^2\rangle_{\rm dS}+\frac{\Gamma\left(D/2-2\right)}{4\pi^{D/2}\alpha^{D+1}\left(r/\eta\right)^6}\left[2\left(4-D\right)c_4(q)+\left(D-1\right)\left(\frac{D}{2}-3\right)c_6(q)\right], \tag{4.42}$$

with the functions (4.36). Note that for $D=5$ the asymptotic (4.42) coincides with the exact result (4.38). For $D=4$ the large distance asymptotic is given by

$$\langle E^2\rangle\approx\langle E^2\rangle_{\rm dS}-\frac{(q^2-1)\ln(r/\eta)}{630\pi^2\alpha^5(r/\eta)^6}(2q^4+23q^2+191). \tag{4.43}$$

Hence, at large distances from the string, $r/\eta \gg 1$, the topological part in the VEV of the electric field squared decays as $(\eta/r)^4$ for $D = 3$, as $\ln(r/\eta)(\eta/r)^6$ for $D = 4$ and as $(\eta/r)^6$ for $D > 4$. The pure dS part $\langle E^2\rangle_{\rm dS}$ is a constant and it dominates in the total VEV at large distances. Note that at large distances from the string the influence of the gravitational field on the VEV is essential. In the Minkowskian case the decay of the VEV is as $1/r^{D+1}$ (see (4.40)) and depends on the number of spatial dimension. For the dS bulk the VEV behaves as $1/r^6$ for all spatial dimensions $D > 4$.

At proper distances from the string smaller than the dS curvature radius one has $r/\eta \ll 1$ and the dominant contribution to the integral in (4.33) comes from large values of u. The topological part dominates near the string and by calculations similar to those for the Minkowskian limit we get

$$\langle E^2\rangle \approx (\eta/\alpha)^{D+1}\langle E^2\rangle^{(M)},\ r/\eta \ll 1, \tag{4.44}$$

with $\langle E^2\rangle^{(M)}$ given by (4.40). This result is natural because near the string the dominant contribution to the VEV comes from the fluctuations with wavelengths smaller than the curvature radius and the influence of the background gravitational field on the corresponding modes is weak.

The VEV of the electric field squared determines the Casimir-Polder interaction energy between the cosmic string and a neutral polarizable microparticle placed close to the string, $U(r) = -\alpha_P\langle E^2\rangle$, where α_P is the polarizability of the particle (in the absence of dispersion). The correlators of the electromagnetic field and the Casimir-Polder potential in the geometry of cosmic string on background of $D = 3$ Minkowski spacetime were investigated in [298, 299].

4.4 Magnetic field correlators and VEV of the energy density

As a next characteristic of the vacuum state we consider the VEV of the Lagrangian density:

$$\langle L\rangle = -\frac{1}{16\pi}g^{\mu\rho}g^{\nu\sigma}\langle F_{\mu\nu}F_{\rho\sigma}\rangle. \tag{4.45}$$

Note that the quantity $g^{\mu\rho}g^{\nu\sigma}\langle F_{\mu\nu}F_{\rho\sigma}\rangle$ is the Abelian analog of the gluon condensate in quantum chromodynamics. The VEV (4.45) is presented as the coincidence limit

$$\langle L\rangle = \lim_{x'\to x} C_L(x,x'), \tag{4.46}$$

with the corresponding correlator

$$C_L(x,x') = -\frac{1}{16\pi} g^{\mu\rho'}(x,x') g^{\nu\sigma'}(x,x') \langle F_{\mu\nu}(x) F_{\rho\sigma}(x') \rangle. \tag{4.47}$$

The latter is decomposed into the electric and magnetic parts as

$$C_L(x,x') = \frac{1}{8\pi} \left[C_E(x,x') - C_M(x,x') \right], \tag{4.48}$$

where the magnetic part is given by the expression

$$\begin{aligned} C_M(x,x') &= \frac{1}{2} g^{lm'}(x,x') g^{np'}(x,x') \langle F_{ln}(x) F_{mp}(x') \rangle \\ &= \left[g^{lm'}(x,x') g^{np'}(x,x') - g^{nm'}(x,x') g^{lp'}(x,x') \right] \partial_l \partial_{m'} \langle A_n(x) A_{p'}(x') \rangle. \end{aligned} \tag{4.49}$$

with the summation over the spatial indices $l,m,n,p = 1,2,\ldots,D$ (for a scheme to measure the correlation functions for cosmological magnetic fields based on TeV blazar observations see [305]).

By using (4.11), after long calculations, the magnetic part is presented in the form

$$\begin{aligned} C_M(x,x') &= \frac{2q\left(\eta\eta'\right)^{D/2+1}}{\pi^2 \left(2\pi\right)^{D-3} \alpha^{D+1}} \sum_{m=0}^{\infty}{}' \\ &\times \left\{ \left[\cos(mq\Delta\phi) \cos\Delta\phi \left(\partial_r \partial_{r'} + \frac{q^2 m^2}{r r'} \right) + \frac{qm}{r r'} \sin(mq\Delta\phi) \sin\Delta\phi \left(r\partial_r + r'\partial_{r'} \right) \right] \right. \\ &\left. \times \left((D-2)\, \mathcal{J}^{(0,1)}_{D/2-1} + 2\mathcal{J}^{(1,0)}_{D/2-1} \right) + \cos(mq\Delta\phi) \left[\mathcal{J}^{(0,2)}_{D/2-1} + (D-3) \mathcal{J}^{(1,1)}_{D/2-1} \right] \right\} \end{aligned} \tag{4.50}$$

By taking into account the representations for the functions $\mathcal{J}^{(n,p)}_{\nu}$ given in Appendix, for the correlator one gets

$$\begin{aligned} C_M(x,x') &= \frac{16q\left(\eta\eta'\right)^{D/2+1}}{\pi^{D/2} \alpha^{D+1}} \int_0^{\infty} du\, u^{D/2} e^{u(\eta^2+\eta'^2-|\Delta\mathbf{z}|^2)} K_{D/2-1}(2\eta\eta' u) \\ &\times \left\{ \left[(D-2)\partial_w w + 2\left(D/2 - 1 - |\Delta\mathbf{z}|^2 u \right) \right] \left[\cos\Delta\phi \left(\partial_w + b \right) - \frac{1}{w} \sin\Delta\phi \partial_{\Delta\phi} \right] \right. \\ &\left. + \partial_w w + (D-3)\left(D/2 - 1 - |\Delta\mathbf{z}|^2 u \right) \right\} \sum_{m=0}^{\infty}{}' \cos(mq\Delta\phi) e^{-bw} I_{qm}(w). \end{aligned} \tag{4.51}$$

The further transformation is similar to that employed for the electric field correlator. By using the formula (4.22) we find

$$C_M(x,x') = C^{(1)}_M(x,x') + \sin\Delta\phi \partial_{\Delta\phi} C^{(2)}_M(x,x'), \tag{4.52}$$

where the functions $C_M^{(i)}(x,x')$ are defined in (4.25) with $J=M$. In the corresponding definition the function $g_M^{(i)}(x,x',y)$ is given by the expression (4.26) with the functions in the integrand

$$\begin{aligned} h_M^{(1)}(y,u) &= \left[1-(D-2)\,y\cos\Delta\phi\right]\left[1-u\left(r^2+r'^2+2rr'y\right)\right] \\ &\quad +(D-3-2y\cos\Delta\phi)\left(D/2-1-|\Delta\mathbf{z}|^2u\right), \end{aligned} \tag{4.53}$$

and $h_M^{(2)}(y,u)=h_E^{(2)}(y,u)$. The contributions of the $l=0$ terms in (4.25) to (4.52) correspond to the correlator in dS spacetime in the absence of the cosmic string ($q=1$):

$$C_M^{(\mathrm{dS})}(x,x')=\frac{2(D-1)}{(2\pi)^{D/2}\alpha^{D+1}}\int_0^\infty du\,u^{D/2}e^{uZ(x,x')}\left(D-u\frac{|\Delta\mathbf{x}|^2}{\eta\eta'}\right)K_{D/2-1}(u), \tag{4.54}$$

For $D=3$ the electric and magnetic correlators coincide and, hence, the correlator for the Lagrangian density vanishes. For close points x and x', the leading term in the corresponding asymptotic expansion coincides with that for the correlator of the electric field, $C_M^{(\mathrm{dS})}(x,x')\approx C_E^{(\mathrm{dS})}(x,x')$, and is given by (4.31).

In (4.52), separating the $l=0$ terms in the expressions (4.25) for the functions $C_M^{(i)}(x,x')$, the remaining part is the contribution induced by the cosmic string. For $r\neq 0$, the latter is finite in the coincidence limit. The renormalization is required for the pure dS part only. Hence, for the VEV of the squared magnetic field,

$$\langle B^2\rangle=\lim_{x'\to x}C_M(x,x'), \tag{4.55}$$

one finds the decomposition

$$\langle B^2\rangle=\langle B^2\rangle_{\mathrm{dS}}+\frac{8\alpha^{-D-1}}{(2\pi)^{D/2}}\left[\sum_{l=1}^{[q/2]}g_M(r/\eta,s_l)-\frac{q}{\pi}\sin(q\pi)\int_0^\infty dy\frac{g_M(r/\eta,\cosh y)}{\cosh(2qy)-\cos(q\pi)}\right], \tag{4.56}$$

with the function

$$\begin{aligned} g_M(x,y) &= \int_0^\infty du\,u^{D/2}K_{D/2-1}(u)e^{u-2x^2y^2u}\left\{(D-1)D/2\right. \\ &\quad \left.-4(D-2)y^2+2x^2y^2u\left[2(D-2)y^2-D+1\right]\right\}. \end{aligned} \tag{4.57}$$

Similar to (4.32), if $q/2$ is an integer, the term $l=q/2$ in (4.56) should be taken with an additional coefficient $1/2$. Note that for $D>3$ the magnetic part of the field tensor is not a spatial vector. In (4.56), $\langle B^2\rangle_{\mathrm{dS}}$ is the corresponding renormalized quantity in the absence of

the cosmic string and, because of the maximal symmetry of dS spacetime, does not depend on the spacetime point. From the dimensional arguments we expect that $\langle B^2\rangle_{\rm dS} = {\rm const}\cdot\alpha^{-D-1}$. For $D = 3$, the VEV of the squared magnetic field has been investigated in [306] by using the adiabatic renormalization procedure. In this special case $\langle B^2\rangle_{\rm dS} = 19/(40\pi\alpha^4)$ (note the different units used here and in [306]).

For odd D, the function $g_M(x,y)$ is expressed in terms of the elementary functions. In particular, for $D = 3$ it coincides with $g_E(x,y)$, given by (4.34), and for $D = 5$ one has

$$g_M(x,y) = \sqrt{\frac{\pi}{2}}\frac{(3+x^2)\,y^2-1}{2x^6y^6},\ D=5. \tag{4.58}$$

In the latter case, the VEV of the squared magnetic field is presented as

$$\langle B^2\rangle = \langle B^2\rangle_{\rm dS} + \frac{(3+r^2/\eta^2)\,c_4(q)-c_6(q)}{2\pi^2\,(\alpha r/\eta)^6}, \tag{4.59}$$

where the functions $c_4(q)$ and $c_6(q)$ are defined in (4.36).

Let us consider the asymptotic behavior of the VEV (4.56) at large and small distances from the string. If the proper distance from the string is much smaller than the curvature radius of the dS spacetime one has $r/\eta \ll 1$. For small x the dominant contribution to (4.57) comes from large values of u. By using the corresponding asymptotic for the Macdonald function, to the leading order we get

$$\langle B^2\rangle \approx (\eta/\alpha)^{D+1}\,\langle B^2\rangle^{(M)}, \tag{4.60}$$

where

$$\langle B^2\rangle^{(M)} = \frac{2\Gamma\left((D+1)/2\right)}{(4\pi)^{(D-1)/2}r^{D+1}}\left[(D-3)\,(D-2)c_{D-1}(q) - \frac{D-1}{2}c_{D+1}(q)\right], \tag{4.61}$$

is the corresponding VEV for the cosmic string in Minkowski bulk. In particular, for $D = 3$ one has $\langle B^2\rangle^{(M)} = \langle E^2\rangle^{(M)}$ with $\langle E^2\rangle^{(M)}$ given by the last term in the right-hand side of (4.37).

At large distances from the string, $r/\eta \gg 1$, we need the asymptotic of the function $g_M(x,y)$ for large x. In this limit, the dominant contribution to the integral in (4.57) comes from the region near the lower limit of the integration and for the leading term one finds

$$g_M(x,y) \approx \frac{2^{D/2-5}}{y^4x^4}(D-1)\,(D-4)\,\Gamma(D/2-1). \tag{4.62}$$

For $D=4$ the leading term vanishes and we need to consider the next to the leading contribution:

$$g_M(x,y) \approx \frac{y^2-3/4}{y^6 x^6}. \tag{4.63}$$

By taking into account (4.36) and (4.62), at distances $r/\eta \gg 1$ one gets

$$\langle B^2 \rangle \approx \langle B^2 \rangle_{\rm dS} + \frac{(D-1)(D-4)\Gamma(D/2-1)}{360\pi^{D/2}\alpha^{D+1}(r/\eta)^4}\left(q^2-1\right)\left(q^2+11\right), \tag{4.64}$$

for $D \neq 4$ and

$$\langle B^2 \rangle \approx \langle B^2 \rangle_{\rm dS} + \frac{4c_4(q)-3c_6(q)}{2\pi^2\alpha^5\left(r/\eta\right)^6}, \tag{4.65}$$

for $D=4$. In the special case $D=3$, the asymptotic (4.64) coincides with the exact result.

In figure 11 we have plotted the topological contributions in the VEVs of the squared electric and magnetic fields, $\langle F^2 \rangle_t = \langle F^2 \rangle - \langle F^2 \rangle_{\rm dS}$, $F = E, B$, for $q = 2.5$ and for spatial dimensions $D = 3, 4, 5$ (the numbers near the curves). The full/dashed curves correspond to the electric/magnetic fields. In the case $D=3$ one has $\langle E^2 \rangle_t = \langle B^2 \rangle_t$. Note that for $D = 4, 5$ the VEVs of the squared electric and magnetic fields have opposite signs. The Casimir-Polder forces acting on a polarizable particle are attractive.

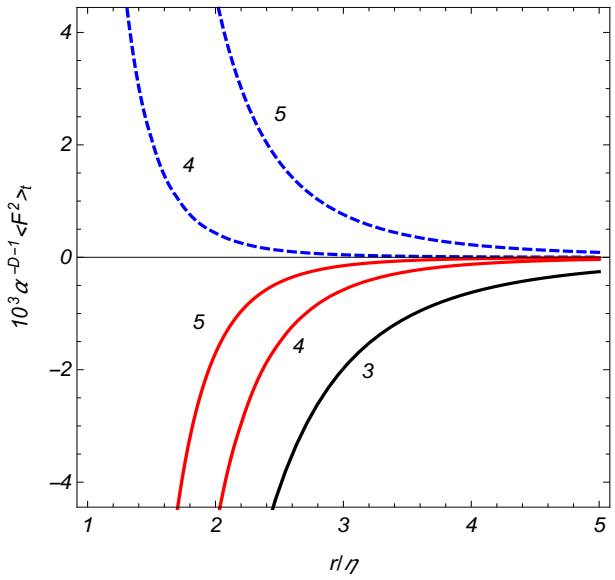

Figure 11: Topological contributions in the VEVs of the squared electric and magnetic fields for $q = 2.5$ and for spatial dimensions $D = 3, 4, 5$ (the numbers near the curves). The full/dashed curves correspond to the electric/magnetic fields.

Among the most interesting features of the inflation is the transition from quantum to classical behavior of quantum fluctuations during the quasiexponential expansion of the universe. An important example of this type of effects is the classicalization of the vacuum fluctuations of the inflaton field which underlies the most popular models of generation of large-scale structure in the universe. A similar effect of classicalization should take place for the electromagnetic fluctuations. In [306], the quantum-to-classical transition of super-Hubble magnetic modes during inflation has been considered as a possible mechanism for the generation of galactic and galaxy cluster magnetic fields (see also [307, 308] for the further discussion). As it has been discussed above, the presence of cosmic string induces shifts in the VEVs of the squared electric and magnetic fields. As a consequence of the quantum-to-classical transition of the corresponding fluctuations during the dS expansion, after inflation these shifts will be imprinted as classical stochastic fluctuations of the electric and magnetic fields surrounding the cosmic string. In the post inflationary radiation dominated era the conductivity is high and the currents in the cosmic plasma eliminate the electric fields whereas the magnetic counterparts are frozen. As a consequence, the cosmic strings will be surrounded by large scale magnetic fields. These fields would be among the distinctive features of the cosmic strings produced during the inflation and also of the corresponding inflationary models. Note that various types of mechanisms for the generation of primordial magnetic fields from cosmic strings in the post-inflationary era have been discussed in the literature (see, for instance, [309]-[316]). For cosmic strings carrying a nonzero magnetic flux in the core, azimuthal currents for charged fields are generated around the string (see [134] and references therein). These currents provide another mechanism for the generation of magnetic fields by the cosmic strings.

Having the VEVs for the squared electric and magnetic fields, we can find the VEV of the energy density ε as

$$\langle\varepsilon\rangle=\frac{\langle E^2\rangle+\langle B^2\rangle}{8\pi}. \tag{4.66}$$

It is decomposed into the pure dS part, $\langle\varepsilon\rangle_{\rm dS}$, and the topological contribution:

$$\langle\varepsilon\rangle=\langle\varepsilon\rangle_{\rm dS}+\frac{2\alpha^{-D-1}}{(2\pi)^{D/2+1}}\left[\sum_{l=1}^{[q/2]}g_0(r/\eta,s_l)-\frac{q}{\pi}\sin(q\pi)\int_0^\infty dy\frac{g_0(r/\eta,\cosh y)}{\cosh(2qy)-\cos(q\pi)}\right], \tag{4.67}$$

with $g_0(x,y)=g_E(x,y)+g_M(x,y)$. If q is equal to an even integer, the term $l=q/2$ in (4.67)

is taken with an additional coefficient 1/2. From the maximal symmetry of the dS spacetime it follows that $\langle\varepsilon\rangle_{\rm dS} = {\rm const}/\alpha^{D+1}$. In the special case $D = 3$ the latter is completely determined by the conformal anomaly (see, for instance, [70]): $\langle\varepsilon\rangle_{\rm dS} = 31/(480\pi^2\alpha^4)$. Combining this with the result for $\langle B^2\rangle_{\rm dS}$ we can find the VEV of the squared electric field: $\langle E^2\rangle_{\rm dS} = 1/(24\pi\alpha^4)$. In this case, the contributions of the electric and magnetic parts to the topological term in the VEV of the energy density are the same and the VEV is conformally related to the corresponding result on the Minkowski bulk found in [317].

Near the string, $r/\eta \ll 1$, the VEV of the energy density is dominated by the topological part and to the leading order one has

$$\langle\varepsilon\rangle \approx \frac{\Gamma\left((D+1)/2\right)}{(4\pi)^{(D+1)/2}(\alpha r/\eta)^{D+1}}\left[(D-3)^2\, c_{D-1}(q) - (D-1)\, c_{D+1}(q)\right]. \tag{4.68}$$

The corresponding VEV in the Minkowski bulk is obtained from the right hand side multiplying by the factor $(\alpha/\eta)^{D+1}$. Depending on the parameters D and q, the energy density (4.68) can be either negative or positive. For $D = 3$ it is always negative. At large distances from the cosmic string and for $D > 4$ the topological contribution in the energy density is dominated by the magnetic part and decays as $(\eta/r)^4$. For $D = 4$ and at large distances the electric part dominates and the energy density decays like $(\eta/r)^6 \ln(r/\eta)$. In figure 12 we display the dependence of the topological contribution in the vacuum energy density as a function of the proper distance from the string (measured in units of dS curvature scale). The graphs are plotted for spatial dimensions $D = 3, 4, 5$. As is seen, in general, the energy density is not a monotonic function of the distance from the string. Moreover, in the case $D = 5$ the energy density changes the sign: it is negative near the string (the electric part dominates) and positive at large distances from the string (the magnetic contribution dominates).

4.5 Appendix A4: Evaluation of the integrals

Here we describe the evaluation of the integrals (4.19) appearing in the expressions of the two-point functions for the electromagnetic field. By using the integral representation [319]

$$K_\nu(e^{-i\pi/2}\eta\omega)K_\nu(e^{i\pi/2}\eta'\omega) = \frac{1}{2}\int_{-\infty}^{+\infty} dy\, e^{-2\nu y}\int_0^\infty \frac{du}{u} e^{-u/2-\omega^2\beta/(2u)}, \tag{4.69}$$

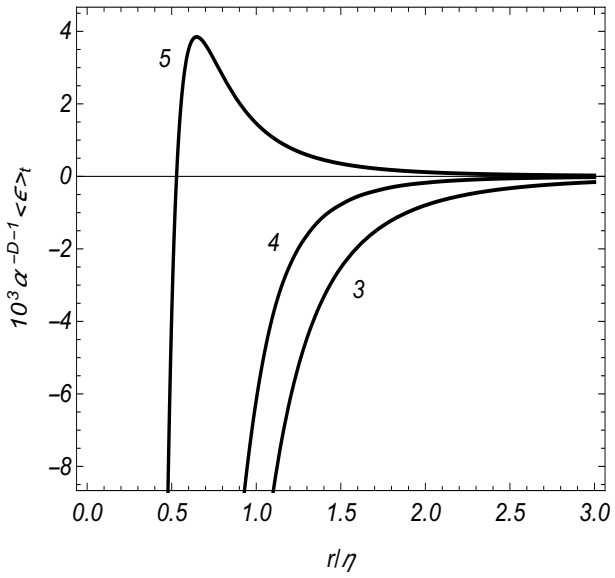

Figure 12: Topological contributions in the VEV of the energy density in spatial dimensions $D = 3, 4, 5$ (the numbers near the curves) for $q = 2.5$.

with the notation

$$\beta = 2\eta\eta' \cosh(2y) - \eta^2 - \eta'^2, \tag{4.70}$$

and redefining the integration variable $u/(2\beta) \to u$, one gets

$$\begin{aligned} \mathcal{J}_\nu^{(n,p)} &= \frac{1}{2} \int d\mathbf{k}\, e^{i\mathbf{k}\cdot\Delta\mathbf{z}} \int_{-\infty}^{+\infty} dy\, e^{-2\nu y} \int_0^\infty \frac{du}{u} e^{-u\beta} \\ &\quad \times \int_0^\infty d\gamma k^{2n} \gamma^{2p-1} e^{-\omega^2/4u} J_{qm}(\gamma r) J_{qm}(\gamma r'). \end{aligned} \tag{4.71}$$

The integration over $\mathbf{k}$ is done with the help of the formula

$$\int d\mathbf{k}\, k^{2n} e^{i\mathbf{k}\cdot\Delta\mathbf{z} - k^2/4u} = (4\pi)^{D/2-1} u^{D/2-1} \left[4u\left(D/2 - 1 - |\Delta\mathbf{z}|^2 u\right)\right]^n e^{-|\Delta\mathbf{z}|^2 u}, \tag{4.72}$$

where $n = 0, 1$. Next, the integral over y is expressed in terms of the function $K_\nu(2\eta\eta' u)$ and we find

$$\begin{aligned} \mathcal{J}_\nu^{(n,p)} &= \frac{1}{2}(4\pi)^{D/2-1} \int_0^\infty du\, u^{D/2-2} \left[4u\left(D/2 - 1 - |\Delta\mathbf{z}|^2 u\right)\right]^n e^{u\left(\eta^2 + \eta'^2 - |\Delta\mathbf{z}|^2\right)} \\ &\quad \times K_\nu(2\eta\eta' u) \int_0^\infty d\gamma \gamma^{2p-1} e^{-\gamma^2/4u} J_{qm}(\gamma r) J_{qm}(\gamma r'). \end{aligned} \tag{4.73}$$

For $p = 1, 2$ the integration over γ is done by using the formula [302]

$$\int_0^\infty d\gamma \gamma^{2p-1} e^{-\gamma^2/4u} J_{qm}(\gamma r) J_{qm}(\gamma r') = 2\left(4u^2 \partial_u\right)^{p-1} \left[u g(r, r', u)\right], \tag{4.74}$$

with the function

$$g(r,r',u) = e^{-(r^2+r'^2)u} I_{qm}(2rr'u). \tag{4.75}$$

For the evaluation of the integral in (4.73) with $p=0$ we use the integral representation

$$e^{-\gamma^2/4u} = \gamma^2 \int_{1/4u}^{\infty} dt\, e^{-t\gamma^2}, \tag{4.76}$$

and then apply the formula (4.74) with $p=1$ for the γ-integral. In this way, we can see that

$$\int_0^{\infty} d\gamma\, \frac{e^{-\gamma^2/4u}}{\gamma} J_{qm}(\gamma r) J_{qm}(\gamma r') = \frac{1}{2}\int_0^u \frac{dx}{x}\, g(r,r',x). \tag{4.77}$$

The corresponding integral in the two-point function (4.18) is acted by the operators with the results

$$(r\partial_r + r'\partial_{r'}) \int_0^u \frac{dx}{x}\, g(r,r',x) = 2e^{-bw} I_{qm}(w), \tag{4.78}$$

and

$$\left(\partial_r\partial_{r'} + \frac{q^2m^2}{rr'}\right) \int_0^u \frac{dx}{x}\, g(r,r',x) = 4ue^{-bw}\partial_w I_{qm}(w), \tag{4.79}$$

with the notations (4.21). In addition we have

$$\left(\partial_r\partial_{r'} + \frac{q^2m^2}{rr'}\right) g(r,r',u) = 4u\partial_w \left(we^{-bw}\partial_w I_{qm}(w)\right). \tag{4.80}$$

Hence, we get the following results

$$\begin{aligned} \mathcal{J}_\nu^{(n,p)} &= (4\pi)^{D/2-1} \int_0^{\infty} du\, u^{D/2-2} \left[4u\left(D/2-1-|\Delta\mathbf{z}|^2 u\right)\right]^n e^{u\left(\eta^2+\eta'^2-|\Delta\mathbf{z}|^2\right)} \\ &\quad \times K_\nu(2\eta\eta' u) \left(4u^2\partial_w\right)^{p-1} \left[we^{-bw} I_{qm}(w)\right], \end{aligned} \tag{4.81}$$

for $p=1,2$ and

$$\begin{aligned} \mathcal{J}_\nu^{(1,0)} &= \frac{1}{4}(4\pi)^{D/2-1} \int_0^{\infty} du\, u^{D/2-2} \left[4u\left(D/2-1-|\Delta\mathbf{z}|^2 u\right)\right]^n e^{u\left(\eta^2+\eta'^2-|\Delta\mathbf{z}|^2\right)} \\ &\quad \times K_\nu(2\eta\eta' u) \int_0^u \frac{dx}{x}\, g(r,r',x). \end{aligned} \tag{4.82}$$

The results for the latter integral after the action of the operators, appearing in (4.18), read

$$\begin{aligned} (r\partial_r + r'\partial_{r'})\, \mathcal{J}_\nu^{(1,0)} &= \frac{1}{2}(4\pi)^{D/2-1} \int_0^{\infty} du\, u^{D/2-2} \left[4u\left(D/2-1-|\Delta\mathbf{z}|^2 u\right)\right]^n \\ &\quad \times e^{u\left(\eta^2+\eta'^2-|\Delta\mathbf{z}|^2\right)} K_\nu(2\eta\eta' u) e^{-bw} I_{qm}(w), \end{aligned} \tag{4.83}$$

and

$$\left(\partial_r\partial_{r'}+\frac{q^2m^2}{rr'}\right)\mathcal{J}_\nu^{(1,0)} = (4\pi)^{D/2-1}\int_0^\infty du\,u^{D/2-1}\left[4u\left(D/2-1-|\Delta\mathbf{z}|^2u\right)\right]^n \times e^{u\left(\eta^2+\eta'^2-|\Delta\mathbf{z}|^2\right)}K_\nu(2\eta\eta'u)\partial_w\left[we^{-bw}\partial_w I_{qm}(w)\right]. \quad (4.84)$$

with w and b defined by (4.21).

4.6 Summary

We have investigated the influence of the cosmic string on the vacuum fluctuations of the electromagnetic field in background of $(D+1)$-dimensional dS spacetime, assuming that the field is prepared in the state which is the analog of the Bunch-Davies vacuum state for a scalar field. In the problem under consideration the only interaction of the quantum electromagnetic field is with the background gravitational field and the information on the vacuum fluctuations is encoded in the two-point functions. As such we have considered the Wightman function. For the evaluation of the latter we have used the direct summation over the complete set of electromagnetic cylindrical modes. The corresponding mode functions for separate polarizations are given by (4.4) and (4.5).

Among the most important characteristics of the electromagnetic vacuum are the VEVs of the squared electric and magnetic fields. The corresponding two-point functions are given by (4.24) and (4.51), respectively, with the function $C_J^{(i)}(x,x')$ defined in (4.25). One of the advantages for these representations is that the contribution corresponding to dS spacetime in the absence of the cosmic string is explicitly extracted. In the model of the cosmic string under consideration the local geometrical characteristics outside the string core are not changed by the presence of the string. Consequently, the divergences and the renormalization procedure for the VEVs are the same as those in pure dS spacetime. The topological parts do not require a renormalization. The renormalized VEVs for the squared electric and magnetic fields are presented in the decomposed form, Eqs. (4.32) and (4.56), respectively, where the first terms in the right-hand sides correspond to the renormalized VEVs in dS spacetime in the absence of the cosmic string. As a consequence of the maximal symmetry of dS spacetime and of the Bunch-Davies vacuum state these contributions do not depend on the spacetime coordinates.

The topological parts in the VEVs depend on the time and the radial coordinate through the ratio r/η which presents the proper distance from the string measured in units of the dS curvature radius. Near the string, the dominant contribution to the VEVs comes from the fluctuations with short wavelengths and the VEVs coincide with those for the string in Minkowski bulk with the distance from the string replaced by the proper distance $\alpha r/\eta$. The influence of the gravitational field on the topological contributions in the VEVs is crucial at proper distances larger than the curvature radius of the background geometry. This contribution in the electric field squared decays as $(\eta/r)^4$ for $D = 3$, as $\ln(r/\eta)(\eta/r)^6$ for $D = 4$ and as $(\eta/r)^6$ for $D > 4$. For the squared magnetic field the topological contribution decays as $(\eta/r)^4$ for $D \geqslant 3$. The exception is the case $D = 4$ where the corresponding coefficient vanishes and the next term in the expansion should be kept. In this case the topological term falls off as $(\eta/r)^6$. In the Minkowskian bulk the decay of the VEVs is as $1/r^{D+1}$ for both the electric and magnetic fields.

The modifications of the electromagnetic field vacuum fluctuations during the dS expansion phase, we have discussed here, will be imprinted in large-scale stochastic perturbations of the electromagnetic fields surrounding the cosmic string in the post-inflationary radiation dominated era. The magnetic fields will be frozen in the cosmic plasma whereas the electric fields will be eliminated by the induced currents.

We have also investigated the VEV of the electromagnetic energy density, induced by a cosmic string. Near the string the topological contribution dominates in the total VEV and the energy density behaves as $(\eta/r)^{D+1}$. At distances from the string larger than the curvature radius of the dS spacetime and for spatial dimensions $D > 4$, the topological part in the energy density is dominated by the magnetic contribution and decays as $(\eta/r)^4$. For $D = 4$ the electric field contribution dominates and at large distances the string-induced energy density behaves as $(\eta/r)^6 \ln(r/\eta)$. For $D = 3$ the topological contribution in the energy density is negative and decays as $(\eta/r)^4$ for all distances. For other spatial dimensions the energy density, in general, is not a monotonic function of the distance from the string. For example, in the case $D = 5$ the energy density is negative near the string and positive at large distances. It has a maximum for some intermediate value of the distance from the string.

CONCLUSIONS

1. For a scalar field with Robin boundary condition on a spherical shell in the background of a constant negative curvature space the Wightman function, the mean field squared and the VEV of the energy-momentum tensor are decomposed into the boundary-free and sphere-induced contributions. This reduces the renormalization procedure to the one for the space without boundaries. The corresponding results are generalized for spaces with spherical bubbles and for cosmological models with negative curvature spaces. For the coefficient in the boundary condition there is a critical value above which the scalar vacuum becomes unstable.

2. At distances from the sphere larger than the curvature scale of the background space the suppression of the vacuum fluctuations in the gravitational field corresponding to the negative curvature space is stronger compared with the case of the Minkowskian bulk. The decay of the VEVs with the distance is exponential for both massive and massless fields.

3. For a charged scalar field in spacetimes with toroidally compactified spatial dimensions and in the presence of planar boundaries, the nontrivial phases in quasiperiodicity conditions along compact dimensions and a constant gauge field induce vacuum current density. It is a periodic function of the magnetic flux, enclosed by compact dimensions, with the period equal to the flux quantum.

4. The current density does not contain surface divergences and for Dirichlet condition it vanishes on the boundaries. The normal derivative of the current density on the boundaries vanishes for both Dirichlet and Neumann conditions. There is a region in the space of the parameters in Robin boundary conditions where the vacuum state becomes unstable. The stability condition depends on the lengths of compact dimensions and is less restrictive than that for background with trivial topology.

5. Complete set of cylindrical modes is constructed for the electromagnetic field inside and outside a cylindrical shell in the background of $(D+1)$-dimensional dS spacetime and

the VEVs of the electric field squared and of the energy-momentum tensor are evaluated for the Bunch-Davies vacuum state. The shell-induced contribution in the electric field squared is positive for both the interior and exterior regions and the corresponding Casimir-Polder forces are directed toward the shell. The vacuum energy-momentum tensor, in addition to the diagonal components, has a nonzero off-diagonal component corresponding to the energy flux along the direction normal to the shell. The flux is directed from the shell in both the exterior and interior regions. The results are extended for confining boundary conditions of flux tube models in quantum chromodynamics.

6. The electromagnetic field correlators around a cosmic string in dS spacetime are presented in the form where the string-induced topological parts are explicitly extracted. With this decomposition, the renormalization of the local VEVs in the coincidence limit is reduced to the one for dS spacetime in the absence of the cosmic string. Near the string the VEVs of the squared electric and magnetic fields, and of the vacuum energy density are dominated by the topological contributions and the effects induced by the gravitational field are small. At distances from the string larger than the curvature radius of the background geometry, the pure dS parts in the VEVs dominate. In this region the influence of the gravitational field on the topological contributions is crucial and the corresponding behavior is essentially different from that for a cosmic string on the Minkowski bulk.

7. It is argued that, as a consequence of the quantum-to-classical transition of super-Hubble electromagnetic fluctuations during cosmological inflation, in the postinflationary era these strings will be surrounded by large scale stochastic magnetic fields. These fields could be among the distinctive features of the cosmic strings produced during the inflation and also of the corresponding inflationary models.

PUBLICATIONS IN THE TOPIC OF THESIS

1. S. Bellucci, A. A. Saharian, N. A. Saharyan, Wightman function and the Casimir effect for a Robin sphere in a constant curvature space, Eur. Phys. J. C **74**, 3047 (2014), 19 pages.

2. S. Bellucci, A. A. Saharian, N. A. Saharyan, Casimir effect for scalar current densities in topologically nontrivial spaces, Eur. Phys. J. C **75**, 378 (2015), 17 pages.

3. A. A. Saharian, V. F. Manukyan, N. A. Saharyan, Electromagnetic Casimir densities for a cylindrical shell on de Sitter space, Int. J. Mod. Phys. A **31**, No. 34, 1650183 (2016), 29 pages.

4. A. A. Saharian, V. F. Manukyan, N. A. Saharyan, Electromagnetic vacuum fluctuations around a cosmic string in de Sitter spacetime, Eur. Phys. J. C **77**, 478 (2017), 13 pages.

5. N. A. Saharyan, Casimir densities outside a constant curvature spherical bubble. Armenian Journal of Physics **10** (3), 112-121 (2017).

6. A. A. Saharian, V. F. Manukyan, N. A. Saharyan, Electromagnetic vacuum densities induced by cosmic string. Particles **1**, 13 (2018), 19 pages.

7. A. S. Kotanjyan, R. M. Avagyan, G. H. Harutunyan, N. A. Saharyan, Dynamics of the quasi-de Sitter model of the Early Universe. Physics of Atomic Nuclei **81**, 894-898 (2018).

ACKNOWLEDGMENTS

I am grateful to my supervisor Professor R. M. Avagyan for the constant help and advise, to my coathors for collaboration and to the members of the Chair of Theoretical Physics of the Yerevan State University for discussions of various questions related to the thesis.

References

[1] H.B.G. Casimir, On the attraction between two perfectly conducting plates. Proc. K. Ned. Akad. Wet. B **51**, 793 (1948).

[2] G. Plunien, B. Müller, W. Greiner, *The Casimir Effect*. Phys. Rep. **134**, 87 (1986).

[3] A.A. Grib, S.G. Mamayev, V.M. Mostepanenko, *Vacuum Quantum Effects in Strong Fields* (Friedmann Laboratory Publishing, St. Petersburg, 1994).

[4] E. Elizalde, S.D. Odintsov, A. Romeo, A.A. Bytsenko, S. Zerbini, *Zeta Regularization Techniques with Applications* (World Scientific, Singapore, 1994).

[5] V.M. Mostepanenko, N.N. Trunov, *The Casimir Effect and its Applications* (Clarendon, Oxford, 1997).

[6] M. Bordag, U. Mohideen, V.M. Mostepanenko, New developments in the Casimir effect. Phys. Rep. **353**, 1 (2001).

[7] K.A. Milton, *The Casimir Effect: Physical Manifestation of Zero-Point Energy* (World Scientific, Singapore, 2002).

[8] K.A. Milton, The Casimir effect: Recent controversies and progress. J. Phys. A **37**, R209 (2004).

[9] G.L. Klimchitskaya, U. Mohideen, V.M. Mostepanenko, The Casimir force between real materials: Experiment and theory. Rev. Mod. Phys. **81**, 1827 (2009).

[10] M. Bordag, G.L. Klimchitskaya, U. Mohideen, V.M. Mostepanenko, *Advances in the Casimir Effect* (Oxford University Press, Oxford, 2009).

[11] *Casimir Physics*, edited by D. Dalvit, P. Milonni, D. Roberts, and F. da Rosa, Lecture Notes in Physics Vol. 834 (Springer-Verlag, Berlin, 2011).

[12] S.K. Lamoreaux, The Casimir force and related effects: The status of the finite temperature correction and limits on new long-range forces. Annu. Rev. Nucl. Part. Sci. **62**, 37 (2012).

[13] H.B.G. Casimir, Introductory remarks on quantum electrodynamics, Physica **19**, 846 (1953).

[14] T.H. Boyer, Quantum Electromagnetic Zero-Point Energy of a Conducting Spherical Shell and the Casimir Model for a Charged Particle, Phys. Rev. **174**, 1764 (1968).

[15] B. Davies, Quantum Electromagnetic Zero-Point Energy of a Conducting Spherical Shell, J. Math. Phys. **13**, 1324 (1972).

[16] R. Balian, B. Duplantier, Electromagnetic waves near perfect conductors. II. Casimir effect, Ann. Phys. (N.Y.) **112**, 165 (1978).

[17] K.A. Milton, L.L. DeRaad, Jr., and J. Schwinger, Casimir effect in dielectrics, Ann. Phys. (N. Y.) **115**, 388 (1978).

[18] A. Romeo, Bessel ζ-function approach to the Casimir effect of a scalar field in a spherical bag, Phys. Rev. D **52**, 7308 (1995).

[19] S. Leseduarte, A. Romeo, Complete zeta-function approach to the electromagnetic Casimir effect for spheres and circles, Ann. Phys. **250**, 448 (1996).

[20] M. Bordag, E. Elizalde, K. Kirsten, Heat kernel coefficients of the Laplace operator on the D-dimensional ball, J. Math. Phys. **37**, 895 (1996).

[21] J.S. Dowker, Robin conditions on the Euclidean ball, Class. Quantum Grav. **13**, 1 (1996).

[22] M. Bordag, E. Elizalde, K. Kirsten, S. Leseduarte, Casimir energies for massive scalar fields in a spherical geometry, Phys. Rev. D **56**, 4896 (1997).

[23] V.V. Nesterenko, I.G. Pirozhenko, Simple method for calculating the Casimir energy for a sphere, Phys. Rev. D **57**, 1284 (1998).

[24] E. Elizalde, M. Bordag, K. Kirsten, Casimir energy for a massive fermionic quantum field with a spherical boundary, J. Phys. A: Math. Gen. **31**, 1743 (1998).

[25] M.E. Bowers, C.R. Hagen, Casimir energy of a spherical shell, Phys. Rev. D **59**, 025007 (1999).

[26] G. Lambiase, V.V. Nesterenko, and M. Bordag, Casimir energy of a ball and cylinder in the zeta function technique, J. Math. Phys. **40**, 6254 (1999).

[27] M. Schaden, L. Spruch, Infinity-free semiclassical evaluation of Casimir effects, Phys. Rev. A **58**, 935 (1998).

[28] M. Schaden, L. Spruch, Focusing virtual photons: Casimir energies for some pairs of conductors, Phys. Rev. Lett. **84**, 459 (2000).

[29] M. Schaden, Semiclassical estimates of electromagnetic Casimir self-energies of spherical and cylindrical metallic shells. Phys. Rev. A **82**, 022113 (2010).

[30] R.L. Jaffe, A. Scardicchio, Casimir effect and geometric optics, Phys. Rev. Lett. **92**, 070402 (2004).

[31] A. Scardicchio, R.L. Jaffe, Casimir effects: an optical approach I. Foundations and examples, Nucl. Phys. B **704**, 552 (2005).

[32] A. Scardicchio, R.L. Jaffe, Casimir effects: An optical approach II. Local observables and thermal corrections, Nucl.Phys. B **743**, 249 (2006).

[33] H. Gies, K. Langfeld, L. Moyaerts, Casimir effect on the worldline, J. High Energy Phys. **06** (2003) 018.

[34] H. Gies, K. Klingmuller, Casimir effect for curved geometries: Proximity-force-approximation validity limits, Phys. Rev. Lett. **96**, 220401 (2006).

[35] H. Gies, K. Klingmuller, Worldline algorithms for Casimir configurations, Phys. Rev. D **74**, 045002 (2006).

[36] M. Bordag, D. Robaschik, E. Wieczorek, Quantum field theoretic treatment of the casimir effect, Ann. Phys. **165**, 192 (1985).

[37] D. Robaschik, K. Scharnhorst, E. Wieczorek, Radiative corrections to the Casimir pressure under the influence of temperature and external fields, Ann. Phys. **174**, 401 (1987).

[38] R. Golestanian, M. Kardar, Mechanical Response of Vacuum, Phys. Rev. Lett. **78**, 3421 (1997).

[39] R. Golestanian, M. Kardar, Path-integral approach to the dynamic Casimir effect with fluctuating boundaries, Phys. Rev. A **58**, 1713 (1998).

[40] T. Emig, A. Hanke, R. Golestanian, M. Kardar, Probing the strong boundary shape dependence of the Casimir force, Phys. Rev. Lett. **87**, 260402 (2001).

[41] T. Emig, A. Hanke, R. Golestanian, M. Kardar, Normal and lateral Casimir forces between deformed plates, Phys. Rev. A **67**, 022114 (2003).

[42] R. Büscher, T. Emig, Geometry and spectrum of Casimir forces, Phys. Rev. Lett. **94**, 133901 (2005).

[43] C. Genet, A. Lambrecht, S. Reynaud, Casimir force and the quantum theory of lossy optical cavities, Phys. Rev. A **67**, 043811 (2003);

[44] A. Lambrecht, P.A. Maia Neto, S. Reynaud, The Casimir effect within scattering theory, New J. Phys. **8**, 243 (2006).

[45] O. Kenneth and I. Klich, Opposites Attract: A Theorem about the Casimir Force, Phys. Rev. Lett. **97**, 160401 (2006).

[46] T. Emig, N. Graham, R.L. Jaffe, M. Kardar, Casimir forces between arbitrary compact objects, Phys. Rev. Lett. **99**, 170403 (2007).

[47] T. Emig, N. Graham, R. L. Jaffe, M. Kardar, Casimir forces between compact objects: The scalar case, Phys. Rev. D **77**, 025005 (2008).

[48] K.A. Milton, J. Wagner, Multiple scattering methods in Casimir calculations, J. Phys. A **41**, 155402 (2008).

[49] O. Kenneth, I. Klich, Casimir forces in a T-operator approach, Phys. Rev. B **78**, 014103 (2008).

[50] P. A. Maia Neto, A. Lambrecht, S. Reynaud, Casimir energy between a plane and a sphere in electromagnetic vacuum, Phys. Rev. A **78**, 012115 (2008).

[51] A. Lambrecht, V.N. Marachevsky, Casimir Interaction of Dielectric Gratings, Phys. Rev. Lett. **101**, 160403 (2008).

[52] S. J. Rahi, T. Emig, N. Graham, R.L. Jaffe, M. Kardar, Scattering theory approach to electrodynamic Casimir forces, Phys. Rev. D **80**, 085021 (2009).

[53] S.J. Rahi, T. Emig, N. Graham, R.L. Jaffe, M. Kardar, Scattering theory approach to electrodynamic Casimir forces, Phys. Rev. D **80**, 085021 (2009).

[54] A.W. Rodriguez, M. Ibanescu, D. Iannuzzi, J.D. Joannopoulos, S.G. Johnson, Virtual photons in imaginary time: Computing exact Casimir forces via standard numerical electromagnetism techniques, Phys. Rev. A **76**, 032106 (2007).

[55] M.T. Homer Reid, A.W. Rodriguez, J. White, S.G. Johnson, Efficient computation of Casimir interactions between arbitrary 3D objects, Phys. Rev. Lett. **103**, 040401 (2009).

[56] C.M. Bender, K.A. Milton, Scalar Casimir effect for a D-dimensional sphere, Phys. Rev. D **50**, 6547 (1994).

[57] K.A. Milton, Vector Casimir effect for a D-dimensional sphere, Phys. Rev. D **55**, 4940 (1997).

[58] E. Cognola, E. Elizalde, K. Kirsten, Casimir energies for spherically symmetric cavities, J. Phys. A **34**, 7311 (2001).

[59] L.P. Teo, Casimir effect of the electromagnetic field in D-dimensional spherically symmetric cavities, Phys. Rev. D **82**, 085009 (2010).

[60] L.P. Teo, The Casimir interaction of a massive vector field between concentric spherical bodies, Phys. Lett. B **696**, 529 (2011).

[61] K. Olaussen, F. Ravndal, Electromagnetic vacuum fields in a spherical cavity, Nucl. Phys. B **192**, 237 (1981).

[62] K. Olaussen, F. Ravndal, Chromomagnetic vacuum fields in a spherical bag, Phys. Lett. B **100**, 497 (1981).

[63] I. Brevik, H. Kolbenstvedt, Electromagnetic Casimir densities in dielectric spherical media, Ann. Phys. (N.Y.) **149**, 237 (1983).

[64] I. Brevik, H. Kolbenstvedt, Casimir stress in spherical media when $\varepsilon\mu = 1$, Can. J. Phys. **62**, 805 (1984).

[65] L.Sh. Grigoryan, A.A. Saharian, Casimir effect for a perfectly conducting spherical surface, Dokl. Akad. Nauk Arm. SSR **83**, 28 (1986).

[66] L.Sh. Grigoryan, A.A. Saharian, Photon vacuum in a spherical layer between perfectly conducting surfaces, Izv. Akad. Nauk. Arm. SSR Fiz. **22**, 3 (1987) [J. Contemp. Phys. **22**, 1 (1987)].

[67] A.A. Saharian, The Generalized Abel-Plana Formula. Applications to Bessel Functions and Casimir Effect, Report No. IC/2000/14; hep-th/0002239.

[68] A.A. Saharian, *The Generalized Abel-Plana Formula with Applications to Bessel Functions and Casimir Effect* (YSU Publishing House, Yerevan, 2008).

[69] A.A. Saharian, Scalar Casimir effect for D-dimensional spherically symmetric Robin boundaries, Phys. Rev. D **63**, 125007 (2001).

[70] N.D. Birrell, P.C.W. Davies, *Quantum Fields in Curved Space* (Cambridge University Press, Cambridge, England, 1982).

[71] I.L. Buchbinder, S.D. Odintsov, I.L. Shapiro, *Effective Action in Quantum Gravity* (Taylor & Francis, New York, 1992).

[72] G. Esposito, A.Yu. Kamenshchik, and G. Pollifrone, *Euclidean Quantum Gravity on Manifolds with Boundary* (Kluwer, Dordrecht, 1997).

[73] S.A. Fulling, *Aspects of Quantum Field Theory in Curved Space-Time* (Cambridge University Press, Cambridge, England, 1996).

[74] V. Mukhanov, S. Winitzki, *Introduction to Quantum Effects in Gravity* (Cambridge University Press, Cambridge, England, 2007).

[75] L. Parker, D. Toms, *Quantum Field Theory in Curved Spacetime: Quantized Fields and Gravity* (Cambridge University Press, Cambridge, England, 2009).

[76] S. Hollands, R.M. Wald, Quantum fields in curved spacetime. Phys. Rep. **574**, 1 (2015).

[77] A.D. Linde, *Particle Physics and Inflationary Cosmology* (Harwood Academic Publishers, Chur, Switzerland 1990).

[78] B.A. Bassett, S. Tsujikawa, D. Wands, Inflation dynamics and reheating, Rev. Mod. Phys. **78**, 537 (2008).

[79] A. Cortijo, F. Guinea, M.A.H. Vozmediano, Geometrical and topological aspects of graphene and related materials, J. Phys. A: Math. Theor. **45**, 383001 (2012).

[80] A. Iorio, G. Lambiase, Quantum field theory in curved graphene spacetimes, Lobachevsky geometry, Weyl symmetry, Hawking effect, and all that. Phys. Rev. D **90**, 025006 (2014).

[81] A.A. Saharian and M.R. Setare, Casimir densities for a spherical shell in the global monopole background, Class. Quantum Grav. **20**, 3765 (2003).

[82] A.A. Saharian and M.R. Setare, Casimir densities for two concentric spherical shells in the global monopole space-time, Int. J. Mod. Phys. A **19**, 4301 (2004).

[83] A.A. Saharian, Quantum vacuum effects in the gravitational field of a global monopole, Astrophys. **47**, 260 (2004).

[84] A.A. Saharian, E.R. Bezerra de Mello, Spinor Casimir densities for a spherical shell in the global monopole spacetime, J. Phys. A **37**, 3543 (2004).

[85] E.R. Bezerra de Mello, A.A. Saharian, Spinor Casimir effect for concentric spherical shells in the global monopole spacetime, Class. Quantum Grav. **23**, 4673 (2006).

[86] E.R. Bezerra de Mello, A.A. Saharian, Vacuum polarization by a global monopole with finite core, J. High Energy Phys. 10(2006)049.

[87] E.R. Bezerra de Mello, A.A. Saharian, Polarization of the fermionic vacuum by a global monopole with finite core, Phys. Rev. D **75**, 065019 (2007).

[88] A.A. Saharian, M.R. Setare, Casimir densities for a spherical brane in Rindler-like spacetimes, Nucl. Phys. B **724**, 406 (2005).

[89] A.A. Saharian, M.R. Setare, Surface Casimir densities on a spherical brane in Rindler-like spacetimes, Phys. Lett. B **637**, 5 (2006).

[90] A.A. Saharian, M.R. Setare, Casimir densities for two spherical branes in Rindler-like spacetimes, J. High Energy Phys. 02(2007)089.

[91] M.R. Setare, R. Mansouri, Casimir effect for a spherical shell in de Sitter space, Class. Quantum Grav. **18**, 2331 (2001).

[92] M.R. Setare, Casimir stress for concentric spheres in de Sitter space, Class. Quant. Grav. **18**, 4823 (2001).

[93] K.A. Milton, A.A. Saharian, Casimir densities for a spherical boundary in de Sitter spacetime. Phys. Rev. D **85**, 064005 (2012).

[94] S. Bellucci, A.A. Saharian, A.H. Yeranyan, Casimir densities from coexisting vacua. Phys. Rev. D **89**, 105006 (2014).

[95] A. Linde, Creation of a compact topologically nontrivial inflationary Universe, JCAP **0410**, 004 (2004).

[96] V.P. Gusynin, S.G. Sharapov, J.P. Carbotte, AC conductivity of graphene: From tight-binding model to 2+1-dimensional quantum electrodynamics, Int. J. Mod. Phys. B **21**, 4611 (2007).

[97] A.H. Castro Neto, F. Guinea, N.M.R. Peres, K.S. Novoselov, A.K. Geim, The electronic properties of graphene, Rev. Mod. Phys. **81**, 109 (2009).

[98] M.J. Duff, B.E.W. Nilsson, C.N. Pope, Kaluza-Klein supergravity, Phys. Rep. **130**, 1 (1986).

[99] R. Camporesi, Harmonic analysis and propagators on homogeneous spaces, Phys. Rep. **196**, 1 (1990).

[100] A.A. Bytsenko, G. Cognola, L. Vanzo, S. Zerbini, Quantum fields and extended objects in space times with constant spatial section, Phys. Rep. **266**, 1 (1996).

[101] A.A. Bytsenko, G. Cognola, E. Elizalde, V. Moretti, S. Zerbini, *Analytic Aspects of Quantum Fields* (World Scientific, Singapore, 2003).

[102] E. Elizalde, *Ten Physical Applications of Spectral Zeta Functions* (Springer Verlag, 2012).

[103] F.C. Khanna, A.P.C. Malbouisson, J.M.C. Malbouisson, A.E. Santana, Quantum field theory on toroidal topology: algebraic structure and applications, Phys. Rep. **539**, 135 (2014).

[104] E. Elizalde, Matching the observational value of the cosmological constant, Phys. Lett. B **516**, 143 (2001).

[105] C.L. Gardner, Primordial inflation and present-day cosmological constant from extra dimensions, Phys. Lett. B **524**, 21 (2002).

[106] K.A. Milton, Dark energy as evidence for extra dimensions, Grav. Cosmol. **9**, 66 (2003).

[107] A.A. Saharian, Surface Casimir densities and induced cosmological constant on parallel branes in AdS spacetime, Phys. Rev. D **70**, 064026 (2004).

[108] E. Elizalde, Uses of zeta regularization in QFT with boundary conditions: a cosmo-topological Casimir effect, J. Phys. A **39**, 6299 (2006).

[109] A.A. Saharian, Surface Casimir densities and induced cosmological constant in higher dimensional braneworlds, Phys. Rev. D **74**, 124009 (2006).

[110] B. Green, J. Levin, Dark energy and stabilization of extra dimensions, J. High Energy Phys. 11 (2007) 096.

[111] P. Burikham, A. Chatrabhuti, P. Patcharamaneepakorn, K. Pimsamarn, Dark energy and moduli stabilization of extra dimensions in $M^{1+3} \times T^2$ spacetime, J. High Energy Phys. 07 (2008) 013.

[112] P. Chen, Dark energy and the hierarchy problem, Nucl. Phys. B (Proc. Suppl.) **173**, s8 (2009).

[113] V.M. Mostepanenko, I.Yu. Sokolov, The Casimir effect leads to new restrictions on long-range force constants, Phys. Lett. A **125**, 405 (1987).

[114] J.C. Long, H.W. Chan, J.C. Price, Experimental status of gravitational-strength forces in the sub-centimeter regime, Nucl. Phys. B **539**, 23 (1999).

[115] R.S. Decca, D. López, E. Fischbach, G.L. Klimchitskaya, D. E. Krause, V. M. Mostepanenko, Precise comparison of theory and new experiment for the Casimir force leads to stronger constraints on thermal quantum effects and long-range interactions, Ann. Phys. (N.Y.) **318**, 37 (2005); Tests of new physics from precise measurements of the Casimir pressure between two gold-coated plates, Phys. Rev. D **75**, 077101 (2007).

[116] G.L. Klimchitskaya, V.M. Mostepanenko, Improved constraints on the coupling constants of axion-like particles to nucleons from recent Casimir-less experiment, Eur. Phys. J. C **75**, 164 (2015).

[117] H.B. Cheng, The asymptotic behavior of Casimir force in the presence of compactified universal extra dimensions, Phys. Lett. B **643**, 311 (2006).

[118] H.B. Cheng, The Casimir force on a piston in the spacetime with extra compactified dimensions, Phys. Lett. B **668**, 72 (2008).

[119] S.A. Fulling, K. Kirsten, The Casimir force on a piston in the spacetime with extra compactified dimensions, Phys. Lett. B **671**, 179 (2009).

[120] K. Kirsten, S.A. Fulling, Kaluza-Klein models as pistons, Phys. Rev. D **79**, 065019 (2009).

[121] E. Elizalde, S.D. Odintsov, A.A. Saharian, Repulsive Casimir effect from extra dimensions and Robin boundary conditions: From branes to pistons, Phys. Rev. D **79**, 065023 (2009).

[122] L.P. Teo, Finite temperature Casimir effect in spacetime with extra compactified dimensions, Phys. Lett. B **672**, 190 (2009); L.P. Teo, Finite temperature Casimir effect in Kaluza-Klein spacetime, Nucl. Phys. B **819**, 431 (2009); L.P. Teo, Finite temperature Casimir effect for scalar field with Robin boundary conditions in spacetime with extra dimensions, J. High Energy Phys. 11 (2009) 095.

[123] K. Poppenhaeger, S. Hossenfelder, S. Hofmann, M. Bleicher, The Casimir effect in the presence of compactified universal extra dimensions, Phys. Lett. B **582**, 1 (2004).

[124] A. Edery, V.N. Marachevsky, Compact dimensions and the Casimir effect: the Proca connection, J. High Energy Phys. 12 (2008) 035.

[125] F. Pascoal, L.F.A. Oliveira, F.S.S. Rosa, C. Farina, Estimative for the size of the compactification radius of a one extra dimension Universe, Braz. J. Phys. **38**, 581 (2008).

[126] L. Perivolaropoulos, Vacuum energy, the cosmological constant, and compact extra dimensions: Constraints from Casimir effect experiments, Phys. Rev. D **77**, 107301 (2008).

[127] L.P. Teo, Electromagnetic Casimir piston in higher-dimensional spacetimes, Phys. Rev. D **83**, 105020 (2011).

[128] S. Bellucci, A.A. Saharian, Fermionic Casimir effect for parallel plates in the presence of compact dimensions with applications to nanotubes, Phys. Rev. D 80, 105003 (2009).

[129] E. Elizalde, S.D. Odintsov, A.A. Saharian, Fermionic condensate and Casimir densities in the presence of compact dimensions with applications to nanotubes, Phys. Rev. D 83, 105023 (2011).

[130] F.S. Khoo, L.P. Teo, Finite temperature Casimir effect of massive fermionic fields in the presence of compact dimensions, Phys. Lett. B 703, 199 (2011).

[131] M.R. Douglas, S. Kachru, Flux compactification, Rev. Mod. Phys. **79**, 733 (2007).

[132] S. Bellucci, A.A. Saharian, V.M. Bardeghyan, Induced fermionic current in toroidally compactified spacetimes with applications to cylindrical and toroidal nanotubes, Phys. Rev. D **82**, 065011 (2010).

[133] S. Bellucci, A.A. Saharian, H.A. Nersisyan, Scalar and fermionic vacuum currents in de Sitter spacetime with compact dimensions, Phys. Rev. D **88**, 024028 (2013).

[134] E.R. Bezerra de Mello, A.A. Saharian, V. Vardanyan, Induced vacuum currents in anti-de Sitter space with toral dimensions, Phys. Lett. B **741**, 155 (2015).

[135] E.R. Bezerra de Mello, A.A. Saharian, Finite temperature current densities and Bose-Einstein condensation in topologically nontrivial spaces, Phys. Rev. D **87**, 045015 (2013).

[136] S. Bellucci, E.R. Bezerra de Mello, A.A. Saharian, Finite temperature fermionic condensate and currents in topologically nontrivial spaces, Phys. Rev. D **89**, 085002 (2014).

[137] S. Bellucci, A.A. Saharian, Fermionic current from topology and boundaries with applications to higher-dimensional models and nanophysics, Phys. Rev. D **87**, 025005 (2013).

[138] S. Bellucci, A.A. Saharian, V. Vardanyan, Vacuum currents in braneworlds on AdS bulk with compact dimensions, JHEP 11(2015)092.

[139] S. Bellucci, A.A. Saharian, V. Vardanyan, Hadamard function and the vacuum currents in braneworlds with compact dimensions: Two-brane geometry. Phys. Rev. D **93**, 084011 (2016).

[140] S. Bellucci, A.A. Saharian, V. Vardanyan, Fermionic currents in AdS spacetime with compact dimensions, Phys. Rev. D **96**, 065025 (2017).

[141] S. Bellucci, A.A. Saharian, D. H. Simonyan, V. Vardanyan, Fermionic currents in topologically nontrivial braneworlds, Phys. Rev. D **98**, 085020 (2018).

[142] P.M. Fishbane, S.G. Gasiorowich, P. Kauss, Long-range dielectric confinement, Phys. Rev. D **36**, 251 (1987); P.M. Fishbane, S.G. Gasiorowich, P. Kauss, Zero-point energy in flux-tube confinement, Phys. Rev. D **37**, 2623 (1988).

[143] B.M. Barbashov, V.V. Nesterenko, *Introduction to the Relativistic String Theory* (World Scientific, Singapore, 1990).

[144] J. Ambjørn, S. Wolfram, Properties of the vacuum. I. Mechanical and thermodynamic, Ann. Phys. **147**, 1 (1983).

[145] M. Brown-Hayes, D.A.R. Dalvit, F.D. Mazzitelli, W.J. Kim, R. Onofrio, Towards a precision measurement of the Casimir force in a cylinder-plane geometry, Phys. Rev. A **72**, 052102 (2005).

[146] R.S. Decca, E. Fischbach, G.L. Klimchitskaya, D.E. Krause, D. López, V.M. Mostepanenko, Possibility of measuring the thermal Casimir interaction between a plate and a cylinder attached to a micromachined oscillator, Phys. Rev. A **82**, 052515 (2010).

[147] E. Noruzifar, T. Emig, U. Mohideen, R. Zandi, Collective charge fluctuations and Casimir interactions for quasi-one-dimensional metals, Phys. Rev. B **86**, 115449 (2012).

[148] L.L. De Raad Jr., K.A. Milton, Casimir self-stress on a perfectly conducting cylindrical shell, Ann. Phys. **136**, 229 (1981).

[149] P. Gosdzinsky, A. Romeo, Energy of the vacuum with a perfectly conducting and infinite cylindrical surface, Phys. Lett. B **441**, 265 (1998).

[150] K.A. Milton, A.V. Nesterenko, V.V. Nesterenko, Mode-by-mode summation for the zero point electromagnetic energy of an infinite cylinder, Phys. Rev. D **59**, 105009 (1999).

[151] I. Cavero-Peláez, K.A. Milton, Green's dyadic approach of the self-stress on a dielectric-diamagnetic cylinder with non-uniform speed of light, J. Phys. A **39**, 6225 (2006); I. Brevik, A. Romeo, Evaluation of the Casimir force for a dielectric-diamagnetic cylinder with light velocity conservation condition and the analogue of Sellmeir's dispersion law, Physics Scripta **76**, 48 (2007).

[152] A.A. Saharian, Vacuum expectation values of the energy–momentum tensor of electromagnetic field inside and outside the perfectly conducting cylindrical surface, Izv. AN Arm. SSR. Fizika **23**, 130 (1988) [Sov. J. Contemp. Phys. **23**, 14 (1988)].

[153] A.A. Saharian, Vacuum expectation values of the energy–momentum tensor of electromagnetic field for regions with cylindrically symmetric boundaries, Dokladi AN Arm. SSR **86**, 112 (1988) (Reports NAS RA, in Russian).

[154] F.D. Mazzitelli, M.J. Sanchez, N.N. Scoccola, J. von Stecher, Casimir interaction between two concentric cylinders: Exact versus semiclassical results, Phys. Rev. A **67**, 013807 (2002).

[155] K. Tatur, L. M. Woods, I. V. Bondarev, Zero-point energy of a cylindrical layer of finite thickness, Phys. Rev. A **78**, 012110 (2008).

[156] A. Romeo, A.A. Saharian, Vacuum densities and zero-point energy for fields obeying Robin conditions on cylindrical surfaces, Phys. Rev. D **63**, 105019 (2001).

[157] A.A. Saharian, A.S. Tarloyan, Scalar Casimir densities for cylindrically symmetric Robin boundaries, J. Phys. A **39**, 13371 (2006).

[158] K. Tatur, L.M. Woods, Zero-point energy of N perfectly conducting concentric cylindrical shells, Phys. Lett. A **372**, 6705 (2008).

[159] D.A.R. Dalvit, F.C. Lombardo, F.D. Mazzitelli, R. Onofrio, Casimir force between eccentric cylinders, Europhys. Lett. **67**, 517 (2004).

[160] F.D. Mazzitelli, D.A.R. Dalvit and F.C. Lombardo, Exact zero-point interaction energy between cylinders, New. J. Phys. **8**, 240 (2006).

[161] D.A.R. Dalvit, F.C. Lombardo, F.D. Mazzitelli, R. Onofrio, Exact Casimir interaction between eccentric cylinders, Phys. Rev. A **74**, 020101(R) (2006).

[162] S.J. Rahi, T. Emig, R.L. Jaffe, M. Kardar, Casimir forces between cylinders and plates, Phys. Rev. A **78**, 012104 (2008).

[163] A.W. Rodriguez, J.N. Munday, J.D. Joannopoulos, F. Capasso, D.A.R. Dalvit, S.G. Johnson, Casimir forces in the time domain: Theory, Phys. Rev. Lett. **101**, 190404 (2008).

[164] M. Bordag, V. Nikolaev, The vacuum energy for two cylinders with one increasing in size, J. Phys. A **42**, 415203 (2009).

[165] F.C. Lombardo, F.D. Mazzitelli, P.I. Villar, D.A.R. Dalvit, Casimir energy between media-separated cylinders: The scalar case, Phys. Rev. A **82**, 042509 (2010).

[166] E. Noruzifar, T. Emig, R. Zandi, Universality versus material dependence of fluctuation forces between metallic wires, Phys. Rev. A **84**, 042501 (2011).

[167] A.R. Kitson, A. Romeo, Perturbative zero-point energy for a cylinder of elliptical section, Phys. Rev. D **74**, 085024 (2006).

[168] J.P. Straley, G.A. White, E.B. Kolomeisky, Casimir energy of a cylindrical shell of elliptical cross section, Phys. Rev. A **87**, 022503 (2013).

[169] N. Graham, Electromagnetic Casimir forces in elliptic cylinder geometries, Phys. Rev. D **87**, 105004 (2013).

[170] V.N. Marachevsky, Casimir interaction of two plates inside a cylinder, Phys. Rev. D **75**, 085019 (2007).

[171] V.V. Nesterenko, G. Lambiase, G. Scarpetta, Casimir energy of a semi-circular infinite cylinder, J. Math. Phys. **42**, 1974 (2001).

[172] A.H. Rezaeian, A.A. Saharian, Local Casimir Energy for a Wedge with circular outer boundary, Class. Quantum Grav. **19**, 3625 (2002).

[173] A.A. Saharian, A.S. Tarloyan, Whightman function and scalar Casimir densities for a wedge with a cylindrical boundary, J. Phys. A **38**, 8763 (2005).

[174] A.A. Saharian, Electromagnetic Casimir densities for a wedge with a coaxial cylindrical shell, Eur. Phys. J. C **52**, 721 (2007).

[175] A.A. Saharian, A.S. Tarloyan, Wightman function and scalar Casimir densities for a wedge with two cylindrical boundaries, Annals Phys. **323**, 1588 (2008).

[176] I. Brevik, S.A. Ellingsen, K. A. Milton, Electrodynamic Casimir effect in a medium-filled wedge, Phys. Rev. E **79**, 041120 (2009).

[177] S.A. Ellingsen, I. Brevik, K.A. Milton, Electrodynamic Casimir effect in a medium-filled wedge. II, Phys. Rev. E **80**, 021125 (2009).

[178] K.A. Milton, J. Wagner, K. Kirsten, Casimir effect for a semitransparent wedge and an annular piston, Phys. Rev. D **80**, 125028 (2009).

[179] S.A. Ellingsen, I. Brevik, K.A. Milton, Casimir effect at nonzero temperature for wedges and cylinders, Phys. Rev. D **81**, 065031 (2010).

[180] I. Brevik, T. Toverud, Electromagnetic energy density around a superconducting cosmic string, Class. Quantum Gravity **12**, 1229 (1995).

[181] E.R. Bezerra de Mello, V.B. Bezerra, A.A. Saharian, A.S. Tarloyan, Vacuum polarization induced by a cylindrical boundary in the cosmic string spacetime, Phys. Rev. D **74**, 025017 (2006).

[182] E.R. Bezerra de Mello, V.B. Bezerra, A.A. Saharian, Electromagnetic Casimir densities induced by a conducting cylindrical shell in the cosmic string spacetime, Phys. Lett. B **645**, 245 (2007).

[183] E.R. Bezerra de Mello, V.B. Bezerra, A.A. Saharian, A.S. Tarloyan, Fermionic vacuum polarization by a cylindrical boundary in the cosmic string spacetime, Phys. Rev. D **78**, 105007 (2008).

[184] V.V. Nesterenko, I.G. Pirozhenko, Vacuum energy in conical space with additional boundary conditions, Class. Quantum Grav. **28**, 175020 (2011).

[185] A.D. Linde, *Particle Physics and Inflationary Cosmology* (Harwood Academic Publishers, Chur, Switzerland 1990).

[186] D.H. Lyth, A. Riotto, Particle Physics Models of Inflation and the Cosmological Density Perturbation, Phys. Rep. **314**, 1 (1999).

[187] B.A. Bassett, S. Tsujikawa, D. Wands, Inflation dynamics and reheating, Rev. Mod. Phys. **78**, 537 (2007).

[188] J. Martin, C. Ringeval, V. Vennin, Encyclopaedia Inflationaris, Phys. Dark Univ. 5-6 (2014) 75-235; arXiv:1303.3787.

[189] A. Linde, Inflationary Cosmology after Planck 2013, arXiv:1402.0526.

[190] A.G. Riess, et al., Astron. J., Observational evidence from supernovae for an accelerating Universe and a cosmological constant, **116**, 1009 (1998).

[191] S. Perlmutter, et al., Measurements of omega and lambda from 42 high-redshift supernovae, Astrophys. J. **517**, 565 (1999).

[192] A.G. Riess et al., New Hubble space telescope discoveries of type Ia supernovae at $z > 1$: Narrowing constraints on the early behavior of dark energy, Astrophys. J. **659**, 98 (2007).

[193] D.N. Spergel et al., Three-year Wilkinson microwave anisotropy probe (WMAP) observations: Implications for cosmology, Astrophys. J. Suppl. Ser. **170**, 377 (2007).

[194] E. Komatsu et al., Five-Year Wilkinson Microwave anisotropy probe (WMAP) observations: Cosmological interpretation, Astrophys. J. Suppl. Ser. **180**, 330 (2009).

[195] P.A.R. Ade et al., Planck 2013 results. XVI. Cosmological parameters, A&A **571**, A16 (2014).

[196] J.A. Frieman, M.S. Turner, D. Huterer, Dark energy and the accelerating Universe, Ann. Rev. Astron. Astrophys. **46**, 385 (2008).

[197] D.H. Weinberg et al., Observational probes of cosmic acceleration, Phys. Rep. **530**, 87 (2013).

[198] A.A. Saharian, T.A. Vardanyan, Casimir densities for a plate in de Sitter spacetime, Classical Quantum Gravity **26**, 195004 (2009).

[199] E. Elizalde, A.A. Saharian, T.A. Vardanyan, Casimir effect for parallel plates in de Sitter spacetime, Phys. Rev. D **81**, 124003 (2010).

[200] A.A. Saharian, Casimir effect in de Sitter spacetime, Int. J. Mod. Phys. A **26**, 3833 (2011).

[201] P. Burda, Casimir effect for a massless minimally coupled scalar field between parallel plates in de Sitter spacetime, JETP Lett. **93**, 632 (2011).

[202] A.A. Saharian, V.F. Manukyan, Scalar Casimir densities induced by a cylindrical shell in de Sitter spacetime, Classical Quantum Gravity **32**, 025009 (2015).

[203] A.A. Saharian, A.S. Kotanjyan, H.A. Nersisyan, Electromagnetic two-point functions and Casimir densities for a conducting plate in de Sitter spacetime, Phys. Lett. B **728**, 141 (2014).

[204] A.S. Kotanjyan, A.A. Saharian, H.A. Nersisyan, Electromagnetic Casimir effect for conducting plates in de Sitter spacetime, Phys. Scr. **90**, 065304 (2015).

[205] B. Allen, T. Jacobson, Vector two-point functions in maximally symmetric spaces, Commun. Math. Phys. **103**, 669 (1986).

[206] N.C. Tsamis, R.P. Woodard, Maximally symmetric vector propagator, J. Math. Phys. **48**, 052306 (2007).

[207] T. Garidi, J.P. Gazeau, S. Rouhani, M.V. Takook, Massless vector field in de Sitter universe, J. Math. Phys. **49**, 032501 (2008).

[208] A. Youssef, Infrared behavior and gauge artifacts in de Sitter spacetime: The Photon Field, Phys. Rev. Lett. **107**, 021101 (2011).

[209] M.B. Fröb, A. Higuchi, Mode-sum construction of the two-point functions for the Stueckelberg vector fields in the Poincaré patch of de Sitter space, J. Math. Phys. **55**, 062301 (2014).

[210] S. Bellucci, A.A. Saharian, Electromagnetic two-point functions and the Casimir effect in Friedmann-Robertson-Walker cosmologies, Phys. Rev. D **88**, 064034 (2013).

[211] O. Aharony, S.S. Gubser, J. Maldacena, H. Ooguri, and Y. Oz, Large N field theories, string theory and gravity, Phys. Rep. **323**, 183 (2000).

[212] H. Năstase, *Introduction to AdS/CFT correspondence* (Cambridge University Press, Cambridge, 2015).

[213] M. Ammon and J. Erdmenger, *Gauge/Gravity Duality: Foundations and Applications* (Cambridge University Press, Cambridge, 2015).

[214] R. Maartens and K. Koyama, Brane-world gravity, Living Rev. Relativity **13**, 5 (2010).

[215] S. Nojiri, S.D. Odintsov, S. Zerbini, Bulk versus boundary (gravitational Casimir) effects in the quantum creation of an inflationary brane-world universe, Class. Quantum Grav. **17**, 4855 (2000).

[216] M. Fabinger and P. Horava, Casimir Effect Between World-Branes in Heterotic M-Theory, Nucl. Phys. B **580**, 243 (2000).

[217] W. Goldberger, I. Rothstein, Quantum stabilization of compactified AdS_5, Phys. Lett. B **491**, 339 (2000).

[218] A. Flachi and D.J. Toms, Quantized bulk scalar fields in the Randall-Sundrum brane-model, Nucl. Phys. B **610**, 144 (2001).

[219] J. Garriga, O. Pujolàs, T. Tanaka, Radion effective potential in the brane-world, Nucl. Phys. B **605**, 192 (2001).

[220] E. Elizalde, S. Nojiri, S.D. Odintsov, S. Ogushi, Casimir effect in de Sitter and anti-de Sitter braneworlds, Phys. Rev. D **67**, 063515 (2003).

[221] A.A. Saharian, M.R. Setare, Casimir energy-momentum tensor for a brane in de Sitter spacetime, Phys. Lett. B **584**, 306 (2004).

[222] A. Knapman, D.J. Toms, Stress-energy tensor for a quantized bulk scalar field in the Randall-Sundrum brane model, Phys. Rev. D **69**, 044023 (2004).

[223] A.A. Saharian, Wightman function and Casimir densities on AdS bulk with application to the Randall-Sundrum braneworld, Nucl. Phys. B **712**, 196 (2005).

[224] A.A. Saharian, Surface Casimir densities and induced cosmological constant on parallel branes in AdS spacetime, Phys. Rev. D **70**, 064026 (2004).

[225] A. Flachi, A. Knapman, W. Naylor, M. Sasaki, Zeta functions in brane world cosmology, Phys. Rev. D **70**, 124011 (2004).

[226] E. Elizalde, S. Nojiri, S.D. Odintsov, P. Wang, Dark energy: Vacuum fluctuations, the effective phantom phase, and holography, Phys. Rev. D **71**, 103504 (2005).

[227] A.A. Saharian, A.L. Mkhitaryan, Wightman function and vacuum densities for a Z2-symmetric thick brane in AdS spacetime, J. High Energy Phys. **08** (2007) 063.

[228] M. Frank, I. Turan, L. Ziegler, Casimir force in Randall-Sundrum models, Phys. Rev. D **76**, 015008 (2007).

[229] L.P. Teo, Casimir effect in spacetime with extra dimensions – From Kaluza-Klein to Randall-Sundrum models, Phys. Lett. B **682**, 259 (2009).

[230] A. Flachi, T. Tanaka, Casimir effect on the brane, Phys. Rev. D **80**, 124022 (2009).

[231] M. Rypestøl, I. Brevik, Finite-temperature Casimir effect in Randall-Sundrum models, New J. Phys **12**, 013022 (2010).

[232] S.-H. Shao, P. Chen, J.-A. Gu, Stress-energy tensor induced by a bulk Dirac spinor in the Randall-Sundrum model, Phys. Rev. D **81**, 084036 (2010).

[233] E. Elizalde, S.D. Odintsov, A.A. Saharian, Fermionic Casimir densities in anti-de Sitter spacetime, Phys. Rev. D **87**, 084003 (2013).

[234] A. Flachi, J. Garriga, O. Pujolàs, T. Tanaka, Moduli stabilization in higher dimensional brane models, J. High Energy Phys. **08** (2003) 053.

[235] A. Flachi, O. Pujolàs, Quantum self-consistency of AdS$\times\Sigma$ brane models, Phys. Rev. D **68**, 025023 (2003).

[236] A.A. Saharian, Wightman function and vacuum fluctuations in higher dimensional brane models, Phys. Rev. D **73**, 044012 (2006).

[237] A.A. Saharian, Bulk Casimir densities and vacuum interaction forces in higher dimensional brane models, Phys. Rev. D **73**, 064019 (2006).

[238] A.A. Saharian, Surface Casimir densities and induced cosmological constant in higher dimensional braneworlds, Phys. Rev. D **74**, 124009 (2006).

[239] E. Elizalde, M. Minamitsuji, W. Naylor, Casimir effect in rugby-ball type flux compactifications, Phys. Rev. D **75**, 064032 (2007).

[240] R. Linares, H.A. Morales-Técotl, O. Pedraza, Casimir force for a scalar field in warped brane worlds, Phys. Rev. D **77**, 066012 (2008).

[241] M. Frank, N. Saad, I. Turan, Casimir force in Randall-Sundrum models with $q+1$ dimensions, Phys. Rev. D **78**, 055014 (2008).

[242] E.R. Bezerra de Mello, A.A. Saharian, M.R. Setare, Vacuum densities for a brane intersecting the AdS boundary, Phys. Rev. D **92**, 104005 (2015).

[243] R. Basu, A. Vilenkin, Evolution of topological defects during inflation, Phys. Rev. D **50**, 7150 (1994).

[244] C.J.A.P. Martins, E.P.S. Shellard, Quantitative string evolution, Phys. Rev. D **54**, 2535 (1996).

[245] C.J.A.P. Martins, E.P.S. Shellard, Extending the velocity-dependent one-scale string evolution model, Phys. Rev. D **65**, 043514 (2002).

[246] P.P. Avelino, C.J.A.P. Martins, E.P.S. Shellard, Effects of inflation on a cosmic string loop population, Phys. Rev. D **76**, 083510 (2007).

[247] M. Hindmarsh, Signals of inflationary models with cosmic strings, Prog. Theor. Phys. Suppl. **190**, 197 (2011); C. Ringeval, Cosmic strings and their induced non-Gaussianities in the cosmic microwave background, arXiv:1005.4842.

[248] A. Vilenkin, Towards the theory of reheating after inflation, Phys. Rev. D **56**, 3258 (1997).

[249] A. Vilenkin, E.P.S. Shellard, *Cosmic Strings and Other Topological Defects* (Cambridge University Press, Cambridge, England, 1994).

[250] E. Witten, Cosmic superstrings, Phys. Lett. B **153**, 243 (1985).

[251] D.F. Chernoff, S.-H. Henry Tye, Inflation, string theory and cosmic strings, Int. J. Mod. Phys. D **24**, 1530010 (2015).

[252] E.J. Copeland, L. Pogosian, T. Vachaspati, Seeking string theory in the cosmos, Class. Quantum Grav. **28**, 204009 (2011).

[253] E.R. Bezerra de Mello, A.A. Saharian, Fermionic vacuum polarization by a flat boundary in cosmic string spacetime, J. High Energy Phys. JHEP04(2009)046.

[254] E.R. Bezerra de Mello, A.A. Saharian, Fermionic vacuum polarization by a cosmic string in de Sitter spacetime, J. High Energy Phys. JHEP08(2010)038.

[255] A. Mohammadi, E.R. Bezerra de Mello, A.A. Saharian, Induced fermionic currents in de Sitter spacetime in the presence of a compactified cosmic string, Class. Quantum Grav. **32**, 135002 (2015).

[256] P.P. Kronberg, Extragalactic magnetic fields, Rep. Prog. Phys. **57**, 325 (1994).

[257] M. Giovannini, The Magnetized Universe, Int. J. Mod. Phys. D **13**, 391 (2004).

[258] A. Kandusa, K.E. Kunze, C.G. Tsagas, Primordial magnetogenesis, Phys. Rep. **505**, 1 (2011).

[259] R. Durrer, A. Neronov, Cosmological Magnetic Fields: Their Generation, Evolution and Observation, Astron. Astrophys. Rev. **21**, 62 (2013).

[260] M. Giovannini, Magnetogenesis and the dynamics of internal dimensions, Phys. Rev. D **62**, 123505 (2000).

[261] J. Ambjorn, S. Wolfram, Properties of the vacuum. 2. Electrodynamic, Ann. Phys. (N.Y.) **147**, 33 (1983).

[262] H. Luckock, Mixed boundary conditions in quantum field theory, J. Math. Phys. **32**, 1755 (1991).

[263] T. Gherghetta, A. Pomarol, Bulk Fields and Supersymmetry in a Slice of AdS, Nucl. Phys. B **586**, 141 (2000).

[264] A.A. Saharian, V.F. Manukyan, N.A. Saharyan, Electromagnetic Casimir densities for a cylindrical shell on de Sitter space, Int. J. Mod. Phys. A **31**, 1650183 (2016).

[265] S.N. Solodukhin, Boundary conditions and the entropy bound, Phys. Rev. D **63**, 044002 (2001).

[266] *Handbook of Mathematical Functions*, edited by M. Abramowitz and I. A. Stegun (Dover, New York, 1972).

[267] A. Erdélyi *et al*, *Higher Transcendental Functions*, Vol. 2 (McGraw Hill, New York, 1953).

[268] A.A. Grib, B.A. Levitskii, V.M. Mostepanenko, Particle creation from vacuum by a non-stationary gravitational field in the canonical formalism, Theor. Math. Phys. **19**, 349 (1974).

[269] A.A. Saharian, A summation formula over the zeros of the associated Legendre function with a physical application, J. Phys. A: Math. Theor. **41**, 415203 (2008).

[270] A.A. Saharian, Energy-momentum tensor for a scalar field on manifolds with boundaries, Phys. Rev. D **69**, 085005 (2004).

[271] G. Kennedy, R. Critchley, and J.S. Dowker, Finite temperature field theory with boundaries: Stress tensor and surface action renormalisation, Ann. Phys. (N.Y.) **125**, 346 (1980).

[272] S.L. Lebedev, Vacuum energy and Casimir force in the presence of a dimensional parameter in the boundary condition, Phys. Atom. Nucl. **64**, 1337 (2001).

[273] A. Romeo, A.A. Saharian, Casimir effect for scalar fields under Robin boundary conditions on plates, J. Phys. A: Math. Gen. **35**, 1297 (2002).

[274] S.A. Fulling, Systematics of the relationship between vacuum energy calculations and heat-kernel coefficients, J. Phys. A **36**, 6857 (2003).

[275] F.R. Klinkhamer, G.E. Volovik, Coexisting vacua and effective gravity, Phys. Lett. A **347**, 8 (2005).

[276] A.A. Saharian, Generalized Abel-Plana formula. Applications to cylindrical functions, Izv. AN Arm. SSR. Matematika **22**, 166 (1987) [Sov. J. Contemp. Math. Analysis, **22**, 70 (1987)].

[277] A.A. Saharian, A summation formula over the zeros of a combination of the associated Legendre functions with a physical application, J. Phys. A: Math. Theor. **42**, 465210 (2009).

[278] C.J. Isham, Twisted quantum fields in a curved space-time, Proc. R. Soc. A **362**, 383 (1978); C. J. Isham, Spinor fields in four dimensional space-time, Proc. R. Soc. A **364**, 591 (1978).

[279] J. Scherk, J.H. Schwartz, Superstrings with spontaneously broken supersymmetry and their effective theories, Phys. Lett. B **82**, 60 (1979).

[280] Y. Hosotani, Dynamical mass generation by compact extra dimensions, Phys. Lett. B **126**, 309 (1983).

[281] A. Higuchi, L. Parker, Aspects of QED and non-Abelian gauge theories in $S^1 \neq^3$ and $S^1 \neq^4$ spacetimes, Phys. Rev. D **37**, 2853 (1988).

[282] Y. Hosotani, Dynamics of non-integrable phases and gauge symmetry breaking, Ann. Phys. (N.Y.) **190**, 233 (1989).

[283] A. Actor, Topological symmetry breaking in ϕ^4 theories on toroidal spacetime, Class. Quantum Grav. **7**, 663 (1990).

[284] K. Kirsten, Topological gauge field mass generation by toroidal spacetime, J. Phys. A: Math. Gen. **26**, 2421 (1993).

[285] C. Ccapa Ttira, C.D. Fosco, A.P.C. Malbouisson, I. Roditi, Vacuum polarization for compactified QED_{4+1} in a magnetic flux background, Phys. Rev. A **81**, 032116 (2010).

[286] D. Deutsch, P. Candelas, Boundary effects in quantum field theory, Phys. Rev. D **20**, 3063 (1979).

[287] P. Candelas, Vacuum energy in the presence of dielectric and conducting surfaces, Ann. Phys. (N.Y.) **143**, 241 (1982).

[288] N. Graham, R.L. Jaffe, V. Khemani, M. Quandt, M. Scandurra, H. Weigel, Calculating vacuum energies in renormalizable quantum field theories: A new approach to the Casimir problem, Nucl. Phys. B **645**, 49 (2002).

[289] N. Graham, R.L. Jaffe, V. Khemani, M. Quandt, O. Schröder, H. Weigel, The Dirichlet Casimir problem, Nucl. Phys. B **677**, 379 (2004).

[290] K.A. Milton, Hard and soft walls, Phys. Rev. D **84**, 065028 (2011).

[291] F.D. Mazzitelli, J.P. Nery, A. Satz, Boundary divergences in vacuum self-energies and quantum field theory in curved spacetime, Phys. Rev. D **84**, 125008 (2011).

[292] R. Estrada, S.A. Fulling, F.D. Mera, Surface vacuum energy in cutoff models: pressure anomaly and distributional gravitational limit, J. Phys. A: Math. Theor. **45**, 455402 (2012).

[293] N. Bartolo, R. Passante, Electromagnetic-field fluctuations near a dielectric-vacuum boundary and surface divergences in the ideal conductor limit, Phys. Rev. A **86**, 012122 (2012).

[294] R. Passante, L. Rizzuto, S. Spagnolo, Vacuum local and global electromagnetic self-energies for a point-like and an extended field source, Eur. Phys. J. C **73**, 2419 (2013).

[295] E.R. Bezerra de Mello, A.A. Saharian, Fermionic vacuum polarization by a composite topological defect in higher-dimensional space-time, Phys. Rev. D **78**, 045021 (2008).

[296] T.S. Bunch, P.C.W. Davies, Quantum field theory in de Sitter space: renormalization by point-splitting, Proc. R. Soc. A **360**, 117 (1978).

[297] E.R. Bezerra de Mello, V.B. Bezerra, A.A. Saharian, Electromagnetic Casimir densities induced by a conducting cylindrical shell in the cosmic string spacetime, Phys. Lett. B **645**, 245 (2007).

[298] V.B. Bezerra, E.R. Bezerra de Mello, G.L. Klimchitskaya, V.M. Mostepanenko, A.A. Saharian, Exact Casimir-Polder potential between a particle and an ideal metal cylindrical shell and the proximity force approximation, Eur. Phys. J. C **71**, 1614 (2011).

[299] A.A. Sahariana, A.S. Kotanjyan, Repulsive Casimir-Polder forces from cosmic strings, Eur. Phys. J. C **71**, 1765 (2011).

[300] P. Candelas, Vacuum energy in the bag model, Ann. Phys. **167**, 257 (1986).

[301] J.D. Jackson, *Classical Electrodynamics* (John Wiley & Sons, 1999).

[302] A.P. Prudnikov, Yu.A. Brychkov, O.I. Marichev, *Integrals and Series* (Gordon and Breach, New York, 1986), Vol. II.

[303] A.M. Ghezelbash, R.B. Mann, Vortices in De Sitter Spacetimes, Phys. Lett. B **537**, 329 (2002).

[304] A.H. Abbassi, A.M. Abbassi, H. Razmi, Cosmological constant influence on cosmic string spacetime, Phys. Rev. D **67**, 103504 (2003).

[305] H. Tashiro, T. Vachaspati, Cosmological magnetic field correlators from blazar induced cascade, Phys. Rev. D 87, 123527 (2013).

[306] L. Campanelli, Origin of Cosmic Magnetic Fields, Phys. Rev. Lett. **111**, 061301 (2013).

[307] R. Durrer, G. Marozzi, M. Rinaldi, Comment on "Origin of Cosmic Magnetic Fields", Phys. Rev. Lett. **111**, 229001 (2013).

[308] L. Campanelli, Campanelli Replies, Phys. Rev. Lett. **111**, 229002 (2013).

[309] T. Vachaspati, A. Vilenkin, Large-scale structure from wiggly cosmic strings, Phys. Rev. Lett. **67**, 1057 (1991).

[310] T. Vachaspati, Structure of wiggly-cosmic-string wakes, Phys. Rev. D **45**, 3487 (1992).

[311] D.N. Vollick, Cosmic string shocks, magnetic fields, and microwave anisotropies, Phys. Rev. D **48**, 3585 (1993).

[312] P.P. Avelino, E.P.S. Shellard, Dynamical friction on cosmic string motion and magnetic field generation, Phys. Rev. D **51**, 5946 (1995).

[313] K. Dimopoulos, Primordial magnetic fields from superconducting cosmic strings, Phys. Rev. D **57**, 4629 (1998).

[314] L. Hollenstein, C. Caprini, R. Crittenden, R. Maartens, Challenges for creating magnetic fields by cosmic defects, Phys. Rev. D **77**, 063517 (2008).

[315] L.V. Zadorozhna, B.I. Hnatyk, Yu.A. Sitenko, Magnetic field of cosmic strings in the Early Universe, Ukr. J. Phys. **58**, 398 (2013).

[316] K. Horiguchi K. Ichiki, N. Sugiyama, Primordial magnetic fields from the string network, Prog. Theor. Exp. Phys. **2016(8)**, 083E02 (2016).

[317] V.P. Frolov, E.M. Serebriany, Vacuum polarization in the gravitational field of a cosmic string, Phys. Rev. D **35**, 3779 (1987).

[318] J.S. Dowker, Vacuum averages for arbitrary spin around a cosmic string, Phys. Rev. D **36**, 3742 (1987).

[319] G.N. Watson, *A Treatise on the Theory of Bessel Functions* (Cambridge University Press, Cambridge, 1966).